Withdrawn NIST Technical Series Publication

Warning Notice

The attached publication has been withdrawn (archived), and is provided solely for historical purposes. It may have been superseded by another publication (indicated below).

Withdrawn Publication	
Series/Number	NIST TN 2230
Title	Fracture Toughness Tests at 77 K and 4 K on 316L Stainless Steel Welded Plates
Publication Date(s)	July 29, 2022
Withdrawal Date	June 6, 2023
Withdrawal Note	Superseded by updated version

Superseding Publication(s) *(if applicable)*

The attached publication has been **superseded by** the following publication(s):

Series/Number	NIST TN 2230-upd1
Title	Fracture Toughness Tests at 77 K and 4 K on 316L Stainless Steel Welded Plates
Author(s)	Jake Benzing; Nick Derimow; Enrico Lucon; Timothy Weeks
Publication Date(s)	June 6, 2023
URL/DOI	https://doi.org/10.6028/NIST.TN.2230-upd1

Additional Information *(if applicable)*	
Contact	
Latest revision of the attached publication	
Related Information	
Withdrawal Announcement Link	

Date updated: June 6, 2023

NIST NATIONAL INSTITUTE OF STANDARDS AND TECHNOLOGY
U.S. DEPARTMENT OF COMMERCE

NIST Technical Note 2230

Fracture Toughness Tests at 77 K and 4 K on 316L Stainless Steel Welded Plates

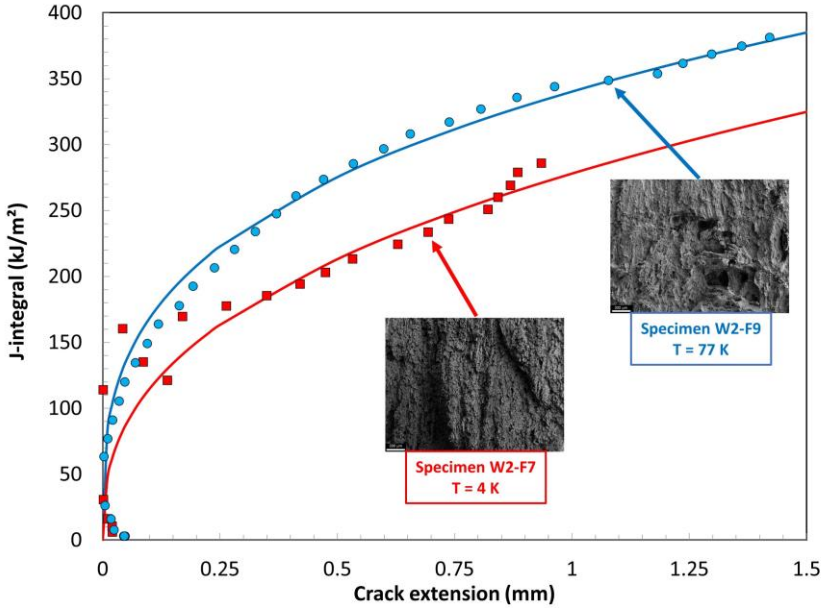

Jake Benzing, Nick Derimow, Enrico Lucon, and Timothy Weeks

This publication is available free of charge from:
https://doi.org/10.6028/NIST.TN.2230

NATIONAL INSTITUTE OF STANDARDS AND TECHNOLOGY
U.S. DEPARTMENT OF COMMERCE

NIST Technical Note 2230

Fracture Toughness Tests at 77 K and 4 K on 316L Stainless Steel Welded Plates

Jake Benzing
Nick Derimow
Enrico Lucon
Timothy Weeks
Applied Chemicals and Materials Division
Material Measurement Laboratory

This publication is available free of charge from:
https://doi.org/10.6028/NIST.TN.2230

July 2022

U.S. Department of Commerce
Gina Raimondo, Secretary

National Institute of Standards and Technology
Laurie E. Locascio, NIST Director and Undersecretary of Commerce for Standards and Technology

National Institute of Standards and Technology Technical Note 2230
Natl. Inst. Stand. Technol. Tech. Note 2230, 219 pages (July 2022)
CODEN: NTNOEF

This publication is available free of charge from:
https://doi.org/10.6028/NIST.TN.2230

Abstract

In the framework of a collaborative project between ASME, NASA, and NIST, quasi-static fracture toughness tests have been performed at liquid nitrogen temperature (77 K, or -196 °C) and liquid helium temperature (4 K, or -269 °C) on weld specimens extracted from the centers of four 316L welded stainless steel plates, each produced by a different vendor. Although the plates were produced in accordance with the same specifications from the same material (316L), large differences in fracture toughness have been observed, with the best weld (W2) exhibiting almost twice the critical toughness of the worst (W1) at 77 K (219 kJ/m^2 vs. 113 kJ/m^2), and about seven times the critical toughness of W1 at 4 K (146 kJ/m^2 as compared to 21 kJ/m^2). The Charpy absorbed energies recorded at 77 K for three of the welds within the same project were found to be strongly linearly correlated with fracture toughness at both test temperatures. The exception was weld W4, which provided the highest impact toughness and the second lowest quasi-static fracture toughness (stable crack initiation and resistance to crack propagation).

Key words

316L stainless steel; apparent negative crack growth; liquid helium; liquid nitrogen; pressure vessels fracture toughness; tearing modulus; welding.

Table of Contents

List of Tables

List of Figures

1. Introduction

Currently, ASME Boiler and Pressure Vessel Code (BPVC) Section VIII [1] and ASME Piping Code B31.12 Hydrogen Piping and Pipelines [2] both require performing Charpy impact tests at liquid nitrogen (LN2) temperature, i.e., 77 K (-196 °C), to assess the fracture performance of austenitic stainless steels at liquid helium (LHe) temperature, i.e., 4 K (-269 °C). The same procedure was also proposed for ASME Piping Code B31.3 Process Piping [3].

Charpy testing provides a relatively inexpensive measurement of the impact toughness of a material, quantified by absorbed energy and lateral expansion [4]. Due to adiabatic heating that occurs at high strain rates during Charpy impact testing [5], conducting Charpy tests at temperatures below 77 K is not technically feasible. The temperature rise during the transfer of the specimens from the cooling medium to the impact position is also a concern at temperatures below 77 K. These infeasibilities call into question the technical justification of using Charpy impact toughness values measured at LN2 temperature to assess the reliability of quasi-static fracture toughness tests conducted on single-edge bend (Charpy-type) specimens at LHe temperature. While actions have been proposed to mitigate the temperature increase due to specimen transfer ([6]-[16]), the heat generated within the specimen during high strain rate deformation and fracture cannot be avoided and is significant [17].

Addressing the use of 77 K Charpy test results to assess material properties at 4 K is the main objective of this work. Specifically, crack propagation through welded sections of 316L stainless steel pipes is the primary mode and material of interest. Charpy impact testing has already been completed on the weld section of four unique lots in welded 316L plates [18]. These four unique lots cover a representative range in welding process, chemical content, and delta ferrite fraction. The framework of this study is a collaborative project between the American Society of Mechanical Engineers (ASME), the National Aeronautics and Space Administration (NASA), and the National Institute for Standards and Technology (NIST). The results presented in this report include quasi-static fracture toughness (as opposed to impact toughness, measured from Charpy tests in [18]) measured on Charpy-type specimens [18] at 77 K and 4 K, extracted from the same four lots of welded 316L plates previously investigated through Charpy impact testing at 77 K and tensile testing at 77 K and 4 K [19]. These results can be applied in energy and aerospace industries.

2. Materials and Test Matrix

Charpy-type single-edge bend, SE(B), fracture toughness specimens were extracted from welds in four welded 316L stainless steel plate samples provided by ASME/Jacob ESSCA Group, identified as W1, W2, W3, and W4. The samples were all in the as-welded condition, and had the following approximate dimensions: 254 mm × 610 mm, thickness = 16 mm. The plates were welded by four different vendors in accordance with ASME Boiler and Pressure Vessel Code requirements, but using 316L plate and weld material individually procured by each vendor, and following each vendor's standard in-house welding procedure specification.

A summary of the welding processing specifications provided by each welding vendor, as well as other pertinent information, is provided in Table 1. Gas tungsten arc welding (GTAW) is sometimes referred to as either tungsten inert gas or heli-arc welding, and does not use flux so as to protect the weld pool from oxidation with an inert gas shield. Flux core arc welding (FCAW) is an automated process involving a wire (thin strip of metal wrapped around a core of flux), such that the flux floats to the surface of the weld upon melting and provides a temporary shield of the weld surface, but is usually assisted by a cover gas. Common issues with using FCAW is that the flux can absorb moisture from the air if not properly stored. Generally, GTAW is used to join smaller pipes since the deposition rate is slower (approximately by a factor 3) than FCAW, which is typically used to join larger pipes. All GTAW processes were performed using straight polarity, whereas FCAW processes use reverse polarity. Notably, all suppliers used GTAW to perform the first few root passes, but only W2 used GTAW to complete the rest of the weld passes (W1, W3, and W4 used FCAW for all other passes after the root). Figure 1 provides a top-view (weld cap) of the final passes used by each welding vendor, which range from one final pass (W1) to four final passes (W2). Additional information about each weld is provided in Appendix F.

Wire chemical composition information reported in welding certifications were provided by each vendor and are shown in Table 2. In Appendix A: Supplemental Information for Each Weld, chemical composition measurements performed by spark emission on surfaces of each plate are provided, as well as rough overviews of the cross sectional ends of each plate, the latter of which guided specimen extraction from the center of each plate. As delta ferrite can form upon cooling, ferrite content measurements were performed on the welds since fracture toughness measurements are centered in each weld. The ferrite measurements were performed using a contact-based Fisher Feritscope[1] FMP30, which was verified using a sample of known ferrite content and are shown in Table 3.

[1] Certain commercial software, equipment, instruments, or materials are identified in this report to adequately specify the experimental procedure. Such identification is not intended to imply recommendation or endorsement by the National Institute of Standards and Technology, nor is it intended to imply that the equipment or materials identified are necessarily the best available for the purpose.

Table 1 – Processing information gleaned from welding process specification reports.

Welded plate	W1		W2		W3		W4	
Process	Root	Cover	Root	Cover	Root	Cover	Root	Cover
	GTAW	FCAW	GTAW, manual	GTAW, manual	GTAW	FCAW	GTAW	FCAW
Tungsten electrode dimensions and composition	0.125", 2% Thoriated		0.094", 2% Thoriated	0.125", 2% Thoriated	0.125", 2% Thoriated		0.125", 2% Thoriated	
Stringer or weave	stringer	stringer	either	either	stringer	either	either	either
Shielding gas	GTAW: Ar, backing Ar	FCAW: CO2	GTAW: 100% Ar, backing: 100% Ar	GTAW: 100% Ar, backing: 100% Ar	GTAW: Ar, backing: Ar	Ar/CO2 75%/25%	Ar 99.997%,	Ar/CO2 75%/25%, backing: Ar 99.997%
Root filler diameter	0.094"		0.094"		0.125"		.0625" and .094"	
Cover filler diameter		0.045"		0.125"		0.045"		0.045"
Interpass temperature	50 °F to 350 °F	50 °F to 350 °F	50 °F to 300 °F	50 °F to 300 °F	70 °F to 350 °F	70 °F to 350 °F	50 °F to 350 °F	50 °F to 350 °F

Figure 1 – Representative view of the top of each weld (weld cap / final cover pass). W1 used a single final pass, W2 used four final passes, W3 used three final passes, and W4 used two final passes.

Table 2 – Wire chemical composition gleaned from welding process specification reports.

Vendor	W1		W2		W3		W4	
	AWS/SFA 5.9 (Root)	AWS/SFA 5.22 (Cover)	Root and Cover have same composition	Root and Cover have same composition	Root	Cover	Root/Hot pass	Cover
C	0.014	0.03	0.02	0.02	0.016	0.03	<.01/<.01	0.022
Cr	18.16	18.89	18.7	18.7	18.3	17.74	18.3/18.0	18.68
Ni	11.81	12.48	11.8	11.8	12.75	12.94	12.2/12.0	11.88
Mo	2.56	2.55	2.3	2.3	2.54	2.1	2.5/2.5	2.72
Mn	1.78	1.14	1.7	1.7	1.89	0.85	1.6/1.5	1.53
Si	0.36	0.7	0.52	0.52	0.35	0.56	0.35/0.37	0.72
P	0.014	0.26	0.02	0.02	0.015	0.025	0.021/.023	0.024
S	0.012	0.005	0.01	0.01	0.012	0.004	0.012/.01	0.008
Cu	0.08	0.21	0.1	0.1	0.1	0.2	0.18/.16	0.12

Table 3 – Ferrite percentage in welds, based on the average of 24 measurements per weld.

Weld	W1		W2		W3		W4	
	Root	Cover	Root	Cover	Root	Cover	Root	Cover
Ferrite (%)	5.64	8.19	4.00	4.25	3.02	2.29	8.04	9.83

The technical drawings of the fracture toughness specimens, whose general dimensions were equivalent to those of the Charpy V-notch specimens according to ASTM E23-18 [4], except for the notched region, are reproduced in Appendix C. The fracture toughness specimens were extracted from the plates at the same time as tensile and Charpy specimens. All specimens were centered on the weld seams. The specimen orientation with respect to the plate thickness and the weld geometry corresponds to orientation “NQ” in Figure 2, which is taken from ISO 15653:2018 [20]. As seen in Figure 2a, the crack grows from the narrower side of the weld (root) to the wider side (cap), which makes it more likely for crack propagation to occur fully within the weld material. After fatigue precracking in accordance with the provisions of ASTM E1820-21 [21], specimens were side-grooved to a total thickness reduction of 20 %, corresponding to 1 mm on each side.

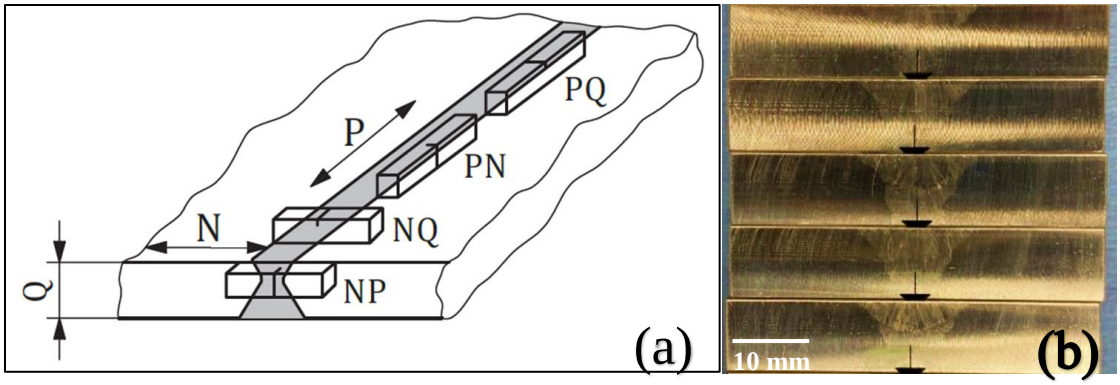

Figure 2 – (a) Possible orientations of Charpy-type fracture toughness specimens extracted from welded plates [20], and (b) photograph of some as-received specimens, showing the location of the weld. The specimens tested in this study correspond to orientation "NQ", where the first letter (N) is the direction normal to the crack plane, and the second (Q) is the expected direction of crack propagation (N = normal to weld direction; Q = weld thickness direction), such that the notch faces the root of the weld and crack propagation moves towards the weld cap.

Details about the experimental procedure are given in Section 3, while Section 4 describes the analytical procedure used for the calculation of critical toughness values and crack resistance curves.

Quasi-static fracture toughness tests were performed in accordance with ASTM E1820-21 [21] at liquid nitrogen temperature (77 K = -196.15 °C = -321.07 °F) and liquid helium temperature (4 K = -269.15 °C = -457.47 °F). On each weld, five or six tests were performed at each temperature, for a total of 43 tests. The complete test matrix is provided in Table 4.

Table 4 - Test matrix for the quasi-static fracture toughness tests.

Weld	T (K)	Number of tests performed
W1	77	6
	4	5
W2	77	5
	4	5
W3	77	6
	4	5
W4	77	5
	4	6

3. Experimental Procedure

3.1. Fatigue Precracking at 77 K (Liquid Nitrogen)

To facilitate straight and efficient fatigue precracking, all specimens were precracked in liquid nitrogen, as room temperature would have been too high with respect to both 77 K and 4 K, and the risk of artificially increasing toughness by the so-called warm prestressing (WPS) effect [22] would have been significant. Prior to precracking, all specimens were polished on both sides to ensure the precrack was visible past the notch. A 50-kip (222 kN) servo-hydraulic load frame, equipped with a 2.5-kip (11 kN) load cell and crack mouth opening ring-shaped clip gage (calibrated in LN2 and verified before testing) was used during precracking and subsequent fracture toughness measurements. A thermocouple was tied to a location well above the specimen to ensure the specimen was constantly submerged in LN2. First, the specimen was placed in the upper bend fixture and the clip gage attached. Then, the lower fixture was inserted over the specimen, and a guide was used to ensure the specimen was centered with respect to all 3 loading pins. Next, a load-bearing sheath was placed over the fixtures and twist-locked into place, with the threaded rod protruding out of the bottom of the sheath. A spherical nut was threaded such that the bottom rod of the lower fixture contacted the sheath. A pre-load was then applied using force control. The entire setup was then slowly lowered into a double-walled cylinder filled with liquid nitrogen, by lowering crosshead with hydraulic pressure. Images showing the pull rod, upper fixture, specimen, clip gage, lower fixture, loading pins, sheath, and double-walled cylinder are provided in Figure 3. If the thermocouple (placed well above the specimen) did not produce a reading consistent with LN2 temperatures (77 K), the cylinder was filled with more LN2.

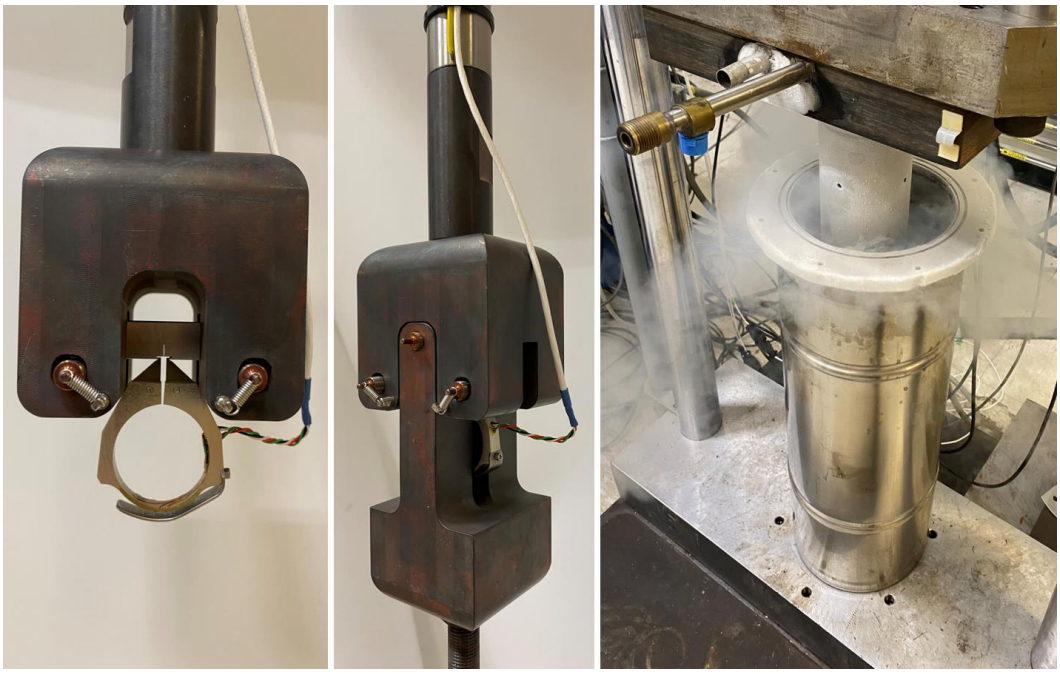

Figure 3 – (Left) Fracture toughness specimen placed in the upper fixture with the clip gage attached and (middle) lower fixture placed over the specimen and 3rd loading pin inserted above the specimen. (Right) The sheath that protects the experimental setup and enables load bearing on the specimen is lowered into a double-walled cylinder filled with LN2.

Every specimen was fatigue precracked with a load shedding procedure, based on a crack size check to verify the expected initial crack size (length of machined notch). Table 5 provides an overview of the parameters chosen for fatigue precracking. After precracking was completed, specimens were 20 % side-grooved, according to the drawings in Appendix C.

Table 5 – Input parameters used during fatigue precracking in LN2.

Item	Input	Units
Precrack Wave Shape	True Sine Taper	–
Precrack Final Crack Limit	5.00	mm
Precrack Frequency	5	Hz
Precrack Load Ratio	0.1	unitless
Precrack Lower Least Squares Fit Percentage	10	%
Precrack Upper Least Squares Fit Percentage	90	%
Precrack Cycle Limit	100,000	count
Precrack Final Maximum Stress Intensity Factor (K_{max})	0.7	kN/mm$^{1.5}$

3.2. Tests at 77 K (Liquid Nitrogen)

Fracture toughness testing in LN2 used the same equipment and experimental setup as described above in 3.1. A custom-written procedure was used to measure crack resistance by means of the Unloading Compliance technique, by recording force, displacement, and CMOD data at a rate of 4 Hz. Once the specimen and fixtures had been submerged in liquid nitrogen for at least 5 minutes, the procedure was initiated. Generally speaking, the following steps were included: operator/specimen input, zero offset of axial channels, pre-load application, elastic unloading and loading, crack extension in small increments with sufficient dwell times and unloading/loading routines, followed by a return of the sample to zero force. After testing, the specimens were heat tinted at 400 °C for 45 minutes and then broken open on a Charpy machine after submerging them for a few minutes in LN2.

3.3. Tests at 4 K (Liquid Helium)

Fracture toughness testing in LHe used similar equipment and software procedures as described for testing in LN2. However, some key equipment-related differences existed. First, the clip gage was re-calibrated and verified in liquid helium. Also, a rod-like liquid level indicator was placed near the specimen/fixtures (as opposed to the thermocouple used in LN2 tests) to monitor the liquid level during testing. To minimize boil-off, a smaller double-walled cylinder was placed in contact with the reaction frame using a tailored silicone seal, and then tightened into place with threaded nuts. Each port on the experiment was equipped with a custom fitting such as: a hose to recover the helium gas, a plug for the liquid transfer line port, a seal around instrumentation wires, and a pressure relief valve. These equipment differences are depicted in Figure 4. Once the specimen and fixtures had been submerged in liquid helium for at least 5 minutes, the same testing procedure as for LN2 tests was initiated.

At both 77 K and 4 K, the typical test duration was between 75 minutes and 90 minutes, except when significant cleavage phenomena occurred.

Figure 4 – (Left) Fracture toughness specimen placed into both fixtures, plus a rod-like liquid helium level indicator is visible behind the fixtures. (Middle) A smaller double-walled cylinder was placed in contact with the reaction frame (silicone seal placed between cylinder and frame) and tightened into place with threaded nuts. Each port on the experiment was either equipped with (middle) a gas recovery hose, a plug, (right) a seal around instrumentation wires, or a pressure relief valve.

4. Analytical Procedure (ASTM E1820-21)

The quasi-static fracture toughness tests performed were analyzed in accordance with ASTM E1820-21 [21], with the objective of establishing for every specimen tested the critical value of fracture toughness (engineering approximation of the *J*-integral value at the initiation of stable crack growth) and the crack resistance, or *J*-*R* (*R* = resistance), curve.

All tests were performed using the Unloading Compliance single-specimen technique, whereby each specimen tested provides a critical value of toughness and a full crack resistance curve, and crack size is measured through the elastic compliance of the cracked specimen at various stages during the test. Elastic compliance is evaluated as the slope of unloading/reloading cycles performed at regular and equally-spaced displacement intervals. Crack sizes are analytically related to compliance for a specific specimen configuration, and depend on the material's elastic modulus at the test temperature.

According to E1820-21, fracture toughness is expressed in terms of *J*-integral, which represents the work spent to propagate the crack. For a SE(B) specimen, it is calculated from the area under the applied force vs. crack mouth opening displacement (CMOD) curve, normalized by the specimen ligament and multiplied by a geometrical factor.

For the calculation of crack size from elastic compliance, the recommendations of Appendix X3 of ASTM E1820-21 were followed. Only the unloading (decreasing force) part of each cycle was used, and the initial and final 5 % of the unloading portion were excluded from the linear regression. According to the same appendix, the uncertainty of the calculated critical toughness due to noise in the unload/reload data is less than 4 % if the value of the non-dimensionalized root-mean square of the standard error of the compliances is less than 400. Based on our calculations, this was found to be the case for all 43 tests performed in this investigation.

Once the *J*-*R* (*J*-integral vs. crack extension Δa) curve is established, the critical toughness is obtained from the intersection between the power law regression curve used to fit qualified *J*-Δa data points and a construction line whose slope depends on the tensile properties of the material at the test temperature, offset by 0.2 mm with respect to the origin of the axes. The value of *J*-integral at this intersection is labeled J_Q, a provisional, size-dependent value of the plane-strain fracture toughness J_{Ic}, which represents the crack-extension resistance under conditions of crack-tip plane strain. J_Q can be qualified as J_{Ic} if a number of validity requirements are fulfilled. Of the 35 toughness tests that provided acceptable *J*-*R* curves (81 % of the 43 tests performed), only 8 yielded J_{Ic} critical values. The cause of invalidity will be detailed in the Results section.

Most of the tests performed exhibited large tearing (ductile) instabilities, accompanied by large crack "jumps" on the *J*-*R* curve, corresponding to significant force drops and sudden increments of CMOD. Some of these crack jumps corresponded to decreases in *J*-integral, particularly after significant crack extensions (1 mm or more). An example is shown in Figure 5 (specimen W4-F5, tested at 4 K, which exhibited three tearing instabilities during the course of the test).

For the test shown in Figure 5, the earliest tearing instability occurred after crack initiation, *i.e.*, the intersection between regression curve and 0.2 mm-offset construction line. Therefore, the critical toughness value to be reported is the *J*-integral at the intersection.

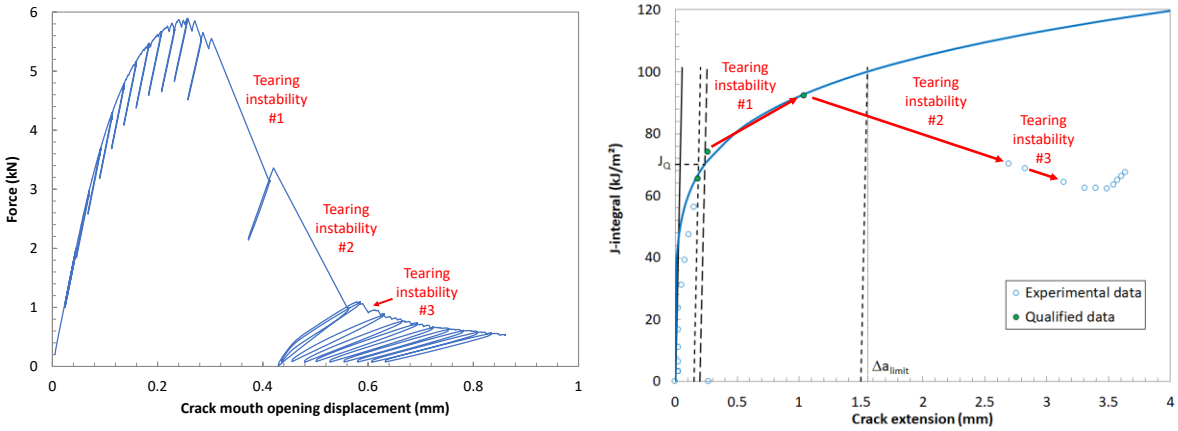

Figure 5 - Specimen W4-F5, force/CMOD curve (left) and *J-R* curve (right). In this case, the first tearing instability occurred just after crack initiation.

If the first tearing instability occurs before crack initiation (example in Figure 6 – specimen W4-F3), J_Q cannot be established, and the critical toughness value to be reported is the *J*-integral at the point of first tearing instability (J_{Qc}). This is defined in Annex A6 of E1820-21 as "a measure of fracture toughness at instability without significant stable crack extension". Provided two specific validity conditions are met, this value is considered independent of the in-plane dimensions of the specimen, and is labeled J_c. Details about the validity or invalidity of J_{Qc} instability values will be provided in the following section.

Only welds W1 and W4 displayed this type of behavior (tearing instability before crack initiation).

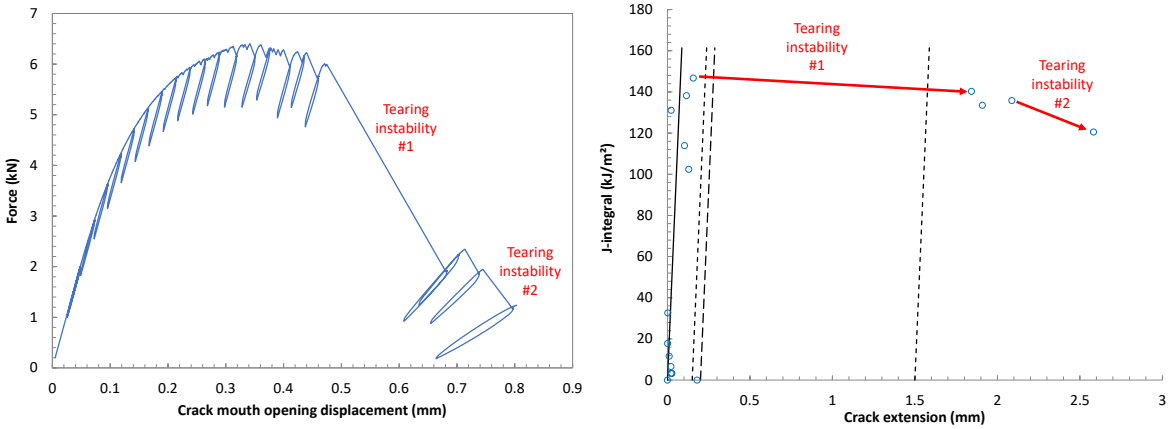

Figure 6 - Specimen W4-F3, force/CMOD curve (left) and *J-R* curve (right). In this case, the first tearing instability occurred before crack initiation.

For welds and test temperatures where different type of fracture behavior were observed, the mean critical toughness value was reported as the average of all calculated values of J_{Qc}, J_c, J_Q, and J_{Ic} (as applicable) for that specific condition.

An additional toughness measure, the tearing modulus *TM* [23], was calculated and reported. Although not included in ASTM E1820, it is considered a useful piece of information for characterizing the fracture toughness of the investigated welds, as it quantifies the slope of the regression curve (*J-R* curve) at the point of crack initiation (J_Q). The higher the tearing modulus, the steeper is the *J-R* curve, and therefore the resistance to crack propagation. It is given by:

$$TM = \frac{E}{\sigma_Y^2}\frac{\mathrm{d}J}{\mathrm{d}a} \tag{1}$$

where E is the Young's modulus, σ_Y is the average of yield and tensile strengths, and $\frac{\mathrm{d}J}{\mathrm{d}a}$ is the slope of the power law regression line calculated at the intersection with the 0.2 mm-offset construction line.

5. Test Results

5.1. Tests at 77 K

5.1.1. Weld W1

Six tests were performed. In five cases, *J-R* curves and corresponding J_Q values were obtained, none of which qualified as J_{Ic}. Significant tearing instabilities were observed for 5 of the 6 tested specimens. Only for specimen W1-F10, the first tearing instability occurred before initiation, and the calculated value of J_{Qc} was found to be dependent on in-plane dimensions. Test results are summarized in Table 6 (including specimen dimensions) and illustrated in Figure 7 (*J*-Δ*a* data points). Detailed test results are provided in Appendix D.

Table 6 – Specimen dimensions and test results for weld W1, T = 77 K. N/A = not available.

Specimen id	W (mm)	B (mm)	B_N (mm)	$a_{o,meas}$ (mm)	a_{oq} (mm)	Δa_{meas} (mm)	Δa_{pred} (mm)	J_{Qc} (kJ/m^2)	J_c (kJ/m^2)	J_Q (kJ/m^2)	J_{Ic} (kJ/m^2)	TM (MPa)	Reasons for J_c or J_{Ic} invalidity
W1-F9	10.02	10.03	8.01	5.22	5.16	3.16	3.21	N/A	N/A	63.81	N/A	36.28	d
W1-F10	10.03	10.02	8.01	5.20	5.17	2.86	2.76	109.31	N/A	N/A	N/A	N/A	k, l
W1-F11	10.02	10.03	8.01	5.28	5.28	1.77	1.40	N/A	N/A	267.44	N/A	69.52	a, d
W1-F12	10.02	10.03	8.00	5.35	5.27	3.06	2.96	N/A	N/A	89.28	N/A	13.99	d
W1-F13	10.03	10.05	8.01	5.36	5.17	3.35	3.31	N/A	N/A	100.52	N/A	34.23	d, f
W1-F14	10.04	10.04	8.01	5.34	5.24	3.39	3.24	N/A	N/A	46.00	N/A	22.50	a, d, e, f, h

Invalidity keys
a – Excessive difference between measured (Δa_{meas}) and predicted (Δa_{pred}) crack extension.
d – Less than 3 data points available to calculate a_{oq}.
e – Less than 3 data points between $0.4J_Q$ and J_Q.
f – Correlation coefficient of the a_{oq} fit < 0.96.
h – Number of data points inside the two exclusion lines < 5.
k – **Only for J_{Qc}/J_c**: thickness $B \leq 100\frac{J_Q}{\sigma_Y}$.
l – **Only for J_{Qc}/J_c**: initial ligament $b_o \leq 100\frac{J_Q}{\sigma_Y}$.

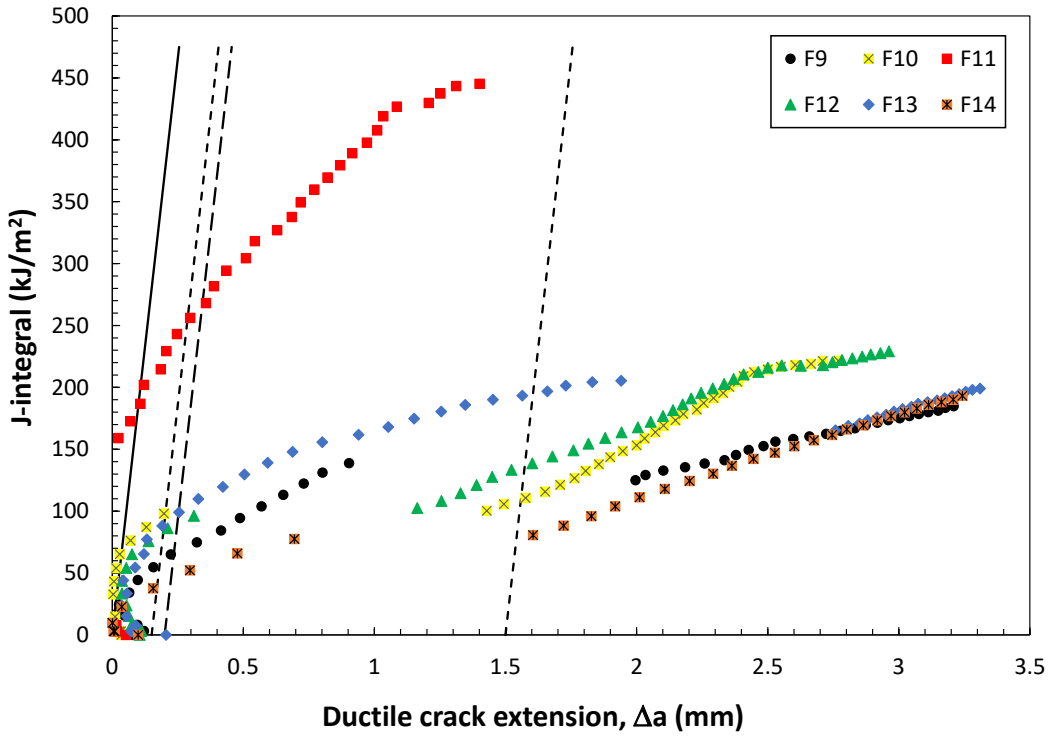

Figure 7 – Experimental data points from the tests performed at 77 K on weld W1.

5.1.2. Weld W2

Five tests were performed. All tests yielded acceptable *J-R* curves with corresponding J_Q values, 4 of which qualified as J_{Ic}. No tearing instabilities were observed. Test results are summarized in Table 7 (including specimen dimensions) and illustrated in Figure 8 (J-Δa data points). Detailed test results are provided in Appendix D.

Table 7 – Specimen dimensions and test results for weld W2, T = 77 K. N/A = not available.

Specimen id	W (mm)	B (mm)	B_N (mm)	$a_{o,meas}$ (mm)	a_{oq} (mm)	Δa_{meas} (mm)	Δa_{pred} (mm)	J_Q (kJ/m^2)	J_{Ic} (kJ/m^2)	TM (MPa)	Reasons for J_c or J_{Ic} invalidity
W2-F8	10.02	10.02	8.01	5.18	4.85	1.57	1.49	N/A	228.13	68.22	
W2-F9	10.03	10.01	8.00	5.22	5.00	1.86	1.80	N/A	243.67	47.34	
W2-F10	10.03	10.02	8.01	5.30	4.90	1.93	1.90	162.15	N/A	63.95	d, f
W2-F11	10.02	10.02	8.00	5.22	4.94	2.15	2.09	N/A	238.23	49.18	
W2-F12	10.02	10.03	8.01	5.16	4.98	1.54	1.40	N/A	224.73	54.55	

Invalidity keys d – Less than 3 data points available to calculate a_{oq}.
f – Correlation coefficient of the a_{oq} fit < 0.96.

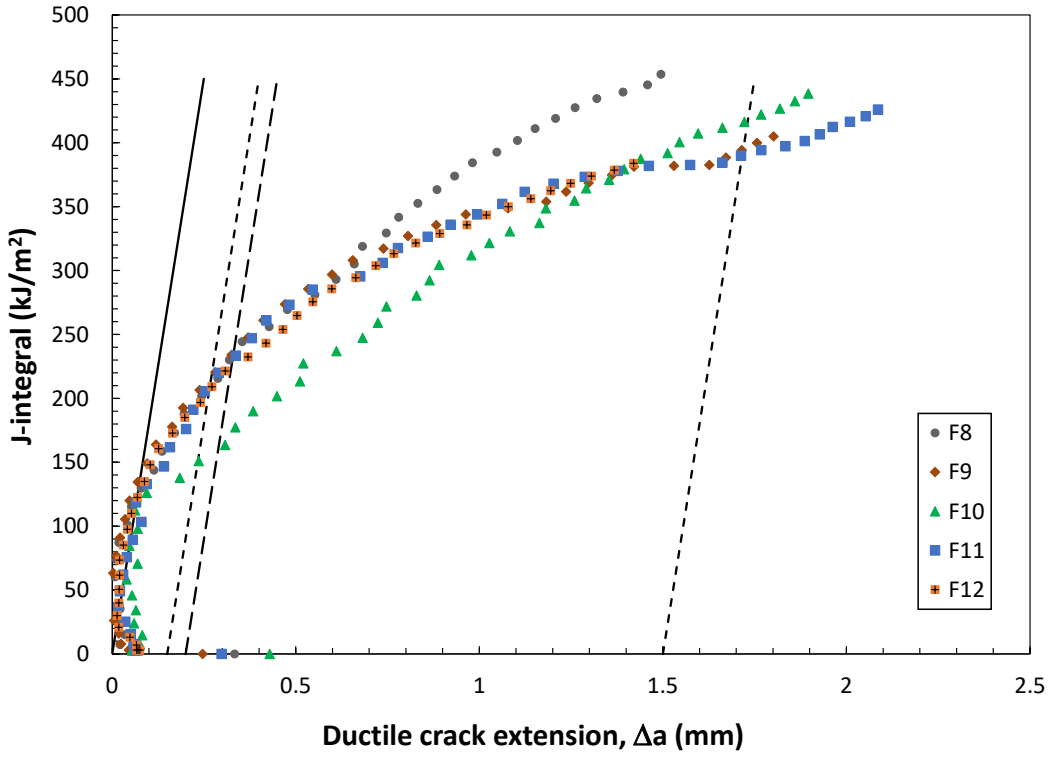

Figure 8 – Experimental data points from the tests performed at 77 K on weld W2.

5.1.3. Weld W3

Six tests were performed. All tests yielded acceptable *J-R* curves with corresponding J_Q values, 4 of which qualified as J_{Ic}. Tearing instabilities were observed for 3 of the tested specimens, all of them occurring after crack initiation. Test results are summarized in Table 8 (including specimen dimensions) and illustrated in Figure 9 (*J*-Δ*a* data points). Detailed test results are provided in Appendix D.

Table 8 – Specimen dimensions and test results for weld W3, T = 77 K. N/A = not available.

Specimen id	W (mm)	B (mm)	B_N (mm)	$a_{o,meas}$ (mm)	a_{oq} (mm)	Δa_{meas} (mm)	Δa_{pred} (mm)	J_Q (kJ/m^2)	J_{Ic} (kJ/m^2)	TM (MPa)	Reasons for J_c or J_{Ic} invalidity
W3-F8	10.02	10.02	7.98	5.21	4.92	1.79	1.72	N/A	213.77	37.73	
W3-F9	9.97	10.02	8.02	5.24	5.00	1.97	1.88	N/A	189.07	37.37	
W3-F10	10.02	10.01	8.01	5.08	5.03	1.98	1.77	123.22	N/A	49.37	a, d
W3-F11	10.02	10.01	7.99	5.29	4.96	2.10	2.05	N/A	168.93	78.71	
W3-F12	10.02	10.02	8.00	5.32	4.93	2.06	2.02	N/A	232.10	41.27	
W3-F13	10.02	10.01	8.00	5.31	5.01	0.72	0.57	186.84	N/A	37.21	a, g

Invalidity keys
a – Excessive difference between measured (Δa_{meas}) and predicted (Δa_{pred}) crack extension.
d – Less than 3 data points available to calculate a_{oq}.
g – Invalid data point distribution between the 0.15 mm and 1.5 mm exclusion lines.

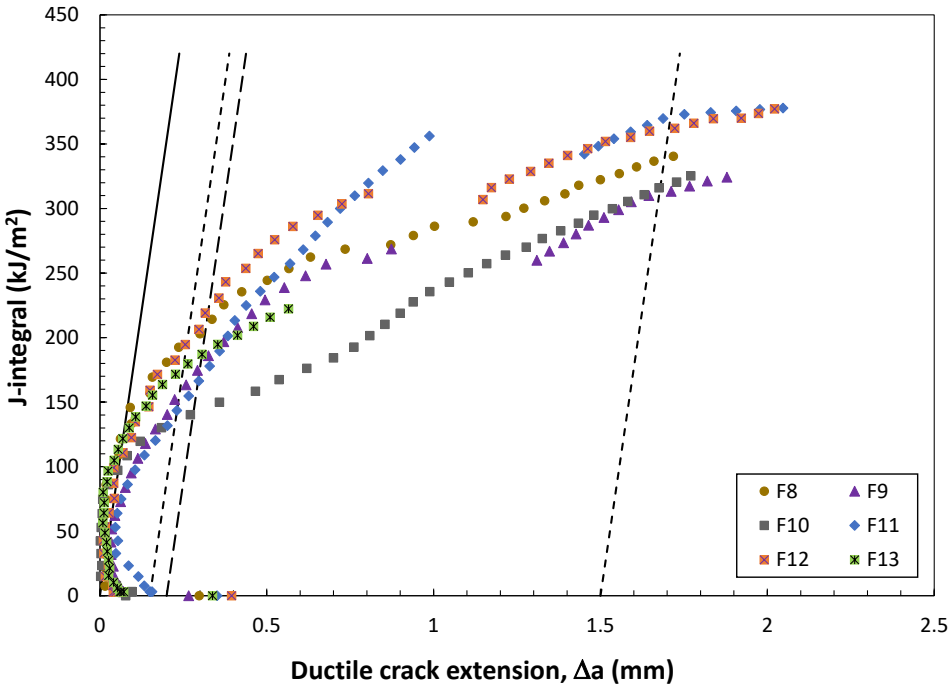

Figure 9 – Experimental data points from the tests performed at 77 K on weld W3.

5.1.4. Weld W4

Five tests were performed. Only one test yielded an acceptable *J-R* curve[2], while the remaining specimens exhibited significant tearing instabilities before the onset of stable crack initiation. Test results are summarized in Table 9 (including specimen dimensions) and illustrated in Figure 10 (*J*-Δ*a* data points). Detailed test results are provided in Appendix D.

Table 9 – Specimen dimensions and results for weld W4, T = 77 K. N/A = not available.

Specimen id	W (mm)	B (mm)	B_N (mm)	$a_{o,meas}$ (mm)	a_{oq} (mm)	Δa_{meas} (mm)	Δa_{pred} (mm)	J_{Qc} (kJ/m²)	J_c (kJ/m²)	J_Q (kJ/m²)	J_{Ic} (kJ/m²)	TM (MPa)	Reasons for J_c or J_{Ic} invalidity
W4-F9	10.01	10.01	8.00	5.20	4.91	0.96	0.50	N/A	N/A	198.73	N/A	20.16	a, g, h
W4-F10	9.99	10.02	8.01	5.18	4.86	3.87	3.93	121.56	N/A	N/A	N/A	N/A	k, l
W4-F11	10.02	10.01	8.00	5.19	4.89	3.81	4.22	116.60	N/A	N/A	N/A	N/A	k, l
W4-F11	10.03	10.02	8.00	5.19	4.90	3.98	4.12	71.53	N/A	N/A	N/A	N/A	l
W4-F13	10.03	10.01	8.00	5.19	5.03	2.04	1.98	106.99	N/A	N/A	N/A	N/A	k, l

Invalidity keys
a – Excessive difference between measured (Δa_{meas}) and predicted (Δa_{pred}) crack extension.
g – Invalid data point distribution between the 0.15 mm and 1.5 mm exclusion lines.
h – Number of qualified data points between the 0.15 mm and 1.5 mm exclusion lines < 5.
k – **Only for J_{Qc}/J_c**: thickness $B \leq 100\frac{J_Q}{\sigma_Y}$.
l – **Only for J_{Qc}/J_c**: initial ligament $b_o \leq 100\frac{J_Q}{\sigma_Y}$.

[2] Even this specimen (W4-F9), however, experienced a large tearing instability after the initiation of stable crack extension.

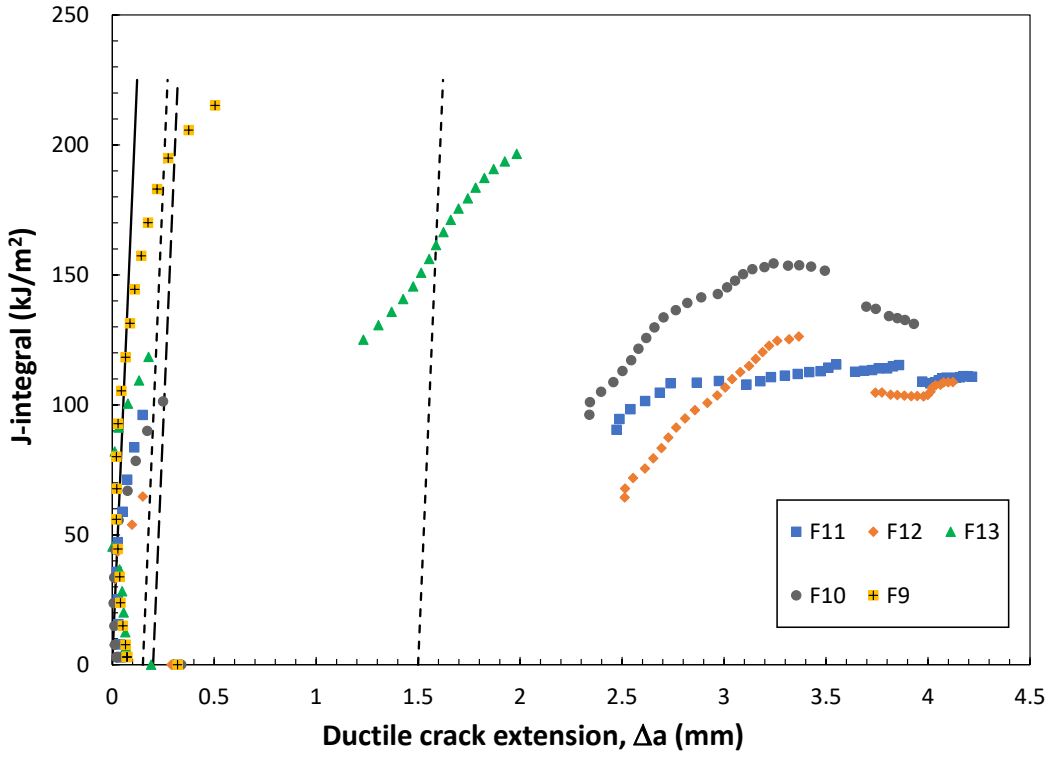

Figure 10 – Experimental data points from the tests performed at 77 K on weld W4.

5.2. Tests at 4 K

In all the fracture toughness tests conducted at liquid helium temperature (4 K), visible serrations were observed on the force-CMOD diagrams of the tested specimens. These serrations appeared as small force drops, accompanied by CMOD increases, and had been already observed during the tensile tests performed at 4 K [19]. These serrations did not occur in tensile or toughness tests performed at liquid nitrogen temperature (77 K), as can be seen in Figure 11.

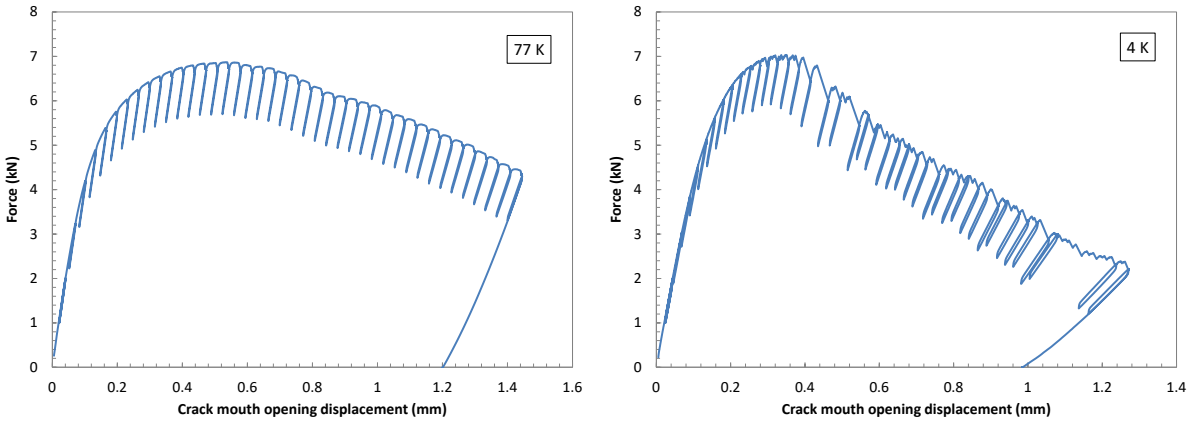

Figure 11 – Force-CMOD curves for a W2 specimen tested at 77 K (left), showing no serrations, and for another W2 specimen tested at 4 K (right), showing serrations.

The quality of the *J-R* curves obtained at 4 K is also significantly worse than at 77 K, in terms of both visible hysteresis of several load/unload cycles (Figure 11), and scatter of the *J*-Δ*a* data points (Figure 12).

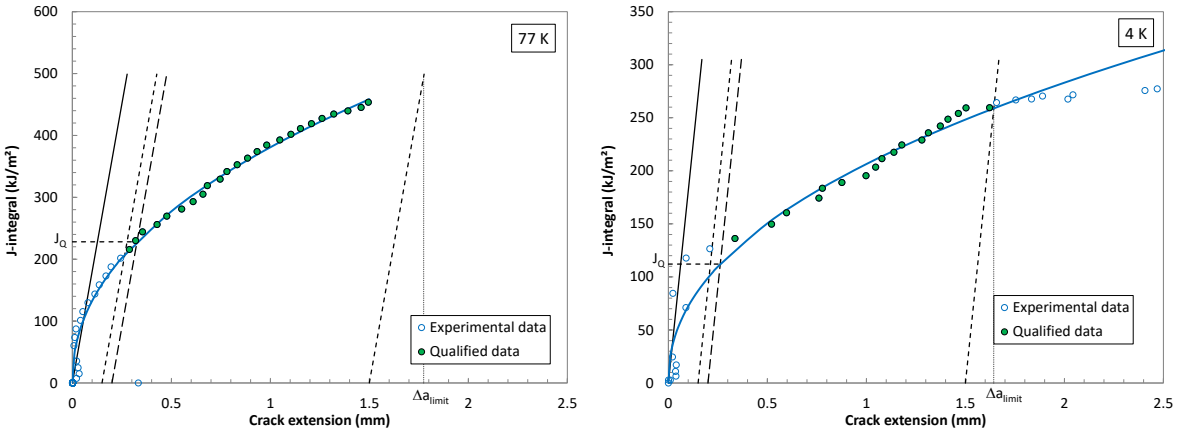

Figure 12 – *J-R* curves for two W2 specimens tested at 77 K (left) and at 4 K (right).

5.2.1. Weld W1

Five tests were performed, all of them providing acceptable *J-R* curves and corresponding J_Q values. No valid J_{Ic} were obtained. All tested specimens exhibited large tearing instabilities, occurring after crack initiation. Test results are summarized in Table 10 (including specimen dimensions) and illustrated in Figure 13 (*J*-Δ*a* data points). Detailed test results are provided in Appendix E.

Table 10 – Specimen dimensions and test results for weld W1, T = 4 K. N/A = not available.

Specimen id	W (mm)	B (mm)	B_N (mm)	$a_{o,meas}$ (mm)	a_{oq} (mm)	Δa_{meas} (mm)	Δa_{pred} (mm)	J_Q (kJ/m^2)	J_{Ic} (kJ/m^2)	TM (MPa)	Reasons for J_c or J_{Ic} invalidity
W1-F4	10.03	10.05	8.00	5.53	5.54	2.65	2.51	16.98	N/A	6.19	a, d, e, g, h
W1-F5	10.04	10.05	8.00	5.76	5.76	2.59	2.13	34.12	N/A	18.95	a
W1-F6	10.04	10.05	8.00	5.30	5.30	2.87	2.58	16.80	N/A	5.50	a, d, e, h
W1-F7	10.04	10.04	8.00	5.31	5.32	2.38	2.02	17.06	N/A	5.30	a, d, e, h
W1-F8	10.03	10.03	8.01	5.37	5.37	2.63	2.36	17.56	N/A	6.12	a, d, e, f

Invalidity keys
a – Excessive difference between measured (Δa_{meas}) and predicted (Δa_{pred}) crack extension.
d – Less than 8 data points available to calculate a_{oq}.
e – Less than 3 data points between $0.4J_Q$ and J_Q.
f – Correlation coefficient of the a_{oq} fit < 0.96.
g – Invalid data point distribution between the 0.15 mm and 1.5 mm exclusion lines.
h – Number of data points inside the two exclusion lines < 5.

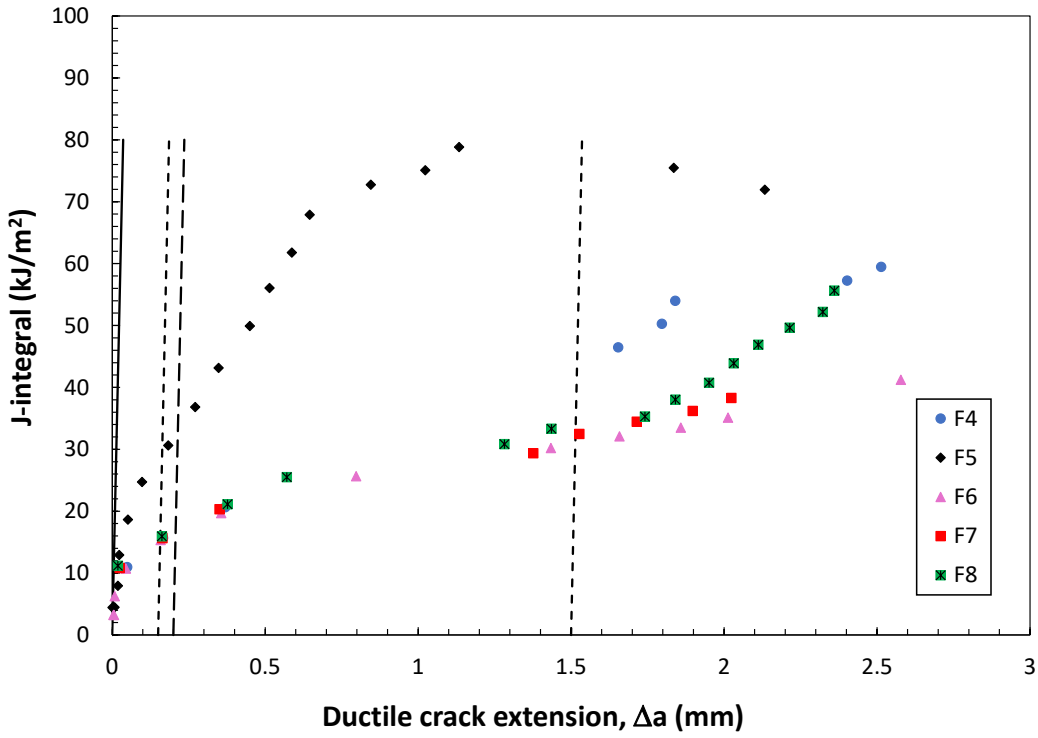

Figure 13 – Experimental data points from the tests performed at 4 K on weld W1.

5.2.2. Weld W2

Five tests were performed. All tests yielded acceptable *J-R* curves with corresponding J_Q values, none of which qualified as J_{Ic}. Large tearing instabilities were observed for 4 of the tested specimens, all occurring after crack initiation. Test results are summarized in Table 11 (including specimen dimensions) and illustrated in Figure 14 (*J*-Δ*a* data points). Detailed test results are provided in Appendix E.

Table 11 – Specimen dimensions and test results for weld W2, T = 4 K. N/A = not available.

Specimen id	W (mm)	B (mm)	B_N (mm)	$a_{o,meas}$ (mm)	a_{oq} (mm)	Δa_{meas} (mm)	Δa_{pred} (mm)	J_Q (kJ/m^2)	J_{Ic} (kJ/m^2)	TM (MPa)	Reasons for J_c or J_{Ic} invalidity
W2-F3	10.02	10.03	8.01	5.29	5.13	2.71	2.44	111.72	N/A	33.38	a, f
W2-F4	10.02	10.02	8.00	5.18	5.16	2.60	1.99	148.99	N/A	33.69	a, f
W2-F5	10.02	10.02	8.00	5.12	5.15	2.68	2.75	131.19	N/A	26.30	f
W2-F6	10.02	10.01	8.01	5.13	5.15	3.07	2.85	164.59	N/A	29.14	a, f
W2-F7	10.03	10.01	8.00	5.28	5.18	3.02	2.68	173.37	N/A	39.00	a, f

Invalidity keys a – Excessive difference between measured (Δa_{meas}) and predicted (Δa_{pred}) crack extension.
f – Correlation coefficient of the a_{oq} fit < 0.96.

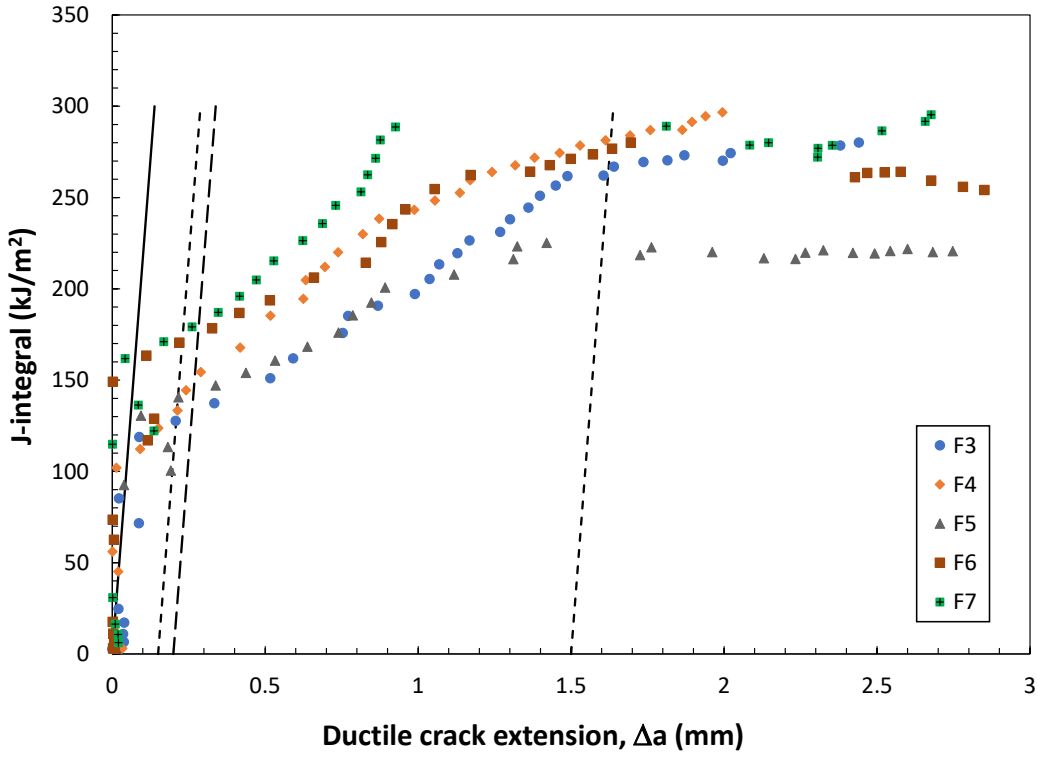

Figure 14 – Experimental data points from the tests performed at 4 K on weld W2.

5.2.3. Weld W3

Five tests were performed, all providing acceptable *J-R* curves with corresponding J_Q values. None qualified as J_{Ic}. Tearing instabilities were observed for 3 of the tested specimens. Test results are summarized in Table 12 (including specimen dimensions) and illustrated in Figure 15 (*J*-Δ*a* data points). Detailed test results are provided in Appendix E.

Table 12 – Specimen dimensions and test results for weld W3, T = 4 K. N/A = not available.

Specimen id	W (mm)	B (mm)	B_N (mm)	$a_{o,meas}$ (mm)	a_{oq} (mm)	Δa_{meas} (mm)	Δa_{pred} (mm)	J_Q (kJ/m^2)	J_{Ic} (kJ/m^2)	TM (MPa)	Reasons for J_c or J_{Ic} invalidity
W3-F3	10.02	10.01	8.06	5.29	5.21	1.59	1.29	85.51	N/A	36.29	a
W3-F4	10.02	10.02	8.00	5.24	5.19	1.72	1.51	98.14	N/A	37.71	a
W3-F5	10.02	9.96	8.06	5.24	5.04	2.42	2.25	101.38	N/A	30.14	a
W3-F6	9.96	10.01	8.00	5.32	5.17	1.82	2.11	96.08	N/A	29.11	a
W3-F7	9.92	10.01	8.07	5.30	5.15	1.86	1.73	104.36	N/A	32.16	f

Invalidity keys a – Excessive difference between measured (Δa_{meas}) and predicted (Δa_{pred}) crack extension.
f – Correlation coefficient of the a_{oq} fit < 0.96.

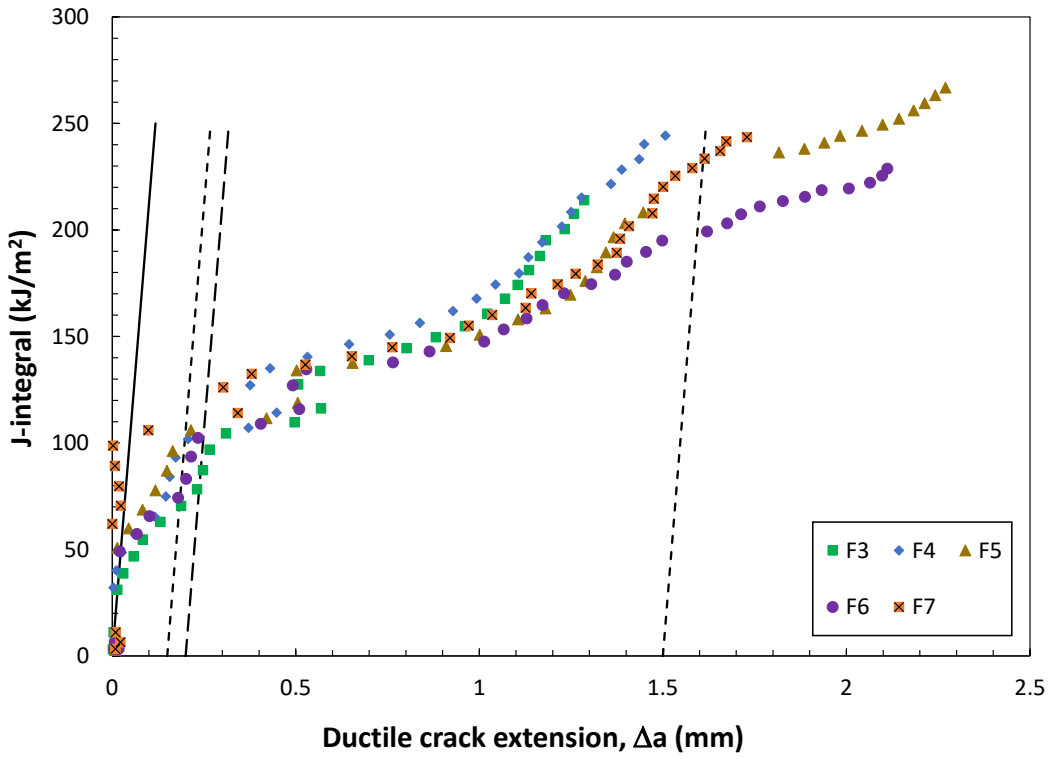

Figure 15 – Experimental data points from the tests performed at 4 K on weld W3.

5.2.4. Weld W4

Six tests were performed. Only 3 tests yielded an acceptable *J-R* curve, while the remaining 3 specimens exhibited significant tearing instabilities before the onset of stable crack initiation. Test results are summarized in Table 13 (including specimen dimensions) and illustrated in Figure 16 (*J*-Δ*a* data points). Detailed test results are provided in Appendix E.

Table 13 – Specimen dimensions and test results for weld W4, T = 4 K. N/A = not available.

Specimen id	W (mm)	B (mm)	B_N (mm)	$a_{o,meas}$ (mm)	a_{oq} (mm)	Δa_{meas} (mm)	Δa_{pred} (mm)	J_{Qc} (kJ/m^2)	J_c (kJ/m^2)	J_Q (kJ/m^2)	J_{Ic} (kJ/m^2)	TM (MPa)	Reasons for J_c or J_{Ic} invalidity
W4-F3	10.01	9.98	8.01	5.24	5.12	2.91	2.57	164.31	N/A	N/A	N/A	N/A	k, l
W4-F4	9.99	10.02	8.01	5.22	5.06	3.34	3.39	N/A	N/A	42.01	N/A	5.98	h
W4-F5	10.01	10.04	8.02	5.23	5.01	3.52	3.62	N/A	N/A	70.32	N/A	7.93	h
W4-F6	10.00	10.02	8.00	5.18	4.99	3.64	3.66	103.96	N/A	N/A	N/A	N/A	k, l
W4-F7	10.01	10.01	8.01	5.13	5.12	3.18	3.18	N/A	N/A	26.99	N/A	6.40	d
W4-F8	10.02	10.02	8.00	5.26	5.07	1.99	3.59	52.34	N/A	N/A	N/A	N/A	k

Invalidity keys
d – Less than 8 data points available to calculate a_{oq}.
g – Invalid data point distribution between the 0.15 mm and 1.5 mm exclusion lines.
k – **Only for J_{Qc}/J_c**: thickness $B \leq 100\frac{J_Q}{\sigma_Y}$.
l – **Only for J_{Qc}/J_c**: initial ligament $b_o \leq 100\frac{J_Q}{\sigma_Y}$.

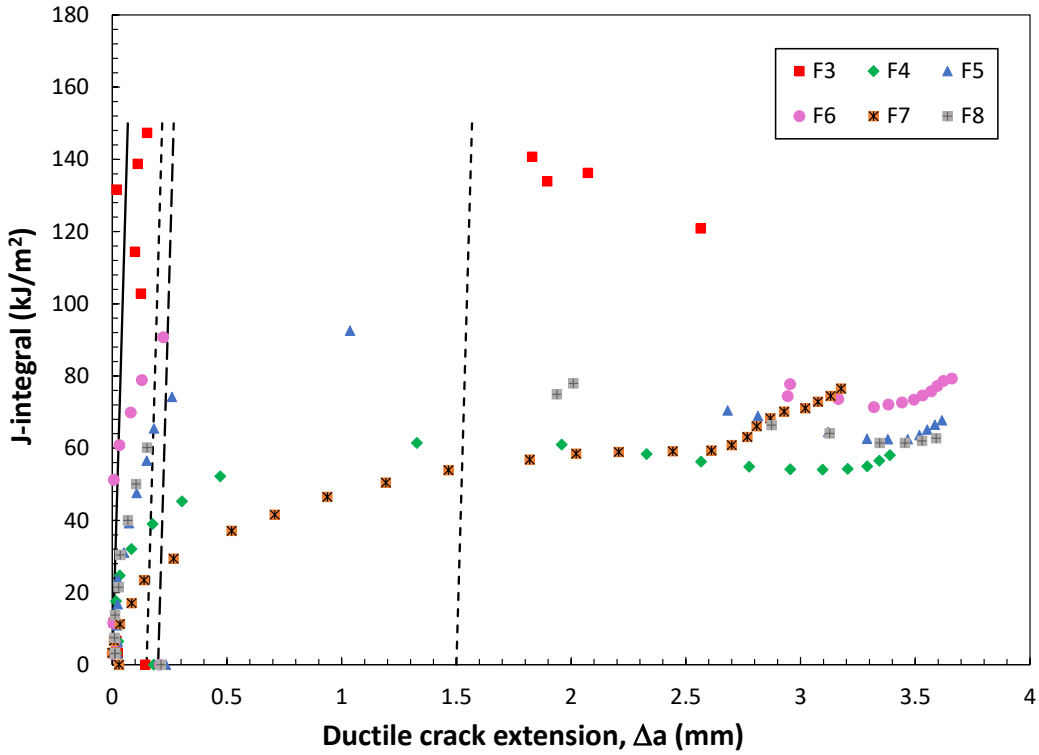

Figure 16 – Experimental data points from the tests performed at 4 K on weld W4.

6. Fractography

6.1. Summary of Fractography of Weld Specimens W1 – W4

Both light optical and SEM-based fractography were performed on all the weld/temperature conditions investigated herein. All weld conditions optical images are presented in Appendix E. Table 14, Table 15, Table 16, and Table 17 summarize the macroscopic features and mechanisms of fracture in the specimens. In the summary tables, green text indicates that SEM fractography was performed in addition to the light optical fractography. Italics represent statements that are inferred from information gathered during SEM of a representative specimen. All SEM conducted on the specimens was such that the precracked region (Figure 17) is directly above the field of view (to the north of the image) and can be found in Appendix E.

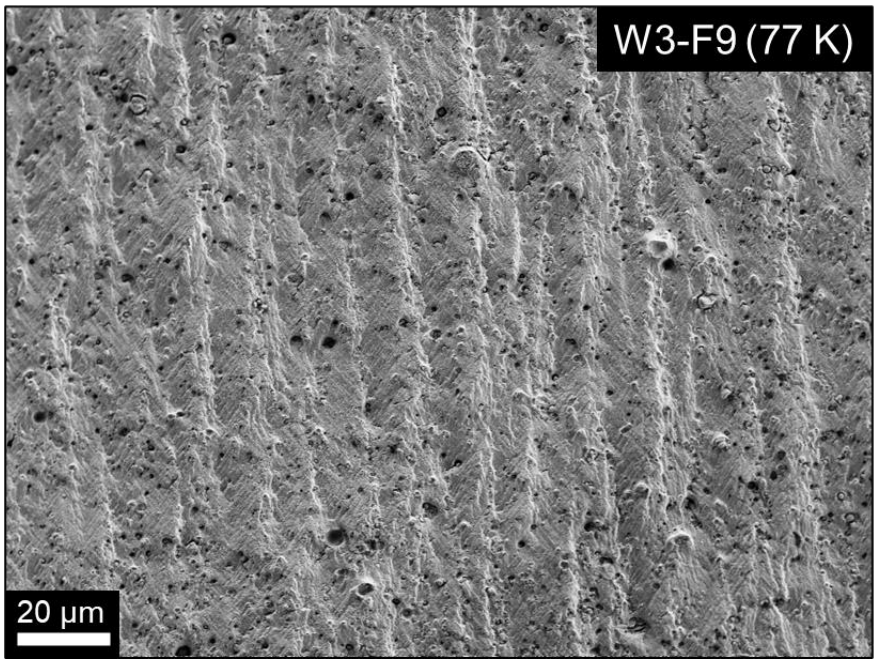

Figure 17 – Representative SE image of the precracked region of a weld specimen.

Table 14 – Summary of the fractography in weld W1 at 4 K and 77 K. Green text indicates that SEM fractography was performed in addition to the light optical fractography. Italics represent statements that are inferred information gathered during SEM of a representative specimen.

Weld	Specimen	T (K)	Macroscopic Features	Mechanism of Fracture
W1	F4	4	Large cracks, lack of fusion porosity, crack jumps	Mixed MVC and brittle fracture (cleavage). Large cleavage present at crack jump. Partially formed microvoids interrupted by cleavage.
	F5	4	Large cracks, small crack jumps	*Mixed MVC and brittle fracture*
	F6	4	Large cracks	*Mixed MVC and brittle fracture*
	F7	4	Large cracks	*Mixed MVC and brittle fracture*
	F8	4	Large cracks	Mixed MVC and brittle fracture (cleavage). Partially formed microvoids interrupted by cleavage.
	F9	77	Wormhole pores, crack jumps	*MVC*
	F10	77	Wormhole pore, crack jumps	*MVC*
	F11	77	Plastic deformation, crack jumps	*MVC*
	F12	77	Large cracks, wormhole pores	*MVC*
	F13	77	Plastic deformation	MVC
	F14	77	Plastic deformation, large cracks, wormhole pore, crack jumps	MVC, wormhole pore surface contains oxides (≈ 2 μm)

Table 15 – Summary of the fractography in weld W2 at 4 K and 77 K.

Weld	Specimen	T (K)	Macroscopic Features	Mechanism of Fracture
W2	F3	4	Plastic deformation	*MVC*
	F4	4	Plastic deformation	MVC, lack of fusion porosity (≈ 200 μm diameter), elongated microvoids ⊥ to crack direction, small signs of brittle fracture, crack jump ≈ 50 μm
	F5	4	Plastic deformation	*MVC*
	F6	4	Plastic deformation	*MVC*
	F7	4	Plastic deformation	*MVC*
	F8	77	Plastic deformation/lack of fusion porosity	*MVC*
	F9	77	Plastic deformation/Lack of fusion porosity, crack jumps	MVC, elongated microvoids ⊥ to crack direction, cracks at MVC, NVC present near MVC, lack of fusion porosity ≈ 150 μm diameter
	F10	77	Plastic deformation, crack jumps	*MVC*
	F11	77	Plastic deformation, crack jumps	*MVC*
	F12	77	Plastic deformation	*MVC*

Table 16 – Summary of the fractography in weld W3 at 4 K and 77 K.

Weld	Specimen	T (K)	Macroscopic Features	Mechanism of Fracture
3	F3	4	Plastic deformation, medium cracks, crack jumps	*Mixed MVC and brittle fracture*
	F4	4	Plastic deformation, medium cracks, crack jumps	Mixed MVC and brittle fracture (cleavage, intragranular, and intergranular). Partially formed microvoids interrupted by cleavage.
	F5	4	Plastic deformation, medium cracks, crack jumps	Mixed MVC and brittle fracture (cleavage). Partially formed microvoids interrupted by cleavage. More cleavage present near precracked region. Crack jumps ≈ 25 μm -- 100 μm
	F6	4	Plastic deformation, medium cracks, crack jumps	*Mixed MVC and brittle fracture*
	F7	4	Plastic deformation, medium cracks, crack jumps	*Mixed MVC and brittle fracture*
	F8	77	Plastic deformation, crack jumps	*MVC*
	F9	77	Plastic deformation, crack jumps	MVC, cracks at MVC
	F10	77	Plastic deformation	*MVC*
	F11	77	Plastic deformation, crack jumps	*MVC*
	F12	77	Plastic deformation	*MVC*
	F13	77	Plastic deformation, crack jumps, very small test region	*MVC*

Table 17 – Summary of the fractography in weld 4 at W4 K and 77 K.

Weld	Specimen	T (K)	Macroscopic Features	Mechanism of Fracture
4	F3	4	Plastic deformation, medium cracks, crack jumps	Mixed MVC and brittle fracture (cleavage)
	F4	4	Large cracks, crack jumps	*Mixed MVC and brittle fracture*
	F5	4	Plastic deformation, large cracks, crack jumps	*Mixed MVC and brittle fracture*
	F6	4	Large cracks	Mixed MVC and brittle fracture (cleavage)
	F7	4	Large cracks	Mixed MVC and brittle fracture (cleavage), possible elongated lack of fusion porosity (≈ 100 μm -- 300 μm)
	F8	4	Large cracks, crack jumps	*Mixed MVC and brittle fracture*
	F9	77	Plastic deformation, crack jumps	*MVC*
	F10	77	Plastic deformation, large cracks	*MVC*
	F11	77	Plastic deformation, large cracks, crack jumps	*MVC*
	F12	77	Plastic deformation, large cracks	MVC
	F13	77	Plastic deformation, crack jumps	*MVC*

6.2. Specimens Tested at 77 K

The macroscopic features in the weld specimens tested at 77 K consisted of large areas of plastic deformation, wormhole pores, crack jumps, and lack of fusion pores (Figure 18). Figure 18a depicts a large wormhole pore present in W1-F14, indicated by a white arrow. The head of the pore is approximately 500 μm across, with the tail measuring approximately 300 μm across. From top to bottom, the wormhole pore is approximately 2 mm in length. Figure 18b depicts W2-F9 with several lack of fusion pores (indicated with white arrows), ranging from approximately 60 μm to 200 μm in diameter. Figure 18c depicts a crack jump in W3-F9, found in several of these specimens. Figure 18d (W4-F12) depicts the general fracture surface morphology.

The wormhole morphology depicted in Figure 18a is shown in greater detail in Figure 19, where a higher magnification (Figure 19a) is presented, detailing some of the inner surface cavity features. Figure 19b and Figure 19c show residual material from the pore formation, with a relative chemical concentration of the hemispherical features shown in Figure 19d. The EDS line scan shows a higher concentration of O and Si relative to the rest of the surrounding material, indicating that these features are likely oxides.

Generally, the fracture mechanism for the 77 K specimens consisted of microvoid coalescence (MVC), which occurred from plastic deformation/stretching during yielding. The MVC occurred mostly around the regions of small inclusions which ranged from approximately 300 nm – 15 μm. The microvoids that formed around the inclusions in the 77 K test specimens are shown in greater detail in Figure 20. A larger FOV depicting several microvoids is shown in Figure 20a, whereas Figure 20b displays the microvoids in greater detail. An EDS line scan (Figure 21) of an inclusion was found to have a higher concentration of Cr and Mn relative to the surrounding material.

Figure 22 displays a higher magnification (Figure 22a) image of a crack jump in W2-F9 with instances of nanovoid formation near the MVC (Figure 22b and Figure 22c). The nanovoids tended to form around very small inclusions (≈ 30 nm – 50 nm), however it is not clear if these nanovoids formed due to the presence of these inclusions leading to weak points in the matrix like the MVC, or if they are present throughout the material at higher magnifications.

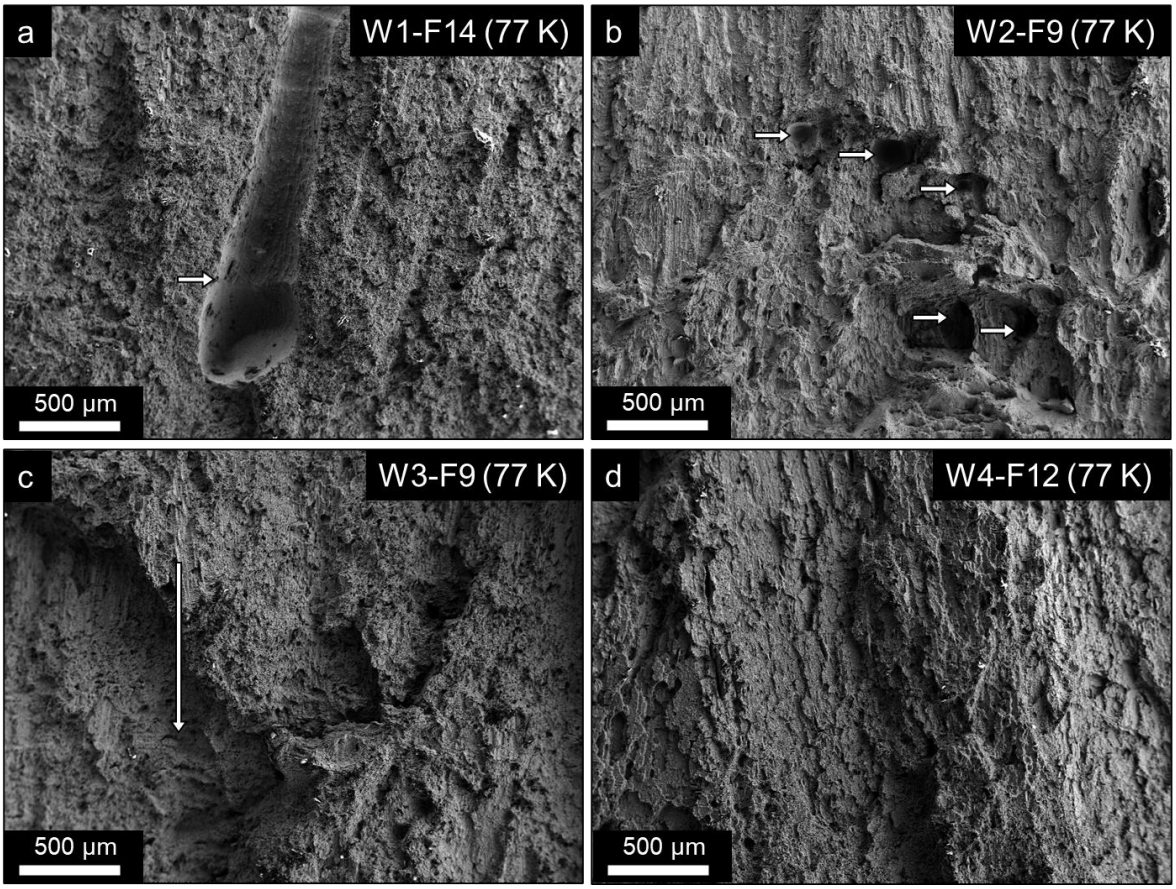

Figure 18 – Representative SE images of the fractographic features. a) wormhole pore, b) lack of fusion porosity, c) crack jumps, d) general fracture surface.

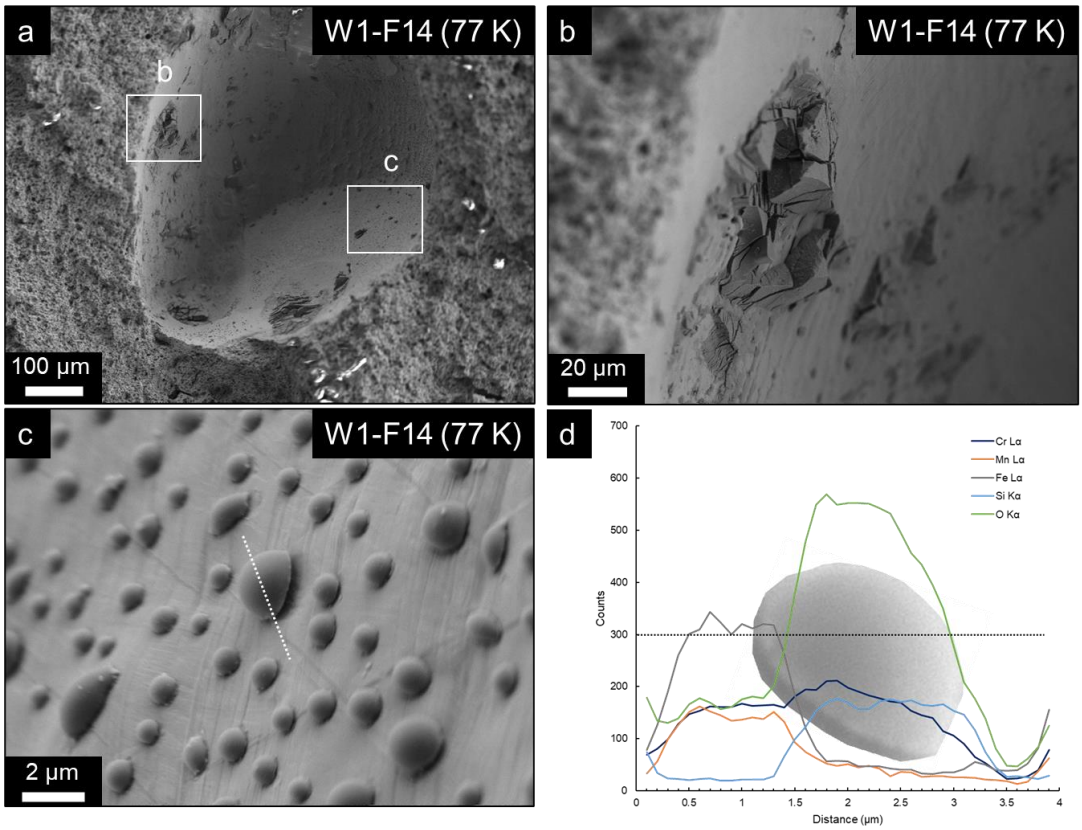

Figure 19 – a) Wormhole morphology at higher magnification, b) signs of residual material from the pre-formation, c) hemispherical inclusions on the surface of the pore cavity with dashed line indicating region of EDS line scan, d) EDS line scan of the hemispherical inclusion.

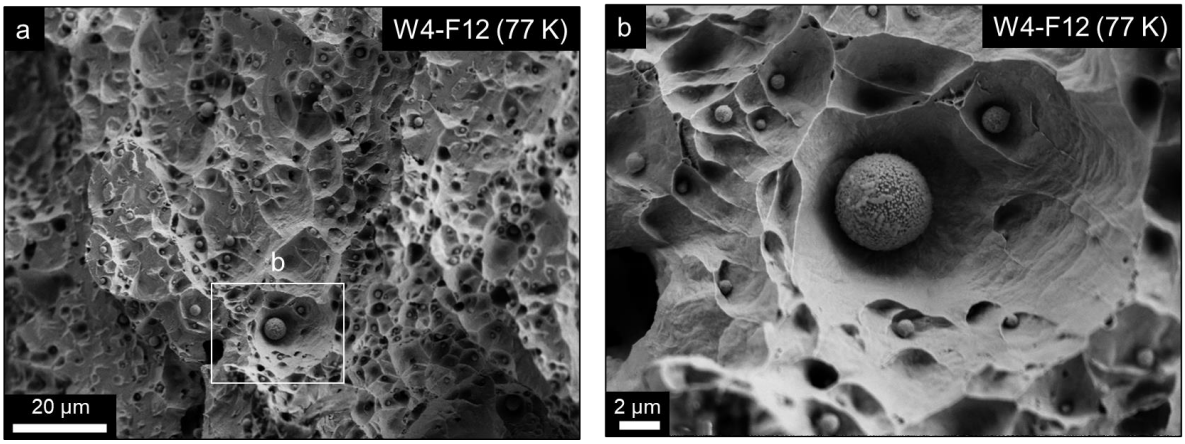

Figure 20 – a) MVC morphology in W4-F12, b) typical inclusion within a microvoid.

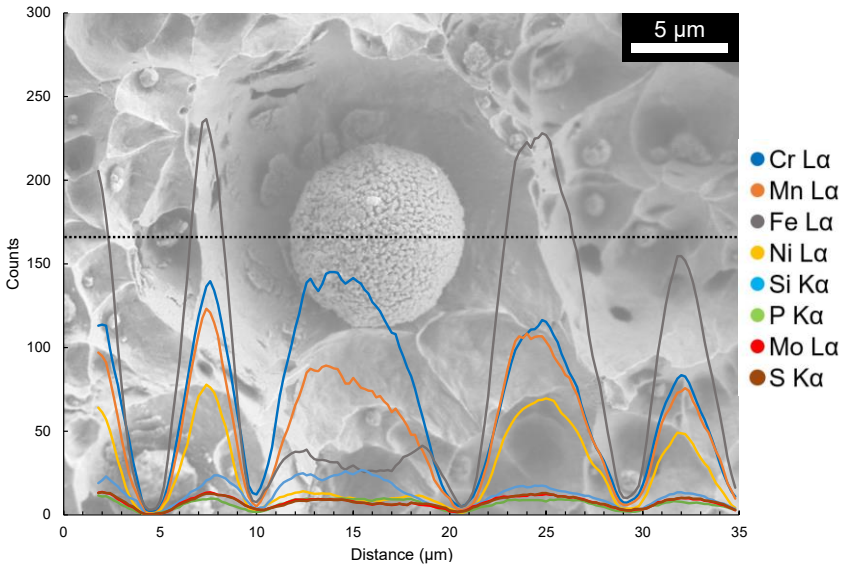

Figure 21 – EDS line scan of an inclusion typically found in a microvoid (W1-F13).

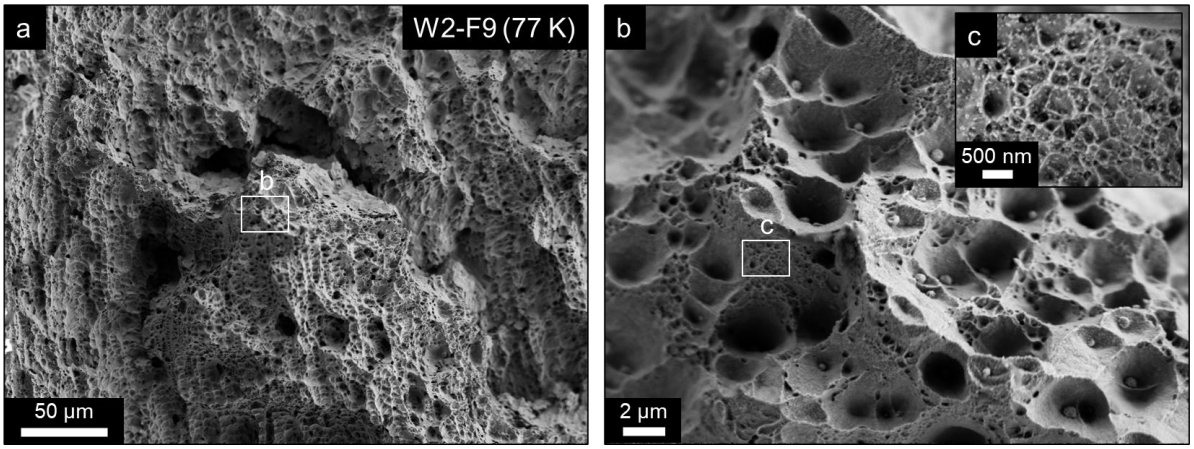

Figure 22 – MVC at a crack jump with nanovoids surrounding the MVC (W2-F9).

6.3. Specimens Tested at 4 K

Unlike the specimens tested at 77 K, those that were tested at 4 K showed less overall plastic deformation. There were macroscopic large cracks present in Welds W1, W3, and W4, whereas Weld W2 showed similar plastic deformation features to specimens tested at 77 K (Appendix E). Similar features such as crack jumps were present in these specimens (Figure 23a), however there were indications of large cleavage fracture (Figure 23b) as indicated by a white arrow. Specimens tested at 4 K displayed both MVC and brittle fracture mechanisms, shown in Figure 24a and in higher magnification in Figure 24b. The inclusions found inside the microvoids of the 77 K tested specimens are now exposed in the 4 K tested specimens without the plastic deformation of the microvoid envelope (Figure 24b). In the areas of strictly brittle fracture/cleavage, there are clear indications of cleavage facets (highlighted by a white arrow) in Figure 24b.

There were many instances of partially formed microvoids that were interrupted by cleavage fracture, shown in Figure 25. There is a large microvoid that began to form in Figure 25 (pictured in the center), which shows signs of cleavage facets that are flat relative to the microvoid formation. This was likely due to regions of the matrix behaving in a ductile fashion until the behavior shifted towards brittle fracture, to which then the microvoid broke apart leaving these partially formed microvoids behind.

Along with the cleavage fracture features, there were small instances of intergranular and intragranular fractures among crack paths, shown in Figure 26. Figure 26a shows the crack paths with signs of cleavage. Figure 26b displays these features at higher magnification, whereas Figure 26c and Figure 26d display signs of intergranular and intragranular fractures indicated with arrows.

Figure 27 displays the fracture surface near the precracked region. Figure 27a shows the crack paths that appear to follow the same path as the fatigue precracks (indicated by a white arrow pointing downward). Figure 27b displays this crack path in higher magnification, among instances of MVC. Figure 27c displays cleavage facets and exposed inclusions. Figure 27d displays clear indications of cleavage fracture, with small voids that could be due to inclusion lift-out from the fracture, as no indications of plastic deformation/coalescence had occurred near the voids.

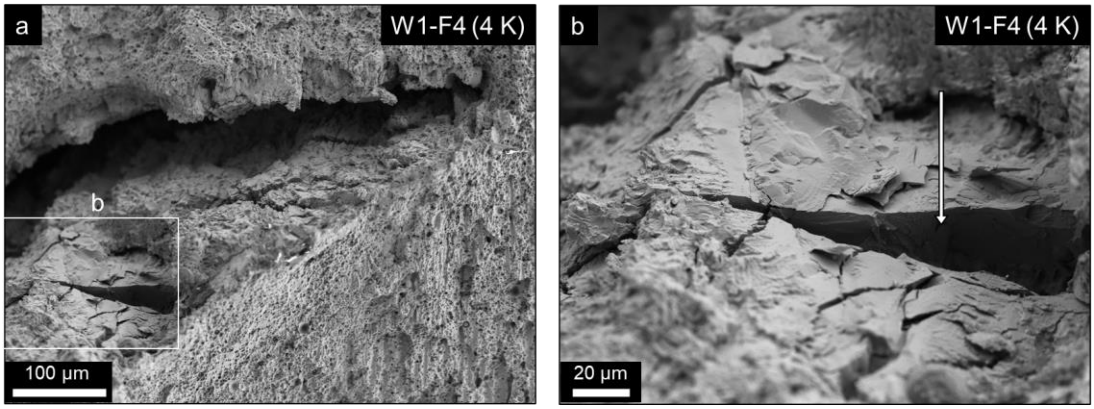

Figure 23 – a) Crack jump displaying a large cleavage-based fracture morphology, b) enhanced view of the cleavage feature.

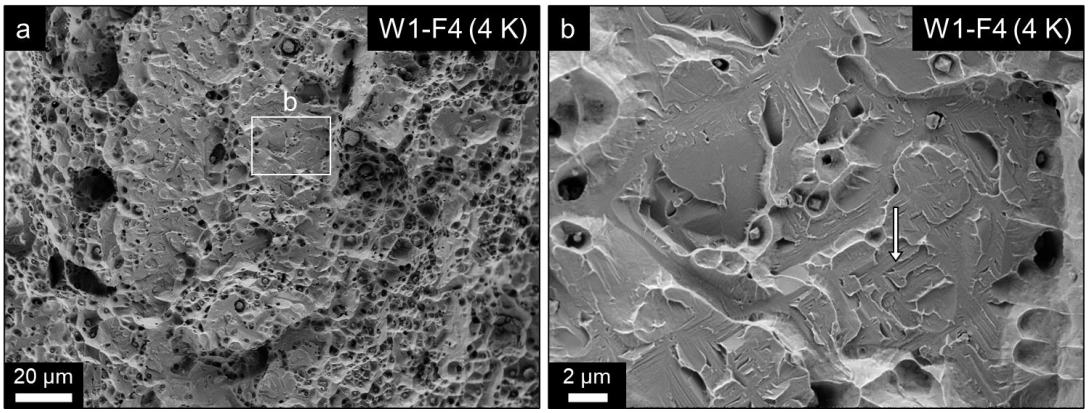

Figure 24 – a) Mixed-mode fracture displaying both MVC and cleavage, b) higher magnification of the cleavage facets.

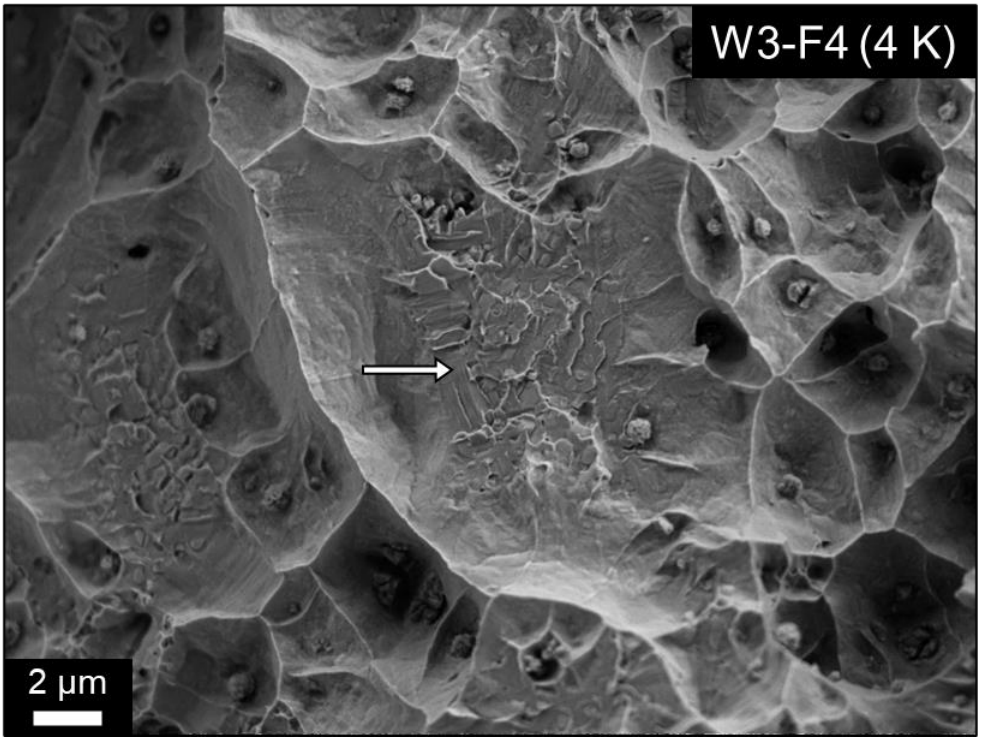

Figure 25 – Partially formed microvoid interrupted by cleavage fracture.

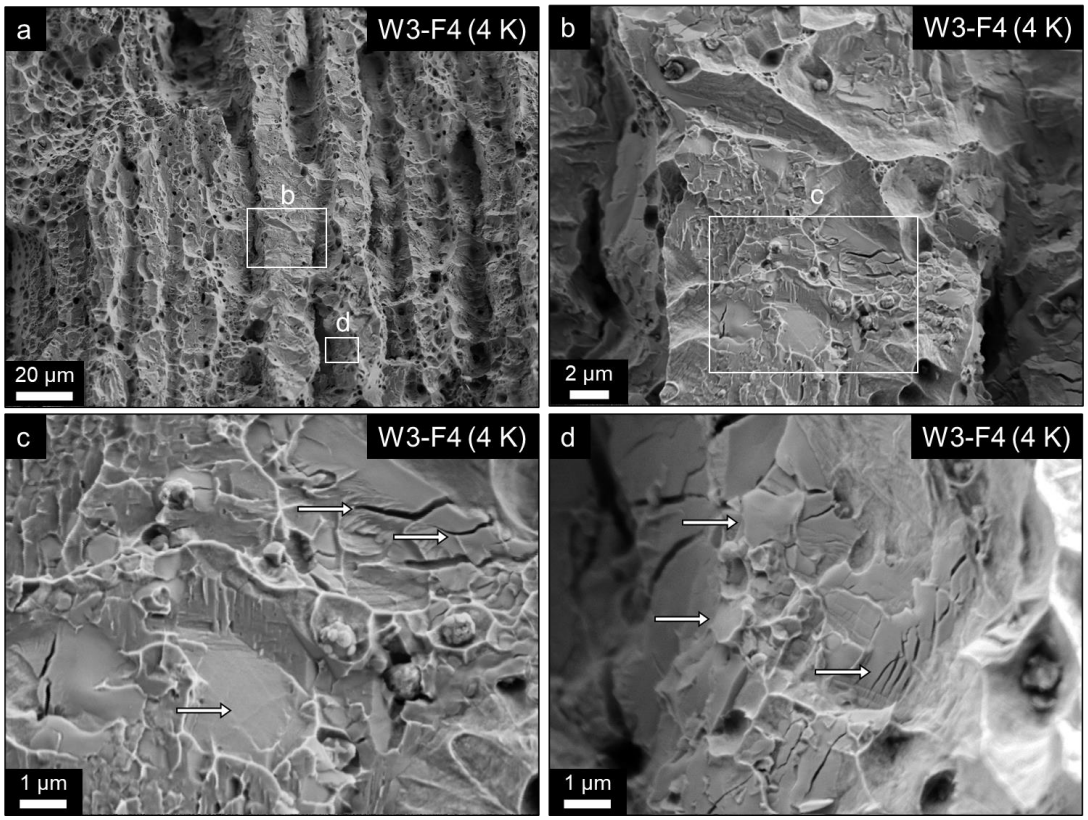

Figure 26 – a) Cleavage fractures along crack paths, b) higher magnification of the crack path, c-d) higher magnifications displaying intergranular fracture.

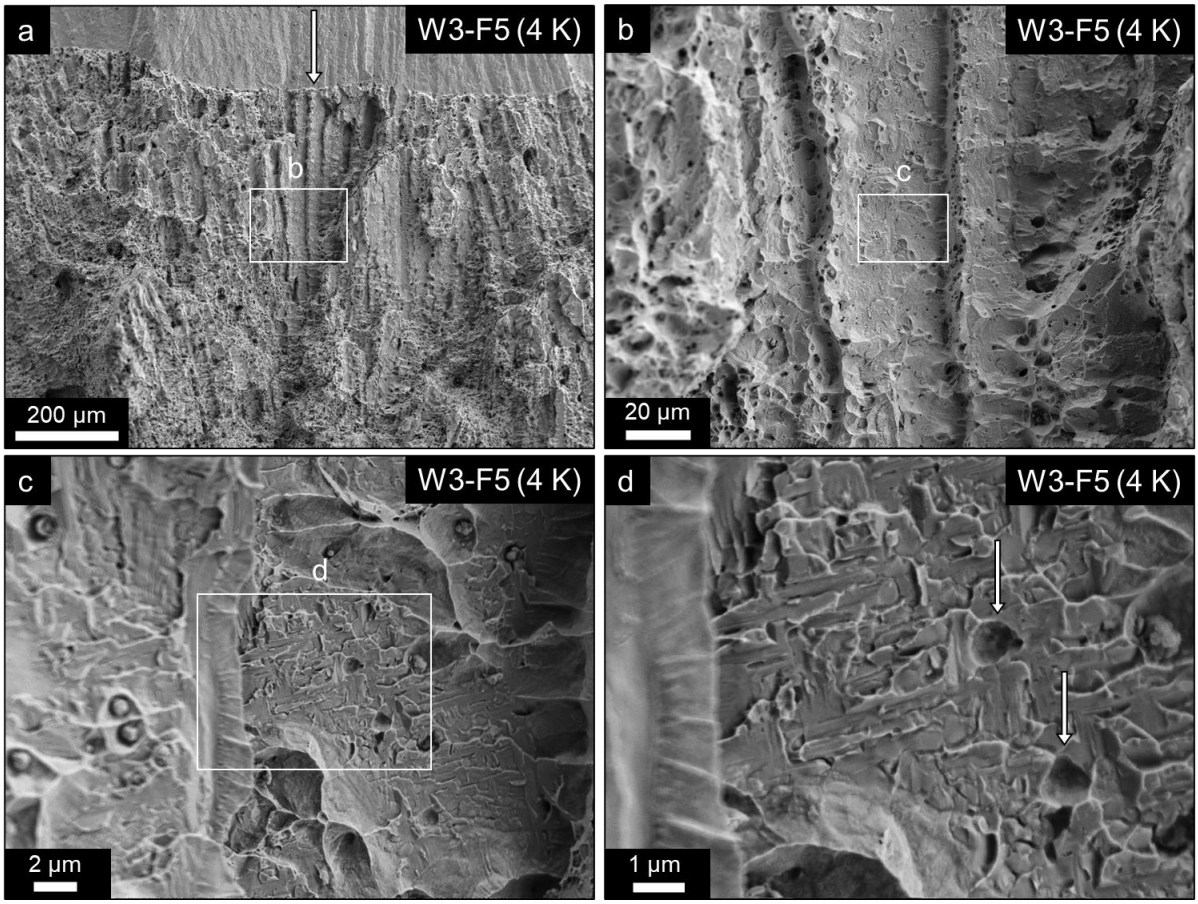

Figure 27 – a) Crack paths that appear to follow the directions of the precracking, b) higher magnification of the crack path, c) cleavage facets among small instances of MVC, d) higher magnification of the cleavage facets and inclusion lift-outs.

7. Discussion

The results of the 43 fracture toughness tests are summarized in Table 18. Average values and standard deviations are based on all types of critical *J*-integral values calculated for each test (J_{Qc}, J_Q, or J_{Ic}).

Table 18 – Summary of critical toughness values measured at 77 K and 4 K on the four 316L welds.

Specimen	T (K)	J_{Qc} (kJ/m^2)	J_Q (kJ/m^2)	J_{Ic} (kJ/m^2)	Comment	Specimen	T (K)	J_{Qc} (kJ/m^2)	J_Q (kJ/m^2)	J_{Ic} (kJ/m^2)	Comment
W1-F9			63.81		Tearing instability after initiation	W1-F4			16.98		Tearing instability after initiation
W1-F10		109.31			Tearing instability before initiation	W1-F5			34.12		Tearing instability after initiation
W1-F11			267.44		Tearing instability after initiation	W1-F6			16.80		Tearing instability after initiation
W1-F12	77		89.28		Tearing instability after initiation	W1-F7	4		17.06		Tearing instability after initiation
W1-F13			100.52		Tearing instability after initiation	W1-F8			17.56		Tearing instability after initiation
W1-F14			46.00		Tearing instability after initiation	**Average**			**20.51**		
Average			**112.73**			**SD**			**7.62**		
SD			**79.36**								
W2-F8				228.13		W2-F3			111.72		Tearing instability after initiation
W2-F9				243.67		W2-F4			148.99		
W2-F10			162.15			W2-F5			131.19		Tearing instability after initiation
W2-F11	77			224.73		W2-F6	4		164.59		Tearing instability after initiation
W2-F12				238.23		W2-F7			173.37		Tearing instability after initiation
Average			**219.38**			**Average**			**145.97**		
SD			**32.89**			**SD**			**24.99**		
W3-F8				213.77	Tearing instability after initiation	W3-F3			85.51		Tearing instability after initiation
W3-F9				189.07	Tearing instability after initiation	W3-F4			98.14		
W3-F10			123.22			W3-F5			101.38		Tearing instability after initiation
W3-F11	77			168.93	Tearing instability after initiation	W3-F6	4		96.08		Tearing instability after initiation
W3-F12				232.10	Tearing instability after initiation	W3-F7			104.36		Tearing instability after initiation
W3-F13			186.84		Tearing instability after initiation	**Average**			**97.10**		
Average			**185.66**			**SD**			**7.20**		
SD			**37.79**								
W4-F9			198.73		Tearing instability after initiation	W4-F3		164.31			Tearing instability before initiation
W4-F10		121.56			Tearing instability before initiation	W4-F4			42.01		Tearing instability after initiation
W4-F11		116.60			Tearing instability before initiation	W4-F5			70.32		Tearing instability after initiation
W4-F12	77	71.53			Tearing instability before initiation	W4-F6	4	103.96			Tearing instability before initiation
W4-F13		106.99			Tearing instability before initiation	W4-F7			26.99		
Average			**123.08**			W4-F8		52.34			Tearing instability before initiation
SD			**46.59**			**Average**			**76.66**		
						SD			**50.45**		

Average values, standard deviations, and coefficients of variation (ratio between standard deviation and average value) are presented in Table 19.

Table 19 – Average values, standard deviations, and coefficients of variation for the fracture toughness tests performed on the four 316L welds.

Weld	T (K)	Average (kJ/m^2)	SD (kJ/m^2)	CV	T (K)	Average (kJ/m^2)	SD (kJ/m^2)	CV
W1	77	112.73	79.36	70%	4	20.51	7.62	37%
W2		219.38	32.89	15%		145.97	24.99	17%
W3		185.66	37.79	20%		97.10	7.20	7%
W4		123.08	46.59	38%		76.66	50.45	66%

7.1. Comparisons Between Welds

Based on the results of the tests performed (Table 18 and Table 19), a clear ranking of the four welds resulted in terms of critical toughness, irrespective of test temperature: from the toughest to the least tough, W2 / W3 / W4 / W1. W2 and W3 also exhibited the smallest scatter at both test temperatures. The same information is also illustrated in Figure 28.

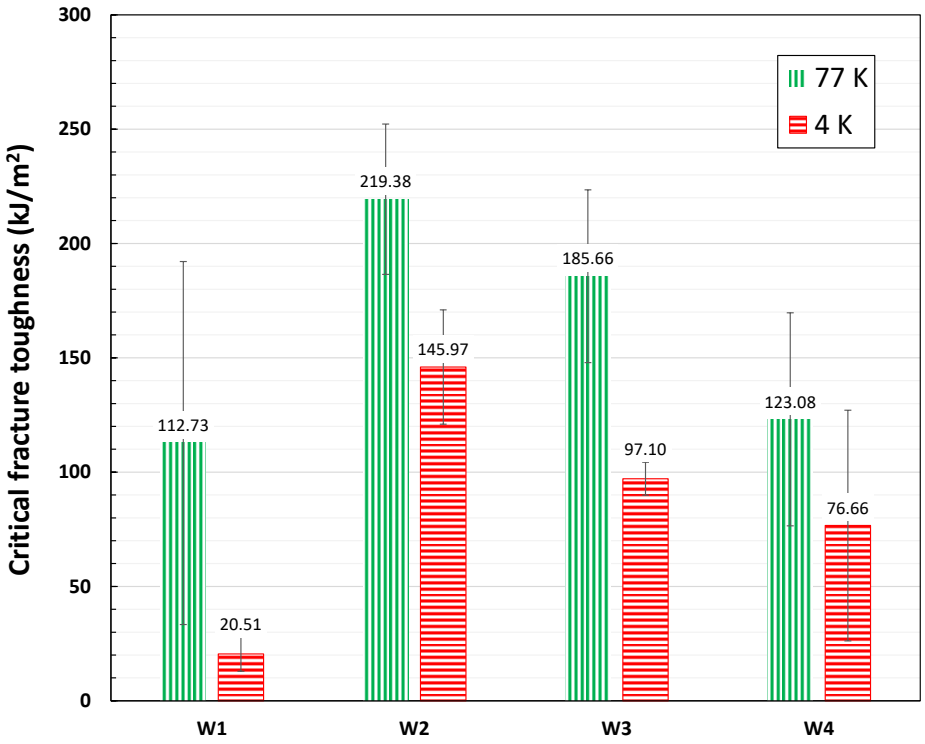

Figure 28 – Average critical fracture toughness values at 77 K and 4 K for the four 316L welds. Error bars correspond to ±1SD.

As far as crack resistance (tearing modulus) is concerned, average values of *TM*, standard deviations, and coefficients of variation are collected in Table 20 and illustrated in Figure 29. These results confirm the ranking observed in terms of critical *J*-integral, although the weld-to-weld differences appear somewhat smaller.

Table 20 – Average values, standard deviations, and coefficients of variation of tearing modulus (*TM*) for the fracture toughness tests performed on the four 316L welds.

Weld	T (K)	*TM* (MPa)	SD (MPa)	CV	T (K)	*TM* (MPa)	SD (MPa)	CV
W1	77	35.31	21.16	60%	4	8.41	5.90	70%
W2		56.65	9.14	16%		32.30	4.84	15%
W3		46.94	16.24	35%		33.08	3.78	11%
W4		20.16	N/A	N/A		6.77	1.03	15%

Another comparison between the investigated welds is provided in Figure 30 and Figure 31, where mean *J-R* curves are presented at 77 K and 4 K respectively. These mean *J-R* curves were obtained by averaging *J* values from all available regression curves at specific crack extension values. The relevant error bars correspond to the standard deviations of those same *J* values.

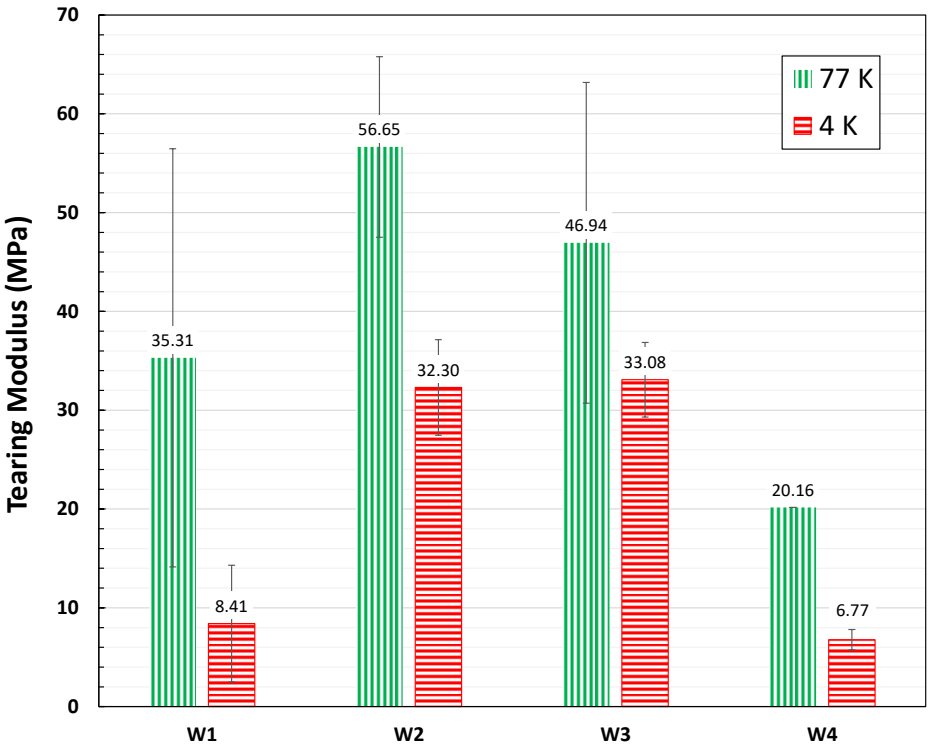

Figure 29 – Average tearing modulus values at 77 K and 4 K for the four 316L welds. Error bars correspond to ±1SD.

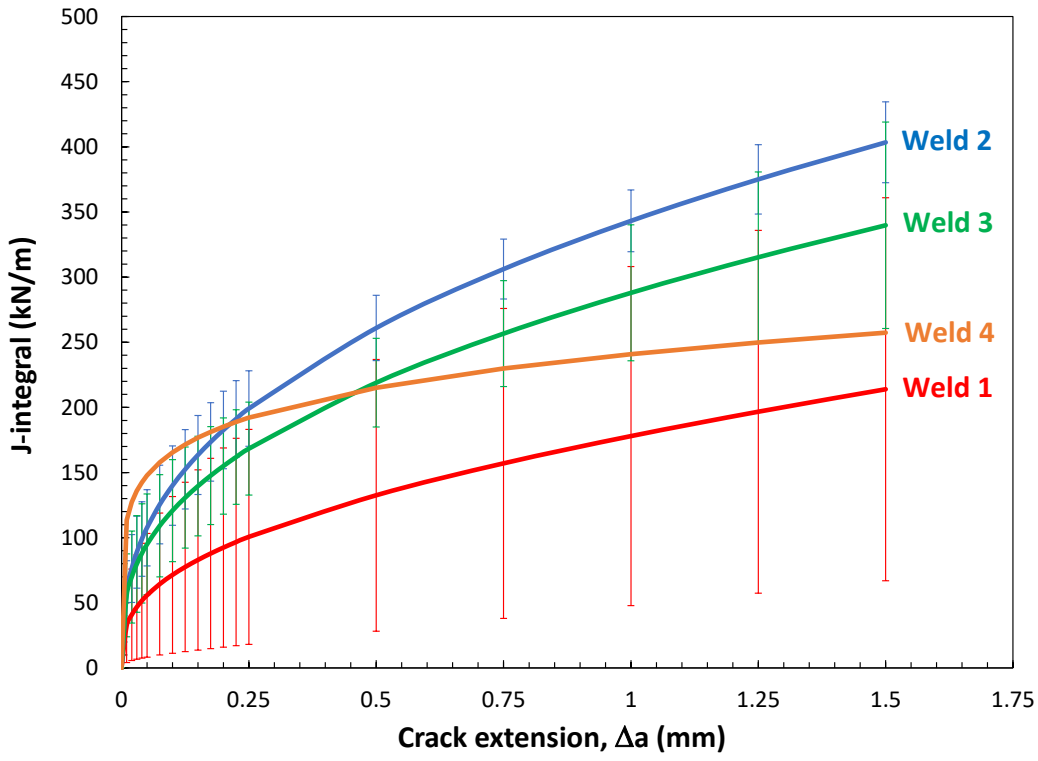

Figure 30 – Mean *J-R* curves for the four 316L welds tested at 77 K. NOTE: there are no error bars for W4, as only one *J-R* curve was obtained.

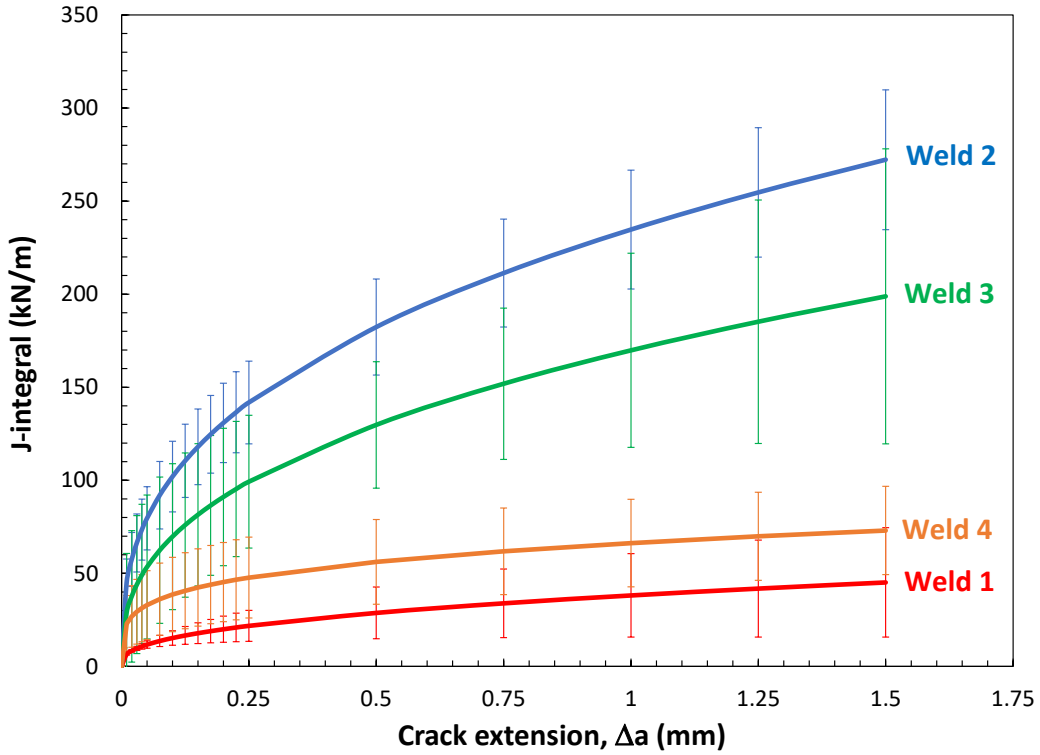

Figure 31 – Mean *J-R* curves for the four 316L welds tested at 4 K.

The four welds also widely differed in terms of the occurrence of significant tearing instabilities. The toughest weld (W2) showed no tearing instabilities at 77 K, while at 4 K 4 out 5 specimens exhibited ductile instabilities, all after crack initiation. Conversely, for the two least tough welds (W1 and W4), all tested specimens exhibited tearing instabilities, except for one W4 specimen tested at 4 K. However, most W1 tests experienced instabilities after crack initiation, while for W4 instabilities occurred before crack initiation for 7 specimens out of 11. This confirms that W4 has the worst fracture toughness of all characterized welds. As for W3, ductile instabilities were observed on 9 tests out of 11, but in every case this occurred after crack initiation.

Differences in toughness between investigated welds depend mostly on welding procedures, inhomogeneities, and ferrite content. As mentioned in section 2, all welding vendors used GTAW to perform the first few root passes, but only W2 used GTAW to complete the rest of the weld passes (W1, W3, and W4 used FCAW for all other passes after the root). In terms of total welding passes used in the final layer (weld cap), W2 contained four passes, W3 contained three passes, W4 contained two passes, and W1 contained a single pass. Typically, residual stresses can be reduced in a weld by increasing the number of passes, reducing the local heat input, and lowering the temperature differential [24]. Of note from fractography, W1 was the only weld that showed signs of wormhole porosity, which is likely due to contamination of the flux core (moisture absorption is a common cause). Also, interstitial content and phase fraction have known effects on the fracture behavior of welds between stainless steels [25], where increases in C and N stabilize the austenite phase and improve crack resistance. In this study, W3 and W2 contained the least amount of ferrite in the weld, whereas W4 and W1 contained the most ferrite in the weld. As W2 exhibited the

highest toughness, there is a clear benefit to using the slower GTAW welding process for both root and subsequent cover passes, finishing the final layer with multiple passes, and minimizing ferrite content. As far as the least tough weld (W1) is concerned, high ferrite content, minimal passes in the final weld layer (weld cap), and excess porosity are the main contributing factors to the significantly lower toughness. Differences between the welds with intermediate toughness (W3 was found to be tougher than W4) can also be attributed to the number of passes in the weld cap and ferrite content, since W3 contained more passes in the weld cap and a lower ferrite content.

While there are many factors that may convolute the comparison of the four 316L welds investigated in this work, such as porosity or welding parameters, a meaningful comparative assessment could be made between welds W3 and W4, neither of which contained a large amount of porosity, and which were manufactured with similar welding parameters (GTAW, then FCAW). In this comparison, the 4 K toughness of W3 was nearly 25 % higher than the 4 K toughness of W4. Also, the ferrite content of W4 was nearly four times that measured in W3. A previous study [26] demonstrates that an increase in ferrite content decreases the toughness of stainless steel welds. This is especially true at cryogenic temperatures, since the body-centered-cubic (BCC) lattice of ferrite becomes brittle as thermal energy is required to activate all possible slip systems. Another factor could be the processing strategy (GTAW, then FCAW or GTAW used in both root and cover passes), where W2 exhibited the greatest toughness at 77 K and 4 K and was the only weld produced by only GTAW processes. The older welds were finished with FCAW processes and were generally less tough at the same temperature, which is consistent with a previous study [27] on the toughness at 4 K of austenitic stainless steel weldments.

In future work, grain size and residual stress will be measured to provide more clarity on differences in the occurrence of tearing instabilities.

7.2. Effect of Test Temperature

As could be expected, decreasing the test temperature from 77 K to 4 K caused a reduction of fracture toughness (critical *J*-integral and tearing modulus) for all investigated welds, as can be seen in Figure 28 and Figure 29. Reductions ranged between 33 % and 82 % for critical *J*, and between 30 % and 55 % for tearing modulus (Table 21). The smallest variations were recorded for W2 (33 % and 30 % respectively).

Table 21 – Fracture toughness variations from 77 K to 4 K for the investigated welds.

Weld	Critical toughness (kJ/m^2)			Tearing modulus (MPa)		
	77 K	4K	Δ (%)	77 K	4K	Δ (%)
W1	112.73	20.51	82%	35.31	8.41	76%
W2	219.38	145.97	33%	56.65	32.30	43%
W3	185.66	97.10	48%	46.94	33.08	30%
W4	123.08	76.66	38%	20.16	6.77	66%

The effect of test temperature can also be appreciated in Figures 32-35, where mean *J-R* curves at 77 K and 4 K with error bars are compared for the four investigated welds.

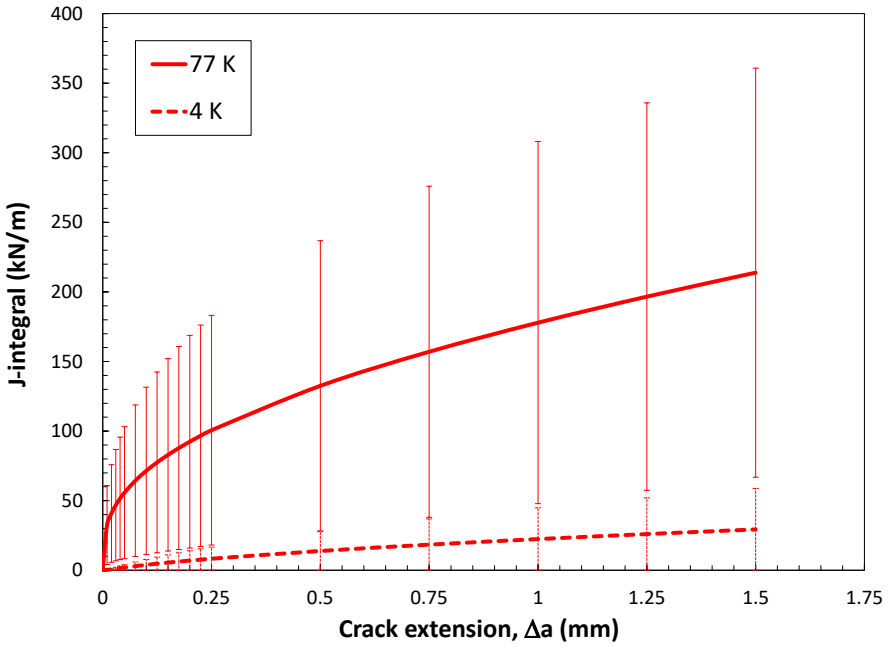

Figure 32 – Mean *J-R* curves at 77 K and 4 K for weld W1.

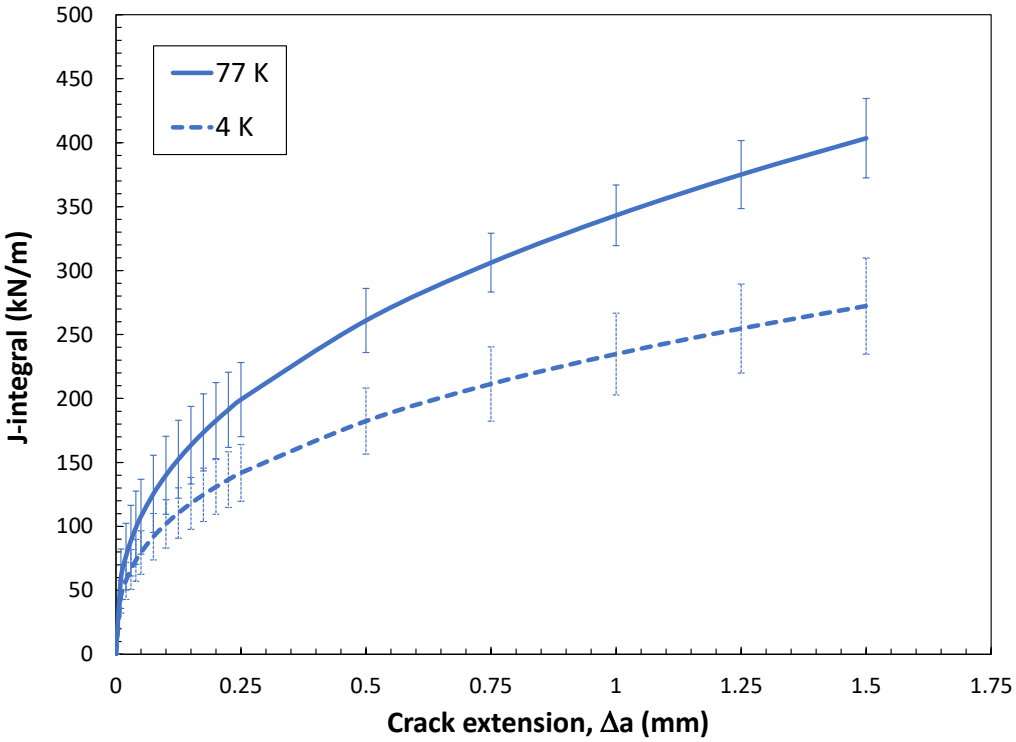

Figure 33 – Mean *J-R* curves at 77 K and 4 K for weld W2.

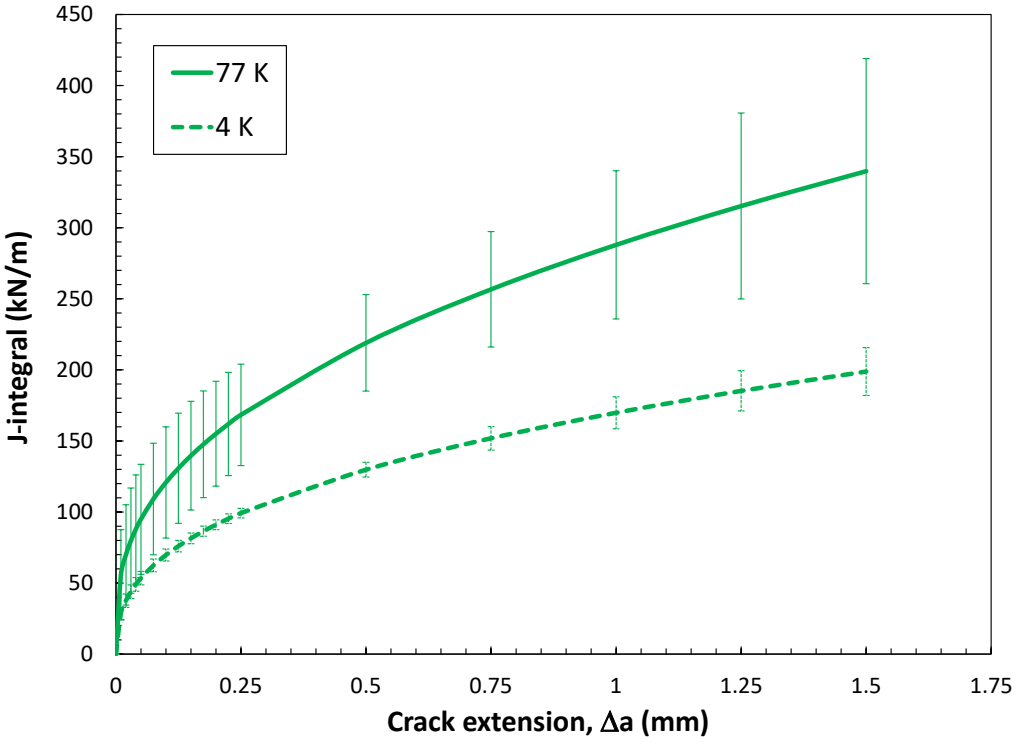

Figure 34 – Mean *J-R* curves at 77 K and 4 K for weld W3.

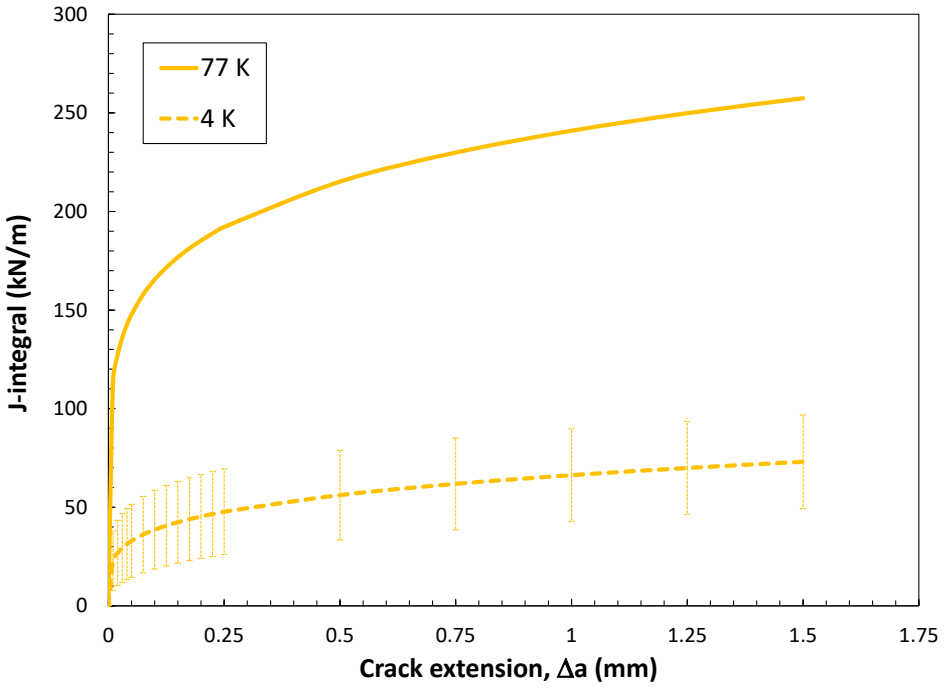

Figure 35 – Mean *J-R* curves at 77 K and 4 K for weld W4. NOTE: only one *J-R* curve is available at 77 K.

A strong linear correlation (Figure 36) was found between average critical toughness values measured at 77 K and 4 K, as indicated by the high value of the Pearson correlation coefficient (r = 0.918).

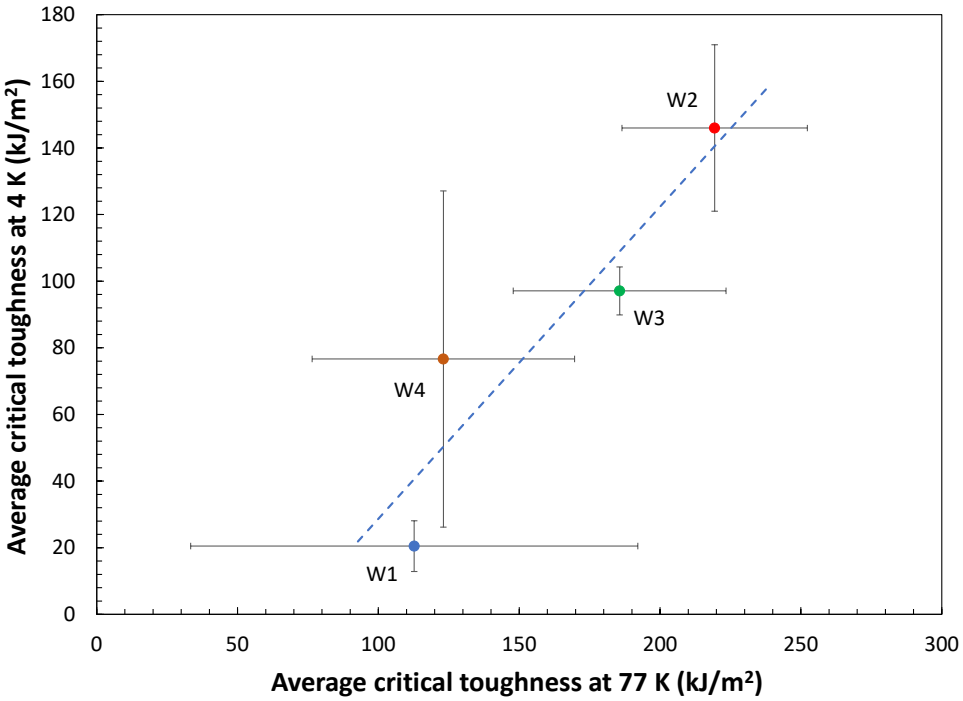

Figure 36 – Relationship between average critical toughness measured on the four welds at 77 K and 4 K. NOTE: error bars correspond to ± 1SD.

On the fracture surface of almost every specimen tested at 77 K, ductile behavior was observed at the microscale (microvoid coalescence). The main distinguishing difference between ductile and brittle fracture behavior is the occurrence of flat cleaved features at the microscale [28].

While all welds experienced a reduction in toughness from 77 K to 4 K, W2 still remained the toughest with the lowest scatter, whereas W4 and W1 showed large scatter and remained the two least tough welds. Toughness reductions from 77 K to 4 K correlated well with fractographical observations. Namely: W2 contained the least amount of cleavage on fracture surfaces, whereas W4 and W1 contained the highest number of occurrences of cleavage at the microscale. Fractography also revealed worm hole porosity on the fracture surfaces of W1, which causes further instability during quasi-static crack growth.

An additional difference between the two test temperatures is the occurrence of serrations at 4 K, which were not observed at 77 K. This is consistent with previous studies on AISI 316 [29] and is considered to be a result of changes in dislocation character, sometimes referred to as low temperature plastic instabilities [30].

7.3. Considerations about J_c and J_{Ic} Validity

We already mentioned in Section 4 that the provisional critical toughness values, J_{Qc} and J_Q, must fulfil several validity requirements in order to be qualified as J_c and J_{Ic}, respectively.

When fracture instability occurs before stable tearing, the requirements are meant to ensure that J_{Qc} is insensitive to the in-plane dimensions of the specimen (*i.e.*, the uncracked ligament size), although it may still be dependent on specimen thickness (length of crack front).

Eight of the 43 fracture toughness tests performed terminated with instability before stable crack initiation (7 on weld W4, 1 on weld W1). None of these J_{Qc} values fulfilled both qualification requirements of ASTM E1820-21, Appendix A6:

(a) Specimen thickness $B > 100\frac{J_{Qc}}{\sigma_Y}$.

(b) Initial ligament $b_o > 100\frac{J_{Qc}}{\sigma_Y}$,

where σ_Y is the material's flow stress at test temperature (average of yield and tensile strengths).

The remaining 35 tests yielded a provisional measure of *J*-integral at the initiation of stable crack extension, J_Q. This provisional value must meet the following 10 requirements to be qualified as size-independent plane-strain fracture toughness, J_{Ic}:

(a) Absolute difference between measured (Δa_{meas}) and predicted (Δa_{pred}) crack extension smaller than 15 % of Δa_{meas} for $\Delta a_{meas} < 0.2 b_o$ or smaller than 3 % of b_o thereafter, with b_o = initial ligament size.
(b) Exponent of the power law regression curve, $C_2 < 1.0$.
(c) Absolute difference between measured (a_o) and calculated (a_{oq}) initial crack size smaller than the larger of 1 % of *W* or 0.5 mm.
(d) Number of data points available to calculate $a_{oq} \geq 8$.
(e) Number of data points between 0.4 J_Q and $J_Q \geq 3$.
(f) Correlation coefficient of the fit used to calculate $a_{oq} \geq 0.96$.
(g) Acceptable data point distribution in the region of qualified data, delimited by the 0.15 mm and 1.5 mm exclusion lines and capped by $J_{limit} = \frac{b_o \sigma_Y}{7.5}$ (at least one point between the 0.15 mm and 0.5 mm exclusion lines, and at least one point between the 0.5 mm and 1.5 mm exclusion lines).
(h) At least 5 data points inside the region of qualified data.
(i) Specimen thickness $B > 10\frac{J_Q}{\sigma_Y}$.
(j) Initial ligament $b_o > 10\frac{J_Q}{\sigma_Y}$.

Among the 27 tests that provided acceptable *J-R* curves, but for which J_Q could not be qualified, the most often violated requirements were:

- requirement (a): 15 tests;
- requirement (d): 12 tests;
- requirement (h): 7 tests.

The remaining violated requirements were: (e) – 4 tests, (f) – 4 tests, and (g) – 3 tests.

Excessive discrepancies between measured and predicted crack extensions, requirement (a), were mostly observed at 4 K (13 tests), and are believed to be caused by the following:

- uncertainties in the elastic moduli used for calculating crack size from compliance;

- additional crack propagation occurring between the last unload/reload cycle, which provides the final predicted crack size, and the effective test termination. This should be particularly relevant at 4 K, where crack resistance is much lower than at 77 K and serrations might also be affecting compliance measurements. Indeed, in all cases, the predicted crack extension was lower than the measured value.

According to E1820-21, the predicted initial crack size a_{oq} is obtained by fitting all [J, a] data points before maximum force. Particularly in case of low resistance to crack propagation, maximum force in a test could be reached before a sufficient number of data points (at least 8) is determined. This type of requirement violation was observed almost equally at both temperatures (7 times at 77 K and 5 times at 4 K).

Finally, whenever tearing instabilities occurred after crack initiation but before a significant amount of crack extension, a significant risk of having less than the minimum number of data points inside the region of qualified data (5) was encountered. This happened more often at 4 K (5 tests) than at 77 K (2 tests).

7.4. Correlations with Charpy Impact Properties

In an earlier part of this project, Charpy impact toughness was measured at 77 K on the four welds [18]. Based on the values of absorbed energy obtained, the toughest weld was W4 ($\overline{KV}$ = 92.3 J) and the least tough was W1 ($\overline{KV}$ = 43.0 J). Overall, the ranking that emerged from the Charpy tests was W4 / W2 / W3 / W1, from the toughest to the least tough. This was reasonably consistent with the outcome of the fracture toughness tests, with the exception of weld W4, which resulted the toughest in Charpy testing but the second least tough in toughness testing, both at 77 K (Figure 37) and 4 K (Figure 38).

The energy absorbed at 77 K in the Charpy tests was found to be strongly linearly correlated to the critical fracture toughness of welds W1, W2, and W3 both at 77 K (r = 0.960) and 4 K (r = 0.981). However, if data for weld W4 are included, the correlation coefficients dramatically drop to 0.295 and 0.650, respectively.

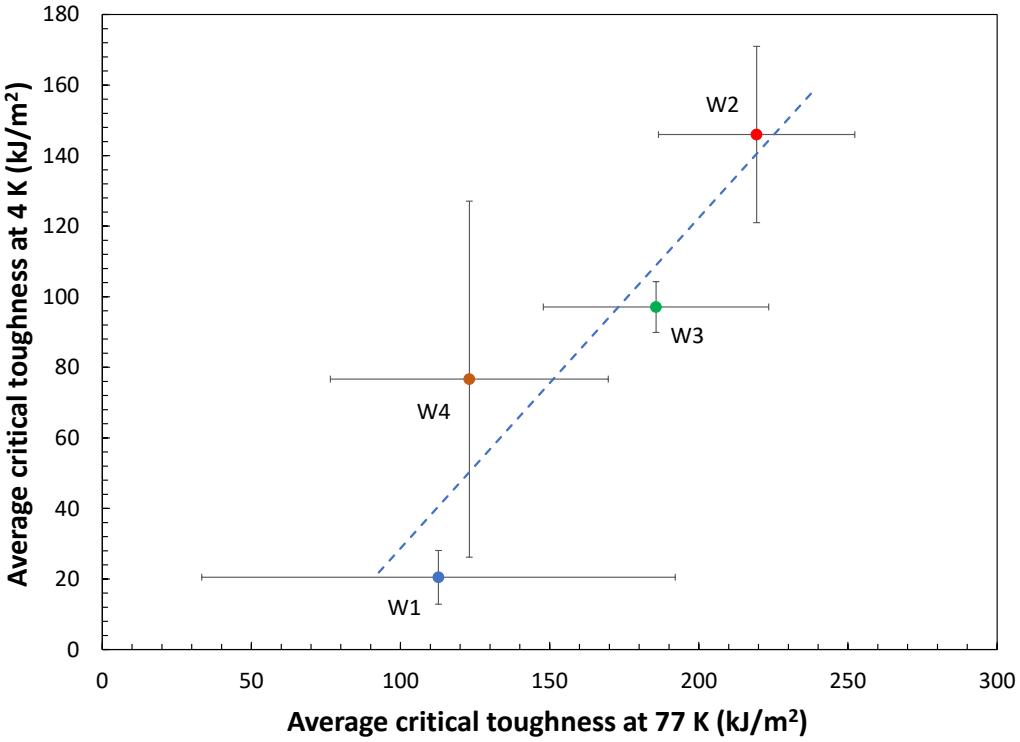

Figure 37 - Correlation between critical toughness and Charpy absorbed energy at 77 K (average values and ±1 SD error bars).

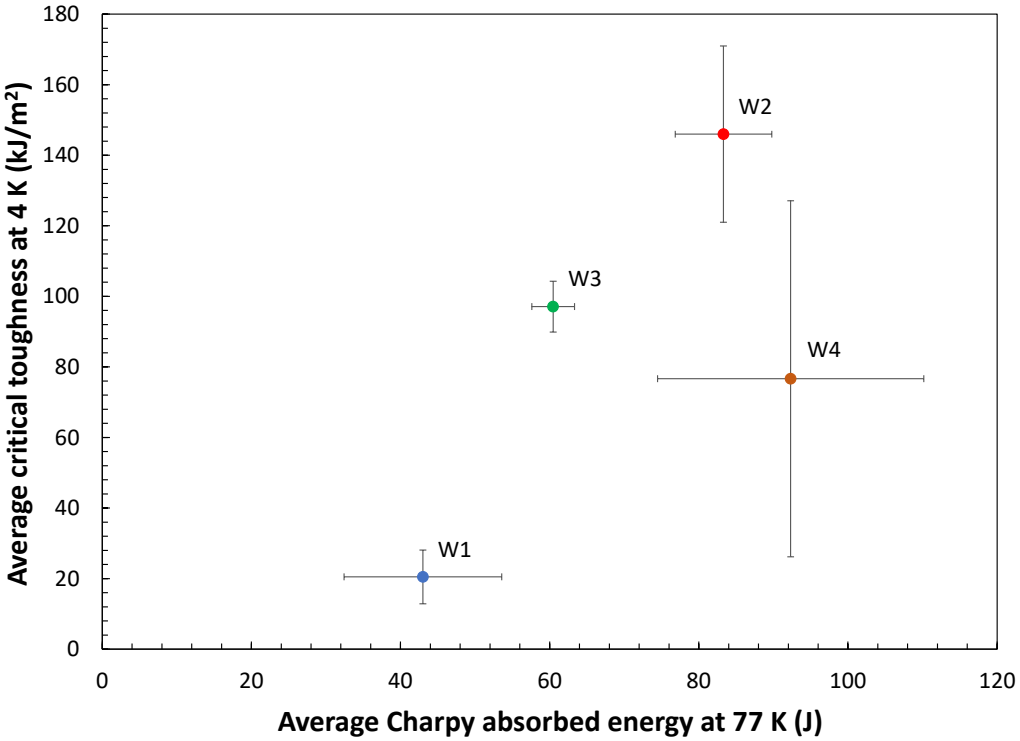

Figure 38 - Correlation between critical toughness at 4 K and Charpy absorbed energy at 77 K (average values and ±1 SD error bars).

7.5. Apparent Negative Crack Growth

Sometimes, when examining the early portion of an elastic compliance fracture toughness test, an unexpected and non-physical phenomenon is apparent, whereby crack size (compliance) decreases with increasing applied *J*-integral. This behavior has been labeled "apparent negative crack growth", and has been extensively studied in the literature ([29],[31]-[36]).

Various causes have been invoked to explain this non-physical behavior, including excessive friction in the test setup, due to round-bottomed clevis holes [31], misalignment in the loading train [32], physical blunting behavior effects [32], compressive residual stresses in the plastic zone surrounding the crack tip during the unloading process [34], and stiffness increase (*i.e.*, compliance decrease) due to strain hardening of the same plastic zone [35]. According to some authors [36], compliance is actually "expected" to decrease for a blunting crack, and therefore the compliance minimum should coincide with the initiation of ductile crack growth.

Different approaches have been proposed to tackle the problem of apparent negative crack growth, such as simply discarding all data points prior to the minimum crack size/compliance ([29],[32]), which is identified as the beginning of ductile crack propagation, or applying analytical corrections to the negative calculated crack extension values [34]. The most convincing approach ([33],[34]), in the opinion of the authors, is associating to the point of minimum compliance the following value of crack extension:

$$\Delta a_{bl} = \frac{J_{MC}}{2\sigma_Y} \quad , \tag{2}$$

where J_{MC} is the *J*-integral value corresponding to the point of minimum compliance, and then shifting all predicted crack extension values by an amount equal to Δa_{bl}. In [33], this procedure clearly improved the agreement between measured and predicted crack extensions.

However, no provisions are contained in ASTM E1820-21 to account for this phenomenon, and the user is required to use all data points preceding maximum force to establish the predicted initial crack size, a_{oq}. Therefore, the analyses in this report were performed strictly in accordance with the E1820-21 procedure.

Apparent negative crack growth was observed on all investigated welds (Figure 39), except for 3 of the 6 tests performed at 4 K on weld W4. This phenomenon had already been reported for a thick-section weld joint of 316 stainless steel tested at 4 K [37].

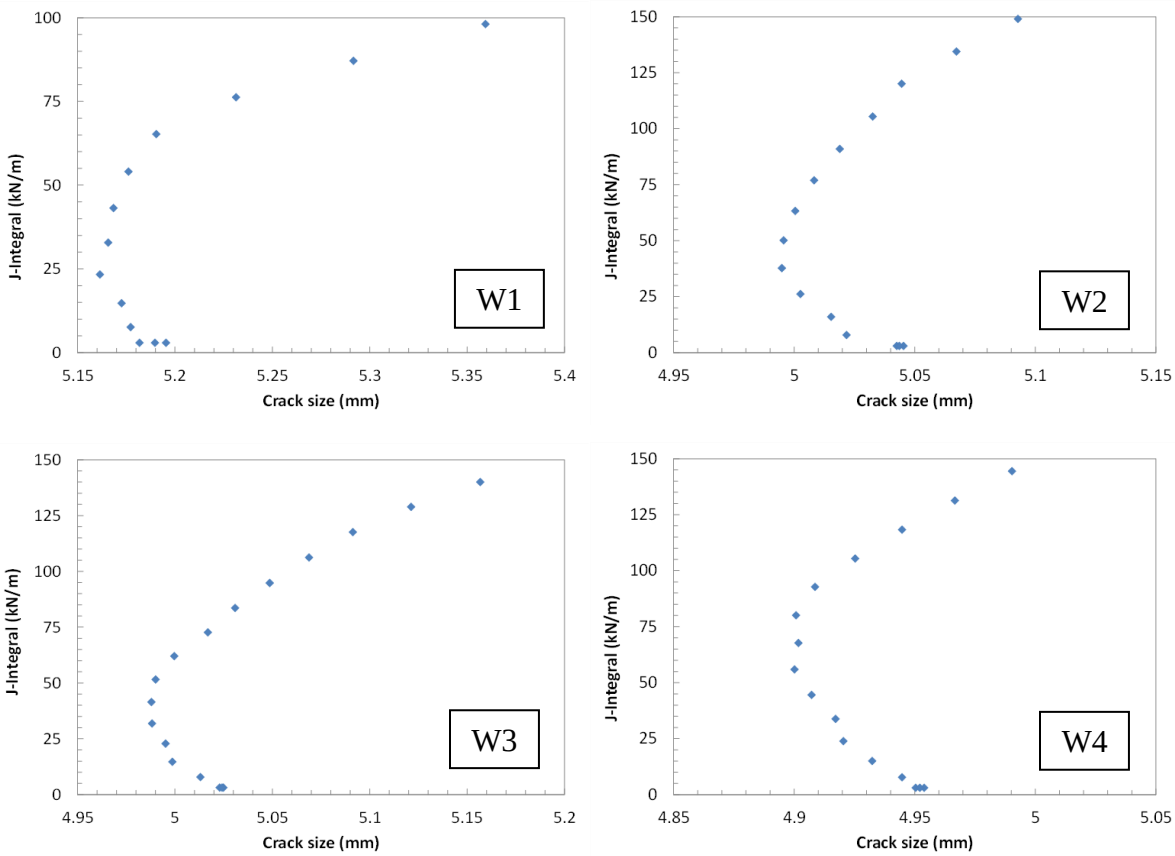

Figure 39 - Examples of apparent negative crack growth observed at 77 K on all investigated welds.

8. Conclusions

The quasi-static fracture toughness of the weld sections of four AISI 316L welded plates was measured at 77 K and 4 K, using Charpy-type single-edge bend specimens and the Unloading Compliance single specimen technique in accordance with ASTM E1820-21. The main findings of this investigation were as follows:

- At both test temperatures (77 K and 4 K), weld W2 turned out to be the toughest and W1 the least tough, based on both critical toughness at crack initiation and resistance to crack propagation. W2 also exhibited the lowest scatter of toughness properties at both temperatures.
- In most of the tests performed, tearing (ductile) instabilities were observed, corresponding to large crack "jumps", which were clearly observed on the fracture surfaces of the tested specimens. In some cases (8 tests out of 43), the earliest tearing instability occurred before stable crack initiation, and the corresponding value of *J*-integral represented the critical toughness value for that particular specimen. The only test condition that did not experience any tearing instability was weld W2 tested at 77 K.
- W2 was the only weld produced using gas tungsten arc welding (GTAW) for both root and subsequent cover passes, whereas all other welds (W1, W3, and W4) used GTAW for the root passes and flux core arc welding (FCAW) during cover passes. Also, the final layer (weld cap) of W2 was created using the most passes (four) when compared to other welds. When comparing welds produced with both GTAW and FCAW, the number of passes in the final layer (weld cap) inversely correlated with toughness, such that the final layer of W1 (least tough) was completed in a single pass, the final layer of W4 (second least tough) was completed with two passes and the final layer of W3 (second toughest) was completed in 3 passes. Ferrite content in the weld covers also likely played a role in toughness, such that W4 and W1 contained the most ferrite, whereas W2 and W3 contained the least amount of ferrite.
- For all investigated welds, quasi-static fracture toughness (both initiation toughness and crack resistance) was significantly reduced from 77 K to 4 K, with W2 exhibiting the smallest reduction and W1 the largest. A strong linear correlation between critical toughness at 77 K and 4 K was found for the welds investigated. While ductile behavior (microvoid coalescence) was observed on the fracture surfaces of all welds tested at 77 K, some instances of brittle failure (cleavage) were observed on the surfaces of the specimens tested at 4 K. The differences in toughness reduction from 77 K to 4 K correlated well with observations from fractography, where W2 showed the least amount of cleavage on fracture surfaces, while W4 and W1 contained the highest number of observable cleavage at the microscale. Fractography also revealed worm hole porosity on the fracture surfaces of W1, which is likely due to contaminated flux core materials.
- Out of 43 specimens tested, only in 8 cases (all at 77 K) the critical value at initiation could be qualified as size-independent plane-strain fracture toughness, J_{Ic}. The most often violated qualification requirements were an excessive difference between measured and predicted crack growth and an insufficient number of data points available to calculate the original crack size from compliance.
- Average critical toughness values at both 77 K and 4 K reasonably correlated with Charpy absorbed energies measured at 77 K, but only for three of the investigated welds (from least tough to toughest, W1 → W3 → W2). The strong linear correlation existing

for weld W1, W2, and W3, however, completely broke down for weld W4, which absorbed the most energy from Charpy tests at 77 K, but resulted the second least tough weld at both 77 K and 4 K.

- Apparent negative crack growth, caused by material stiffening in the plastic zone around the crack tip during the blunting phase, was observed in 40 of the 43 tests performed. This seemingly non-physical phenomenon, however, is currently not acknowledged by the ASTM E1820-21 test standard and was not accounted for in the analyses performed and was therefore not accounted for in the analyses performed.

Acknowledgements

This research used resources provided by the American Society of Mechanical Engineers (ASME) and the NASA Office of Safety and Mission Assurance. We would like to acknowledge our colleagues who were instrumental in many aspects of this research.

National Institute of Standards and Technology:

- David McColskey for guidance on fixture design and proper implementation of ASTM standards.
- Ted Stauffer for retrofitting the load frame to enable recovery of helium gas, which was necessary during a global helium shortage.
- Ross Rentz for producing technical drawings of all specimen geometries, swift implementation of necessary changes to the experimental setup, and assistance during liquid helium fracture toughness testing.
- Matthew Connolly for assistance during liquid helium fracture toughness testing.
- Nik Hrabe for assistance during liquid helium fracture toughness testing.

NASA and NASA contractors:

- Levi Shelton for coordinating materials delivery and providing guidance on proper implementation of ASTM standards.
- Owen Greulich for guidance on interpretation of welding procedure specifications for each welding lot, which enabled deconvolution of key parameters influencing fracture toughness, as well as discussion of relevant ASME pressure vessel codes.

Swagelok Company:

- Shelly Tang for completing ferroscope measurements on welds and base plates, plus guidance on interpretation of welding procedure specifications for each welding lot, which enabled deconvolution of key parameters that influencing fracture toughness.

Sperko Engineering Services:

- Walter Sperko for guidance on interpretation of welding procedure specifications for each welding lot, which enabled deconvolution of key parameters influencing fracture toughness.

Finally, we would like to acknowledge the welding vendors, in no particular order, for providing their services: Nooter, Team Industries, Atlas, and Boardman.

References

[1] The American Society of Mechanical Engineers (2021) Boiler and Pressure Vessel Code, BPVC Section VIII-Rules for Construction of Pressure Vessels, Division 1, BVPC-VIII-1, ASME.

[2] The American Society of Mechanical Engineers (2019), Hydrogen Piping and Pipelines, B31.12, ASME.

[3] The American Society of Mechanical Engineers (2020) Process Piping, ASME Code for Pressure Piping, B31, ASME.

[4] ASTM E23 (2018) Standard Test Methods for Notched Bar Impact Testing of Metallic Materials. American Society for Testing and Material International, West Conshohocken, PA.

[5] Vazquez-Fernandez NI, Soares GC, Smith JL, Seidt JD, Isakov M, Gilat A, Kuokkala VT, Hokka M (2019) Adiabatic Heating of Austenitic Stainless Steels at Different Strain Rates. *Journal of Dynamic Behavior of Materials* 5, pp. 221-229. http://dx.doi.org/10.1007/s40870-019-00204-z

[6] Tobler RL, Reed RP, Hwang IS, Morra MM, Ballinger RG, Nakajima H, Shimamoto S (1991) Charpy Impact Tests Near Absolute Zero. *Journal of Testing and Evaluation* 19(1), pp. 34-40. https://doi.org/10.1520/JTE12527J

[7] Zambrow JL, Fontana MG (1949) Mechanical Properties, Including Fatigue, of Aircraft Alloys at Very Low Temperatures. *Transaction of ASM* 41, pp. 480-518.

[8] Kiefer TF, Keys RD, Schwartzberg FR (1965) Charpy Impact Testing at 20 K. *Advances in Cryogenic Engineering* (10), pp. 56-62. http://dx.doi.org/10.1007/978-1-4684-3108-7_7

[9] Long HM (1974), Comment in Advances in Cryogenic Engineering (19), p. 378.

[10] Jin S, Horwood WA, Morris JW, Jr., Zackay VF (1974) A Simplified Method for Charpy Impact Testing Below 6 K. *Advances in Cryogenic Engineering* (19), pp. 373-378.

[11] Ogata T, Hiraga K, Nagai K, Ishikawa K (1982) A Simplified Method for Charpy Impact Testing Near Liquid Helium Temperature. *Cryogenics* (22), pp. 481-482. http://dx.doi.org/10.1016/0011-2275(82)90135-7,

[12] Ogata T, Hiraga K, Nagai K, Ishikawa K (1984) A Simple Method for Charpy Impact Test at Liquid Helium Temperature. *Transactions of the National Research Institute for Metals* (26), pp. 238-242.

[13] Takahashi Y, Yoshida K, Shimada M, Tada E, Miura R, Shimamoto S (1982) *Advances in Cryogenic Engineering* (28), pp. 73-81.

[14] Matsumoto T, Satoh H, Wadayama Y, Hataya F (1987) Mechanical Properties of Fully Austenitic Weld Deposits for Cryogenic Structures. *Welding Research Supplement* (66), pp. 120-126s.

[15] Mori T, Kuroda T (1985) Prediction of Energy Absorbed in Impact for Austenitic Weld Metals at 4.2 K. *Cryogenics* (25), pp. 243-248. http://dx.doi.org/10.1016/0011-2275(85)90203-6

[16] DeSisto TS (1958) Automatic Impact Testing to 8 K. Technical Report 112/93. Watertown Arsenal Laboratories, Watertown, Massachusetts.

[17] Dobson WG, Johnson DL (1984) Effect of Strain Rate on Measured Mechanical Properties of Stainless Steel at 4 K. *Advances in Cryogenics Engineering* (30), pp. 185-192.
[18] Lucon E, Benzing J (2021) Instrumented Charpy Tests at 77 K on 316L Stainless Steel Welded Plates. National Institute of Standards and Technology, NIST Technical Note 2196, Boulder, Colorado. https://doi.org/10.6028/NIST.TN.2196
[19] Weeks T, Derimow N, Benzing J (2022) Tensile Tests at 77 K and 4 K on 316L Stainless Steel Welded Plates. National Institute of Standards and Technology, NIST Technical Note 2229, Boulder, Colorado. https://doi.org/10.6028/NIST.TN.2229
[20] ISO 15653 (2018) Metallic materials — Method of test for the determination of quasistatic fracture toughness of welds. International Standards Organization, Geneva (Switzerland).
[21] ASTM E1820 (2021) Standard Test Method for Measurement of Fracture Toughness. American Society for Testing and Material International, West Conshohocken, PA.
[22] Van Gelderen DGA, Booker JD, Smith DJ (2015) Evaluating the conditions when warm pre-stressing does not produce a benefit in apparent toughness. *Materials Today: Proceedings 2S*, S401 – S407. https://doi.org/10.1016/j.matpr.2015.05.055
[23] Paris PC, Tada H, Zahoor A, Ernst H (1977) A Treatment of the Subject of Tearing Instability. U.S. Nuclear Regulatory Commission, Washington, DC, Report No. NUREG-0311.
[24] Greulich O, Jawad MH (2022) Fabrication of Metallic Pressure Vessels. John Wiley & Sons-ASME Press, 1st Edition.
[25] Tobler RL, Reed RP (1984) Interstitial Carbon and Nitrogen Effects on the Cryogenic Fatigue Crack Growth of AISI 304 Type Stainless Steels. *Journal of Testing and Evaluation*, JTEVA, Vol. 12, No. 6, pp. 364-370. https://doi.org/10.1520/JTE10741J
[26] Read DT, McHenry HI, Steinmeyer PA, Thomas RD Jr. (1979) Metallurgical factors affecting the toughness of 316L SMA weldments at cryogenic temperatures (NBSIR--79-1609), Reed, R.P. (Ed.), United States.
[27] Goodwin GM (1984) Fracture toughness of austenitic stainless steel weld metal at 4 K. Oak Ridge National Laboratory Technical Report, ORNL/TM-9172, Oak Ridge, TN. https://doi.org/10.2172/6569271
[28] Hertzberg RW, Vinci RP, Hertzberg JL (2012) Deformation and Fracture Mechanics of Engineering Materials. Wiley, 5th Edition.
[29] Fernandez-Pisón P, Rodríguez-Martínez JA, García-Tabarés E, Avilés-Santillana I, Sgobba S (2021) Flow and Fracture of Austenitic Stainless Steels at Cryogenic Temperatures. *Engineering Fracture Mechanics* 258, 108042 https://doi.org/10.1016/j.engfracmech.2021.108042
[30] Obst B, Nyilas A (1991) Experimental evidence on the dislocation mechanism of serrated yielding in f.c.c. metals and alloys at low temperatures. *Mater. Sci. Eng. A.* 137 (1991), pp. 141–150. https://doi.org/https://doi.org/10.1016/0921-5093(91)90328-K
[31] Voss B, Mayville RA (1985) The Use of the Partial Unloading Compliance Method for the Determination of J_I-R Curves and J_{Ic}. *Elastic-Plastic Fracture Test Methods: The User's Experience*, ASTM STP 856, ET Wessel and FJ Loss, Eds., American Society for Testing and Materials, Philadelphia, PA, pp. 117-130. https://doi.org/10.1520/STP856-EB

[32] Rosenthal YA, Tobler RL, Purtscher PT (1990) J_{Ic} Data Analysis Methods with a "Negative Crack Growth" Correction Procedure. *Journal of Testing and Evaluation*, JTEVA, Vol. 18, No. 4, pp. 301-304. https://doi.org/10.1520/JTE12488J

[33] Underwood JH, Troiano EJ, Abbott RT (1994) Simpler J_{Ic} Test and Data Analysis Procedures for High-Strength Steels. *Fracture Mechanics: Twenty-Fourth Volume*, ASTM STP 1207, JD Landes, DE McCabe, JA Boulet, Eds., American Society for Testing and Materials, Philadelphia, PA, pp. 410-421. https://doi.org/10.1520/STP1207-EB

[34] Seok C-S (2000) Correction Methods of an Apparent Negative Crack Growth Phenomenon. *International Journal of Fracture* **102**, pp. 259-269. https://doi.org/10.1023/A:1007680608587

[35] Weiss K, Nyilas A (2006) Specific Aspects on Crack Advance During *J*-test Method for Structural Materials at Cryogenic Temperatures. *Fatigue and Fracture of Engineering Materials and Structures*, Vol. 29, No. 2, pp. 83-92. http://dx.doi.org/10.1111/j.1460-2695.2006.00963.x

[36] Verstraete MA, Hertelé S, Denys RM, Van Minnebruggen K, De Waele W (2014) Evaluation and Interpretation of Ductile Crack Extension in SENT Specimens Using Unloading Compliance Technique. *Engineering Fracture Mechanics* 115, pp. 190-203. http://dx.doi.org/10.1016/j.engfracmech.2013.11.004

[37] Nishimura A, Tobler RL, Tamura H, Imagawa S, Yamamoto J (1998) Fracture Toughness of Thick-Section Weld joint of SUS 316 at cryogenic temperature. *Fusion Engineering and Design*, Vol. 42, No. 1-4, pp. 425-430. https://doi.org/10.1016/S0920-3796(98)00104-5

Appendix A: Supplemental Information for Each Weld

Base plate composition (average of 3 measurements) in % mass fraction provided by NASA MSFC. Measurements were performed via spark emission along the surface of each plate.

Welded plate	C	Si	Mn	P	S	Cr	Mo	Ni	Al	Co	Cu	Nb	Ti	V	W	Pb	Sn	As	Zr	Ca	B	Fe
W1	0.045	0.28	1.19	0.047	0.01	15	2.13	10.22	0.007	0.4	0.47	0.039	0.022	0.076	0.058	0.011	0.01	0.005	0.003	0.001	0.0005	70
W2	0.039	0.24	1.14	0.054	0.007	15.2	2.11	10.17	0.008	0.31	0.49	0.005	0.018	0.083	0.05	0.013	0.011	0.005	0.003	0.001	0.0005	70.1
W3	0.033	0.31	1.28	0.048	0.008	14.88	2.14	10.24	0.006	0.36	0.33	0.028	0.017	0.058	0.065	0.011	0.007	0.005	0.003	0.0007	0.0005	70.2
W4	0.053	0.29	1.13	0.046	0.006	15.25	2.14	10.15	0.008	0.33	0.35	0.0009	0.02	0.13	0.089	0.011	0.008	0.005	0.003	0.001	0.0005	70

Weld composition (average of 3 measurements) in % mass fraction provided by NASA MSFC. Measurements were performed via spark emission along the surface of each weld.

Welded plate	C	Si	Mn	P	S	Cr	Mo	Ni	Al	Co	Cu	Nb	Ti	V	W	Pb	Sn	As	Zr	Ca	B	Fe
W1	0.049	0.47	1.07	0.049	0.012	16.84	2.71	12.41	0.009	0.1	0.22	0.01	0.044	0.071	0.04	0.011	0.008	0.005	0.004	0.0009	0.0005	65.9
W2	0.07	0.41	1.88	0.031	0.039	16.69	2.94	13.23	0.018	0.053	0.12	0.013	0.016	0.032	0.04	0.016	0.006	0.005	0.003	0.002	0.0008	64.4
W3	0.064	0.52	0.82	0.046	0.011	15.89	2.23	12.87	0.007	0.11	0.22	0.027	0.039	0.078	0.04	0.01	0.008	0.005	0.003	0.001	0.0005	67
W4	0.074	0.64	1.4	0.038	0.026	16.71	2.96	11.96	0.04	0.19	0.12	0.005	0.084	0.092	0.04	0.013	0.003	0.005	0.003	0.002	0.0005	65.6

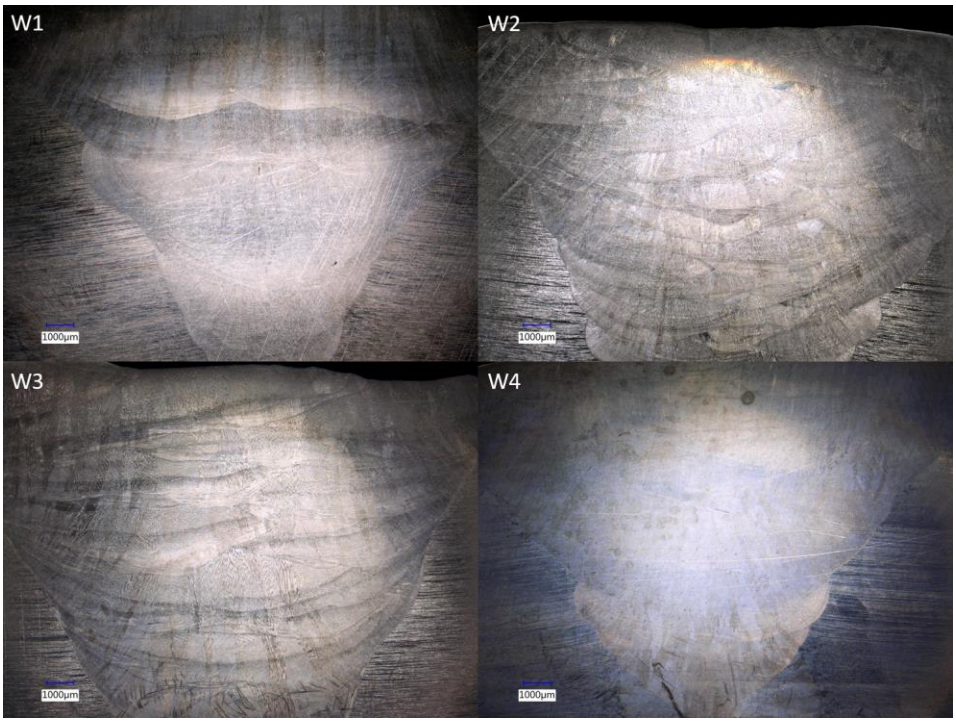

Optical image of weld cross sections after mechanical polishing and etching (Kalling's No. 2: 5 g $CuCl_2$, 40 ml HCl, 30 ml H_2O).

Appendix B: Technical Drawings of the Charpy-type Specimens for Fracture Toughness Testing

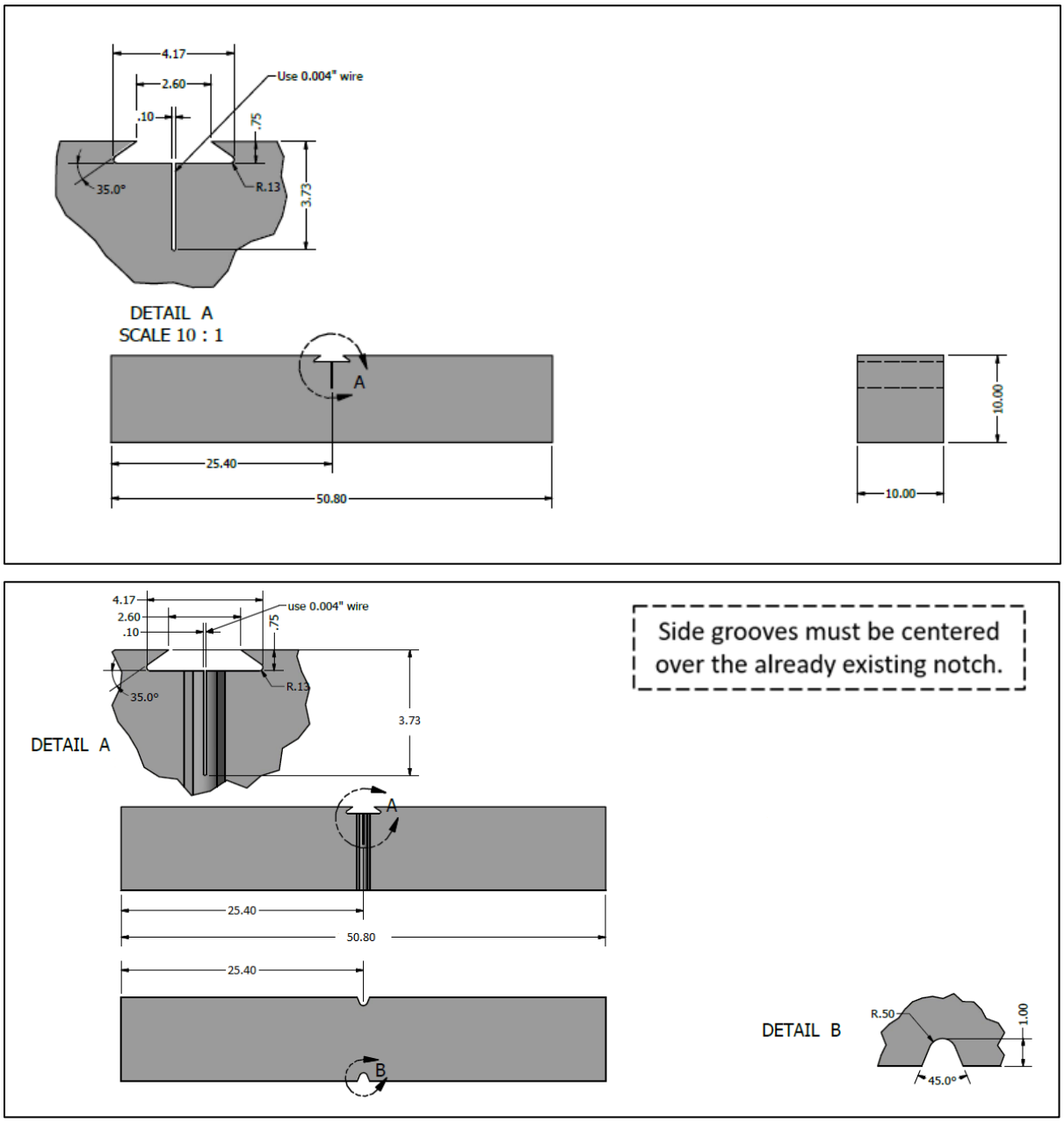

NOTES: all dimensions in millimeters. Default tolerances are ± 0.1 mm and ± 1°. Default surface finish, unless specified, is < 1.6 µm.

Top: general drawing of the specimen before side-grooving – Bottom: details of side-grooves (machined after fatigue precracking).

Appendix C: Digital Pictures of the Fracture Surfaces of the Tested Specimens

Specimens Tested at 77 K


W1-F11

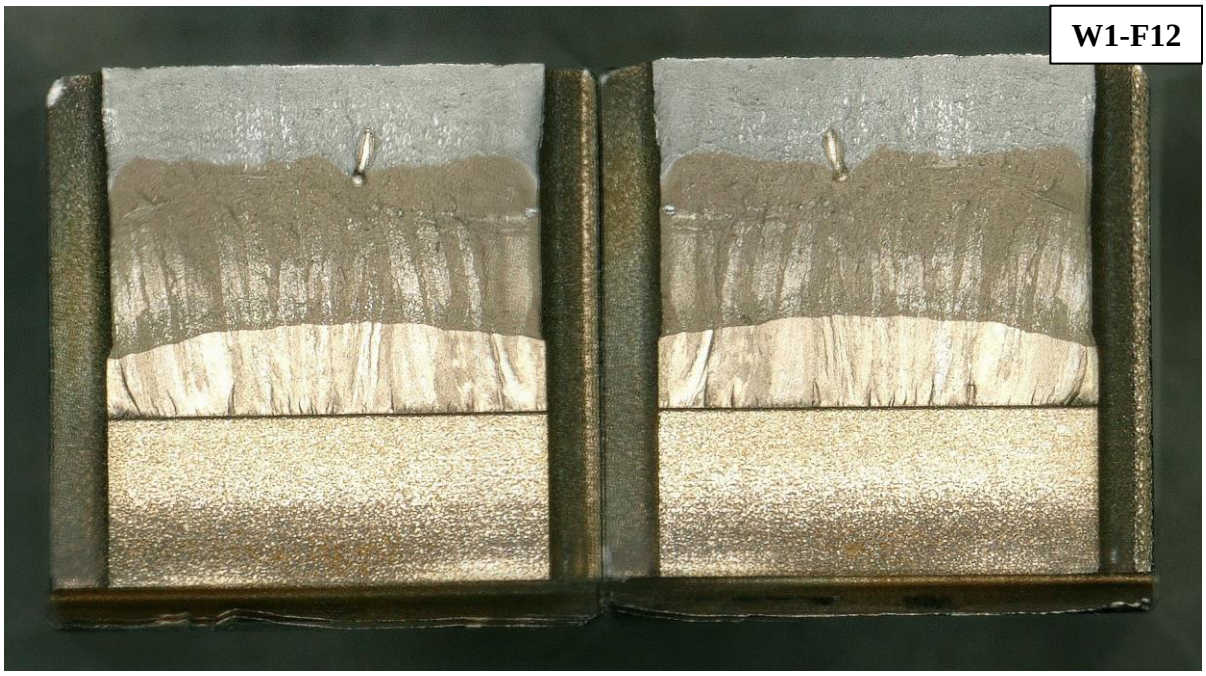
W1-F12


W1-F13

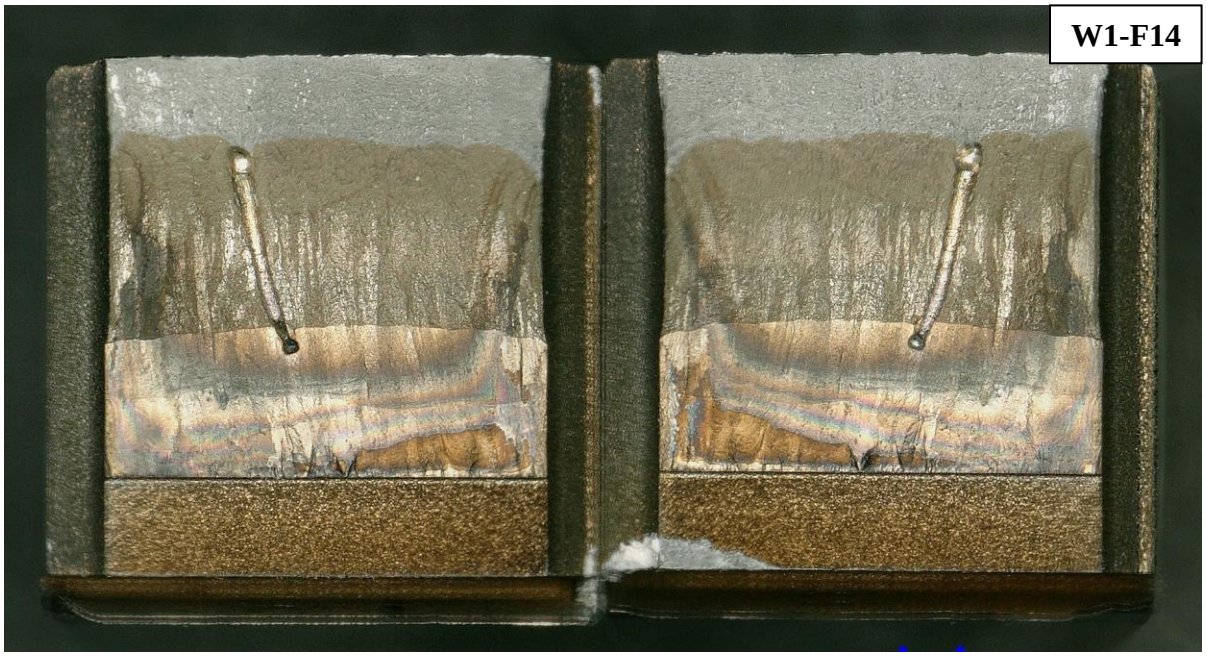
W1-F14


W2-F8

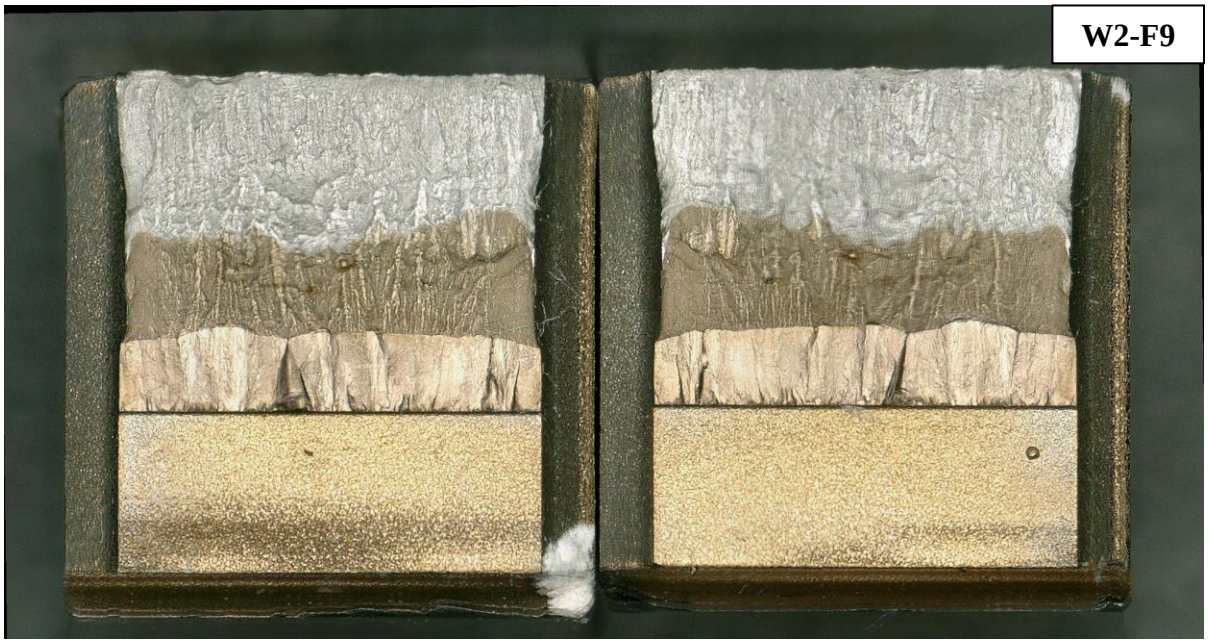
W2-F9


W2-F10


W2-F11


W2-F12

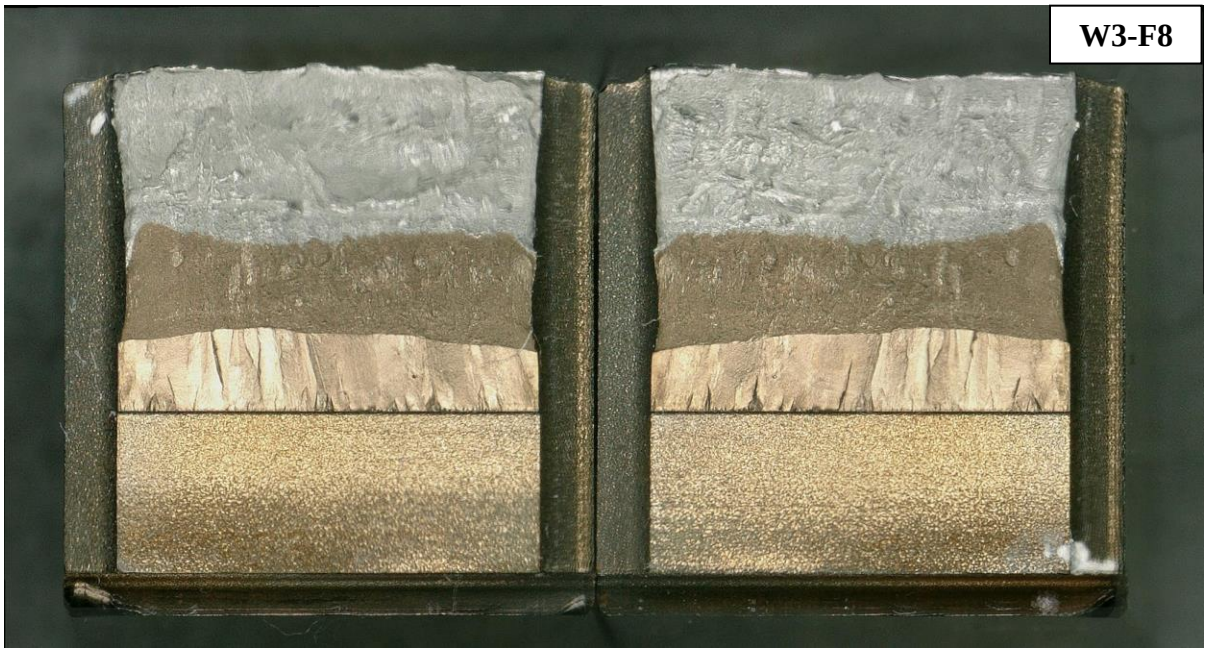
W3-F8

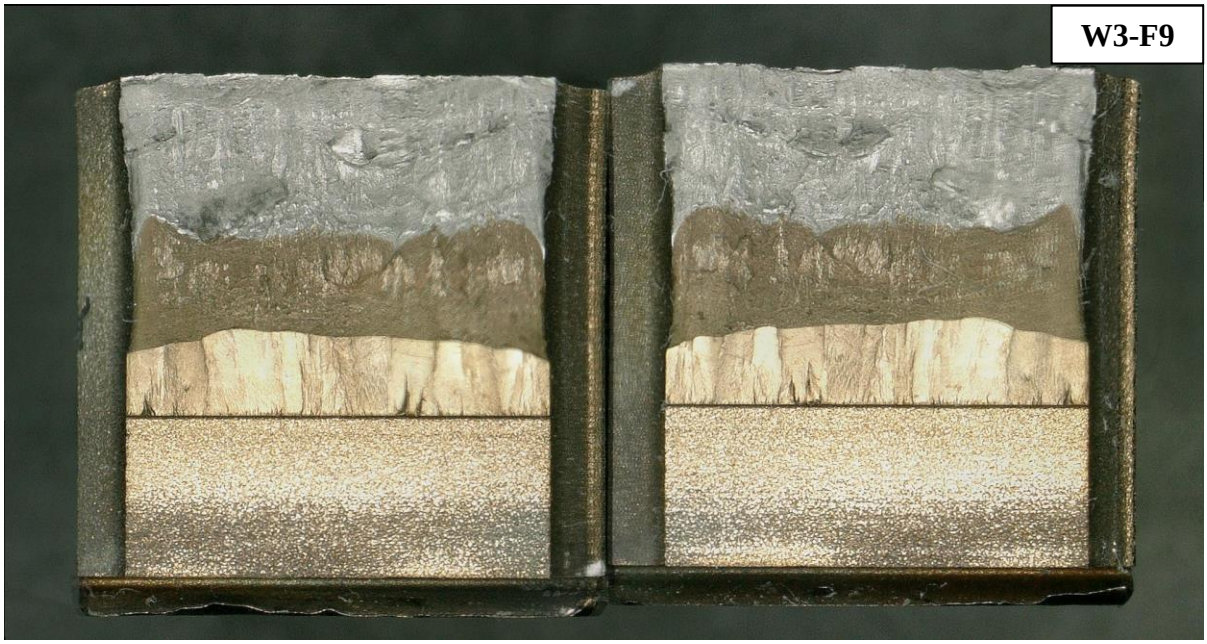
W3-F9

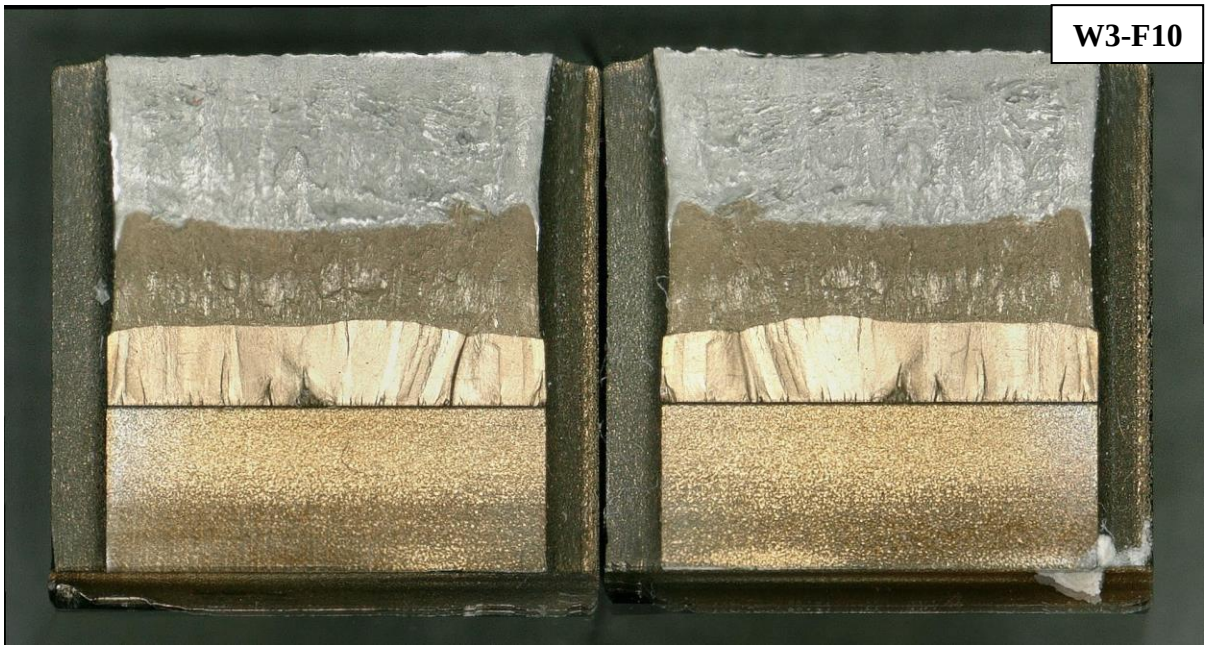
W3-F10

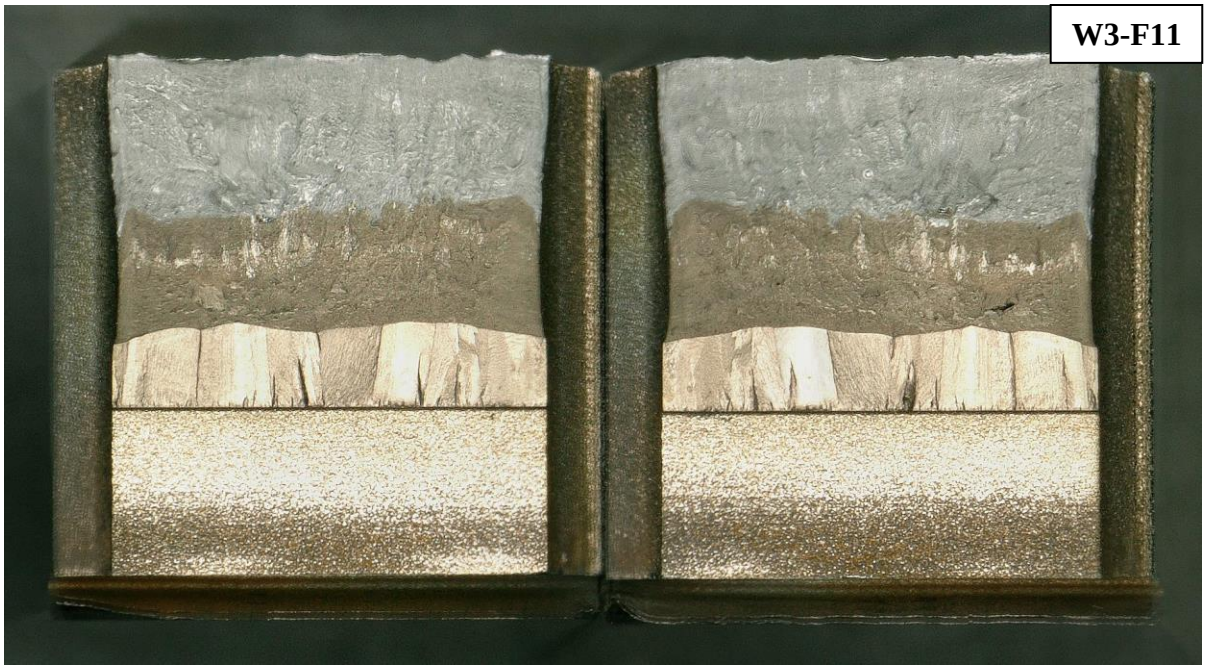
W3-F11

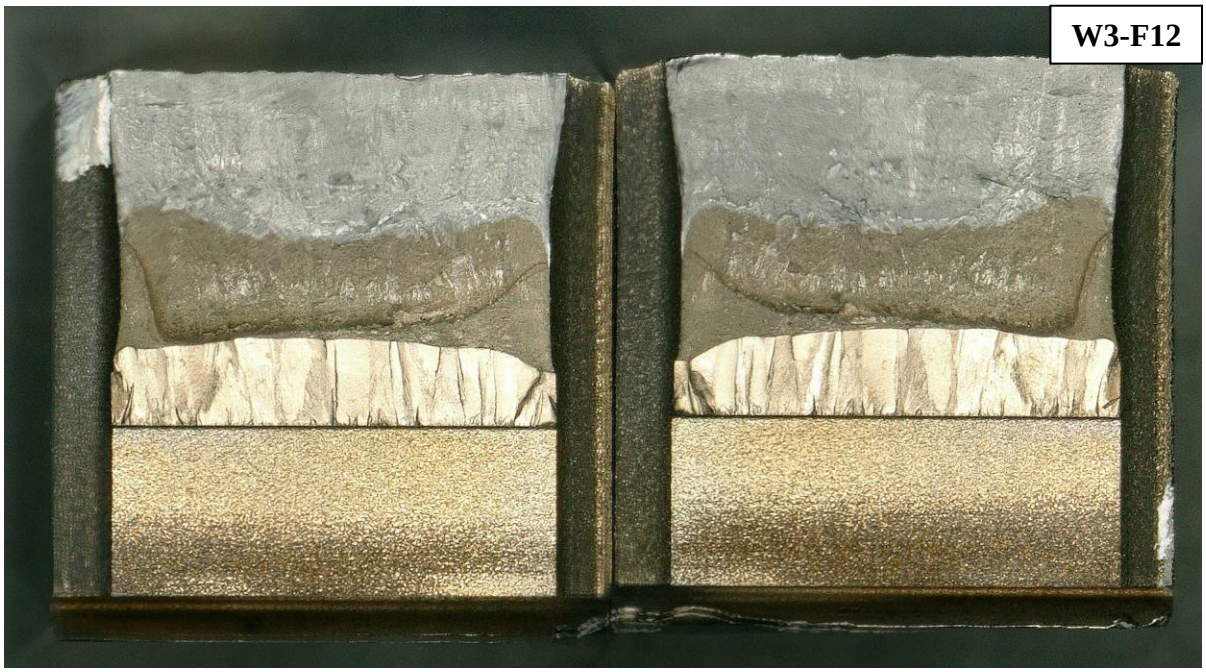
W3-F12

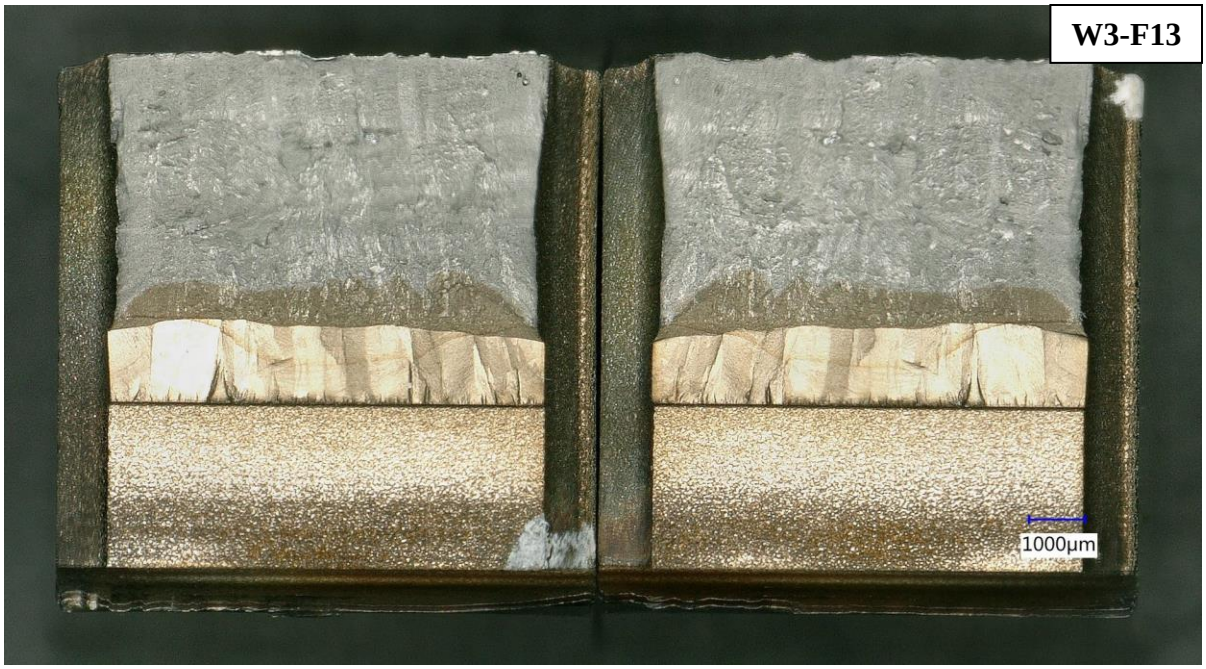
W3-F13
1000µm

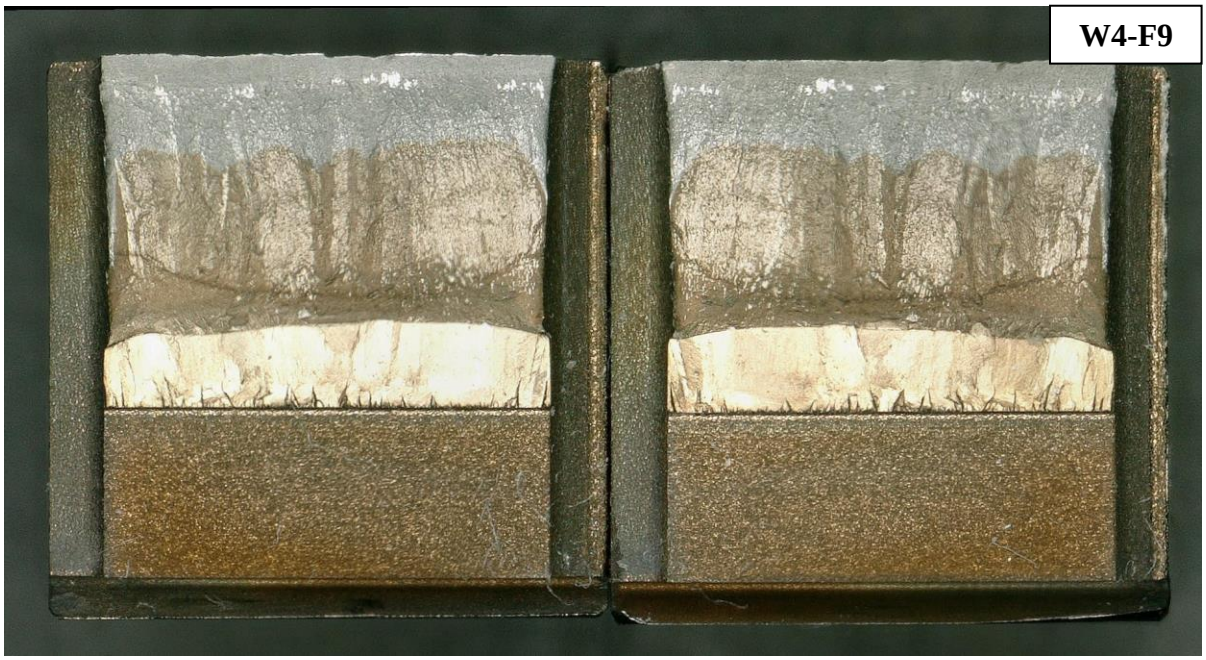
W4-F9


W4-F10

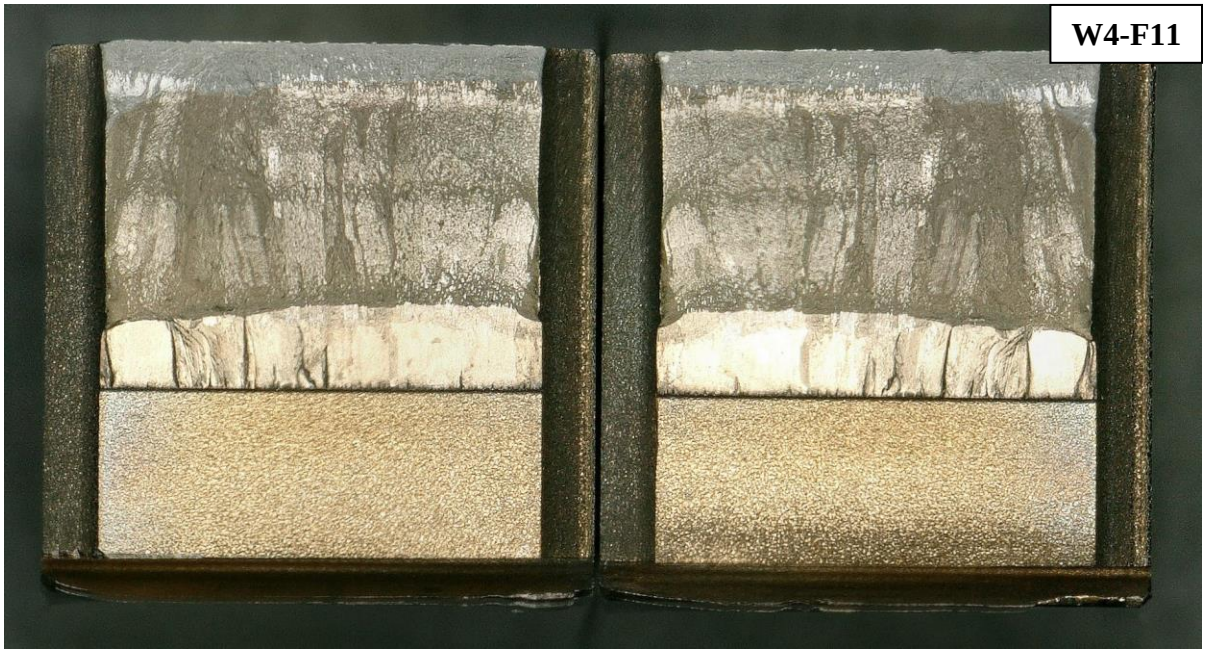
W4-F11


W4-F12

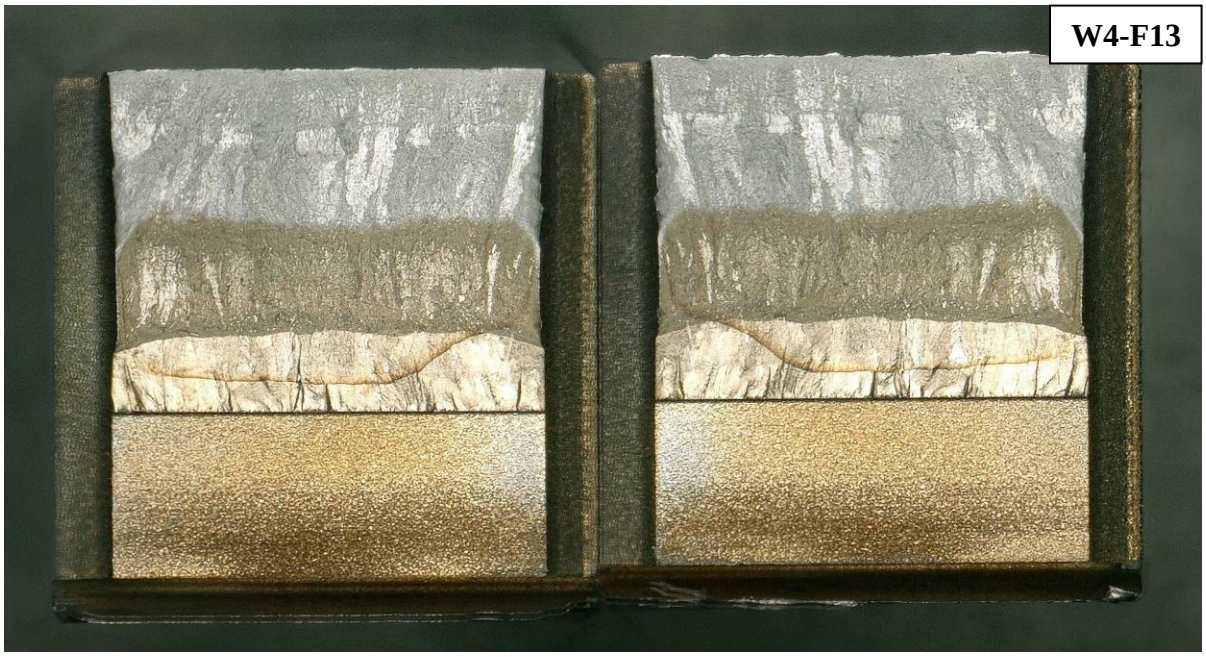
W4-F13

Specimens Tested at 4 K


W1-F6


W1-F7


W1-F8


W2-F3

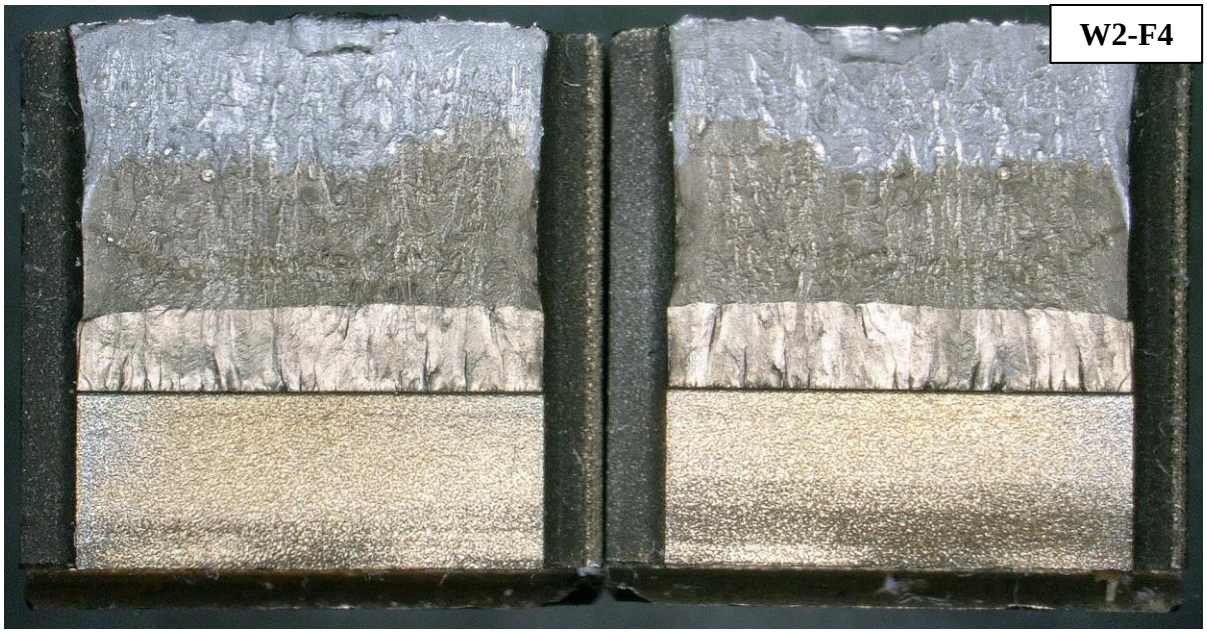
W2-F4


W2-F5


W2-F6


W2-F7

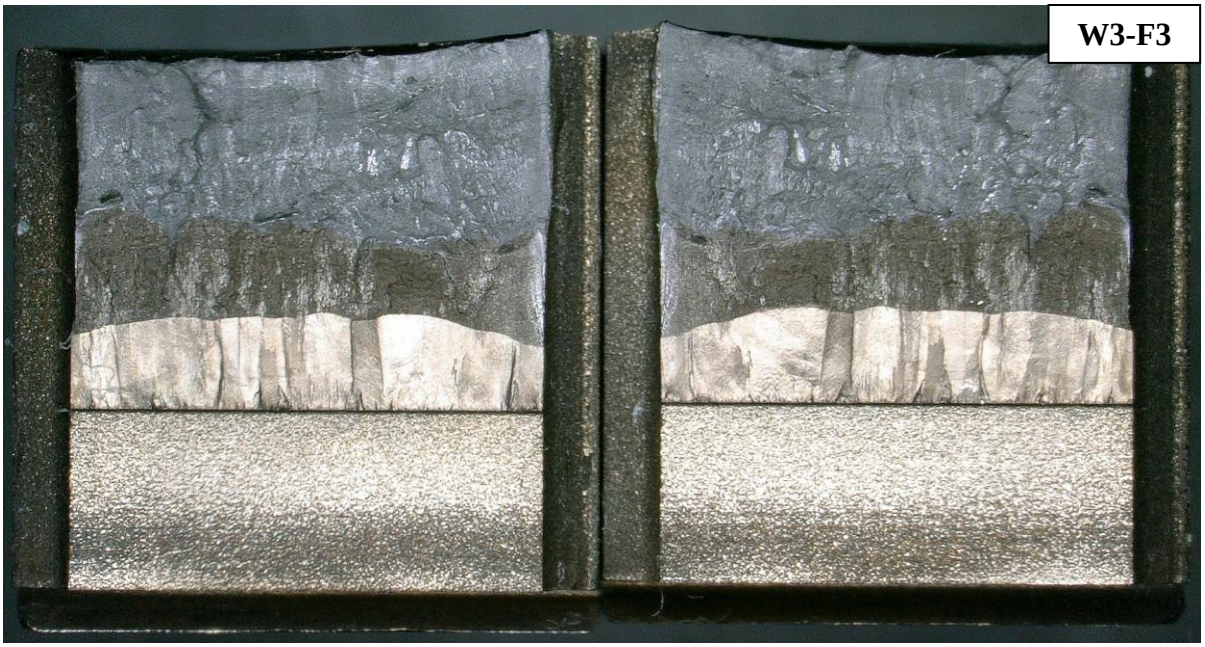
W3-F3

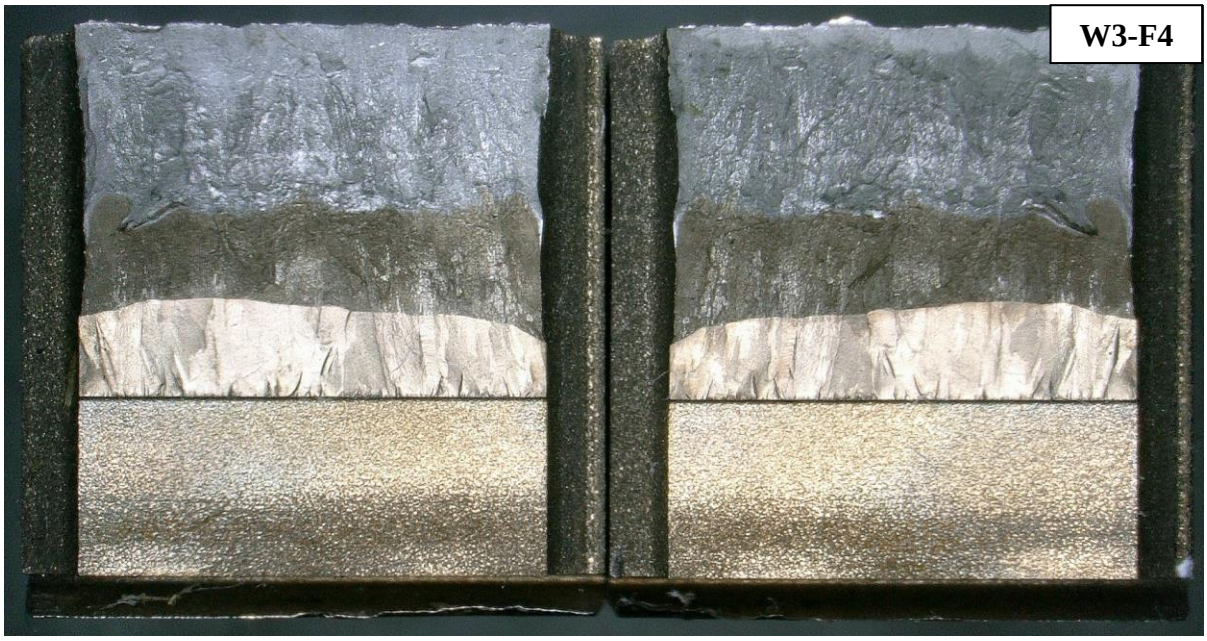
W3-F4


W3-F5


W3-F6


W3-F7


W4-F3

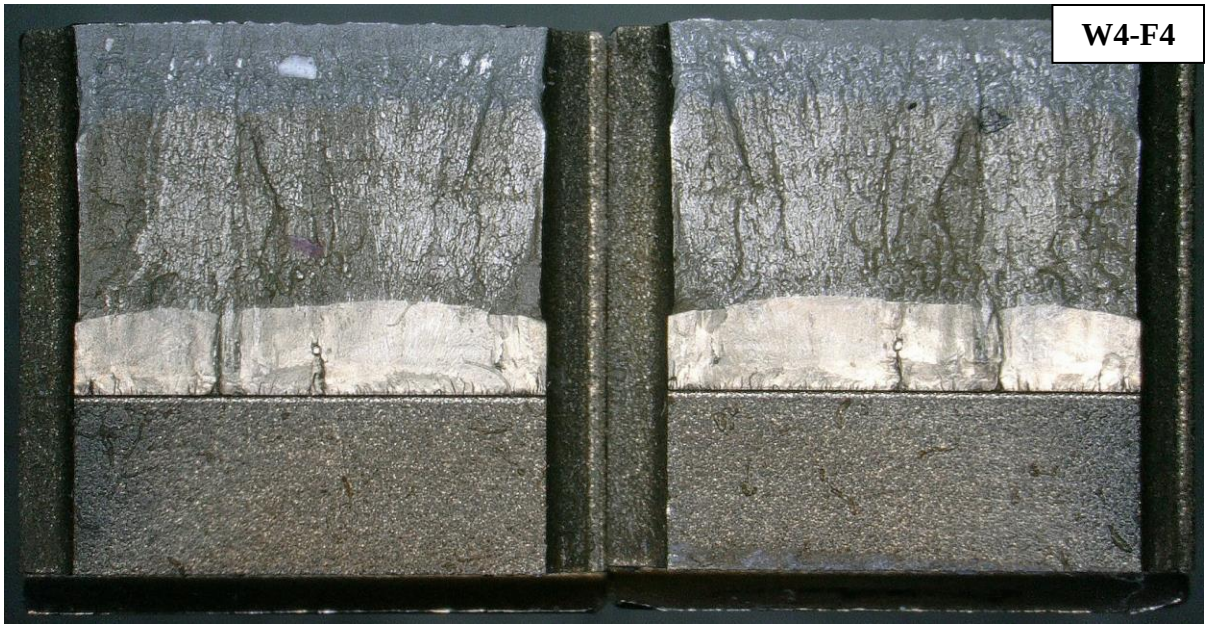
W4-F4

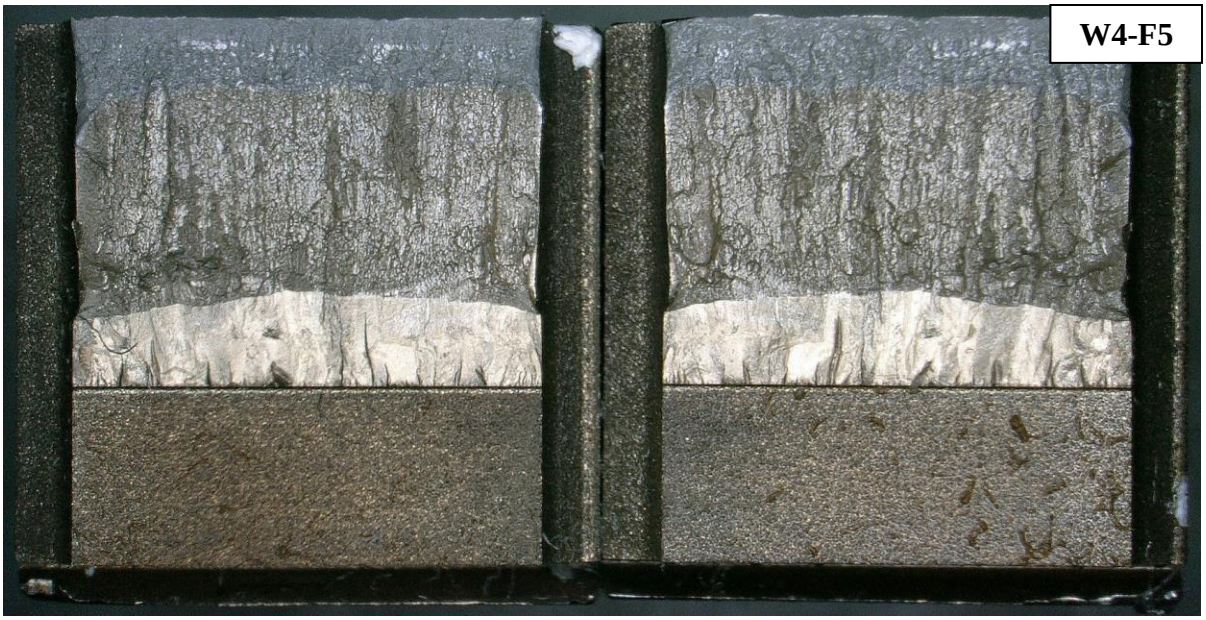
W4-F5

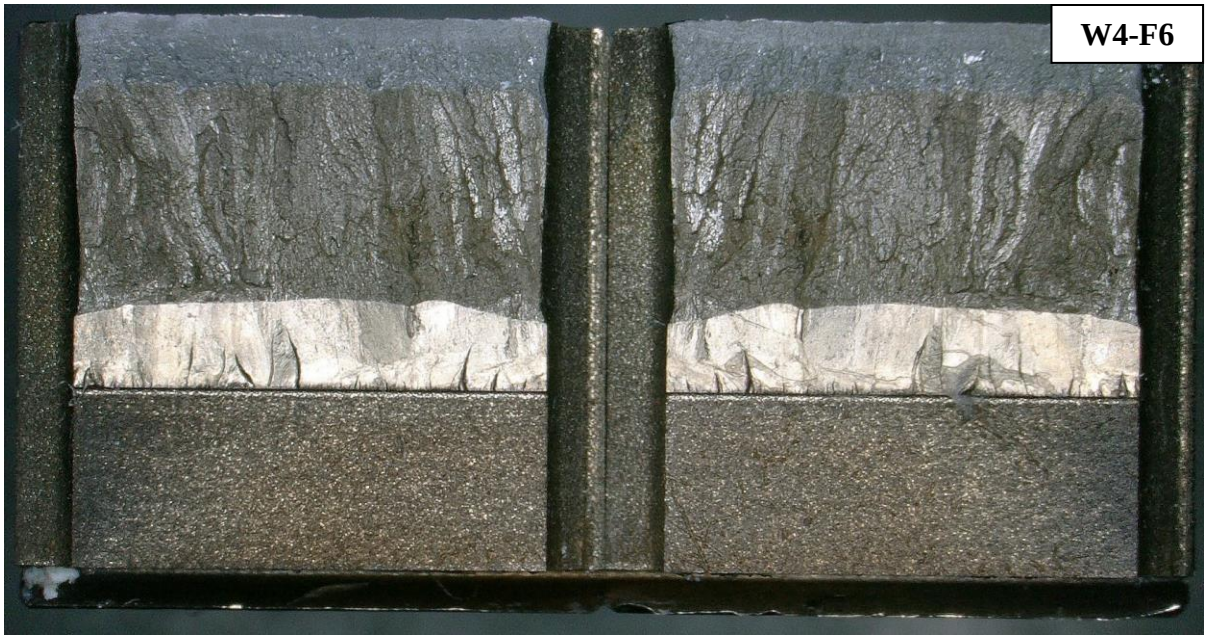
W4-F6

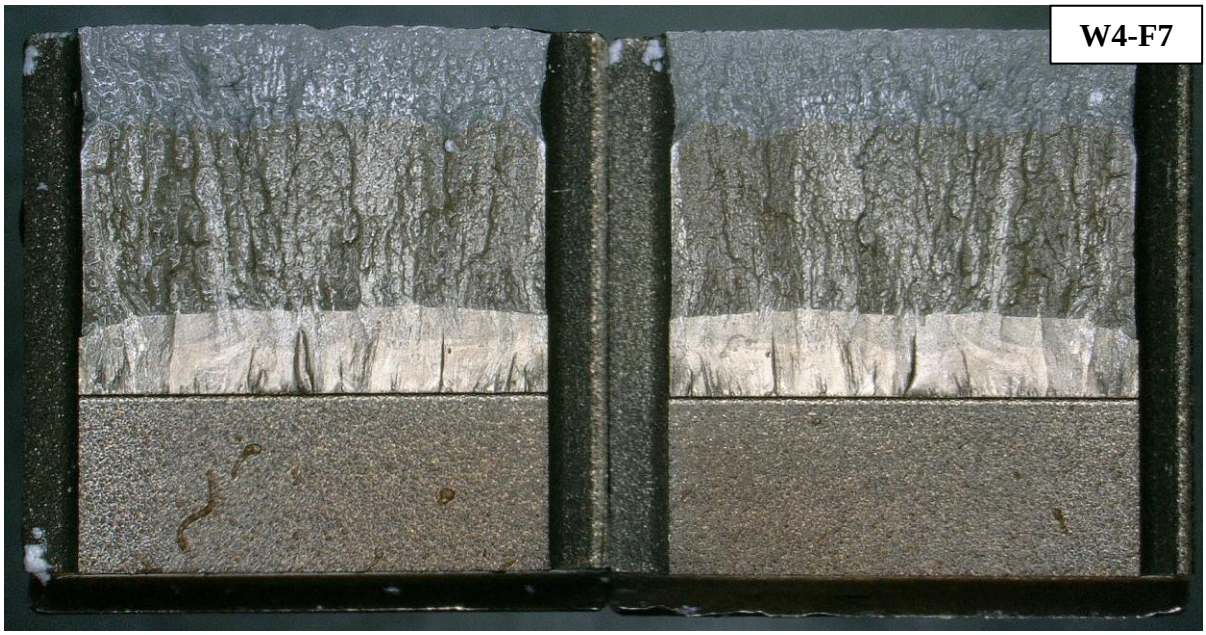
W4-F7


W4-F8

Appendix D: Detailed Results of the Fracture Toughness Tests

Weld W1, T = 77 K

TEST REPORT

Specimen Information

Type = SE(B)
Identification = W1-F9
Orientation = N/A

Basic dimensions

B =	10.03	mm
B_N =	8.01	mm
W =	10.02	mm

Other dimensions

S =	40.00	mm

Tensile Properties

E =	192	GPa
ν =	0.3	
σ_{YS} =	582.0	MPa
σ_{TS} =	1221.0	MPa

Crack Size Information

a_0 =	5.22	mm
a_{0q} =	5.16	mm
a_f =	8.38	mm
Δa_p =	3.16	mm
$\Delta a_{predicted}$ =	3.21	mm

Test temperature: -196 °C

Analysis of Results

Fracture type = stable tearing

Critical Fracture Toughness

J_Q = 63.81 kJ/m²

TM = 36.3 MPa

QUALIFICATION OF DATA

Estimates of initial crack size:	$a_{0q,1}$ =	5.268	mm	Diff :	0.009	< 0.002W =	0.0200 mm
	$a_{0q,2}$ =	5.282	mm		0.005	< 0.002W =	0.0200 mm
	$a_{0,q3}$ =	5.281	mm		0.004	< 0.002W =	0.0200 mm
	$a_{0,qmean}$ =	5.277	mm				

Qualification of data

Crack extension prediction	Δa_p =	3.16	mm (measured)	
	Δa_{pred} =	3.21	mm (predicted)	
	Difference =	0.05	mm	(PREDICTION ACCEPTABLE)

J_Q - Qualification of data

Power coefficient C_2 =	0.566498	< 1.0	→ QUALIFIED
$\lvert a_{0q} - a_0 \rvert$ =	0.06	mm	→ DATA SET ADEQUATE
# of data available to calculate a_{0q} :	4	< 8	→ DATA SET NOT ADEQUATE
# of data between $0.4J_q$ and J_q :	3	≥ 3	→ QUALIFIED
Correlation coefficient a_{0q} fit :	0.997	≥ 0.96	→ DATA SET ADEQUATE
Data points distribution :	VALID		
Number of qualified data points :	VALID		

Qualification of J_Q as J_{Ic}

Thickness B =	10.03	mm > 10 JQ/Sy	→ QUALIFIED
Initial ligament b_0 =	4.80	mm > 10 JQ/Sy	→ QUALIFIED

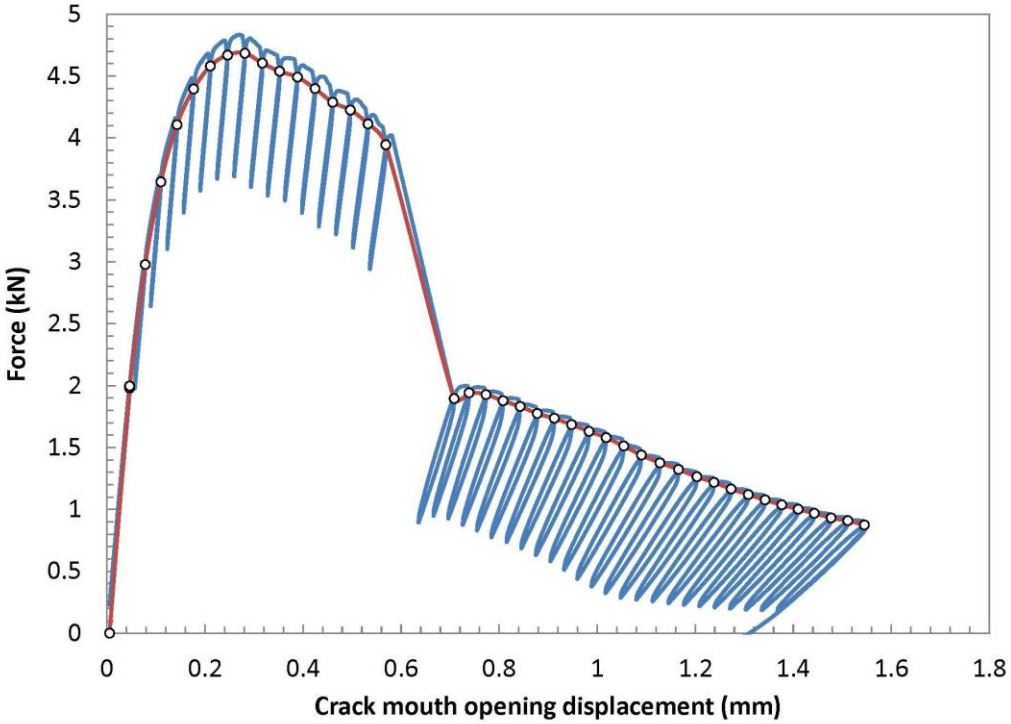
Force (kN)
Crack mouth opening displacement (mm)
0
0.5
1
1.5
2
2.5
3
3.5
4
4.5
5
0
0.2
0.4
0.6
0.8
1
1.2
1.4
1.6
1.8

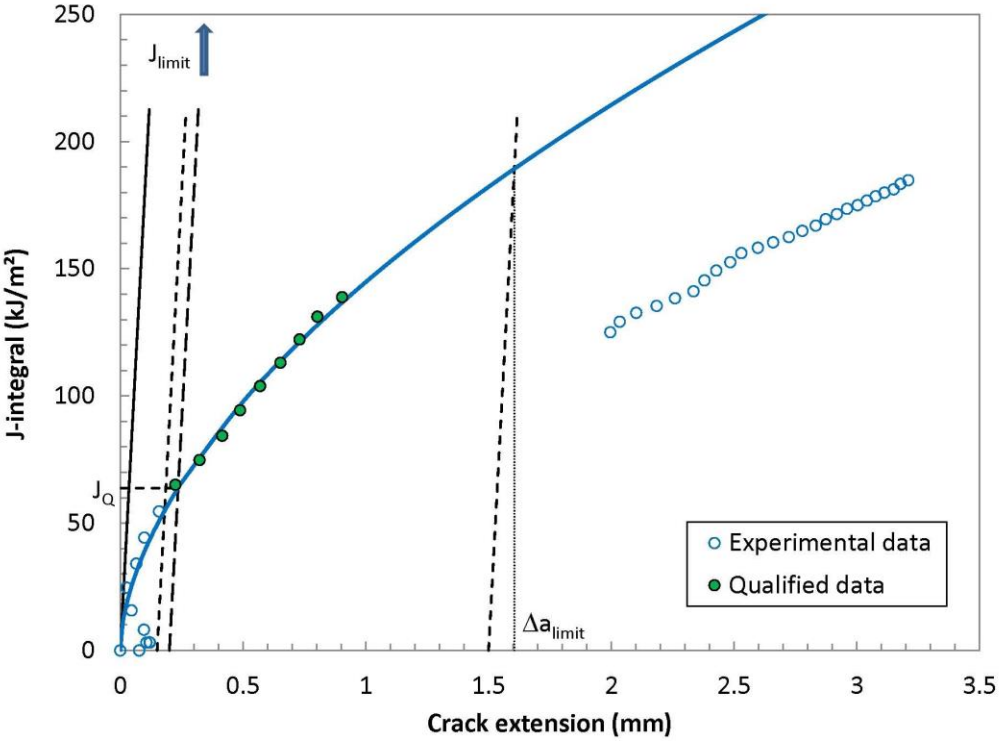
J-integral (kJ/m²)
Crack extension (mm)
J_limit
J_Q
Δa_limit
Experimental data
Qualified data
0
50
100
150
200
250
0
0.5
1
1.5
2
2.5
3
3.5

TEST REPORT

Specimen Information

Type = SE(B)
Identification = W1-F10
Orientation = N/A

Basic dimensions

B =	10.02	mm
B_N =	8.01	mm
W =	10.03	mm

Other dimensions

S =	40.00	mm

Tensile Properties

E =	192	MPa
ν =	0.3	
σ_{YS} =	582.0	MPa
σ_{TS} =	1221.0	MPa

Crack Size Information

a_0 =	5.20	mm
a_{0q} =	5.17	mm
a_f =	8.06	mm
Δa_p =	2.86	mm
$\Delta a_{predicted}$ =	2.76	mm

Test temperature: -196 °C

Analysis of Results

Fracture type = stable tearing

Critical Fracture Toughness

J_Q = #N/A kJ/m²

TM = #N/A MPa

QUALIFICATION OF DATA

Estimates of initial crack size:

$a_{0q,1}$ =	5.182	mm	Diff :	0.007	< 0.002W =	0.0201	mm
$a_{0q,2}$ =	5.195	mm		0.006	< 0.002W =	0.0201	mm
$a_{0,q3}$ =	5.190	mm		0.001	< 0.002W =	0.0201	mm
$a_{0,qmean}$ =	5.189	mm					

Qualification of data

Crack extension prediction	Δa_p =	2.86	mm (measured)	
	Δa_{pred} =	2.76	mm (predicted)	
	Difference =	-0.10	mm	(PREDICTION ACCEPTABLE)

J_Q - Qualification of data

Power coefficient C_2 =	1.181008	≥ 1.0	→ NOT QUALIFIED
$\lvert a_{0q} - a_0 \rvert$ =	0.02	mm	→ DATA SET ADEQUATE
# of data available to calculate a_{0q} :	6	< 8	→ DATA SET NOT ADEQUATE
# of data between $0.4J_q$ and J_q :	0	< 3	→ NOT QUALIFIED
Correlation coefficient a_{0q} fit :	0.993	≥ 0.96	→ DATA SET ADEQUATE
Data points distribution :	NOT VALID		
Number of qualified data points :	NOT VALID		

Qualification of J_Q as J_{Ic}

Thickness B =	10.02	#N/A	#N/A
Initial ligament b_0 =	4.83	#N/A	#N/A

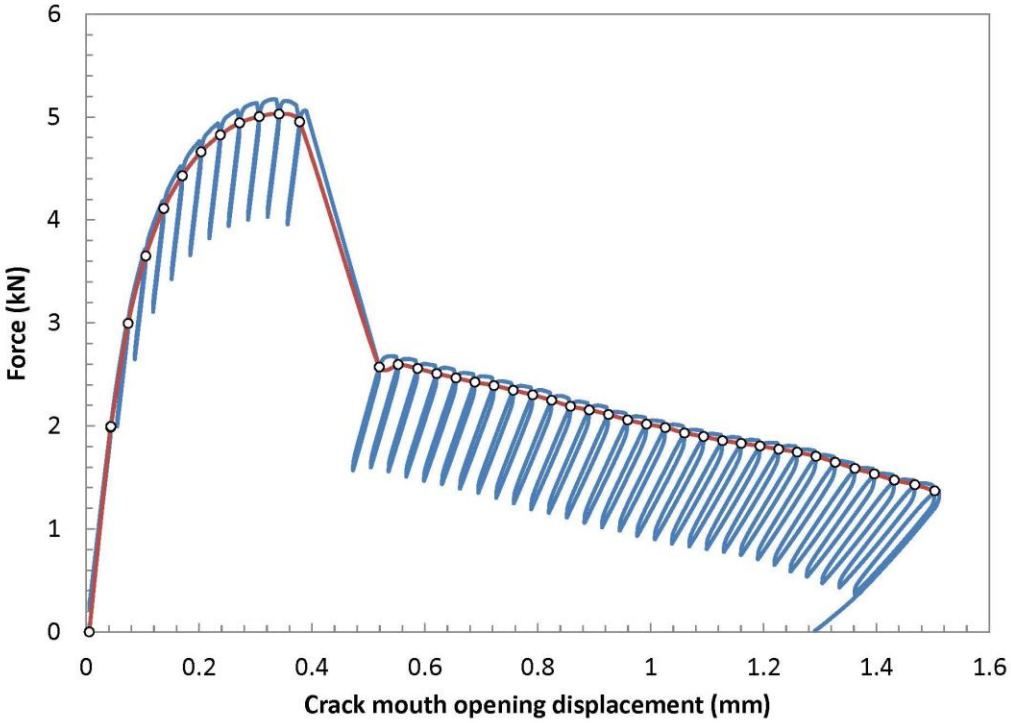
Force (kN)
Crack mouth opening displacement (mm)
0
1
2
3
4
5
6
0
0.2
0.4
0.6
0.8
1
1.2
1.4
1.6

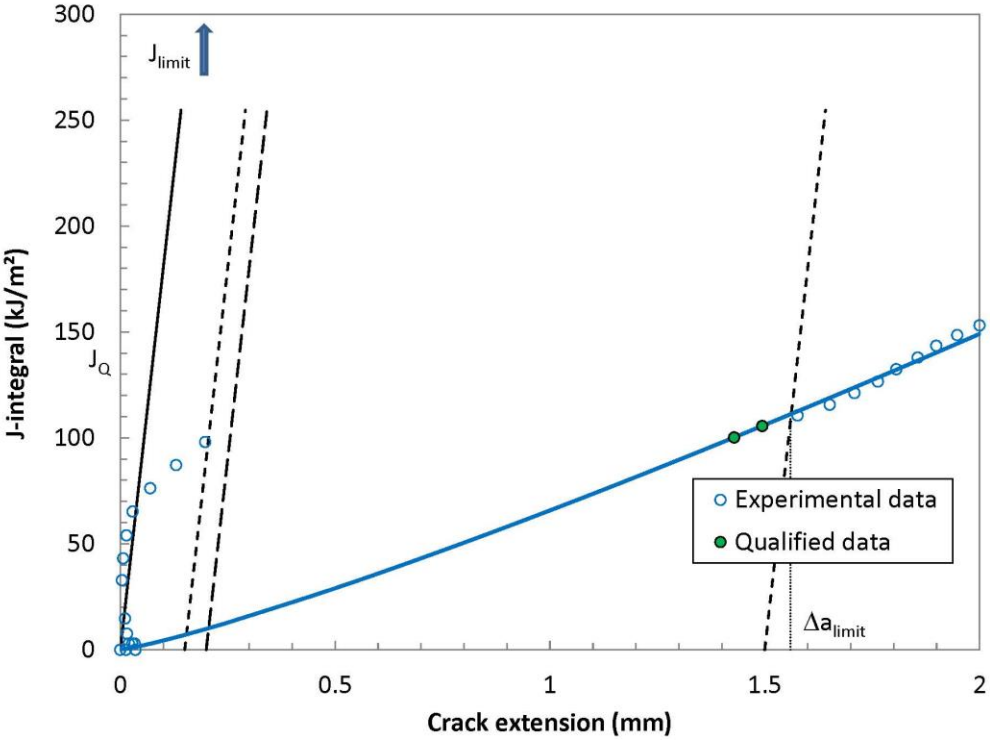
J-integral (kJ/m²)
Crack extension (mm)
J_limit
J_Q
Δa_limit
Experimental data
Qualified data
0
50
100
150
200
250
300
0
0.5
1
1.5
2

TEST REPORT

Specimen Information

Type = SE(B)
Identification = W1-F11
Orientation = N/A

Basic dimensions

B =	10.03	mm
B_N =	8.01	mm
W =	10.02	mm

Other dimensions

S =	40.00	mm

Tensile Properties

E =	192	MPa
ν =	0.3	
σ_{YS} =	582.0	MPa
σ_{TS} =	1221.0	MPa

Crack Size Information

a_0 =	5.28	mm
a_{0q} =	5.28	mm
a_f =	7.05	mm
Δa_p =	1.77	mm
$\Delta a_{predicted}$ =	1.40	mm

Test temperature: -196 °C

Analysis of Results

Fracture type = stable tearing

Critical Fracture Toughness

J_Q = 267.44 kJ/m²

TM = 69.5 MPa

QUALIFICATION OF DATA

Estimates of initial crack size:	$a_{0q,1}$ =	5.235	mm	Diff :	0.005	< 0.002W =	0.0200	mm
	$a_{0q,2}$ =	5.246	mm		0.005	< 0.002W =	0.0200	mm
	$a_{0,q3}$ =	5.240	mm		0.000	< 0.002W =	0.0200	mm
	$a_{0,qmean}$ =	5.241	mm					

Qualification of data

Crack extension prediction	Δa_p =	1.77	mm (measured)	
	Δa_{pred} =	1.40	mm (predicted)	
	Difference =	-0.37	mm	PREDICTION NOT ACCEPTABLE

J_Q - Qualification of data

Power coefficient C_2 =	0.383282	< 1.0	→ QUALIFIED
$\lvert a_{0q} - a_0 \rvert$ =	0.00	mm	→ DATA SET ADEQUATE
# of data available to calculate a_{0q} :	7	< 8	→ DATA SET NOT ADEQUATE
# of data between $0.4J_q$ and J_q :	11	≥ 3	→ QUALIFIED
Correlation coefficient a_{0q} fit :	0.990	≥ 0.96	→ DATA SET ADEQUATE

Data points distribution : VALID
Number of qualified data points : VALID

Qualification of J_Q as J_{Ic}

Thickness B =	10.03	mm > 10 JQ/Sy	→ QUALIFIED
Initial ligament b_0 =	4.74	mm > 10 JQ/Sy	→ QUALIFIED

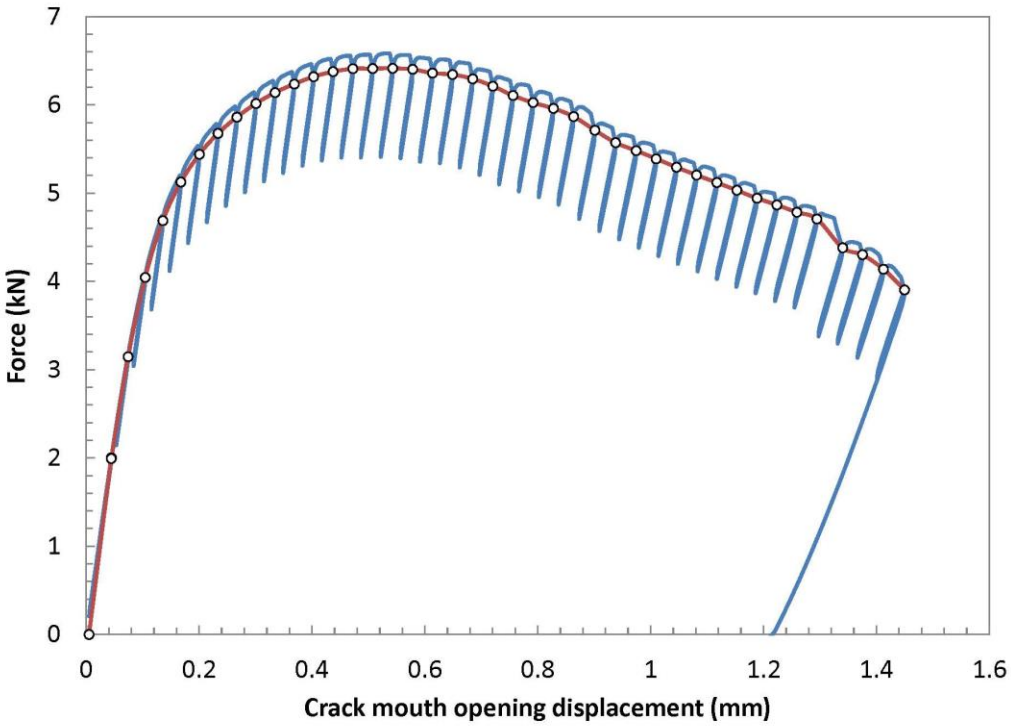
Force (kN)
Crack mouth opening displacement (mm)
0
1
2
3
4
5
6
7
0
0.2
0.4
0.6
0.8
1
1.2
1.4
1.6

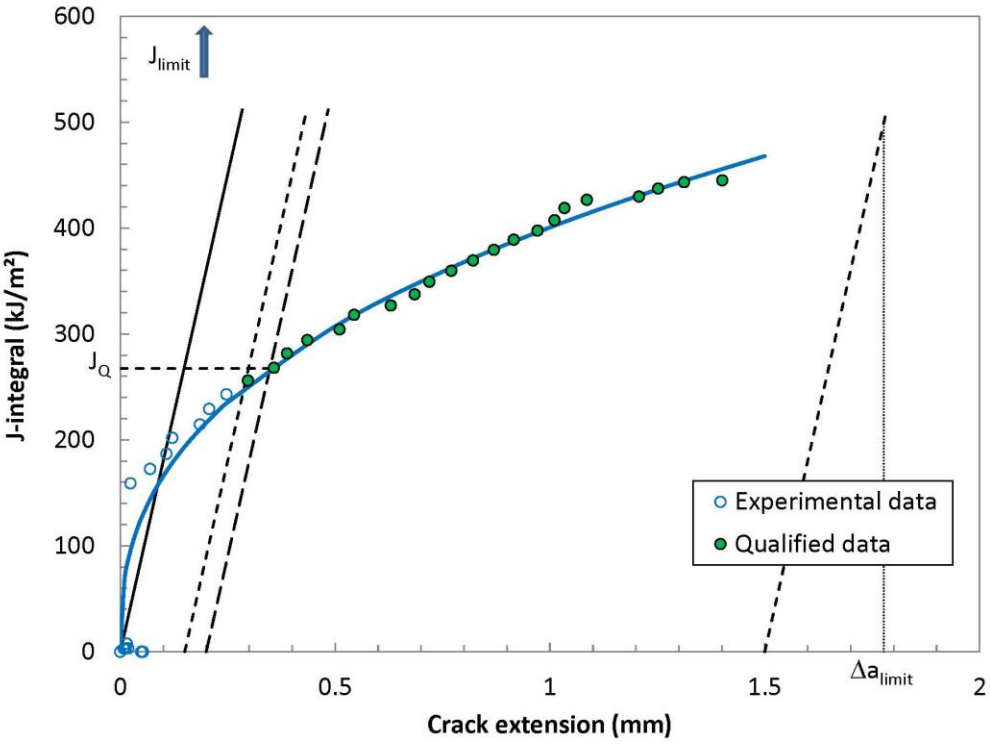
J-integral (kJ/m²)
Crack extension (mm)
J_limit
J_Q
Δa_limit
Experimental data
Qualified data
0
100
200
300
400
500
600
0
0.5
1
1.5
2

TEST REPORT

Specimen Information

Type = SE(B)
Identification = W1-F12
Orientation = N/A

Basic dimensions

B =	10.03	mm
B_N =	8.00	mm
W =	10.02	mm

Other dimensions

S =	40.00	mm

Tensile Properties

E =	192	MPa
ν =	0.3	
σ_{YS} =	582.0	MPa
σ_{TS} =	1221.0	MPa

Crack Size Information

a_0 =	5.35	mm
a_{0q} =	5.27	mm
a_f =	8.41	mm
Δa_p =	3.06	mm
$\Delta a_{predicted}$ =	2.96	mm

Test temperature: -196 °C

Analysis of Results

Fracture type = stable tearing

Critical Fracture Toughness

J_Q = 89.28 kJ/m²

TM = 14.0 MPa

QUALIFICATION OF DATA

Estimates of initial crack size:

$a_{0q,1}$ =	5.360	mm	Diff :	0.004	< 0.002W =	0.0200	mm
$a_{0q,2}$ =	5.355	mm		0.001	< 0.002W =	0.0200	mm
$a_{0,q3}$ =	5.354	mm		0.003	< 0.002W =	0.0200	mm
$a_{0,qmean}$ =	5.356	mm					

Qualification of data

Crack extension prediction	Δa_p =	3.06	mm (measured)	
	Δa_{pred} =	2.96	mm (predicted)	
	Difference =	-0.10	mm	(PREDICTION ACCEPTABLE)

J_Q - Qualification of data

Power coefficient C_2 =	0.165488	< 1.0	→ QUALIFIED
$\lvert a_{0q} - a_0 \rvert$ =	0.08	mm	→ DATA SET ADEQUATE
# of data available to calculate a_{0q} :	3	< 8	→ DATA SET NOT ADEQUATE
# of data between $0.4J_q$ and J_q :	5	≥ 3	→ QUALIFIED
Correlation coefficient a_{0q} fit :	1.000	≥ 0.96	→ DATA SET ADEQUATE
Data points distribution :	VALID		
Number of qualified data points :	VALID		

Qualification of J_Q as J_{Ic}

Thickness B =	10.03	mm > 10 JQ/Sy	→ QUALIFIED
Initial ligament b_0 =	4.67	mm > 10 JQ/Sy	→ QUALIFIED

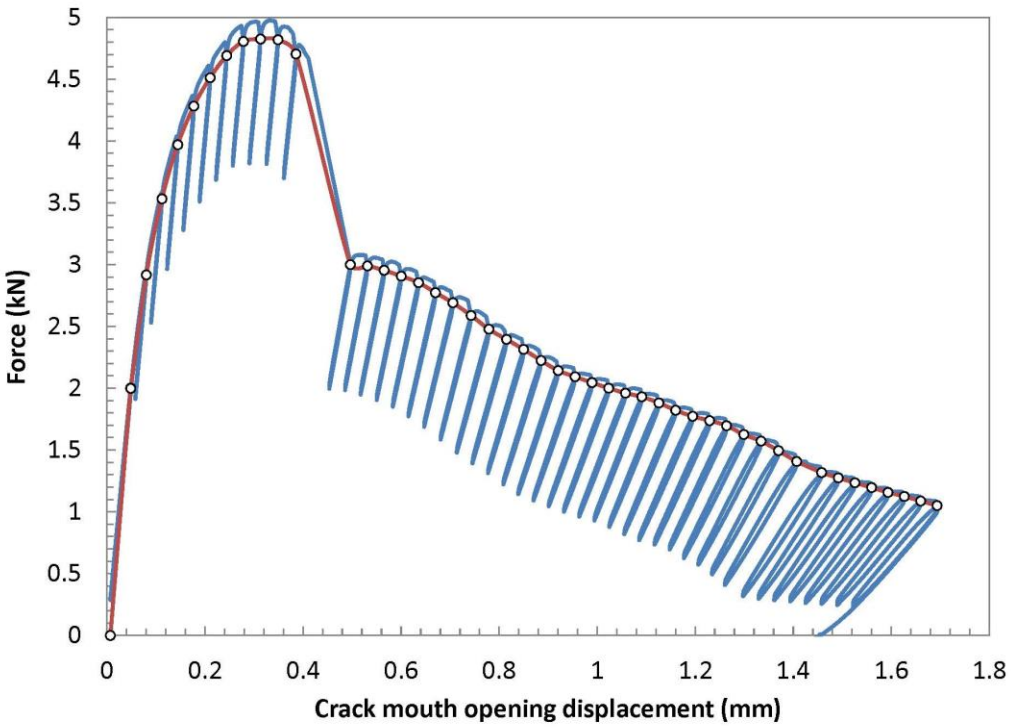
Force (kN)
Crack mouth opening displacement (mm)
0
0.5
1
1.5
2
2.5
3
3.5
4
4.5
5
0
0.2
0.4
0.6
0.8
1
1.2
1.4
1.6
1.8

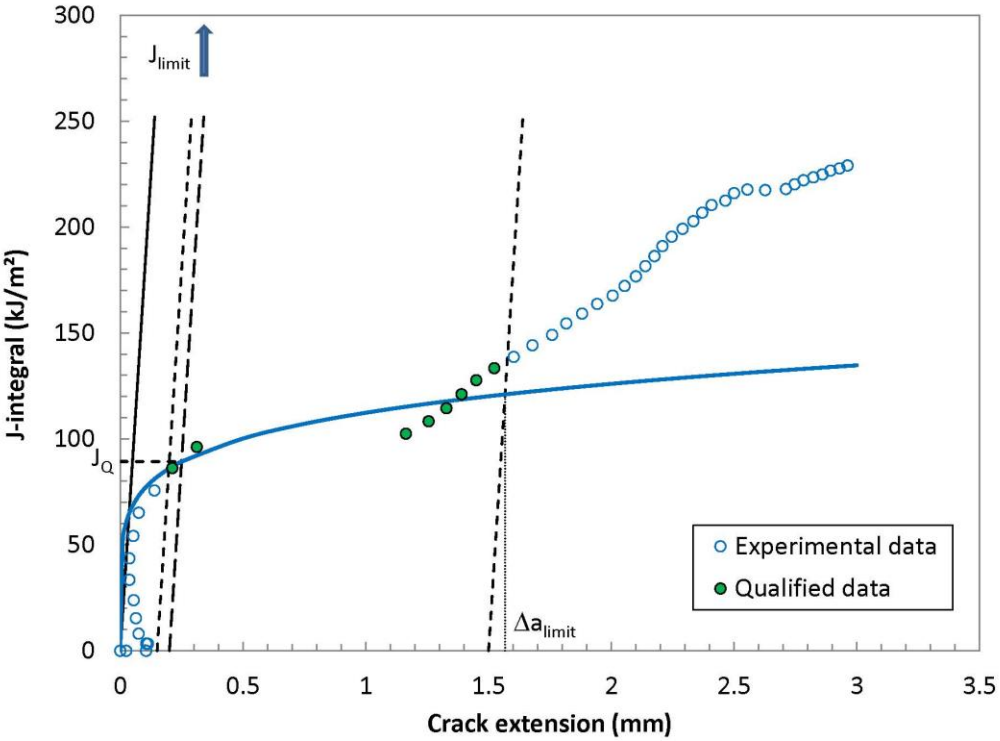
J-integral (kJ/m²)
Crack extension (mm)
J_limit
J_Q
Δa_limit
Experimental data
Qualified data
0
50
100
150
200
250
300
0
0.5
1
1.5
2
2.5
3
3.5

TEST REPORT

Specimen Information

Type = SE(B)
Identification = W1-F13
Orientation = N/A

Basic dimensions

B =	10.05	mm
B_N =	8.01	mm
W =	10.03	mm

Other dimensions

S =	40.00	mm

Tensile Properties

E =	192	MPa
ν =	0.3	
σ_{YS} =	582.0	MPa
σ_{TS} =	1221.0	MPa

Crack Size Information

a_0 =	5.36	mm
a_{0q} =	5.17	mm
a_f =	8.71	mm
Δa_p =	3.35	mm
$\Delta a_{predicted}$ =	3.31	mm

Test temperature: -196 °C

Analysis of Results

Fracture type = stable tearing

Critical Fracture Toughness

J_Q = 100.52 kJ/m²

TM = 34.2 MPa

QUALIFICATION OF DATA

Estimates of initial crack size:

$a_{0q,1}$ =	5.227	mm	Diff :	0.004	< 0.002W =	0.0201	mm
$a_{0q,2}$ =	5.230	mm		0.001	< 0.002W =	0.0201	mm
$a_{0,q3}$ =	5.236	mm		0.005	< 0.002W =	0.0201	mm
$a_{0,qmean}$ =	5.231	mm					

Qualification of data				
Crack extension prediction	Δa_p =	3.35	mm (measured)	
	Δa_{pred} =	3.31	mm (predicted)	
	Difference =	-0.04	mm	(PREDICTION ACCEPTABLE)

J_Q - Qualification of data			
Power coefficient C_2 =	0.368659	< 1.0	→ QUALIFIED
$\lvert a_{0q} - a_0 \rvert$ =	0.19 mm		→ DATA SET ADEQUATE
# of data available to calculate a_{0q} :	6	< 8	→ DATA SET NOT ADEQUATE
# of data between $0.4J_q$ and J_q :	6	≥ 3	→ QUALIFIED
Correlation coefficient a_{0q} fit :	0.953	< 0.96	→ DATA SET NOT ADEQUATE
Data points distribution : VALID			
Number of qualified data points : VALID			

Qualification of J_Q as J_{Ic}			
Thickness B =	10.05	mm > 10 JQ/Sy	→ QUALIFIED
Initial ligament b_0 =	4.67	mm > 10 JQ/Sy	→ QUALIFIED

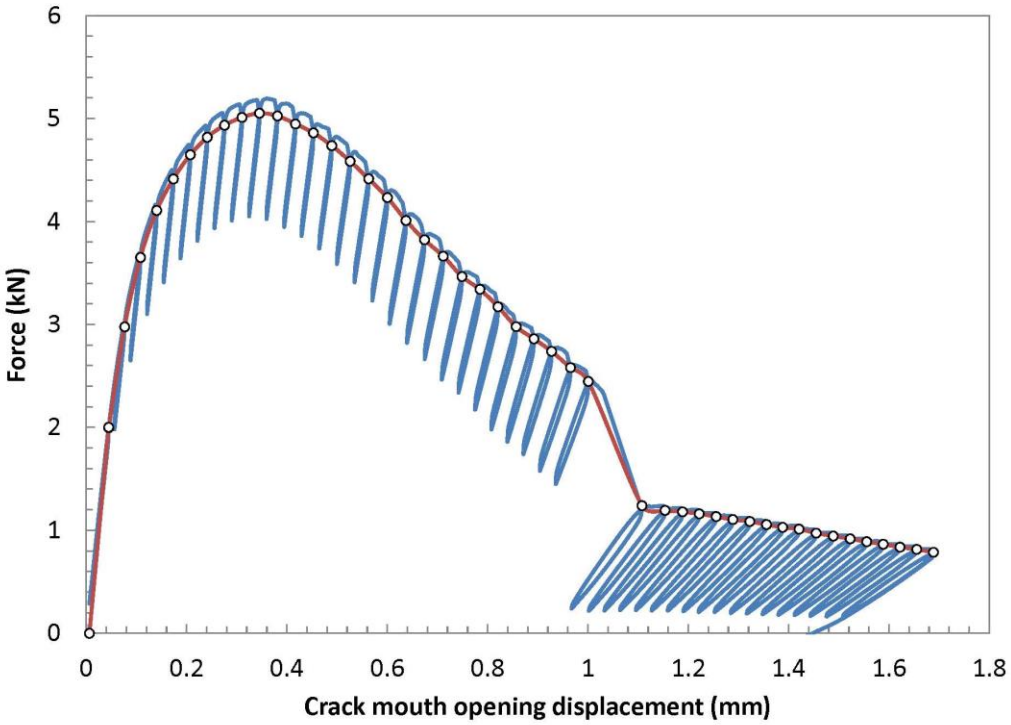
Force (kN)
Crack mouth opening displacement (mm)
0
1
2
3
4
5
6
0
0.2
0.4
0.6
0.8
1
1.2
1.4
1.6
1.8

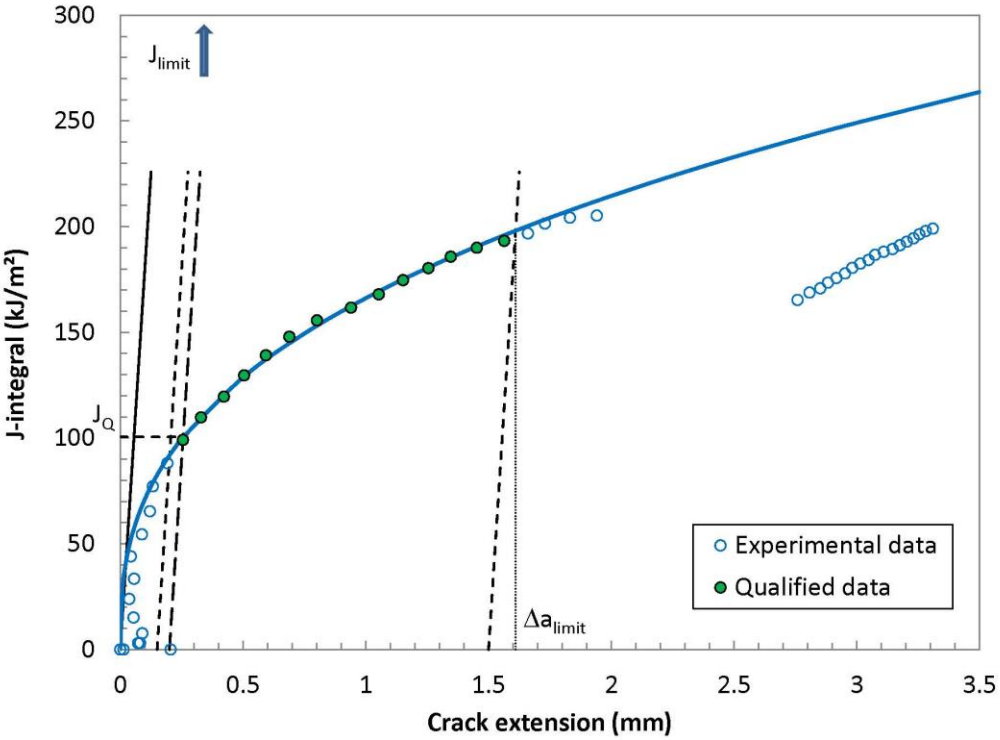
J-integral (kJ/m²)
Crack extension (mm)
J_limit
J_Q
Δa_limit
Experimental data
Qualified data
0
50
100
150
200
250
300
0
0.5
1
1.5
2
2.5
3
3.5

TEST REPORT

Specimen Information

Type = SE(B)
Identification = W1-F14
Orientation = N/A

Basic dimensions

B =	10.04	mm
B_N =	8.01	mm
W =	10.04	mm

Other dimensions

S =	40.00	mm

Tensile Properties

E =	192	MPa
ν =	0.3	
σ_{YS} =	582.0	MPa
σ_{TS} =	1221.0	MPa

Crack Size Information

a_0 =	5.34	mm
a_{0q} =	5.24	mm
a_f =	8.72	mm
Δa_p =	3.39	mm
$\Delta a_{predicted}$ =	3.24	mm

Test temperature: -196 °C

Analysis of Results

Fracture type = stable tearing

Critical Fracture Toughness

J_Q = 46.00 kJ/m²

TM = 22.5 MPa

QUALIFICATION OF DATA

Estimates of initial crack size:	$a_{0q,1}$ =	5.226	mm	Diff :	0.013	< 0.002W =	0.0201	mm
	$a_{0q,2}$ =	5.243	mm		0.004	< 0.002W =	0.0201	mm
	$a_{0,q3}$ =	5.248	mm		0.009	< 0.002W =	0.0201	mm
	$a_{0,qmean}$ =	5.239	mm					

Qualification of data

Crack extension prediction	Δa_p =	3.39	mm (measured)	
	Δa_{pred} =	3.24	mm (predicted)	
	Difference =	-0.15	mm	PREDICTION NOT ACCEPTABLE

J_Q - Qualification of data

Power coefficient C_2 =	0.466923	< 1.0	→ QUALIFIED
$\lvert a_{0q} - a_0 \rvert$ =	0.10	mm	→ DATA SET ADEQUATE
# of data available to calculate a_{0q} :	5	< 8	→ DATA SET NOT ADEQUATE
# of data between $0.4J_q$ and J_q :	2	< 3	→ NOT QUALIFIED
Correlation coefficient a_{0q} fit :	0.895	< 0.96	→ DATA SET NOT ADEQUATE

Data points distribution : VALID
Number of qualified data points : NOT VALID

Qualification of J_Q as J_{Ic}

Thickness B =	10.04	mm > 10 JQ/Sy	→ QUALIFIED
Initial ligament b_0 =	4.70	mm > 10 JQ/Sy	→ QUALIFIED

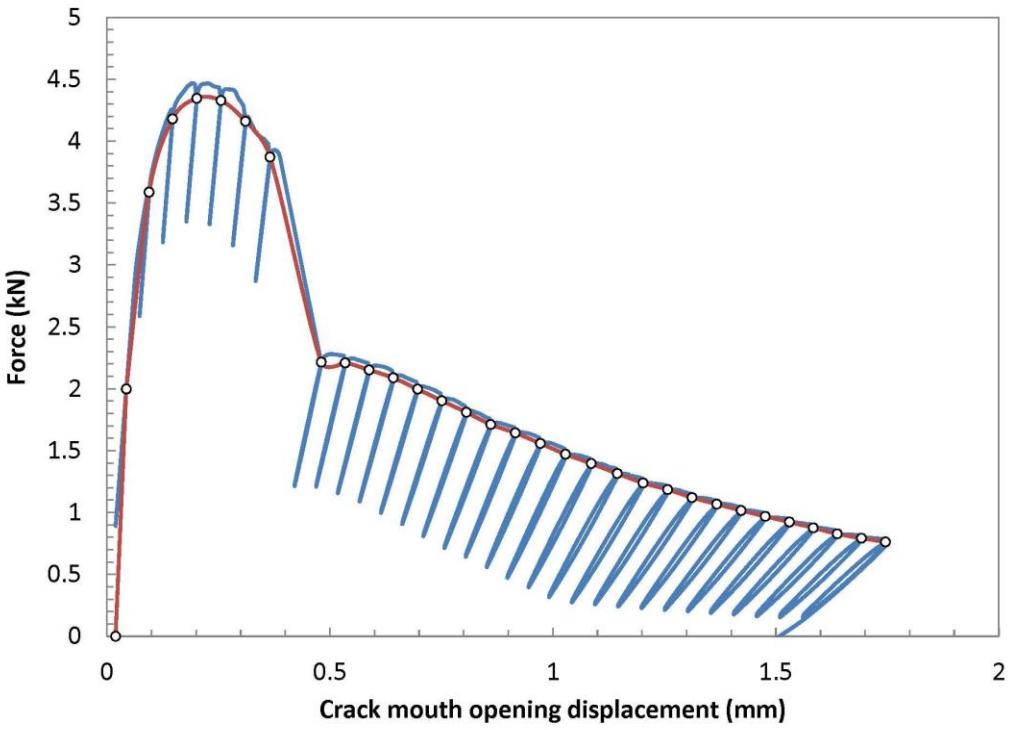
Force (kN)
Crack mouth opening displacement (mm)
0
0.5
1
1.5
2
2.5
3
3.5
4
4.5
5

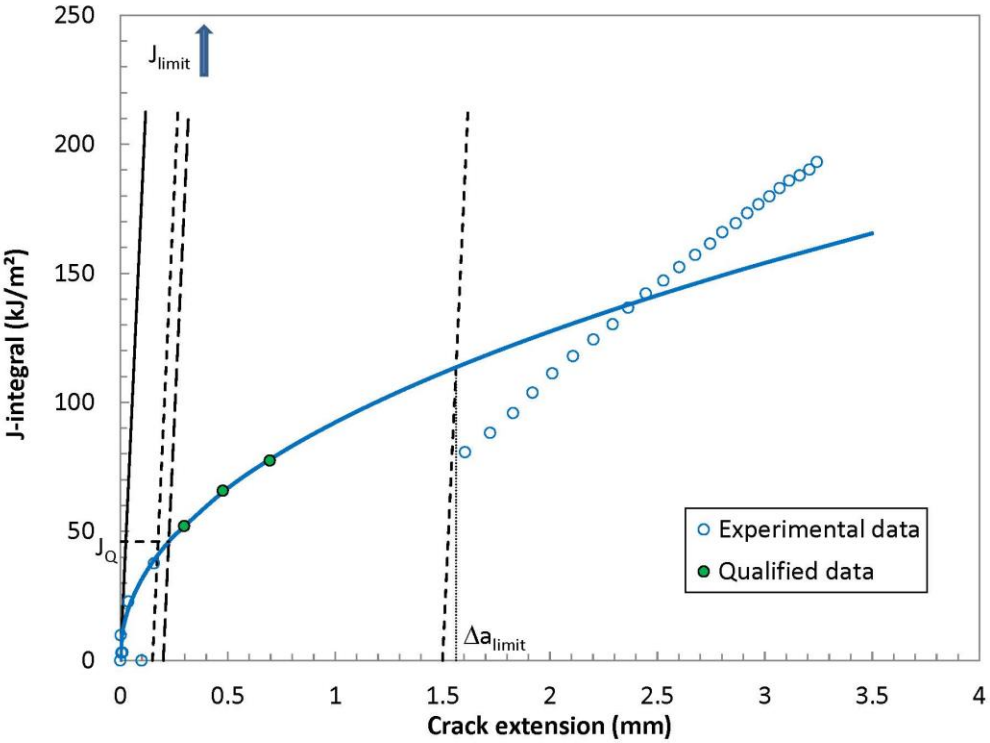
J-integral (kJ/m²)
Crack extension (mm)
J_limit
J_Q
Δa_limit
Experimental data
Qualified data
0
50
100
150
200
250
0.5
1
1.5
2
2.5
3
3.5
4

Weld W2, T = 77 K

TEST REPORT

Specimen Information

Type = SE(B)
Identification = W2-F8
Orientation = N/A

Basic dimensions

B =	10.02	mm
B_N =	8.01	mm
W =	10.02	mm

Other dimensions

S =	40.00	mm

Tensile Properties

E =	173	MPa
ν =	0.3	
σ_{YS} =	581.0	MPa
σ_{TS} =	1220.0	MPa

Crack Size Information

a_0 =	5.18	mm
a_{0q} =	4.85	mm
a_f =	6.75	mm
Δa_p =	1.57	mm
$\Delta a_{predicted}$ =	1.49	mm

Test temperature: -196 °C

Analysis of Results

Fracture type = stable tearing

Critical Fracture Toughness

J_Ic = 228.13 kJ/m²

TM = 68.2 MPa

QUALIFICATION OF DATA

Estimates of initial crack size:	$a_{0q,1}$ =	4.838	mm	Diff :	0.001	< 0.002W =	0.0200	mm
	$a_{0q,2}$ =	4.839	mm		0.000	< 0.002W =	0.0200	mm
	a_{0q3} =	4.840	mm		0.001	< 0.002W =	0.0200	mm
	$a_{0,qmean}$ =	4.839	mm					

Qualification of data

Crack extension prediction	Δa_p =	1.57	mm (measured)	
	Δa_{pred} =	1.49	mm (predicted)	
	Difference =	-0.07	mm	(PREDICTION ACCEPTABLE)

J_Q - Qualification of data

Power coefficient C_2 =	0.457869	< 1.0	→ QUALIFIED
$\lvert a_{0q} - a_0 \rvert$ =	0.33	mm	→ DATA SET ADEQUATE
# of data available to calculate a_{0q} :	17	≥ 8	→ DATA SET ADEQUATE
# of data between 0.4J_q and J_q :	9	≥ 3	→ QUALIFIED
Correlation coefficient a_{0q} fit :	0.966	≥ 0.96	→ DATA SET ADEQUATE
Data points distribution :	VALID		
Number of qualified data points :	VALID		

Qualification of J_Q as J_{Ic}

Thickness B =	10.02	mm > 10 JQ/Sy	→ QUALIFIED
Initial ligament b_0 =	4.83	mm > 10 JQ/Sy	→ QUALIFIED

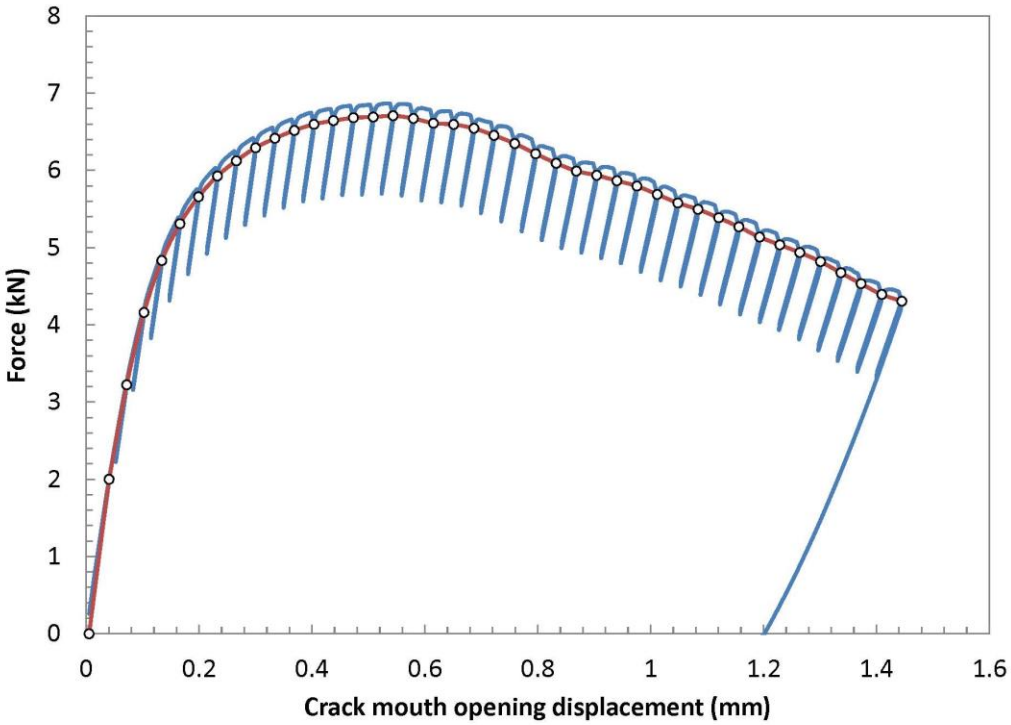
Force (kN)
Crack mouth opening displacement (mm)
0
1
2
3
4
5
6
7
8
0
0.2
0.4
0.6
0.8
1
1.2
1.4
1.6

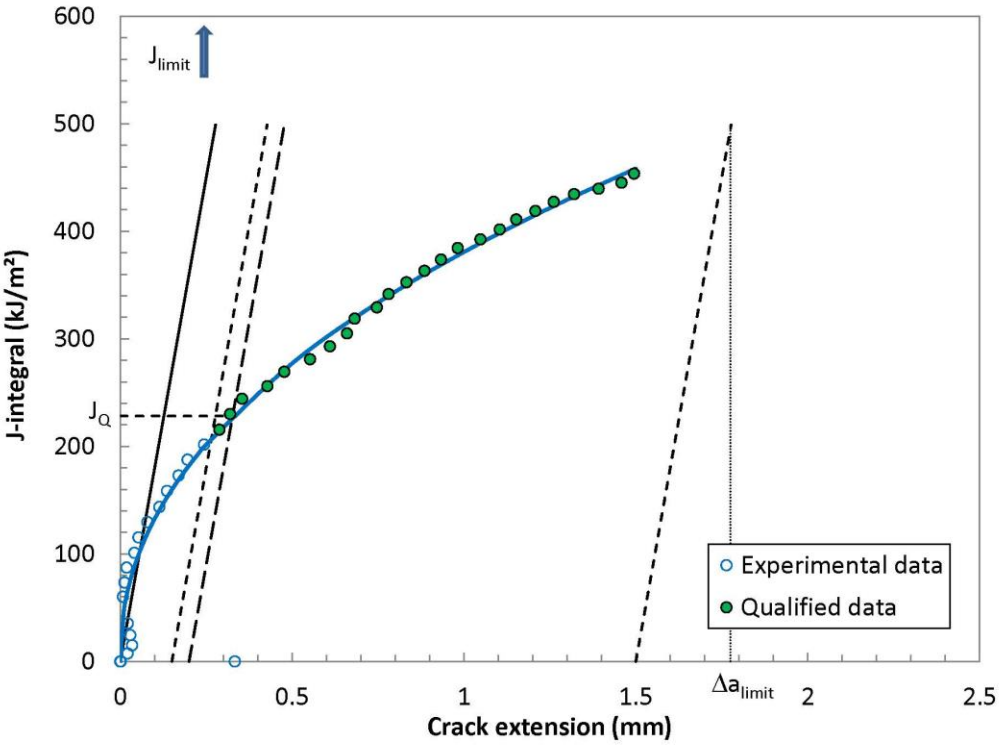
J-integral (kJ/m²)
Crack extension (mm)
J_limit
J_Q
Δa_limit
Experimental data
Qualified data
0
100
200
300
400
500
600
0
0.5
1
1.5
2
2.5

TEST REPORT

Specimen Information

Type = SE(B)
Identification = W2-F9
Orientation = N/A

Basic dimensions

B =	10.01	mm
B_N =	8.00	mm
W =	10.03	mm

Other dimensions

S =	40.00	mm

Tensile Properties

E =	173	MPa
ν =	0.3	
σ_{YS} =	581.0	MPa
σ_{TS} =	1220.0	MPa

Crack Size Information

a_0 =	5.22	mm
a_{0q} =	5.00	mm
a_f =	7.09	mm
Δa_p =	1.86	mm
$\Delta a_{predicted}$ =	1.80	mm

Test temperature: -196 °C

Analysis of Results

Fracture type = stable tearing

Critical Fracture Toughness

J_Ic = 243.67 kJ/m²

TM = 47.3 MPa

QUALIFICATION OF DATA

Estimates of initial crack size:	$a_{0q,1}$ =	5.043	mm	Diff :	0.001	< 0.002W =	0.0201	mm
	$a_{0q,2}$ =	5.045	mm		0.001	< 0.002W =	0.0201	mm
	$a_{0,q3}$ =	5.044	mm		0.000	< 0.002W =	0.0201	mm
	$a_{0,qmean}$ =	5.044	mm					

Qualification of data

Crack extension prediction	Δa_p =	1.86	mm (measured)	
	Δa_{pred} =	1.80	mm (predicted)	
	Difference =	-0.06	mm	(PREDICTION ACCEPTABLE)

J_Q - Qualification of data

Power coefficient C_2 =	0.30534	< 1.0	→ QUALIFIED
$\lvert a_{0q} - a_0 \rvert$ =	0.23	mm	→ DATA SET ADEQUATE
# of data available to calculate a_{0q} :	9	≥ 8	→ DATA SET ADEQUATE
# of data between $0.4J_q$ and J_q :	10	≥ 3	→ QUALIFIED
Correlation coefficient a_{0q} fit :	0.999	≥ 0.96	→ DATA SET ADEQUATE

Data points distribution : VALID
Number of qualified data points : VALID

Qualification of J_Q as J_{Ic}

Thickness B =	10.01	mm > 10 JQ/Sy	→ QUALIFIED
Initial ligament b_0 =	4.80	mm > 10 JQ/Sy	→ QUALIFIED

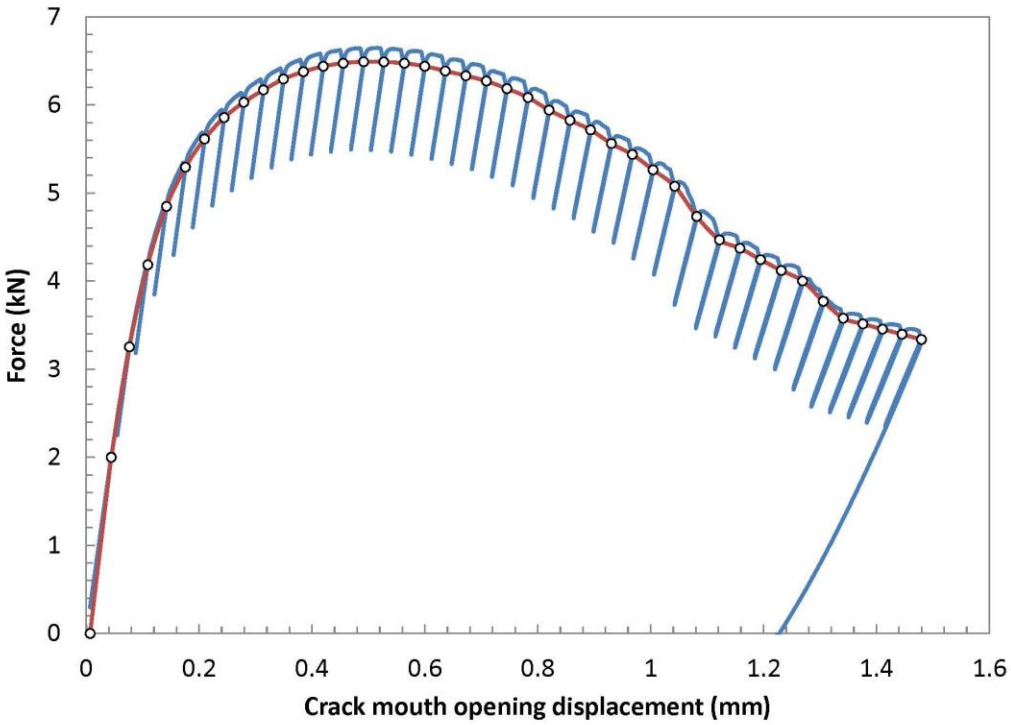
Force (kN)
Crack mouth opening displacement (mm)
0
1
2
3
4
5
6
7
0
0.2
0.4
0.6
0.8
1
1.2
1.4
1.6

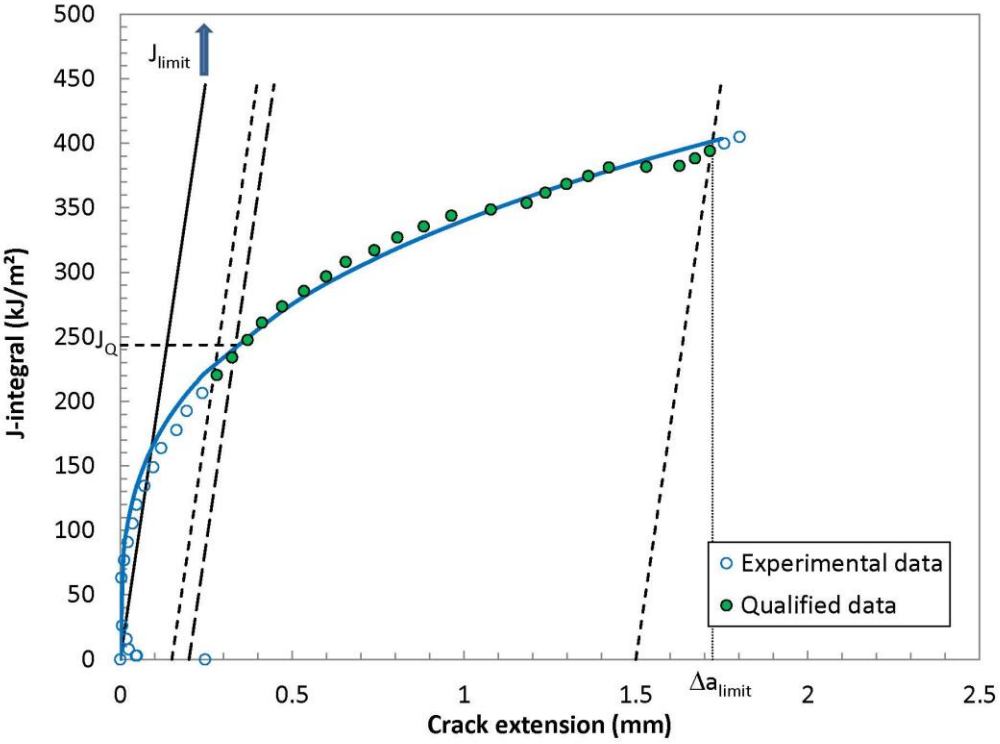
J-integral (kJ/m²)
Crack extension (mm)
J_limit
J_Q
Δa_limit
Experimental data
Qualified data
0
50
100
150
200
250
300
350
400
450
500
0
0.5
1
1.5
2
2.5

TEST REPORT

Specimen Information

Type = SE(B)
Identification = W2-F10
Orientation = N/A

Basic dimensions

B =	10.02	mm
B_N =	8.01	mm
W =	10.03	mm

Other dimensions

S =	40.00	mm

Tensile Properties

E =	173	MPa
ν =	0.3	
σ_{YS} =	581.0	MPa
σ_{TS} =	1220.0	MPa

Crack Size Information

a_0 =	5.30	mm
a_{0q} =	4.90	mm
a_f =	7.23	mm
Δa_p =	1.93	mm
$\Delta a_{predicted}$ =	1.90	mm

Test temperature: -196 °C

Analysis of Results

Fracture type = stable tearing

Critical Fracture Toughness

J_Q = 162.15 kJ/m²

TM = 64.0 MPa

QUALIFICATION OF DATA

Estimates of initial crack size:	$a_{0q,1}$ =	4.927	mm	Diff :	0.002	< 0.002W =	0.0201 mm
	$a_{0q,2}$ =	4.921	mm		0.005	< 0.002W =	0.0201 mm
	$a_{0,q3}$ =	4.928	mm		0.003	< 0.002W =	0.0201 mm
	$a_{0,qmean}$ =	4.925	mm				

Qualification of data

Crack extension prediction	Δa_p =	1.93	mm (measured)	
	Δa_{pred} =	1.90	mm (predicted)	
	Difference =	-0.03	mm	(PREDICTION ACCEPTABLE)

J_Q - Qualification of data

Power coefficient C_2 =	0.536198	< 1.0	→ QUALIFIED
$\lvert a_{0q} - a_0 \rvert$ =	0.40	mm	→ DATA SET ADEQUATE
# of data available to calculate a_{0q} :	5	< 8	→ DATA SET NOT ADEQUATE
# of data between $0.4J_q$ and J_q :	7	≥ 3	→ QUALIFIED
Correlation coefficient a_{0q} fit :	0.578	< 0.96	→ DATA SET NOT ADEQUATE
Data points distribution :	VALID		
Number of qualified data points :	VALID		

Qualification of J_Q as J_{Ic}

Thickness B =	10.02	mm > 10 JQ/Sy	→ QUALIFIED
Initial ligament b_0 =	4.73	mm > 10 JQ/Sy	→ QUALIFIED

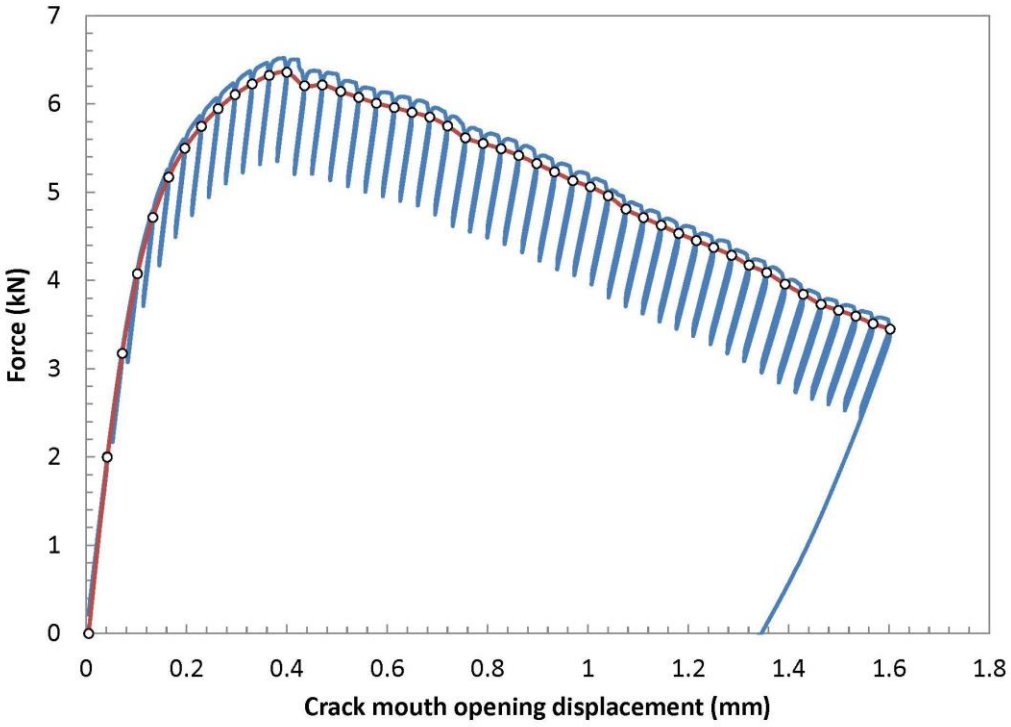
Force (kN)
Crack mouth opening displacement (mm)
0
1
2
3
4
5
6
7
0
0.2
0.4
0.6
0.8
1
1.2
1.4
1.6
1.8

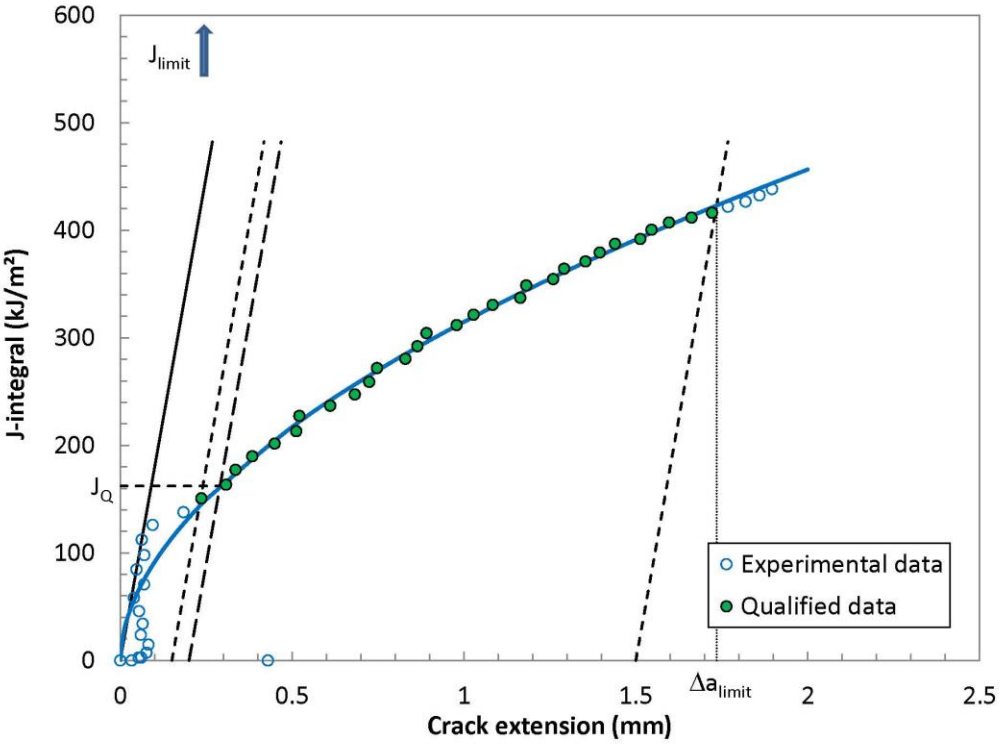
J-integral (kJ/m²)
Crack extension (mm)
J_limit
J_Q
Δa_limit
Experimental data
Qualified data
0
100
200
300
400
500
600
0
0.5
1
1.5
2
2.5

TEST REPORT

Specimen Information

Type = SE(B)
Identification = W2-F11
Orientation = N/A

Basic dimensions

B =	10.02	mm
B_N =	8.00	mm
W =	10.02	mm

Other dimensions

S =	40.00	mm

Tensile Properties

E =	173	MPa
ν =	0.3	
σ_{YS} =	581.0	MPa
σ_{TS} =	1220.0	MPa

Crack Size Information

a_0 =	5.22	mm
a_{0q} =	4.94	mm
a_f =	7.37	mm
Δa_p =	2.15	mm
$\Delta a_{predicted}$ =	2.09	mm

Test temperature: -196 °C

Analysis of Results

Fracture type = stable tearing

Critical Fracture Toughness

J_Ic = 238.23 kJ/m²

TM = 49.2 MPa

QUALIFICATION OF DATA

Estimates of initial crack size:

$a_{0q,1}$ =	4.988	mm	Diff :	0.001	< 0.002W =	0.0200	mm
$a_{0q,2}$ =	4.983	mm		0.004	< 0.002W =	0.0200	mm
a_{0q3} =	4.989	mm		0.003	< 0.002W =	0.0200	mm
$a_{0,qmean}$ =	4.987	mm					

Qualification of data				
Crack extension prediction	Δa_p =	2.15	mm (measured)	
	Δa_{pred} =	2.09	mm (predicted)	
	Difference =	-0.06	mm	(PREDICTION ACCEPTABLE)

J_Q - Qualification of data			
Power coefficient C_2 =	0.32155	< 1.0	→ QUALIFIED
$\lvert a_{0q} - a_0 \rvert$ =	0.28	mm	→ DATA SET ADEQUATE
# of data available to calculate a_{0q} :	11	≥ 8	→ DATA SET ADEQUATE
# of data between $0.4J_q$ and J_q :	10	≥ 3	→ QUALIFIED
Correlation coefficient a_{0q} fit :	0.988	≥ 0.96	→ DATA SET ADEQUATE
Data points distribution :	VALID		
Number of qualified data points :	VALID		

Qualification of J_Q as J_{Ic}			
Thickness B =	10.02	mm > 10 JQ/Sy	→ QUALIFIED
Initial ligament b_0 =	4.80	mm > 10 JQ/Sy	→ QUALIFIED

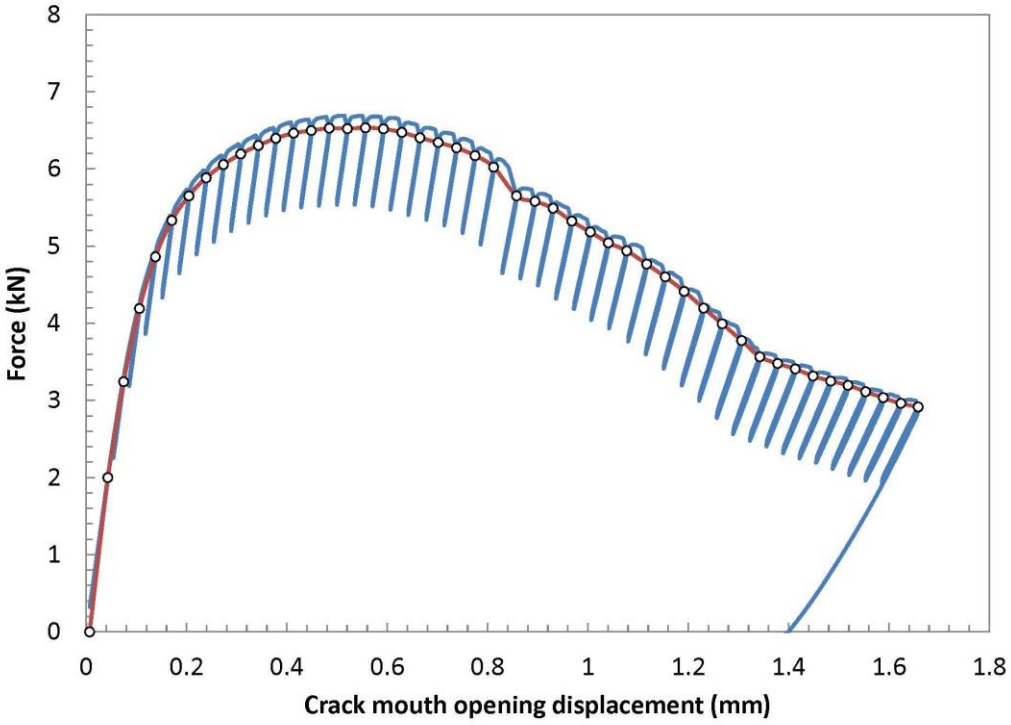
Force (kN)
Crack mouth opening displacement (mm)
0
1
2
3
4
5
6
7
8
0
0.2
0.4
0.6
0.8
1
1.2
1.4
1.6
1.8

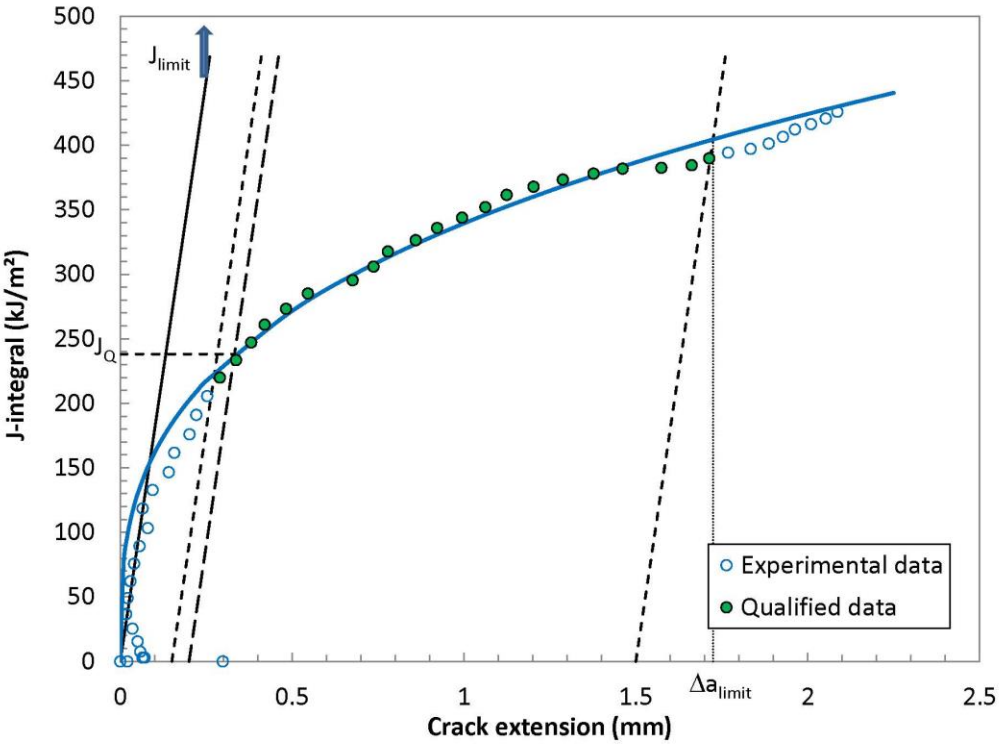
J-integral (kJ/m²)
Crack extension (mm)
J_limit
J_Q
Δa_limit
Experimental data
Qualified data
0
50
100
150
200
250
300
350
400
450
500
0
0.5
1
1.5
2
2.5

TEST REPORT

Specimen Information

Type = SE(B)
Identification = W2-F12
Orientation = N/A

Basic dimensions

B =	10.03	mm
B_N =	8.01	mm
W =	10.02	mm

Other dimensions

S =	40.00	mm

Tensile Properties

E =	173	MPa
ν =	0.3	
σ_{YS} =	581.0	MPa
σ_{TS} =	1220.0	MPa

Crack Size Information

a_0 =	5.16	mm
a_{0q} =	4.98	mm
a_f =	6.70	mm
Δa_p =	1.54	mm
$\Delta a_{predicted}$ =	1.40	mm

Test temperature: -196 °C

Analysis of Results

Fracture type = stable tearing

Critical Fracture Toughness

J_Ic = 224.73 kJ/m²

TM = 54.6 MPa

QUALIFICATION OF DATA

Estimates of initial crack size:	$a_{0q,1}$ =	5.032	mm	Diff :	0.004	< 0.002W =	0.0200 mm
	$a_{0q,2}$ =	5.041	mm		0.004	< 0.002W =	0.0200 mm
	$a_{0,q3}$ =	5.036	mm		0.000	< 0.002W =	0.0200 mm
	$a_{0,qmean}$ =	5.036	mm				

Qualification of data

Crack extension prediction	Δa_p =	1.54	mm (measured)	
	Δa_{pred} =	1.40	mm (predicted)	
	Difference =	-0.14	mm	(PREDICTION ACCEPTABLE)

J_Q - Qualification of data

Power coefficient C_2 =	0.36955	< 1.0	→ QUALIFIED
$\lvert a_{0q} - a_0 \rvert$ =	0.17	mm	→ DATA SET ADEQUATE
# of data available to calculate a_{0q} :	11	≥ 8	→ DATA SET ADEQUATE
# of data between $0.4J_q$ and J_q :	11	≥ 3	→ QUALIFIED
Correlation coefficient a_{0q} fit :	0.995	≥ 0.96	→ DATA SET ADEQUATE
Data points distribution :	VALID		
Number of qualified data points :	VALID		

Qualification of J_Q as J_{Ic}

Thickness B =	10.03	mm > 10 JQ/Sy	→ QUALIFIED
Initial ligament b_0 =	4.87	mm > 10 JQ/Sy	→ QUALIFIED

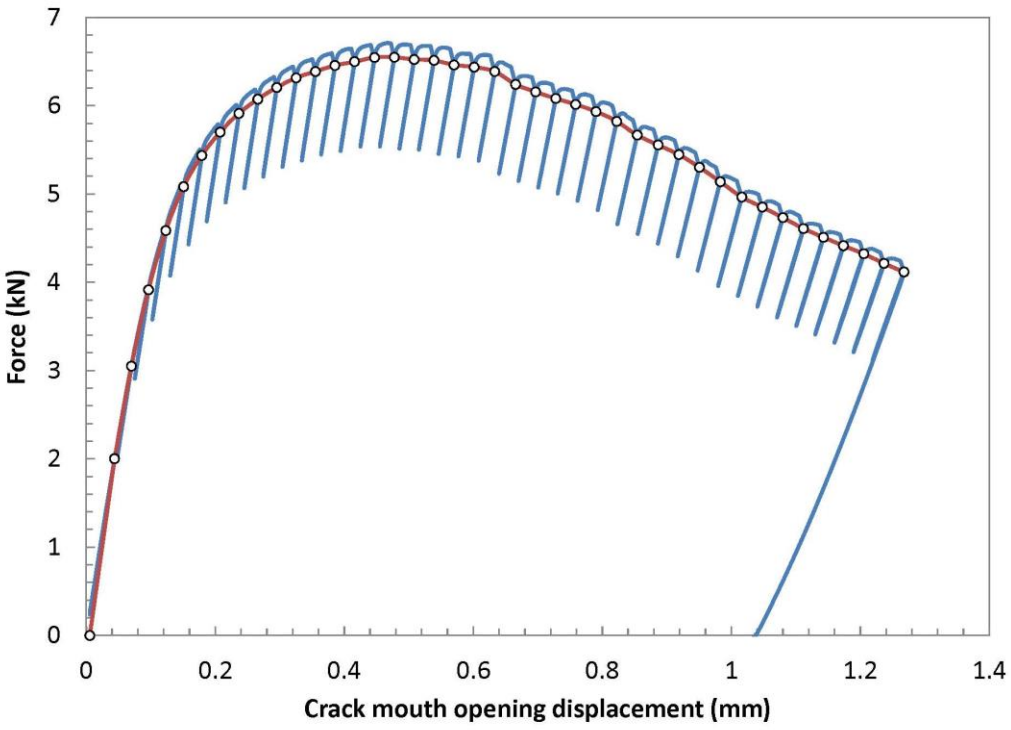
Force (kN)
Crack mouth opening displacement (mm)
0
1
2
3
4
5
6
7
0
0.2
0.4
0.6
0.8
1
1.2
1.4

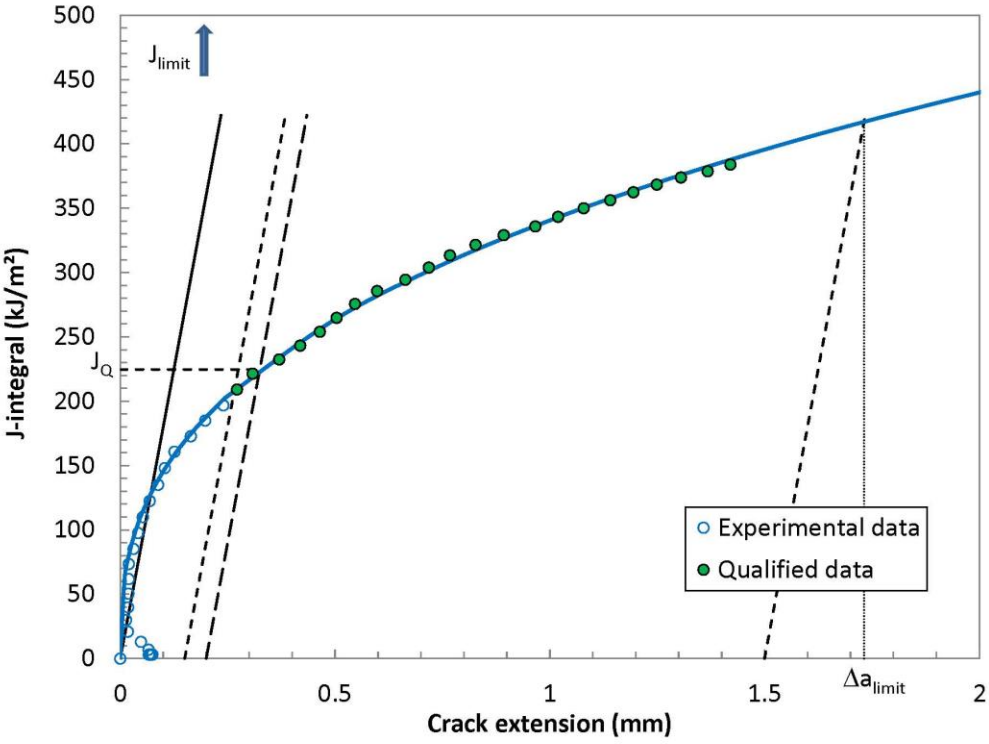
J-integral (kJ/m²)
Crack extension (mm)
J_limit
J_Q
Δa_limit
Experimental data
Qualified data
0
50
100
150
200
250
300
350
400
450
500
0
0.5
1
1.5
2

Weld W3, T = 77 K

TEST REPORT

Specimen Information

Type = SE(B)
Identification = W3-F8
Orientation = N/A

Basic dimensions

B =	10.02	mm
B_N =	7.98	mm
W =	10.02	mm

Other dimensions

S =	40.00	mm

Tensile Properties

E =	173	MPa
ν =	0.3	
σ_{YS} =	544.0	MPa
σ_{TS} =	1244.0	MPa

Crack Size Information

a_0 =	5.21	mm
a_{0q} =	4.92	mm
a_f =	7.00	mm
Δa_p =	1.79	mm
$\Delta a_{predicted}$ =	1.72	mm

Test temperature: -196 °C

Analysis of Results

Fracture type = stable tearing

Critical Fracture Toughness

J_Ic = 213.77 kJ/m²

TM = 37.7 MPa

QUALIFICATION OF DATA

Estimates of initial crack size:	$a_{0q,1}$ =	4.911	mm	Diff :	0.000	< 0.002W =	0.0200	mm
	$a_{0q,2}$ =	4.912	mm		0.000	< 0.002W =	0.0200	mm
	$a_{0,q3}$ =	4.912	mm		0.000	< 0.002W =	0.0200	mm
	$a_{0,qmean}$ =	4.912	mm					

Qualification of data

Crack extension prediction	Δa_p =	1.79	mm (measured)	
	Δa_{pred} =	1.72	mm (predicted)	
	Difference =	-0.07	mm	(PREDICTION ACCEPTABLE)

J_Q - Qualification of data

Power coefficient C_2 =	0.260591	< 1.0	→ QUALIFIED
$\lvert a_{0q} - a_0 \rvert$ =	0.29	mm	→ DATA SET ADEQUATE
# of data available to calculate a_{0q} :	17	≥ 8	→ DATA SET ADEQUATE
# of data between $0.4J_q$ and J_q :	11	≥ 3	→ QUALIFIED
Correlation coefficient a_{0q} fit :	0.961	≥ 0.96	→ DATA SET ADEQUATE
Data points distribution :	VALID		
Number of qualified data points :	VALID		

Qualification of J_Q as J_{Ic}

Thickness B =	10.02	mm > 10 JQ/Sy	→ QUALIFIED
Initial ligament b_0 =	4.81	mm > 10 JQ/Sy	→ QUALIFIED

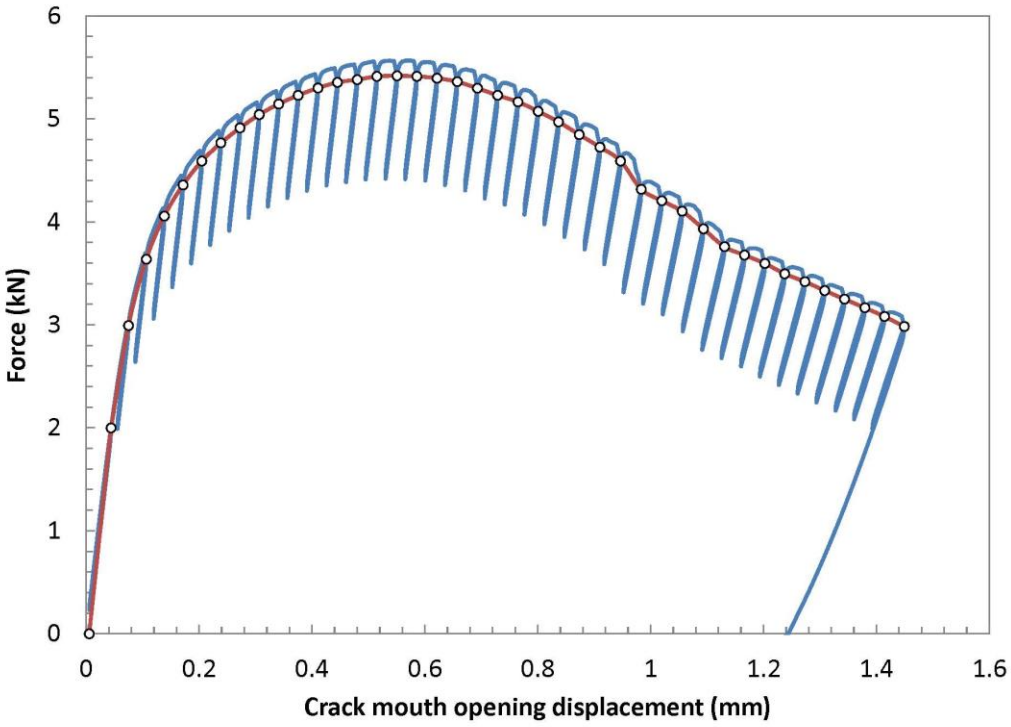
Force (kN)
Crack mouth opening displacement (mm)
0
1
2
3
4
5
6
0
0.2
0.4
0.6
0.8
1
1.2
1.4
1.6

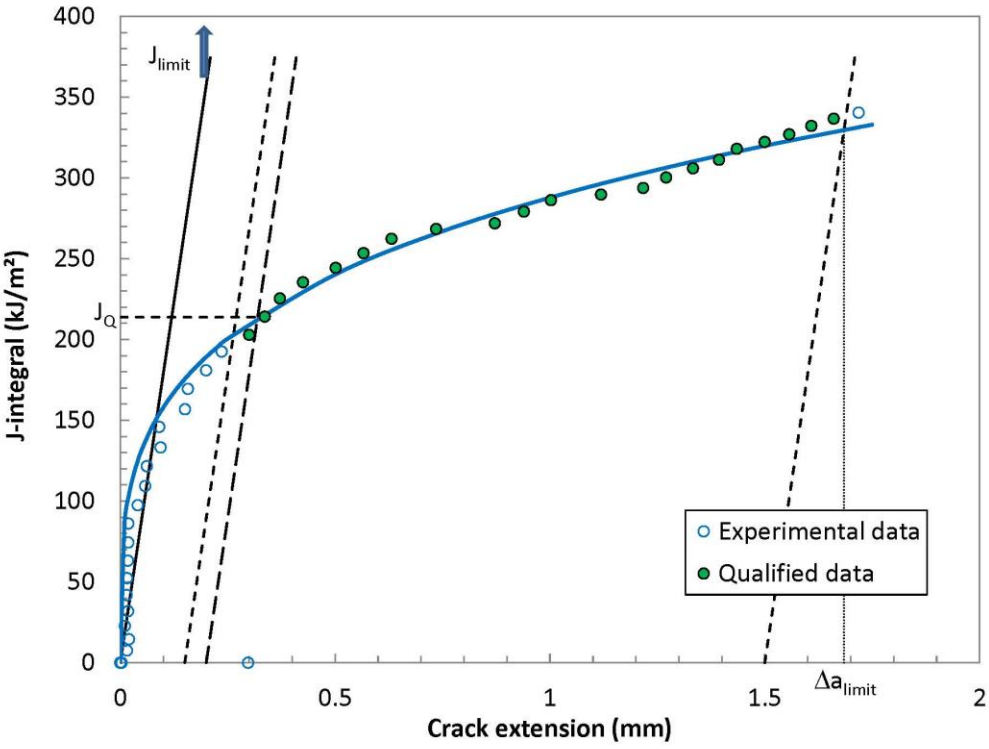
J-integral (kJ/m²)
Crack extension (mm)
J_limit
J_Q
Δa_limit
Experimental data
Qualified data
0
50
100
150
200
250
300
350
400
0
0.5
1
1.5
2

TEST REPORT

Specimen Information

Type = SE(B)
Identification = W3-F9
Orientation = N/A

Basic dimensions

B =	10.02	mm
B_N =	8.02	mm
W =	9.97	mm

Other dimensions

S =	40.00	mm

Tensile Properties

E =	173	MPa
ν =	0.3	
σ_{YS} =	544.0	MPa
σ_{TS} =	1244.0	MPa

Crack Size Information

a_0 =	5.24	mm
a_{0q} =	5.00	mm
a_f =	7.21	mm
Δa_p =	1.97	mm
$\Delta a_{predicted}$ =	1.88	mm

Test temperature: -196 °C

Analysis of Results

Fracture type = stable tearing

Critical Fracture Toughness

J_Ic = 189.07 kJ/m²

TM = 37.4 MPa

QUALIFICATION OF DATA

Estimates of initial crack size:	$a_{0q,1}$ =	5.046	mm	Diff :	0.001	< 0.002W =	0.0199	mm
	$a_{0q,2}$ =	5.044	mm		0.001	< 0.002W =	0.0199	mm
	$a_{0,q3}$ =	5.045	mm		0.000	< 0.002W =	0.0199	mm
	$a_{0,qmean}$ =	5.045	mm					

Qualification of data

Crack extension prediction	Δa_p =	1.97	mm (measured)	
	Δa_{pred} =	1.88	mm (predicted)	
	Difference =	-0.09	mm	(PREDICTION ACCEPTABLE)

J_Q - Qualification of data

Power coefficient C_2 =	0.279189	< 1.0	→ QUALIFIED
$\lvert a_{0q} - a_0 \rvert$ =	0.24	mm	→ DATA SET ADEQUATE
# of data available to calculate a_{0q} :	11	≥ 8	→ DATA SET ADEQUATE
# of data between $0.4J_q$ and J_q :	10	≥ 3	→ QUALIFIED
Correlation coefficient a_{0q} fit :	0.999	≥ 0.96	→ DATA SET ADEQUATE
Data points distribution :	VALID		
Number of qualified data points :	VALID		

Qualification of J_Q as J_{Ic}

Thickness B =	10.02	mm > 10 JQ/Sy	→ QUALIFIED
Initial ligament b_0 =	4.73	mm > 10 JQ/Sy	→ QUALIFIED

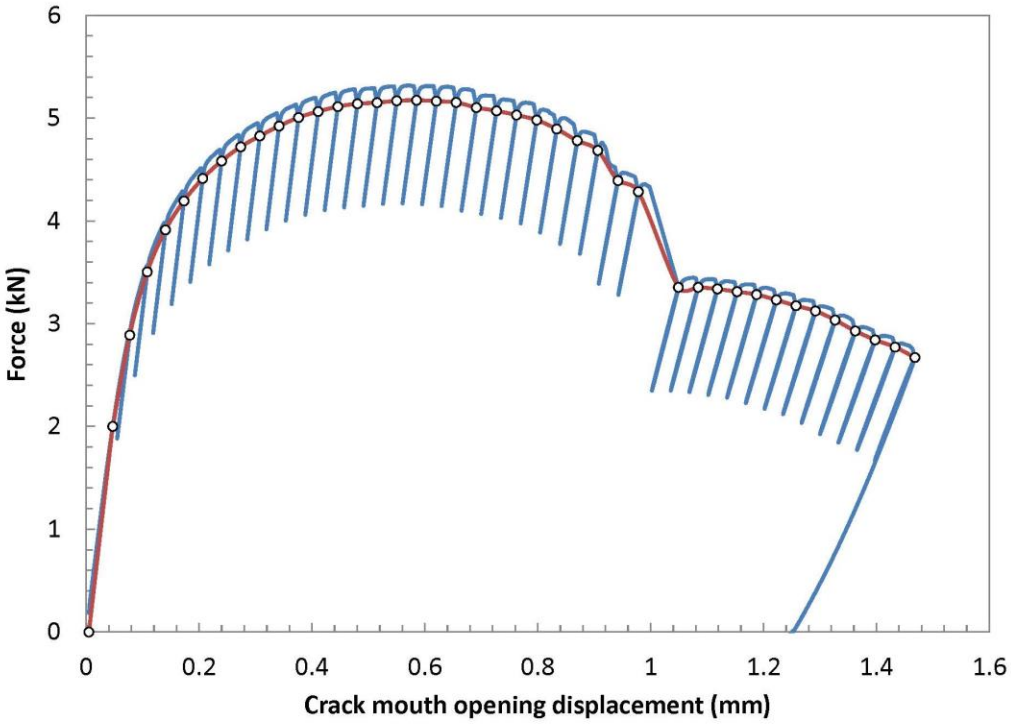
Force (kN)
Crack mouth opening displacement (mm)
0
1
2
3
4
5
6
0
0.2
0.4
0.6
0.8
1
1.2
1.4
1.6

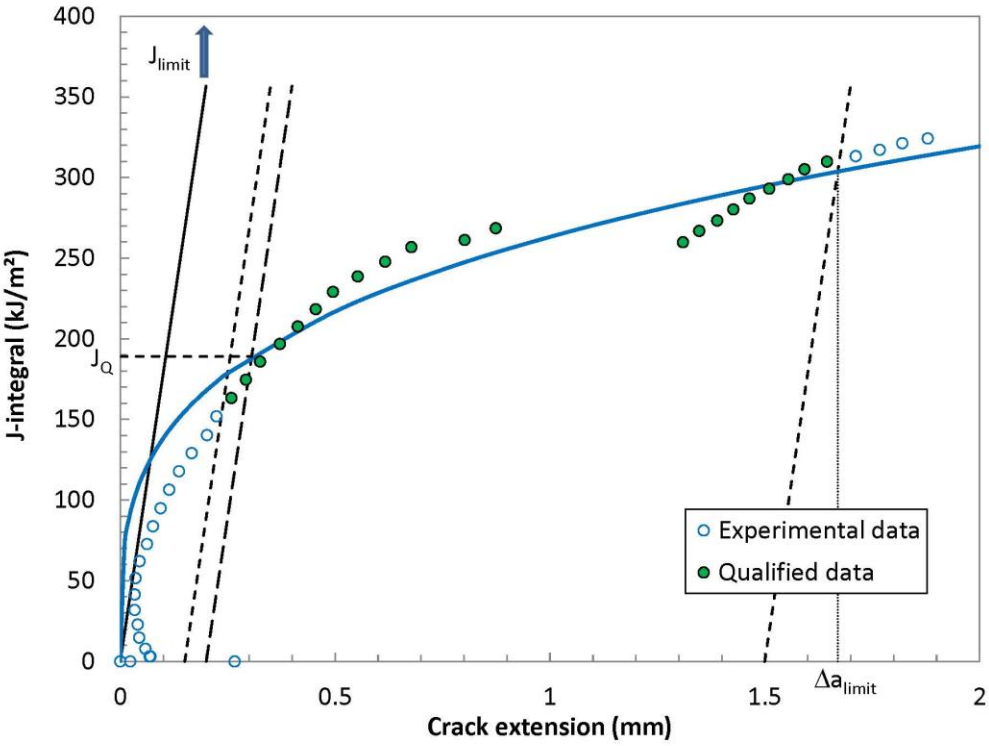
J-integral (kJ/m²)
Crack extension (mm)
J_limit
J_Q
Δa_limit
Experimental data
Qualified data
0
50
100
150
200
250
300
350
400
0
0.5
1
1.5
2

TEST REPORT

Specimen Information

Type = SE(B)
Identification = W3-F10
Orientation = N/A

Basic dimensions

B =	10.01	mm
B_N =	8.01	mm
W =	10.02	mm

Other dimensions

S =	40.00	mm

Tensile Properties

E =	173	MPa
ν =	0.3	
σ_{YS} =	544.0	MPa
σ_{TS} =	1244.0	MPa

Crack Size Information

a_0 =	5.08	mm
a_{0q} =	5.03	mm
a_f =	7.06	mm
Δa_p =	1.98	mm
$\Delta a_{predicted}$ =	1.77	mm

Test temperature: -196 °C

Analysis of Results

Fracture type = stable tearing

Critical Fracture Toughness

J_Q = 123.22 kJ/m²

TM = 49.4 MPa

QUALIFICATION OF DATA

Estimates of initial crack size:	$a_{0q,1}$ =	5.099	mm	Diff :	0.000	< 0.002W =	0.0200	mm
	$a_{0q,2}$ =	5.099	mm		0.001	< 0.002W =	0.0200	mm
	$a_{0,q3}$ =	5.098	mm		0.001	< 0.002W =	0.0200	mm
	$a_{0,qmean}$ =	5.099	mm					

Qualification of data				
Crack extension prediction	Δa_p =	1.98	mm (measured)	
	Δa_{pred} =	1.77	mm (predicted)	
	Difference =	-0.21	mm	PREDICTION NOT ACCEPTABLE

J_Q - Qualification of data			
Power coefficient C_2 =	0.497747	< 1.0	→ QUALIFIED
$\lvert a_{0q} - a_0 \rvert$ =	0.05	mm	→ DATA SET ADEQUATE
# of data available to calculate a_{0q} :	7	< 8	→ DATA SET NOT ADEQUATE
# of data between $0.4J_q$ and J_q :	7	≥ 3	→ QUALIFIED
Correlation coefficient a_{0q} fit :	0.996	≥ 0.96	→ DATA SET ADEQUATE
Data points distribution :	VALID		
Number of qualified data points :	VALID		

Qualification of J_Q as J_{Ic}			
Thickness B =	10.01	mm > 10 JQ/Sy	→ QUALIFIED
Initial ligament b_0 =	4.94	mm > 10 JQ/Sy	→ QUALIFIED

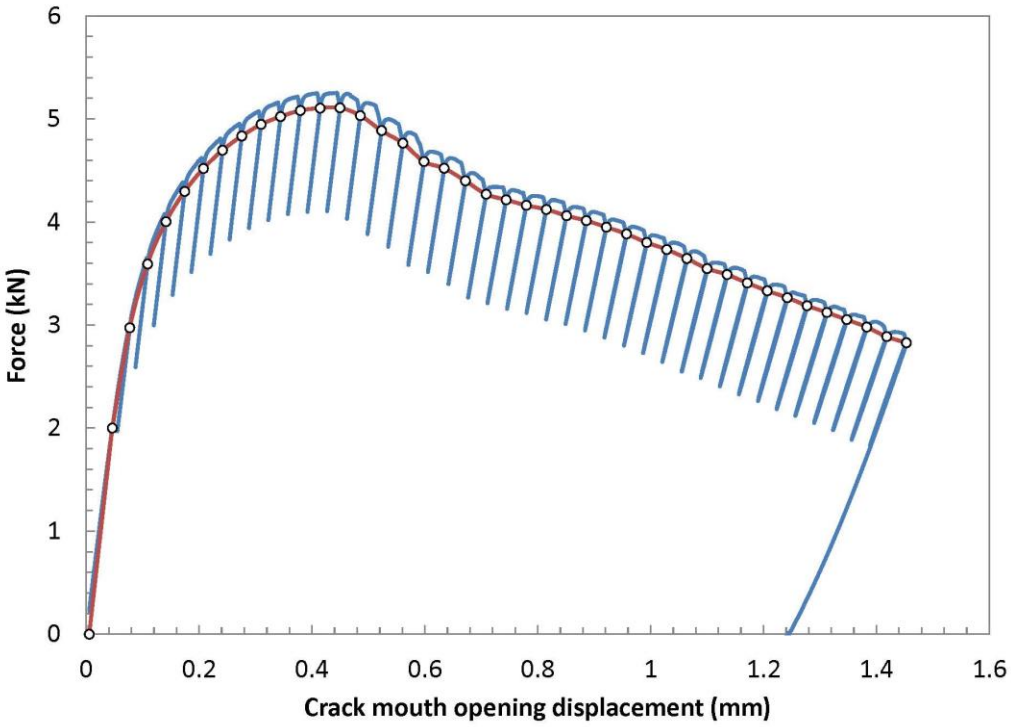
Force (kN)
Crack mouth opening displacement (mm)
0
1
2
3
4
5
6
0
0.2
0.4
0.6
0.8
1
1.2
1.4
1.6

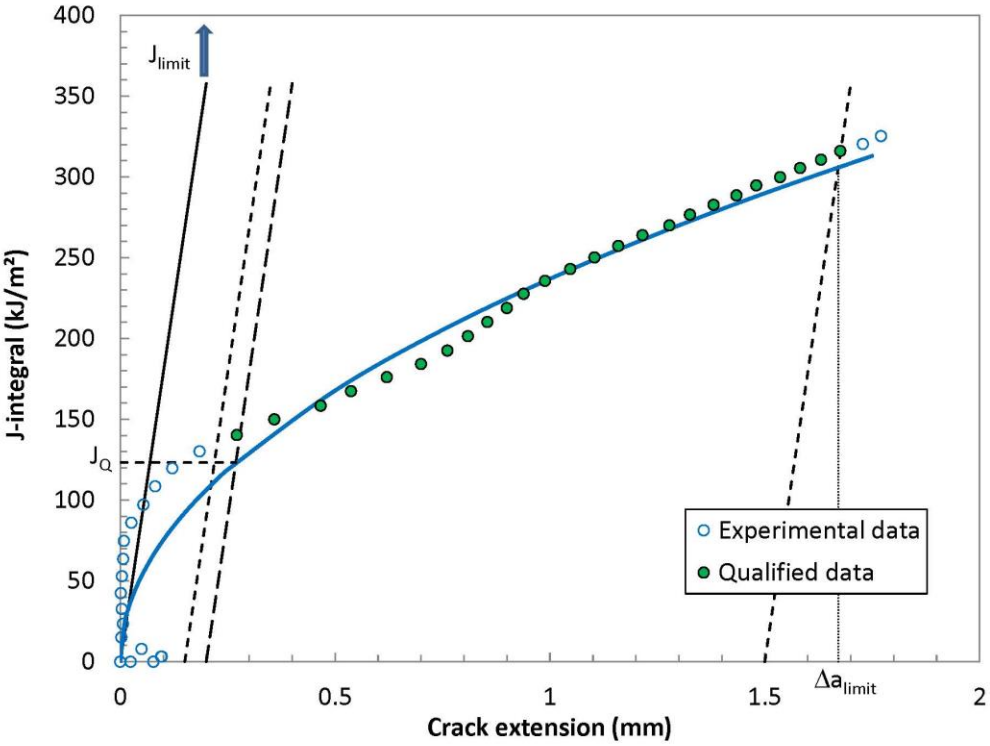
J-integral (kJ/m²)
Crack extension (mm)
J_limit
J_Q
Δa_limit
Experimental data
Qualified data
0
50
100
150
200
250
300
350
400
0
0.5
1
1.5
2

TEST REPORT

Specimen Information

Type = SE(B)
Identification = W3-F11
Orientation = N/A

Basic dimensions

B =	10.01	mm
B_N =	7.99	mm
W =	10.02	mm

Other dimensions

S =	40.00	mm

Tensile Properties

E =	173	MPa
ν =	0.3	
σ_{YS} =	544.0	MPa
σ_{TS} =	1244.0	MPa

Crack Size Information

a_0 =	5.29	mm
a_{0q} =	4.96	mm
a_f =	7.39	mm
Δa_p =	2.10	mm
$\Delta a_{predicted}$ =	2.05	mm

Test temperature: -196 °C

Analysis of Results

Fracture type = stable tearing

Critical Fracture Toughness

J_Ic = 168.93 kJ/m²

TM = 78.7 MPa

QUALIFICATION OF DATA

Estimates of initial crack size:

$a_{0q,1}$ =	5.091	mm	Diff :	0.002	< 0.002W =	0.0200	mm
$a_{0q,2}$ =	5.092	mm		0.002	< 0.002W =	0.0200	mm
$a_{0,q3}$ =	5.098	mm		0.004	< 0.002W =	0.0200	mm
$a_{0,qmean}$ =	5.094	mm					

Qualification of data

Crack extension prediction	Δa_p =	2.10	mm (measured)	
	Δa_{pred} =	2.05	mm (predicted)	
	Difference =	-0.05	mm	(PREDICTION ACCEPTABLE)

J_Q - Qualification of data

Power coefficient C_2 =	0.633872	< 1.0	→ QUALIFIED
$\lvert a_{0q} - a_0 \rvert$ =	0.33	mm	→ DATA SET ADEQUATE
# of data available to calculate a_{0q} :	16	≥ 8	→ DATA SET ADEQUATE
# of data between $0.4J_q$ and J_q :	9	≥ 3	→ QUALIFIED
Correlation coefficient a_{0q} fit :	0.994	≥ 0.96	→ DATA SET ADEQUATE

Data points distribution : VALID
Number of qualified data points : VALID

Qualification of J_Q as J_{Ic}

Thickness B =	10.01	mm > 10 JQ/Sy	→ QUALIFIED
Initial ligament b_0 =	4.73	mm > 10 JQ/Sy	→ QUALIFIED

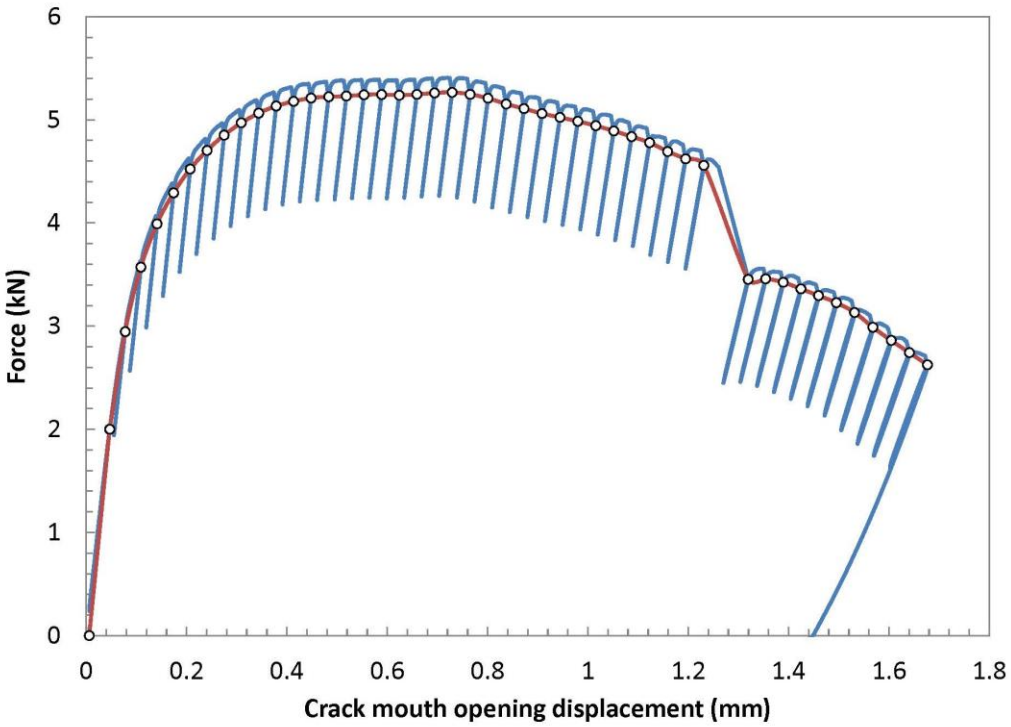
Force (kN)
Crack mouth opening displacement (mm)
0
1
2
3
4
5
6
0
0.2
0.4
0.6
0.8
1
1.2
1.4
1.6
1.8

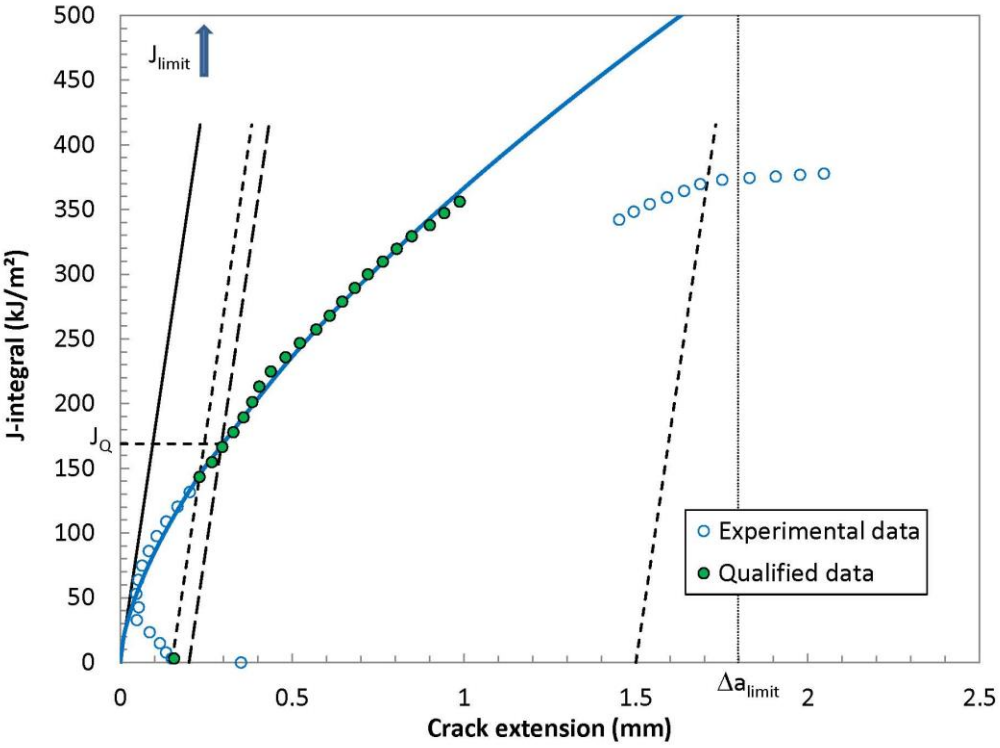
J-integral (kJ/m²)
Crack extension (mm)
J_limit
J_Q
Δa_limit
Experimental data
Qualified data
0
50
100
150
200
250
300
350
400
450
500
0
0.5
1
1.5
2
2.5

TEST REPORT

Specimen Information

Type = SE(B)
Identification = W3-F12
Orientation = N/A

Basic dimensions

B =	10.02	mm
B_N =	8.00	mm
W =	10.02	mm

Other dimensions

S =	40.00	mm

Tensile Properties

E =	173	MPa
ν =	0.3	
σ_{YS} =	544.0	MPa
σ_{TS} =	1244.0	MPa

Crack Size Information

a_0 =	5.32	mm
a_{0q} =	4.93	mm
a_f =	7.38	mm
Δa_p =	2.06	mm
$\Delta a_{predicted}$ =	2.02	mm

Test temperature: -196 °C

Analysis of Results

Fracture type = stable tearing

Critical Fracture Toughness

J_Ic = 232.10 kJ/m²

TM = 41.3 MPa

QUALIFICATION OF DATA

Estimates of initial crack size:

$a_{0q,1}$ =	4.966	mm	Diff :	0.008	< 0.002W =	0.0200	mm
$a_{0q,2}$ =	4.982	mm		0.009	< 0.002W =	0.0200	mm
$a_{0,q3}$ =	4.972	mm		0.001	< 0.002W =	0.0200	mm
$a_{0,qmean}$ =	4.973	mm					

Qualification of data

Crack extension prediction	Δa_p =	2.06	mm (measured)	
	Δa_{pred} =	2.02	mm (predicted)	
	Difference =	-0.04	mm	(PREDICTION ACCEPTABLE)

J_Q - Qualification of data

Power coefficient C_2 =	0.270909	< 1.0	→ QUALIFIED
$\lvert a_{0q} - a_0 \rvert$ =	0.39	mm	→ DATA SET ADEQUATE
# of data available to calculate a_{0q} :	16	≥ 8	→ DATA SET ADEQUATE
# of data between $0.4J_q$ and J_q :	12	≥ 3	→ QUALIFIED
Correlation coefficient a_{0q} fit :	0.988	≥ 0.96	→ DATA SET ADEQUATE
Data points distribution :	VALID		
Number of qualified data points :	VALID		

Qualification of J_Q as J_{Ic}

Thickness B =	10.02	mm > 10 JQ/Sy	→ QUALIFIED
Initial ligament b_0 =	4.70	mm > 10 JQ/Sy	→ QUALIFIED

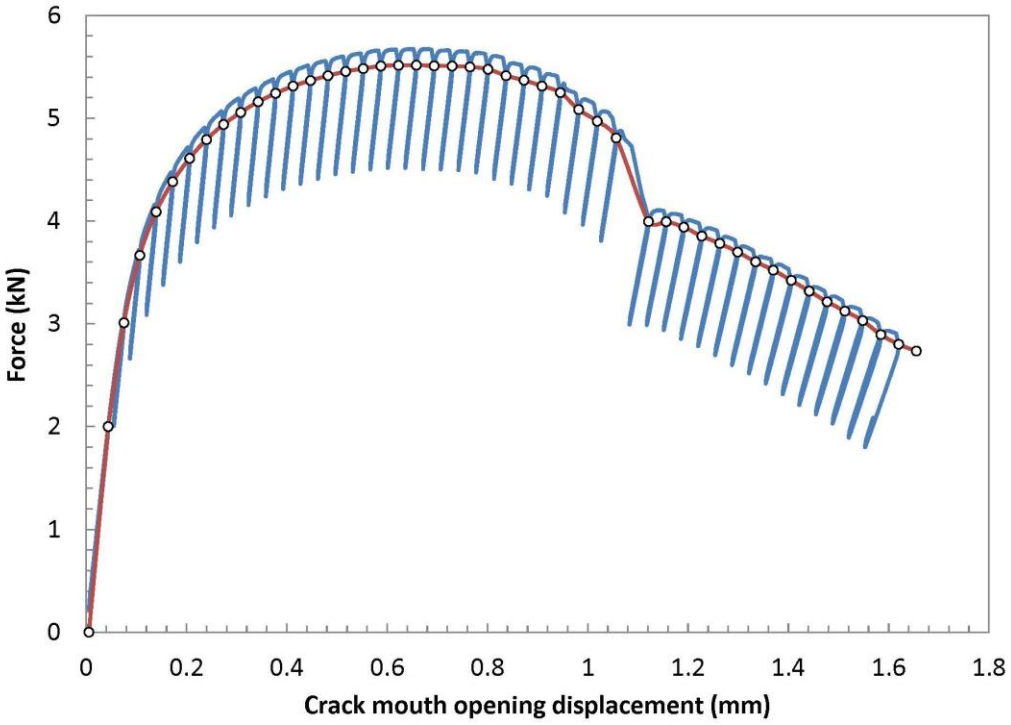
Force (kN)
Crack mouth opening displacement (mm)
0
1
2
3
4
5
6
0
0.2
0.4
0.6
0.8
1
1.2
1.4
1.6
1.8

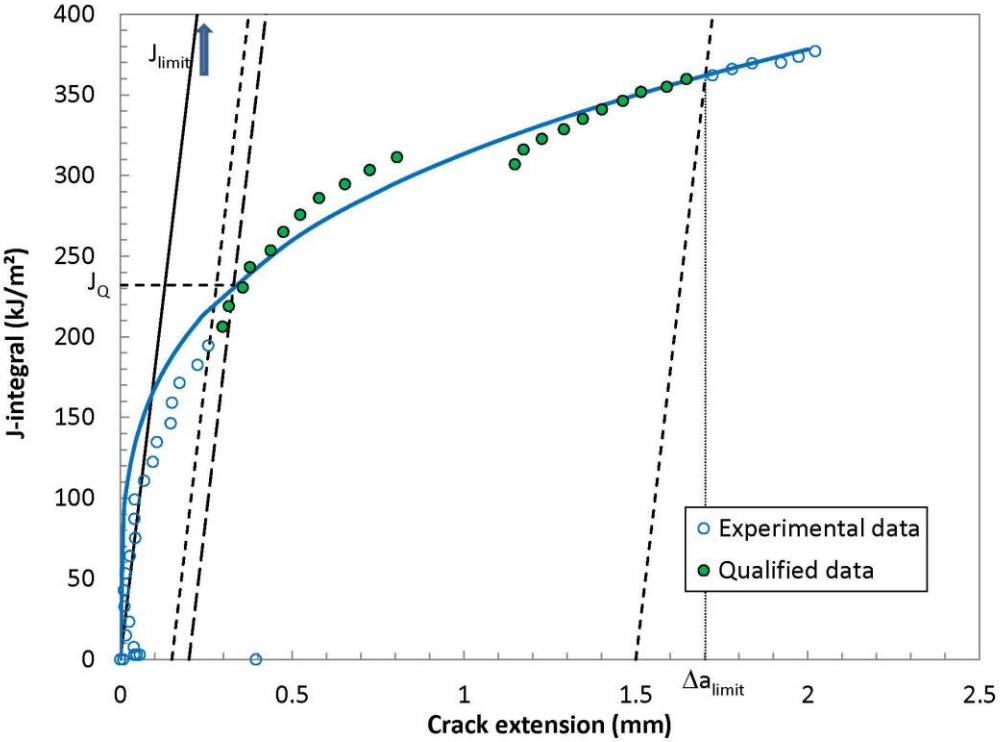
J-integral (kJ/m²)
Crack extension (mm)
J_limit
J_Q
Δa_limit
Experimental data
Qualified data
0
50
100
150
200
250
300
350
400
0
0.5
1
1.5
2
2.5

TEST REPORT

Specimen Information

Type = SE(B)
Identification = W3-F13
Orientation = N/A

Basic dimensions

B =	10.01	mm
B_N =	8.00	mm
W =	10.02	mm

Other dimensions

S =	40.00	mm

Tensile Properties

E =	171	MPa
ν =	0.3	
σ_{YS} =	545.0	MPa
σ_{TS} =	1220.0	MPa

Crack Size Information

a_0 =	5.31	mm
a_{0q} =	5.01	mm
a_f =	6.04	mm
Δa_p =	0.72	mm
$\Delta a_{predicted}$ =	0.57	mm

Test temperature: -196 °C

Analysis of Results

Fracture type = stable tearing

Critical Fracture Toughness

J_Q = 186.84 kJ/m²

TM = 37.2 MPa

QUALIFICATION OF DATA

Estimates of initial crack size:	$a_{0q,1}$ =	5.041	mm	Diff :	0.001	< 0.002W =	0.0200 mm
	$a_{0q,2}$ =	5.037	mm		0.005	< 0.002W =	0.0200 mm
	$a_{0,q3}$ =	5.048	mm		0.006	< 0.002W =	0.0200 mm
	$a_{0,qmean}$ =	5.042	mm				

Qualification of data

Crack extension prediction	Δa_p =	0.72	mm (measured)	
	Δa_{pred} =	0.57	mm (predicted)	
	Difference =	-0.16	mm	(PREDICTION NOT ACCEPTABLE)

J_Q - Qualification of data

Power coefficient C_2 =	0.277409	< 1.0	→ QUALIFIED
$\lvert a_{0q} - a_0 \rvert$ =	0.31	mm	→ DATA SET ADEQUATE
# of data available to calculate a_{0q} :	10	≥ 8	→ DATA SET ADEQUATE
# of data between $0.4J_q$ and J_q :	13	≥ 3	→ QUALIFIED
Correlation coefficient a_{0q} fit :	0.994	≥ 0.96	→ DATA SET ADEQUATE
Data points distribution :	NOT VALID		
Number of qualified data points :	VALID		

Qualification of J_Q as J_{Ic}

Thickness B =	10.01	mm > 10 JQ/Sy	→ QUALIFIED
Initial ligament b_0 =	4.71	mm > 10 JQ/Sy	→ QUALIFIED

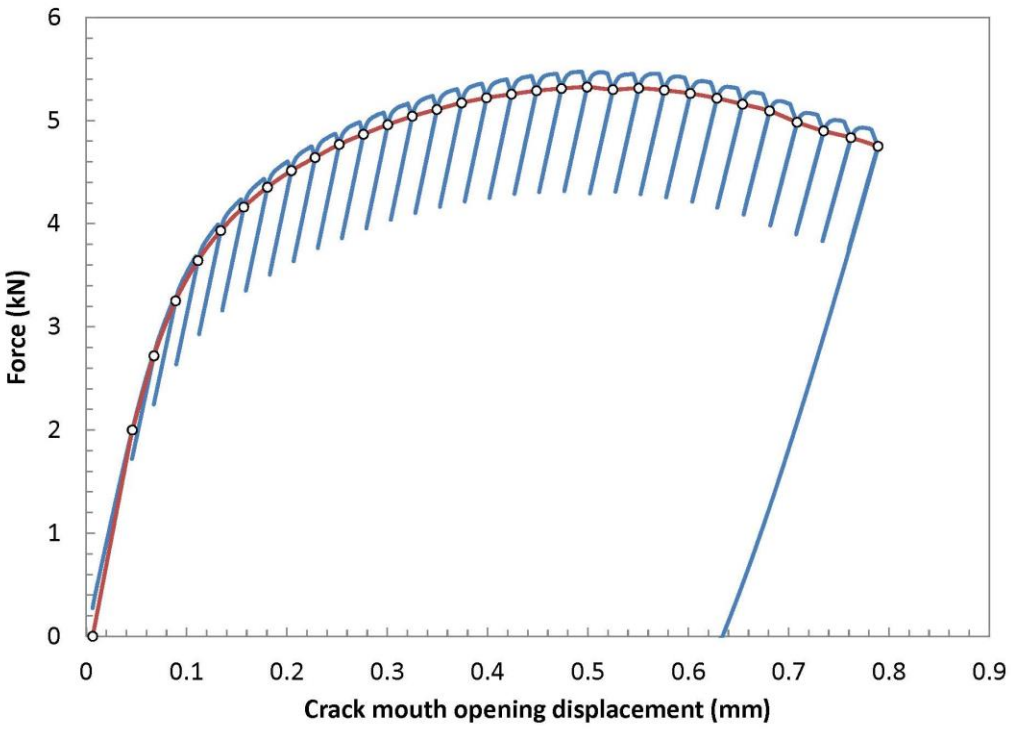
Force (kN)
Crack mouth opening displacement (mm)
0
1
2
3
4
5
6
0
0.1
0.2
0.3
0.4
0.5
0.6
0.7
0.8
0.9

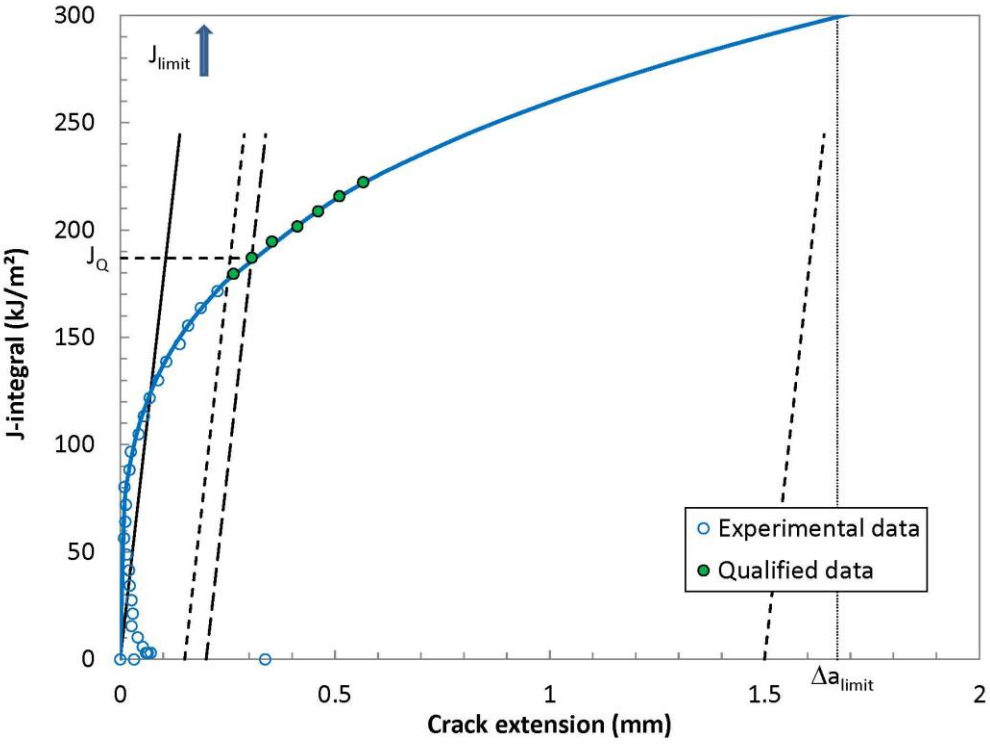
J-integral (kJ/m²)
Crack extension (mm)
J_limit
J_Q
Δa_limit
Experimental data
Qualified data
0
50
100
150
200
250
300
0
0.5
1
1.5
2

Weld W4, T = 77 K

TEST REPORT

Specimen Information

Type = SE(B)
Identification = W4-F9
Orientation = N/A

Basic dimensions

B =	10.01	mm
B_N =	8.00	mm
W =	10.01	mm

Other dimensions

S =	40.00	mm

Tensile Properties

E =	163	MPa
ν =	0.3	
σ_{YS} =	565.0	MPa
σ_{TS} =	1282.0	MPa

Crack Size Information

a_0 =	5.20	mm
a_{0q} =	4.91	mm
a_f =	6.16	mm
Δa_p =	0.96	mm
$\Delta a_{predicted}$ =	0.50	mm

Test temperature: -196 °C

Analysis of Results

Fracture type = stable tearing

Critical Fracture Toughness

J_Q = 198.73 kJ/m²

TM = 20.2 MPa

QUALIFICATION OF DATA

Estimates of initial crack size:	$a_{0q,1}$ =	4.950	mm	Diff :	0.002	< 0.002W =	0.0200	mm
	$a_{0q,2}$ =	4.954	mm		0.002	< 0.002W =	0.0200	mm
	$a_{0,q3}$ =	4.952	mm		0.000	< 0.002W =	0.0200	mm
	$a_{0,qmean}$ =	4.952	mm					

Qualification of data

Crack extension prediction	Δa_p =	0.96	mm (measured)	
	Δa_{pred} =	0.50	mm (predicted)	
	Difference =	-0.45	mm	(PREDICTION NOT ACCEPTABLE)

J_Q - Qualification of data

Power coefficient C_2 =	0.163232	< 1.0	→ QUALIFIED
$\lvert a_{0q} - a_0 \rvert$ =	0.29	mm	→ DATA SET ADEQUATE
# of data available to calculate a_{0q} :	9	≥ 8	→ DATA SET ADEQUATE
# of data between $0.4J_q$ and J_q :	10	≥ 3	→ QUALIFIED
Correlation coefficient a_{0q} fit :	0.997	≥ 0.96	→ DATA SET ADEQUATE
Data points distribution :	NOT VALID		
Number of qualified data points :	NOT VALID		

Qualification of J_Q as J_{Ic}

Thickness B =	10.01	mm > 10 JQ/Sy	→ QUALIFIED
Initial ligament b_0 =	4.81	mm > 10 JQ/Sy	→ QUALIFIED

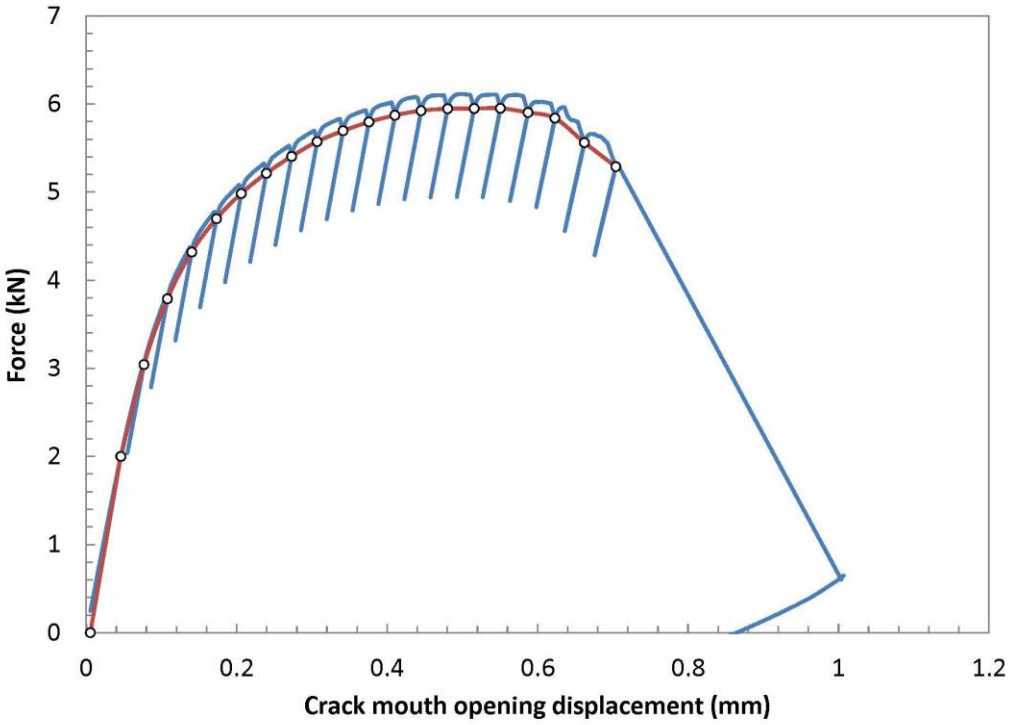
Force (kN)
Crack mouth opening displacement (mm)
0
1
2
3
4
5
6
7
0
0.2
0.4
0.6
0.8
1
1.2

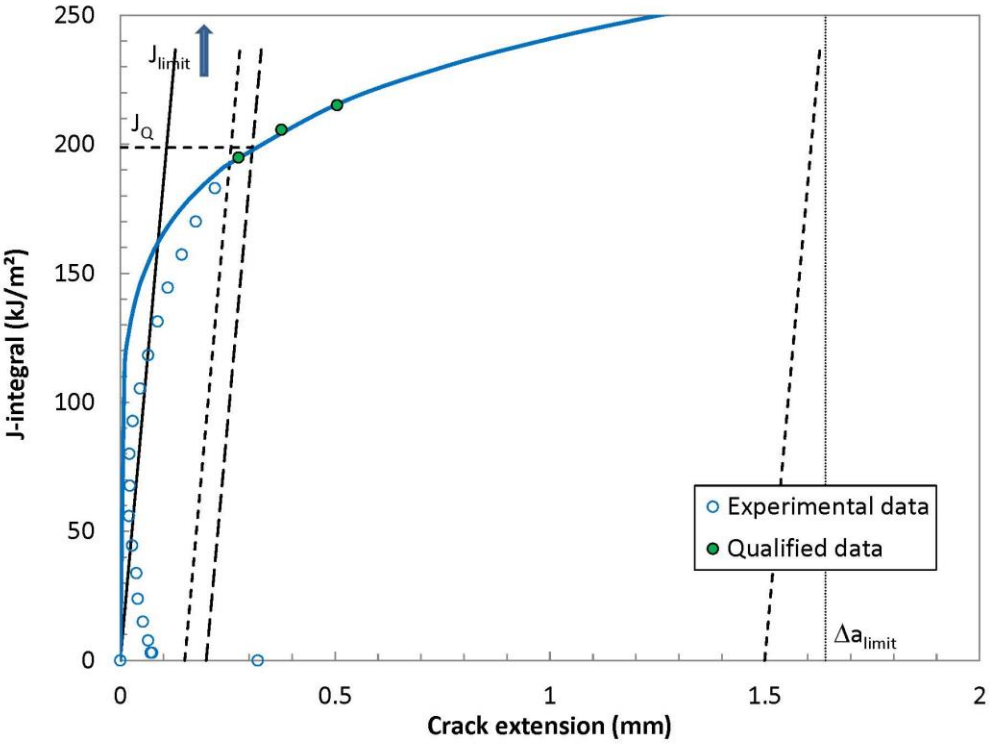
J-integral (kJ/m²)
Crack extension (mm)
J_limit
J_Q
Experimental data
Qualified data
Δa_limit
0
50
100
150
200
250
0
0.5
1
1.5
2

TEST REPORT

Specimen Information

Type = SE(B)
Identification = W4-F10
Orientation = N/A

Basic dimensions

B =	10.02	mm
B_N =	8.01	mm
W =	9.99	mm

Other dimensions

S =	40.00	mm

Tensile Properties

E =	163	MPa
ν =	0.3	
σ_{YS} =	565.0	MPa
σ_{TS} =	1282.0	MPa

Crack Size Information

a_0 =	5.18	mm
a_{0q} =	4.86	mm
a_f =	9.06	mm
Δa_p =	3.87	mm
$\Delta a_{predicted}$ =	3.93	mm

Test temperature: -196 °C

Analysis of Results

Fracture type = stable tearing

Critical Fracture Toughness

J_Q = #N/A kJ/m²

TM = #N/A MPa

QUALIFICATION OF DATA

Estimates of initial crack size:	$a_{0q,1}$ =	4.866	mm	Diff :	0.001	< 0.002W =	0.0200	mm
	$a_{0q,2}$ =	4.864	mm		0.003	< 0.002W =	0.0200	mm
	$a_{0,q3}$ =	4.871	mm		0.004	< 0.002W =	0.0200	mm
	$a_{0,qmean}$ =	4.867	mm					

Qualification of data

Crack extension prediction	Δa_p =	3.87	mm (measured)	
	Δa_{pred} =	3.93	mm (predicted)	
	Difference =	0.06	mm	(PREDICTION ACCEPTABLE)

J_Q - Qualification of data

Power coefficient C_2 =	#DIV/0!	#DIV/0!	#DIV/0!
$\lvert a_{0q} - a_0 \rvert$ =	0.33	mm	→ DATA SET ADEQUATE
# of data available to calculate a_{0q} :	6	< 8	→ DATA SET NOT ADEQUATE
# of data between $0.4J_q$ and J_q :	0	< 3	→ NOT QUALIFIED
Correlation coefficient a_{0q} fit :	0.995	≥ 0.96	→ DATA SET ADEQUATE
Data points distribution :	NOT VALID		
Number of qualified data points :	NOT VALID		

Qualification of J_Q as J_{Ic}

Thickness B =	10.02	#N/A	#N/A
Initial ligament b_0 =	4.81	#N/A	#N/A

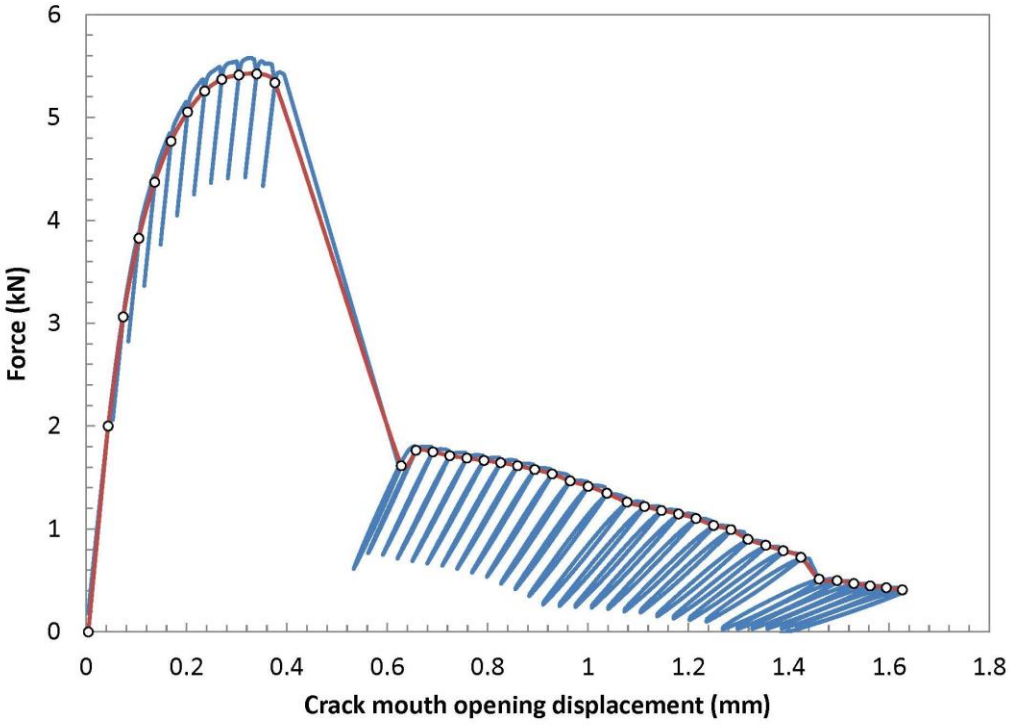
Force (kN)
Crack mouth opening displacement (mm)
0
1
2
3
4
5
6
0
0.2
0.4
0.6
0.8
1
1.2
1.4
1.6
1.8

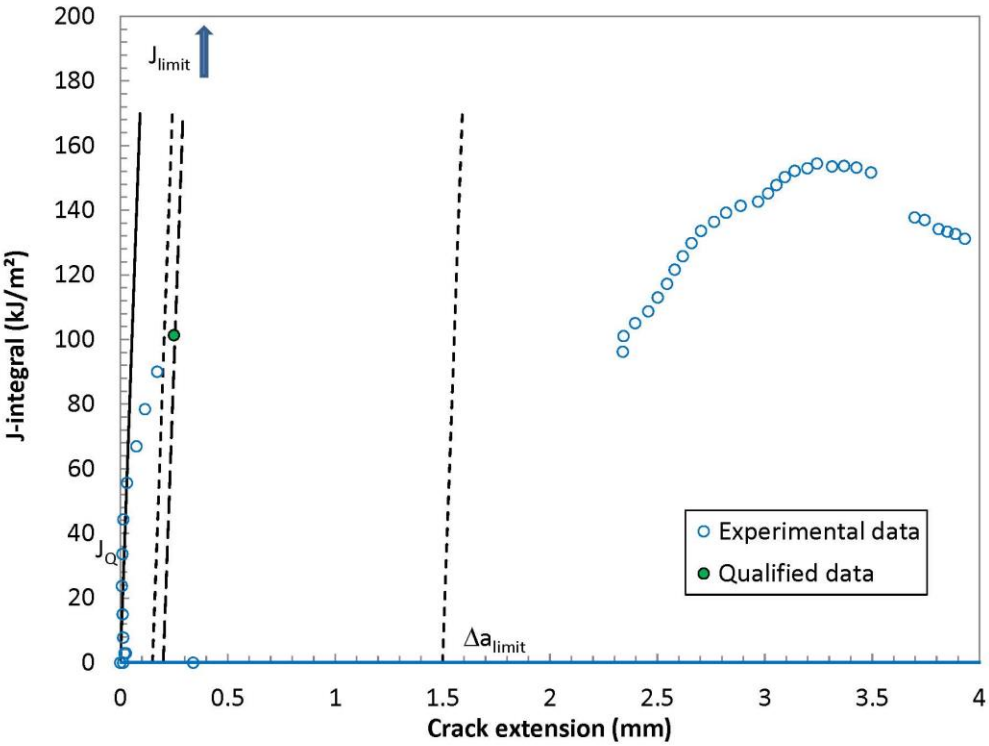
J-integral (kJ/m²)
Crack extension (mm)
J_limit
J_Q
Δa_limit
Experimental data
Qualified data
0
20
40
60
80
100
120
140
160
180
200
0
0.5
1
1.5
2
2.5
3
3.5
4

Specimen :	W4-F10			Δa =	0.25	mm	
F_c =	5.42	kN		K_e =	68.53	MPa$\sqrt{m}$	
B =	10.0156	mm		J_e =	26.22	kJ/m²	
B_N =	8.0074	mm					
W =	9.99	mm		η =	2.643751		
a_0 =	5.184	mm					
a_0/W =	0.519			J_{pl} =	97.00	kJ/m²	
S =	40	mm					
				J_c =	**121.56**	**kJ/m²**	NOT VALID
f(a/W) =	2.828988			**K_{Jc} =**	**147.56**	**MPa$\sqrt{m}$**	
T =	-196	°C			σ_Y =	923.5	MPa
E =	163.00	GPa =	163000 MPa	.00	J_{Qc}/σ_Y =	13.2	mm
ν =	0.3						
A_{tot} =	1.73	kN.mm					
			Limits for compliance calculation:		**F_{low} =**	**0.5**	**kN**
C_o =	0.021656	mm/kN			**F_{high} =**	**1.7**	**kN**
A_{el} =	0.32	kN.mm					
A_{pl} =	1.41	kN.mm			Intercept:	-0.00432	mm

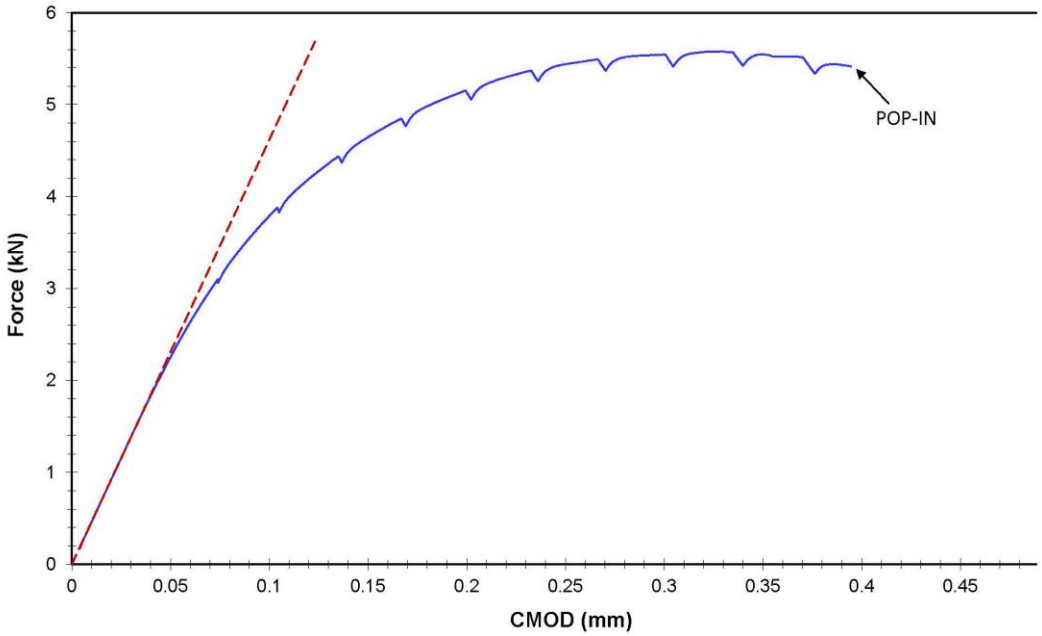

TEST REPORT

Specimen Information

Type = SE(B)
Identification = W4-F11
Orientation = N/A

Basic dimensions

B =	10.01	mm
B_N =	8.00	mm
W =	10.02	mm

Other dimensions

S =	40.00	mm

Tensile Properties

E =	163	MPa
ν =	0.3	
σ_{YS} =	565.0	MPa
σ_{TS} =	1282.0	MPa

Crack Size Information

a_0 =	5.19	mm
a_{0q} =	4.89	mm
a_f =	9.00	mm
Δa_p =	3.81	mm
$\Delta a_{predicted}$ =	4.22	mm

Test temperature: -196 °C

Analysis of Results

Fracture type = stable tearing

Critical Fracture Toughness

J_Q = #N/A kJ/m²

TM = #N/A MPa

QUALIFICATION OF DATA

Estimates of initial crack size:

$a_{0q,1}$ =	4.914	mm	Diff :	0.001	< 0.002W =	0.0200	mm
$a_{0q,2}$ =	4.916	mm		0.001	< 0.002W =	0.0200	mm
a_{0q3} =	4.915	mm		0.000	< 0.002W =	0.0200	mm
$a_{0,qmean}$ =	4.915	mm					

Qualification of data

Crack extension prediction	Δa_p =	3.81	mm (measured)	
	Δa_{pred} =	4.22	mm (predicted)	
	Difference =	0.41	mm	PREDICTION NOT ACCEPTABLE

J_Q - Qualification of data

Power coefficient C_2 =	#DIV/0!	#DIV/0!	#DIV/0!
$\lvert a_{0q} - a_0 \rvert$ =	0.30	mm	→ DATA SET ADEQUATE
# of data available to calculate a_{0q} :	5	< 8	→ DATA SET NOT ADEQUATE
# of data between $0.4J_q$ and J_q :	0	< 3	→ NOT QUALIFIED
Correlation coefficient a_{0q} fit :	0.997	≥ 0.96	→ DATA SET ADEQUATE
Data points distribution :	NOT VALID		
Number of qualified data points :	NOT VALID		

Qualification of J_Q as J_{Ic}

Thickness B =	10.01	#N/A	#N/A
Initial ligament b_0 =	4.83	#N/A	#N/A

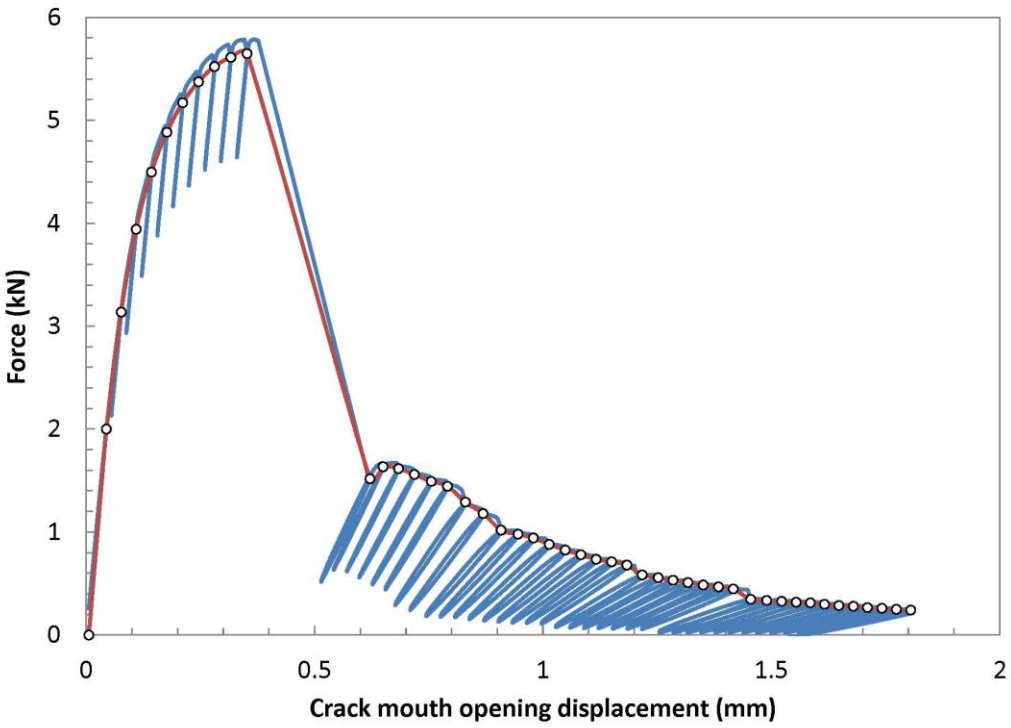
Force (kN)
Crack mouth opening displacement (mm)
0
1
2
3
4
5
6
0
0.5
1
1.5
2

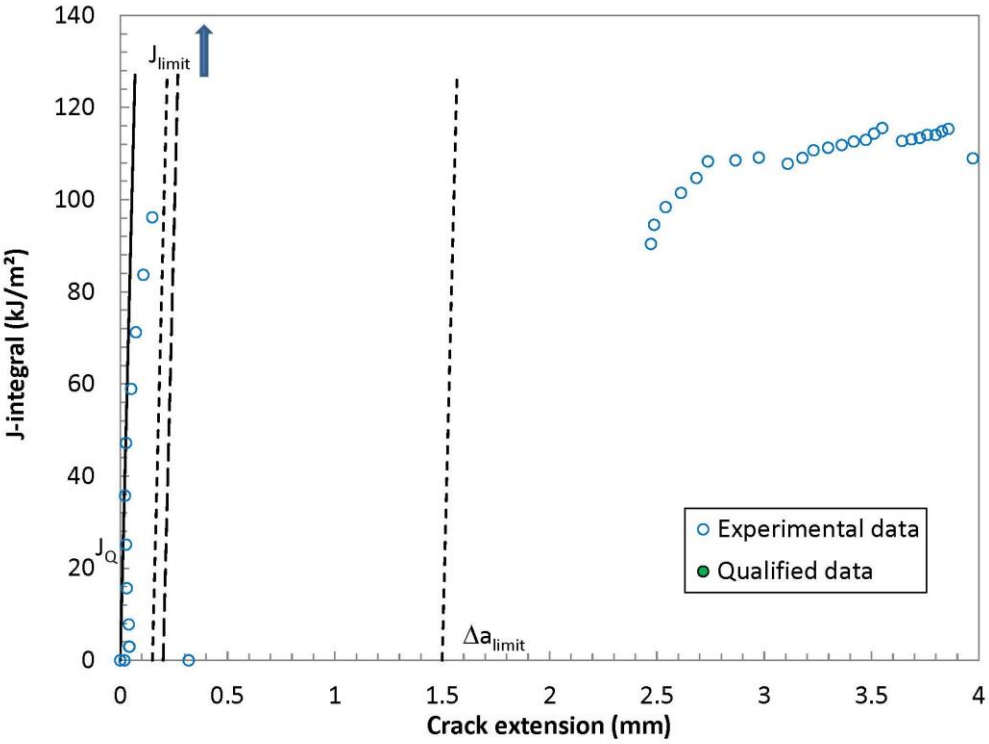
J-integral (kJ/m²)
Crack extension (mm)
J_limit
J_Q
Δa_limit
Experimental data
Qualified data
0
20
40
60
80
100
120
140
0
0.5
1
1.5
2
2.5
3
3.5
4

Specimen :	W4-F11			Δa =	0.25	mm	
F_c =	5.77	kN		K_e =	72.62	MPa$\sqrt{m}$	
B =	10.014	mm		J_e =	29.44	kJ/m²	
B_N =	8.004	mm					
W =	10.02	mm		η =	2.644796		
a_0 =	5.192	mm					
a_0/W =	0.518			J_{pl} =	88.66	kJ/m²	
S =	40	mm					
				J_c =	**116.60**	**kJ/m²**	NOT VALID
f(a/W) =	2.823448			**K_{Jc} =**	**144.52**	**MPa$\sqrt{m}$**	
T =	-196	°C			σ_Y =	923.5	MPa
E =	163.00	GPa =	163000 MPa	.00	J_{Qc}/σ_Y =	12.6	mm
ν =	0.3						
A_{tot} =	1.66	kN.mm					
			Limits for compliance calculation:		**F_{low} =**	**0.6**	**kN**
C_o =	0.021984	mm/kN			**F_{high} =**	**2**	**kN**
A_{el} =	0.37	kN.mm					
A_{pl} =	1.30	kN.mm			Intercept:	-0.00617	mm

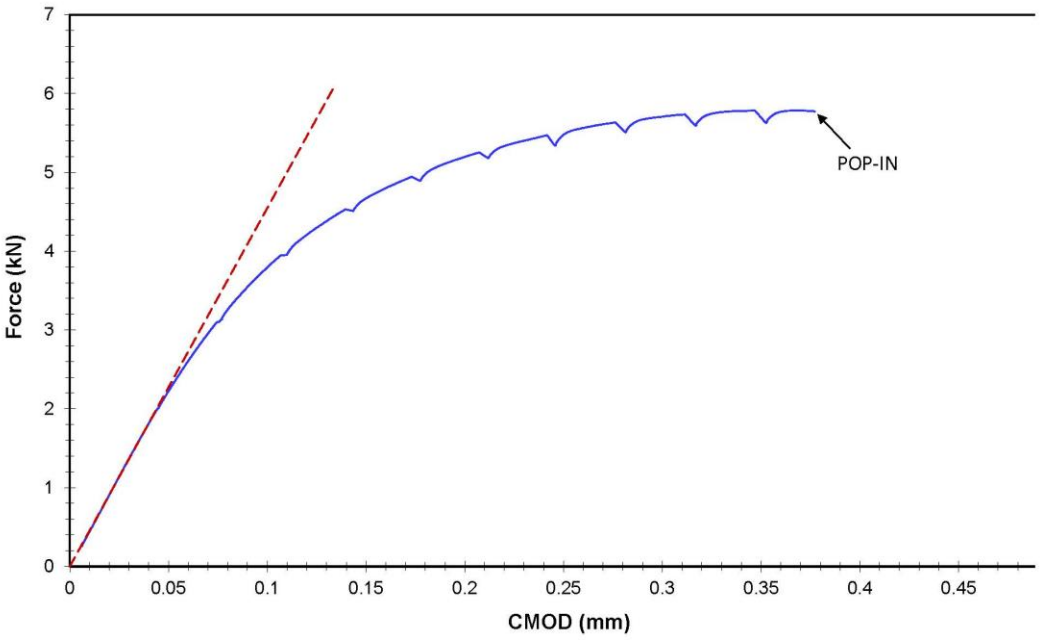

TEST REPORT

Specimen Information

Type = SE(B)
Identification = W4-F11
Orientation = N/A

Basic dimensions

B = 10.02 mm
B_N = 8.00 mm
W = 10.03 mm

Other dimensions

S = 40.00 mm

Tensile Properties

E = 163 MPa
ν = 0.3
σ_{YS} = 565.0 MPa
σ_{TS} = 1282.0 MPa

Crack Size Information

a_0 = 5.19 mm
a_{0q} = 4.90 mm
a_f = 9.17 mm
Δa_p = 3.98 mm
$\Delta a_{predicted}$ = 4.12 mm

Test temperature: -196 °C

Analysis of Results

Fracture type = stable tearing

Critical Fracture Toughness

J_Q = #N/A kJ/m²

TM = #N/A MPa

QUALIFICATION OF DATA

Estimates of initial crack size:

$a_{0q,1}$ =	4.929	mm	Diff :	0.007	< 0.002W =	0.0201	mm
$a_{0q,2}$ =	4.921	mm		0.001	< 0.002W =	0.0201	mm
a_{0q3} =	4.917	mm		0.006	< 0.002W =	0.0201	mm
$a_{0,qmean}$ =	4.922	mm					

Qualification of data

Crack extension prediction	Δa_p =	3.98	mm (measured)	
	Δa_{pred} =	4.12	mm (predicted)	
	Difference =	0.14	mm	(PREDICTION ACCEPTABLE)

J_Q - Qualification of data

Power coefficient C_2 =	#DIV/0!	#DIV/0!	#DIV/0!
$\lvert a_{0q} - a_0 \rvert$ =	0.28	mm	→ DATA SET ADEQUATE
# of data available to calculate a_{0q} :	5	< 8	→ DATA SET NOT ADEQUATE
# of data between $0.4J_q$ and J_q :	0	< 3	→ NOT QUALIFIED
Correlation coefficient a_{0q} fit :	0.990	≥ 0.96	→ DATA SET ADEQUATE
Data points distribution :	NOT VALID		
Number of qualified data points :	NOT VALID		

Qualification of J_Q as J_{Ic}

Thickness B =	10.02	#N/A	#N/A
Initial ligament b_0 =	4.84	#N/A	#N/A

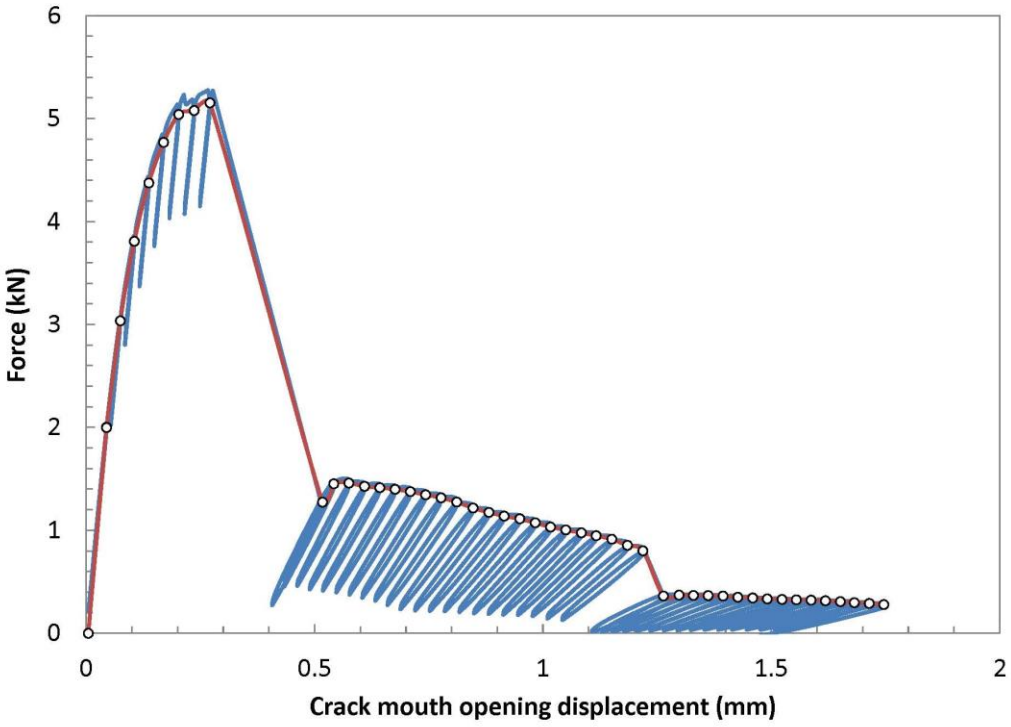
Force (kN)
Crack mouth opening displacement (mm)
0
1
2
3
4
5
6
0
0.5
1
1.5
2

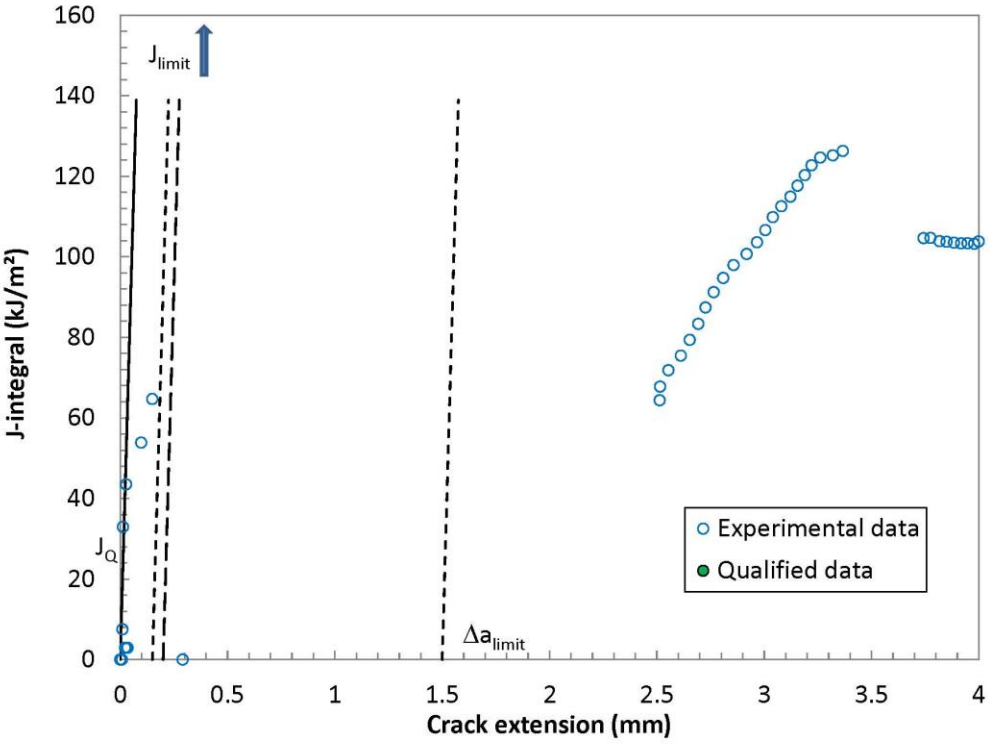
J-integral (kJ/m²)
Crack extension (mm)
J_limit
J_Q
Δa_limit
Experimental data
Qualified data
0
20
40
60
80
100
120
140
160
0
0.5
1
1.5
2
2.5
3
3.5
4

Specimen :	W4-F12			Δa =	0.25	mm
F_c =	5.28	kN		K_e =	65.99	MPa√m
B =	10.019	mm		J_e =	24.31	kJ/m²
B_N =	8.005	mm				
W =	10.03	mm		η =	2.646834	
a_0 =	5.186	mm				
a_0/W =	0.517			J_{pl} =	48.03	kJ/m²
S =	40	mm				
				J_c =	**71.53**	**kJ/m²** NOT VALID
f(a/W) =	2.812702			**K_{Jc} =**	**113.19**	**MPa√m**
T =	-196	°C		σ_Y =	923.5	MPa
E =	163.00	GPa = 163000	MPa	.00 J_{Qc}/σ_Y =	7.7	mm
ν =	0.3					
A_{tot} =	1.01	kN.mm				
			Limits for compliance calculation:	**F_{low} =**	**0.6**	**kN**
C_o =	0.022254	mm/kN		**F_{high} =**	**2**	**kN**
A_{el} =	0.31	kN.mm				
A_{pl} =	0.70	kN.mm		Intercept:	-0.00516	mm

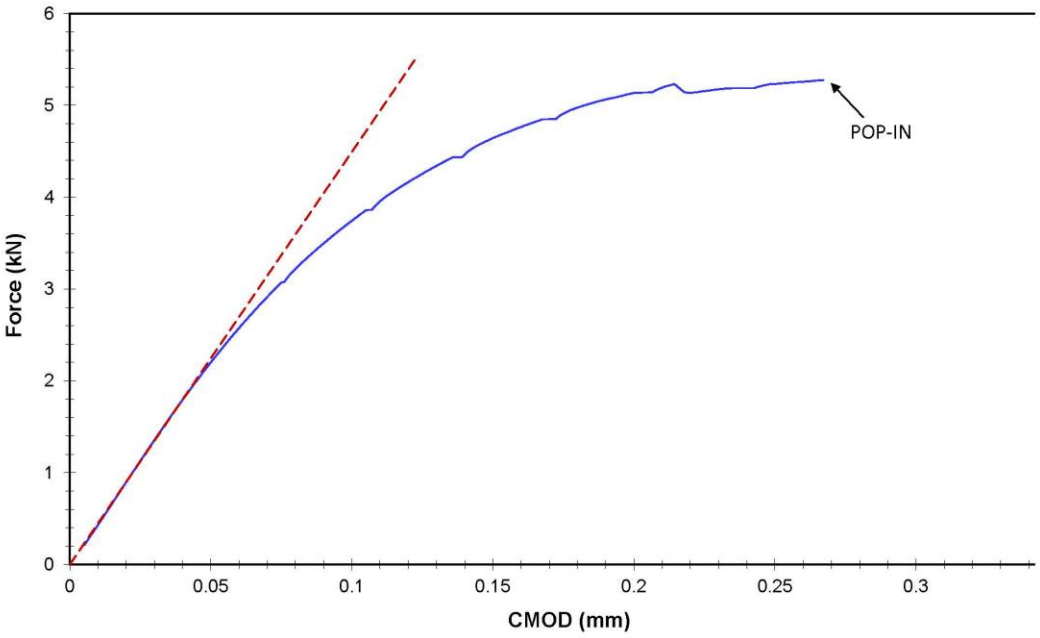

TEST REPORT

Specimen Information

Type = SE(B)
Identification = W4-F13
Orientation = N/A

Basic dimensions

B =	10.01	mm
B_N =	8.00	mm
W =	10.03	mm

Other dimensions

S =	40.00	mm

Tensile Properties

E =	163	MPa
ν =	0.3	
σ_{YS} =	565.0	MPa
σ_{TS} =	1282.0	MPa

Crack Size Information

a_0 =	5.19	mm
a_{0q} =	5.03	mm
a_f =	7.23	mm
Δa_p =	2.04	mm
$\Delta a_{predicted}$ =	1.98	mm

Test temperature: -196 °C

Analysis of Results

Fracture type = stable tearing

Critical Fracture Toughness

J_Q = #N/A kJ/m²

TM = #N/A MPa

QUALIFICATION OF DATA

Estimates of initial crack size:	$a_{0q,1}$ =	5.070	mm	Diff :	0.005	< 0.002W =	0.0201 mm
	$a_{0q,2}$ =	5.064	mm		0.001	< 0.002W =	0.0201 mm
	$a_{0,q3}$ =	5.061	mm		0.004	< 0.002W =	0.0201 mm
	$a_{0,qmean}$ =	5.065	mm				

Qualification of data

Crack extension prediction	Δa_p =	2.04	mm (measured)	
	Δa_{pred} =	1.98	mm (predicted)	
	Difference =	-0.06	mm	(PREDICTION ACCEPTABLE)

J_Q - Qualification of data

Power coefficient C_2 =	0	< 1.0	→ QUALIFIED
$\lvert a_{0q} - a_0 \rvert$ =	0.16	mm	→ DATA SET ADEQUATE
# of data available to calculate a_{0q} :	4	< 8	→ DATA SET NOT ADEQUATE
# of data between $0.4J_q$ and J_q :	0	< 3	→ NOT QUALIFIED
Correlation coefficient a_{0q} fit :	0.996	≥ 0.96	→ DATA SET ADEQUATE

Data points distribution : NOT VALID
Number of qualified data points : VALID

Qualification of J_Q as J_{Ic}

Thickness B =	10.01	#N/A	#N/A
Initial ligament b_0 =	4.84	#N/A	#N/A

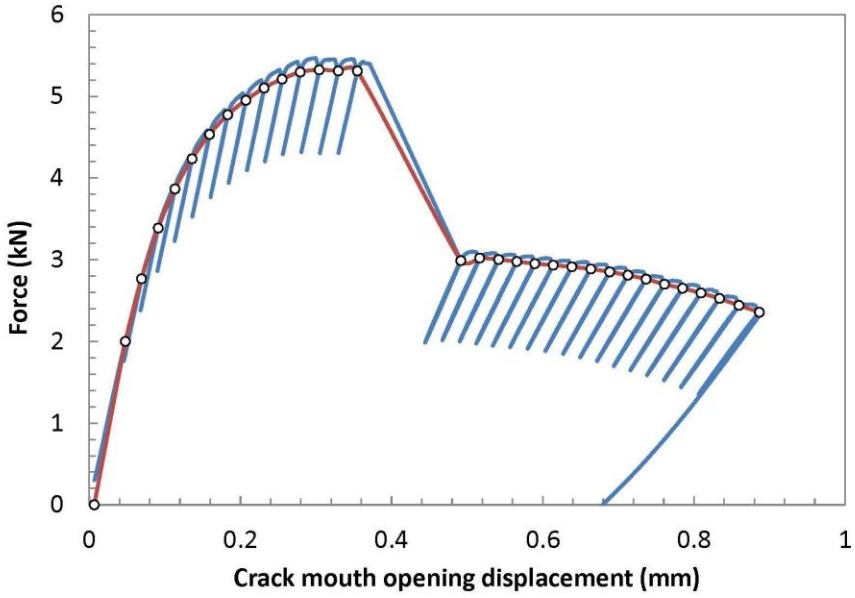
Force (kN)
Crack mouth opening displacement (mm)
0
1
2
3
4
5
6
0
0.2
0.4
0.6
0.8
1

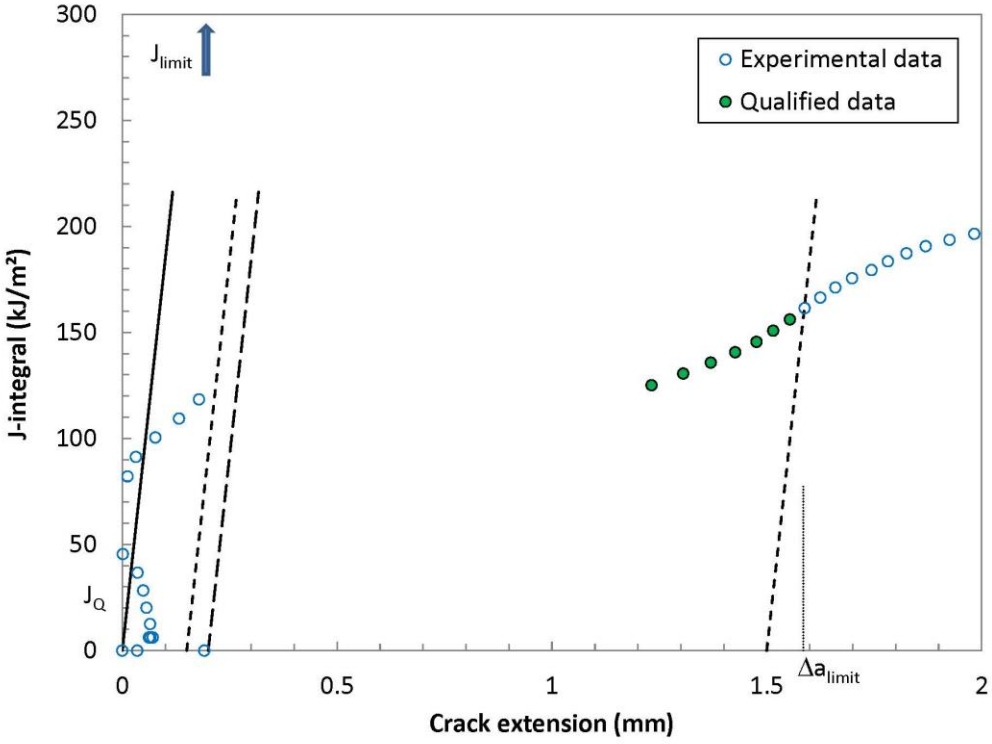
J-integral (kJ/m²)
Crack extension (mm)
J_limit
Experimental data
Qualified data
J_Q
Δa_limit
0
50
100
150
200
250
300
0
0.5
1
1.5
2

Specimen :	W4-F13			Δa =	0.25	mm	
F_c =	5.40	kN		K_e =	67.70	MPa$\sqrt{m}$	
B =	10.011	mm		J_e =	25.59	kJ/m²	
B_N =	8.001	mm					
W =	10.03	mm		η =	2.645787		
a_0 =	5.189	mm					
a_0/W =	0.518			J_{pl} =	82.80	kJ/m²	
S =	40	mm					
				J_c =	**106.99**	**kJ/m²**	NOT VALID
f(a/W) =	2.818212			**K_{Jc} =**	**138.43**	**MPa$\sqrt{m}$**	
T =	-196	°C		σ_Y =	923.5	MPa	
E =	163.00	GPa =	163000 MPa	.00 J_{QC}/σ_Y =	11.6	mm	
ν =	0.3						
A_{tot} =	1.55	kN.mm					
			Limits for compliance calculation:	**F_{low} =**	**0.6**	**kN**	
C_o =	0.023522	mm/kN		**F_{high} =**	**1.8**	**kN**	
A_{el} =	0.34	kN.mm					
A_{pl} =	1.21	kN.mm		Intercept:	-0.00661	mm	

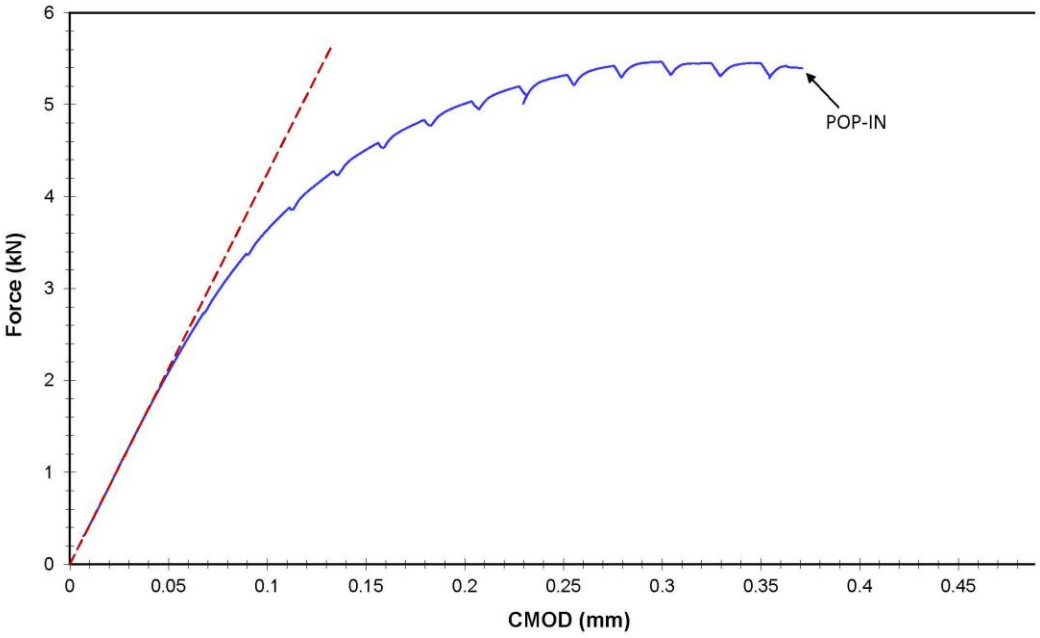

Weld W1, T = 4 K

TEST REPORT

Specimen Information

Type = SE(B)
Identification = W1-F4
Orientation = N/A

Basic dimensions

B =	10.05	mm
B_N =	8.00	mm
W =	10.03	mm

Other dimensions

S =	40.00	mm

Tensile Properties

E =	187	MPa
ν =	0.3	
σ_{YS} =	663.0	MPa
σ_{TS} =	1171.0	MPa

Crack Size Information

a_0 =	5.53	mm
a_{0q} =	5.54	mm
a_f =	8.18	mm
Δa_p =	2.65	mm
$\Delta a_{predicted}$ =	2.51	mm

Test temperature: -269 °C

Analysis of Results

Fracture type = stable tearing

Critical Fracture Toughness

J_Q = 16.98 kJ/m²

TM = 6.2 MPa

QUALIFICATION OF DATA

Estimates of initial crack size:	$a_{0q,1}$ =	5.530	mm	Diff :	0.000	< 0.002W =	0.0201 mm
	$a_{0q,2}$ =	5.533	mm		0.003	< 0.002W =	0.0201 mm
	a_{0q3} =	5.527	mm		0.003	< 0.002W =	0.0201 mm
	$a_{0,qmean}$ =	5.530	mm				

Qualification of data

Crack extension prediction	Δa_p =	2.65	mm (measured)	
	Δa_{pred} =	2.51	mm (predicted)	
	Difference =	-0.14	mm	PREDICTION NOT ACCEPTABLE

J_Q - Qualification of data

Power coefficient C_2 =	0.342887	< 1.0	→ QUALIFIED
$\lvert a_{0q} - a_0 \rvert$ =	0.01	mm	→ DATA SET ADEQUATE
# of data available to calculate a_{0q} :	5	< 8	→ DATA SET NOT ADEQUATE
# of data between $0.4J_q$ and J_q :	2	< 3	→ NOT QUALIFIED
Correlation coefficient a_{0q} fit :	0.997	≥ 0.96	→ DATA SET ADEQUATE
Data points distribution :	NOT VALID		
Number of qualified data points :	NOT VALID		

Qualification of J_Q as J_{Ic}

Thickness B =	10.05	mm > 10 JQ/Sy	→ QUALIFIED
Initial ligament b_0 =	4.50	mm > 10 JQ/Sy	→ QUALIFIED

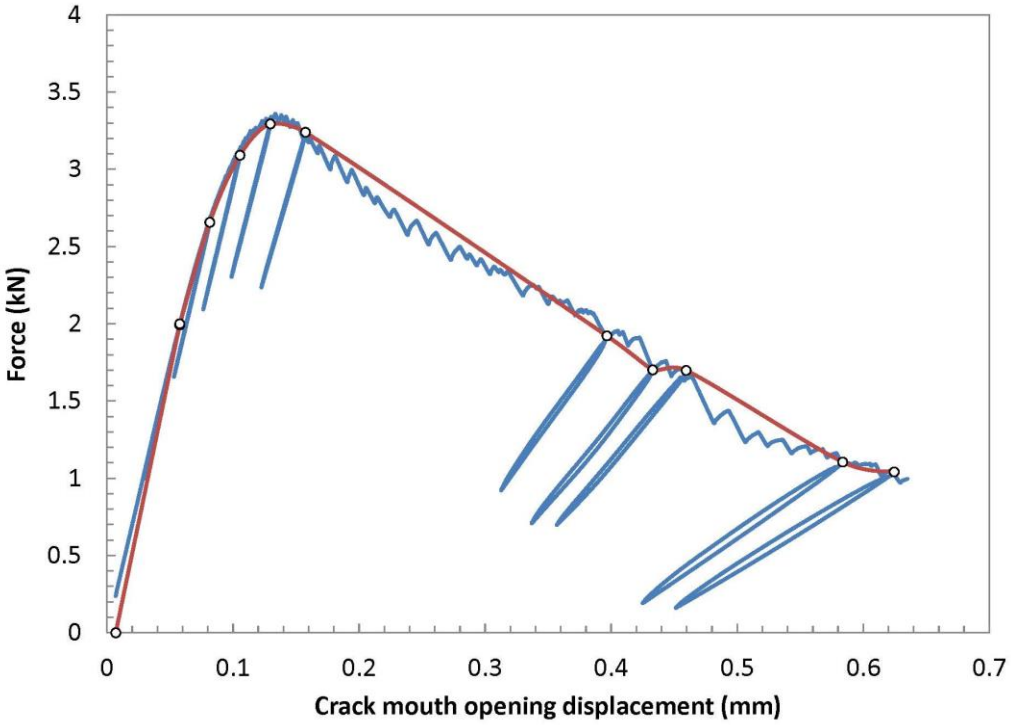
Force (kN)
Crack mouth opening displacement (mm)
0
0.5
1
1.5
2
2.5
3
3.5
4
0
0.1
0.2
0.3
0.4
0.5
0.6
0.7

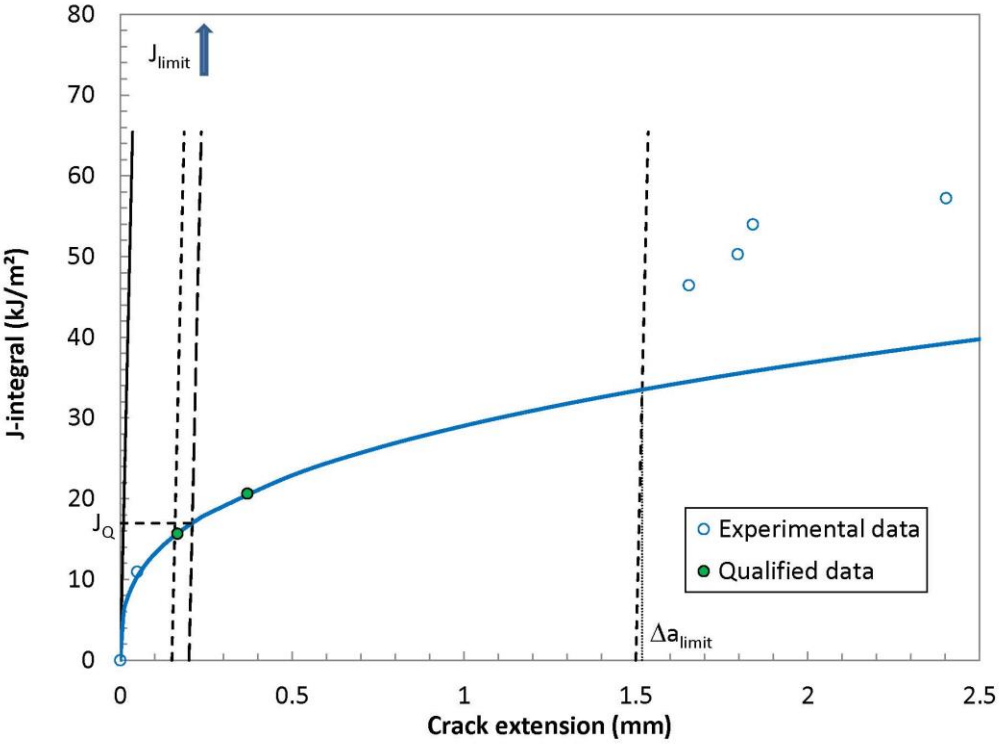
J-integral (kJ/m²)
Crack extension (mm)
J_limit
J_Q
Δa_limit
Experimental data
Qualified data
0
10
20
30
40
50
60
70
80
0
0.5
1
1.5
2
2.5

TEST REPORT

Specimen Information

Type = SE(B)
Identification = W1-F5
Orientation = N/A

Basic dimensions

B =	10.05	mm
B_N =	8.00	mm
W =	10.04	mm

Other dimensions

S =	40.00	mm

Tensile Properties

E =	187	MPa
ν =	0.3	
σ_{YS} =	663.0	MPa
σ_{TS} =	1171.0	MPa

Crack Size Information

a_0 =	5.76	mm
a_{0q} =	5.76	mm
a_f =	8.35	mm
Δa_p =	2.59	mm
$\Delta a_{predicted}$ =	2.13	mm

Test temperature: -269 °C

Analysis of Results

Fracture type = stable tearing

Critical Fracture Toughness

J_Q = 34.12 kJ/m²

TM = 19.0 MPa

QUALIFICATION OF DATA

Estimates of initial crack size:	$a_{0q,1}$ =	5.758	mm	Diff :	0.002	< 0.002W =	0.0201	mm
	$a_{0q,2}$ =	5.757	mm		0.003	< 0.002W =	0.0201	mm
	$a_{0,q3}$ =	5.765	mm		0.005	< 0.002W =	0.0201	mm
	$a_{0,qmean}$ =	5.760	mm					

Qualification of data

Crack extension prediction	Δa_p =	2.59	mm (measured)	
	Δa_{pred} =	2.13	mm (predicted)	
	Difference =	-0.46	mm	PREDICTION NOT ACCEPTABLE

J_Q - Qualification of data

Power coefficient C_2 =	0.545987	< 1.0	→ QUALIFIED
$\lvert a_{0q} - a_0 \rvert$ =	0.00	mm	→ DATA SET ADEQUATE
# of data available to calculate a_{0q} :	9	≥ 8	→ DATA SET ADEQUATE
# of data between 0.4J_q and J_q :	3	≥ 3	→ QUALIFIED
Correlation coefficient a_{0q} fit :	0.998	≥ 0.96	→ DATA SET ADEQUATE
Data points distribution :	VALID		
Number of qualified data points :	VALID		

Qualification of J_Q as J_{Ic}

Thickness B =	10.05	mm > 10 JQ/Sy	→ QUALIFIED
Initial ligament b_0 =	4.28	mm > 10 JQ/Sy	→ QUALIFIED

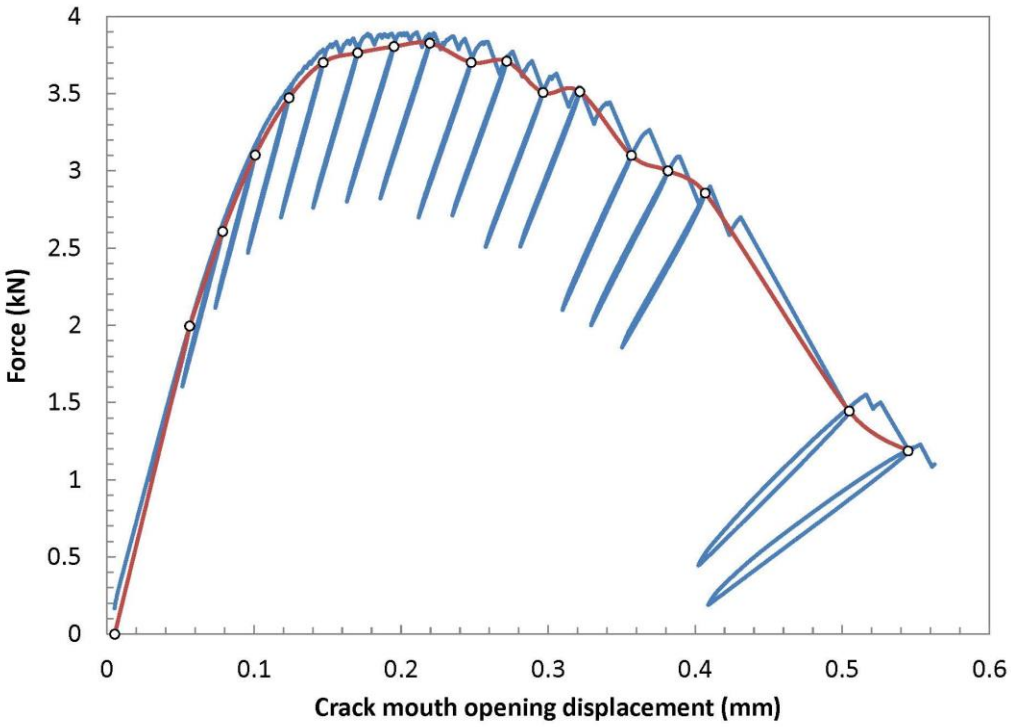
Force (kN)
Crack mouth opening displacement (mm)
0
0.5
1
1.5
2
2.5
3
3.5
4
0
0.1
0.2
0.3
0.4
0.5
0.6

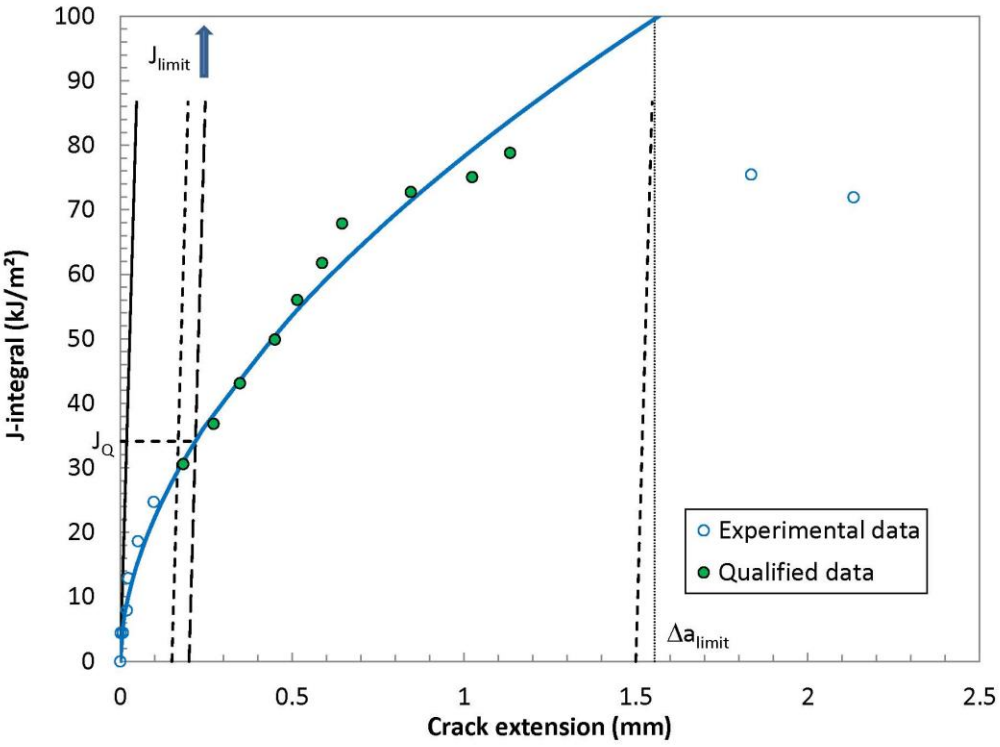
J-integral (kJ/m²)
Crack extension (mm)
J_limit
J_Q
Δa_limit
Experimental data
Qualified data
0
10
20
30
40
50
60
70
80
90
100
0
0.5
1
1.5
2
2.5

TEST REPORT

Specimen Information

Type = SE(B)
Identification = W1-F6
Orientation = N/A

Basic dimensions

B =	10.05	mm
B_N =	8.00	mm
W =	10.04	mm

Other dimensions

S =	40.00	mm

Tensile Properties

E =	187	MPa
ν =	0.3	
σ_{YS} =	663.0	MPa
σ_{TS} =	1171.0	MPa

Crack Size Information

a_0 =	5.30	mm
a_{0q} =	5.30	mm
a_f =	8.17	mm
Δa_p =	2.87	mm
$\Delta a_{predicted}$ =	2.58	mm

Test temperature: -269 °C

Analysis of Results

Fracture type = stable tearing

Critical Fracture Toughness

J_Q = 16.80 kJ/m²

TM = 5.5 MPa

QUALIFICATION OF DATA

Estimates of initial crack size:	$a_{0q,1}$ =	5.294	mm	Diff :	0.006	< 0.002W =	0.0201 mm
	$a_{0q,2}$ =	5.302	mm		0.002	< 0.002W =	0.0201 mm
	$a_{0,q3}$ =	5.304	mm		0.004	< 0.002W =	0.0201 mm
	$a_{0,qmean}$ =	5.300	mm				

Qualification of data

Crack extension prediction	Δa_p =	2.87	mm (measured)	
	Δa_{pred} =	2.58	mm (predicted)	
	Difference =	-0.29	mm	PREDICTION NOT ACCEPTABLE

J_Q - Qualification of data

Power coefficient C_2 =	0.307914	< 1.0	→ QUALIFIED
$\lvert a_{0q} - a_0 \rvert$ =	0.00	mm	→ DATA SET ADEQUATE
# of data available to calculate a_{0q} :	5	< 8	→ DATA SET NOT ADEQUATE
# of data between $0.4J_q$ and J_q :	2	< 3	→ NOT QUALIFIED
Correlation coefficient a_{0q} fit :	0.979	≥ 0.96	→ DATA SET ADEQUATE

Data points distribution : VALID
Number of qualified data points : NOT VALID

Qualification of J_Q as J_{Ic}

Thickness B =	10.05	mm > 10 JQ/Sy	→ QUALIFIED
Initial ligament b_0 =	4.74	mm > 10 JQ/Sy	→ QUALIFIED

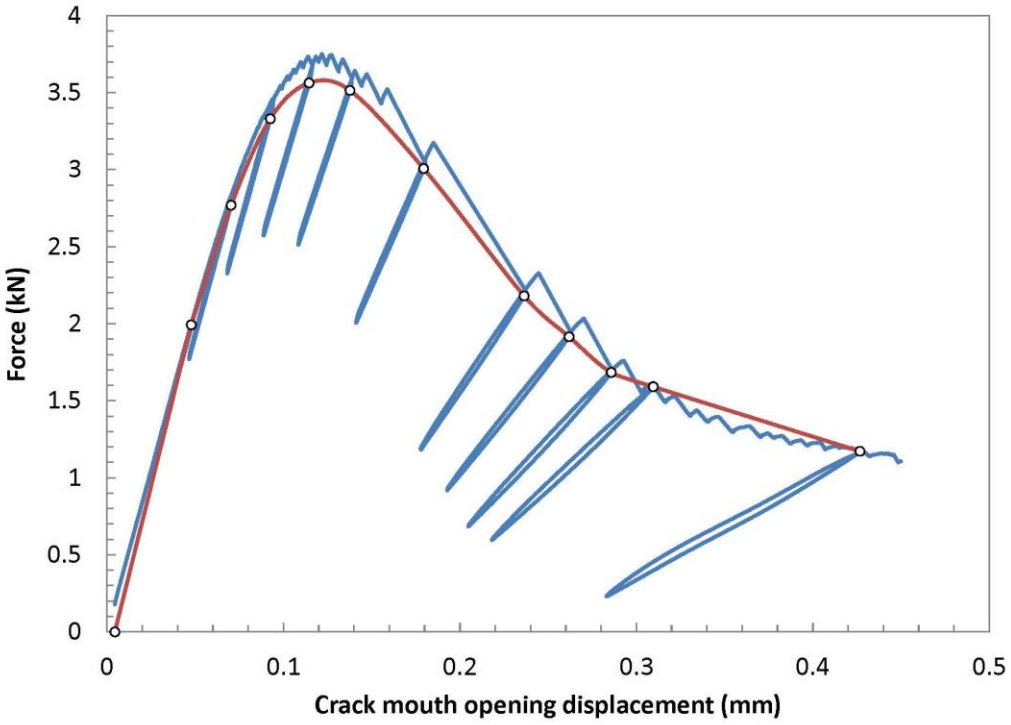
Force (kN)
Crack mouth opening displacement (mm)
0
0.5
1
1.5
2
2.5
3
3.5
4
0
0.1
0.2
0.3
0.4
0.5

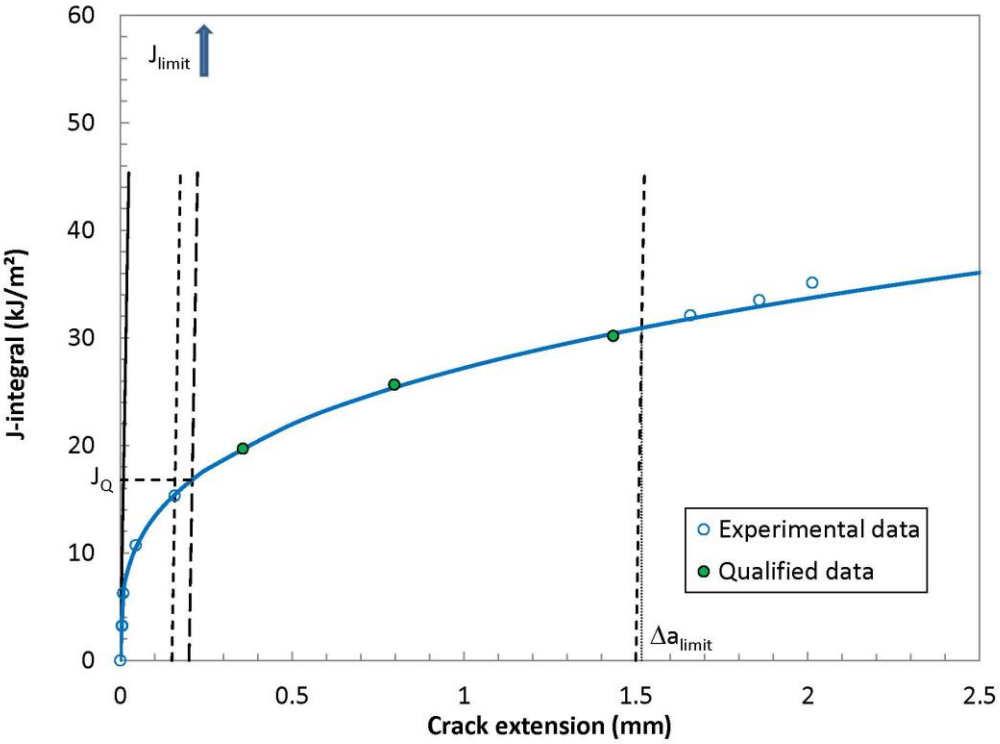
J-integral (kJ/m²)
Crack extension (mm)
J_limit
J_Q
Δa_limit
Experimental data
Qualified data
0
10
20
30
40
50
60
0
0.5
1
1.5
2
2.5

TEST REPORT

Specimen Information

Type = SE(B)
Identification = W1-F7
Orientation = N/A

Basic dimensions

B =	10.04	mm
B_N =	8.00	mm
W =	10.04	mm

Other dimensions

S =	40.00	mm

Tensile Properties

E =	187	MPa
ν =	0.3	
σ_{YS} =	663.0	MPa
σ_{TS} =	1171.0	MPa

Crack Size Information

a_0 =	5.31	mm
a_{0q} =	5.32	mm
a_f =	7.69	mm
Δa_p =	2.38	mm
$\Delta a_{predicted}$ =	2.02	mm

Test temperature: -269 °C

Analysis of Results

Fracture type = stable tearing

Critical Fracture Toughness

J_Q = 17.06 kJ/m²

TM = 5.3 MPa

QUALIFICATION OF DATA

Estimates of initial crack size:	$a_{0q,1}$ =	5.313	mm	Diff :	0.003	< 0.002W =	0.0201	mm
	$a_{0q,2}$ =	5.312	mm		0.002	< 0.002W =	0.0201	mm
	$a_{0,q3}$ =	5.306	mm		0.004	< 0.002W =	0.0201	mm
	$a_{0,qmean}$ =	5.310	mm					

Qualification of data

Crack extension prediction	Δa_p =	2.38	mm (measured)	
	Δa_{pred} =	2.02	mm (predicted)	
	Difference =	-0.36	mm	PREDICTION NOT ACCEPTABLE

J_Q - Qualification of data

Power coefficient C_2 =	0.292352	< 1.0	→ QUALIFIED
$\lvert a_{0q} - a_0 \rvert$ =	0.01	mm	→ DATA SET ADEQUATE
# of data available to calculate a_{0q} :	5	< 8	→ DATA SET NOT ADEQUATE
# of data between $0.4J_q$ and J_q :	2	< 3	→ NOT QUALIFIED
Correlation coefficient a_{0q} fit :	0.984	≥ 0.96	→ DATA SET ADEQUATE

Data points distribution : VALID
Number of qualified data points : NOT VALID

Qualification of J_Q as J_{Ic}

Thickness B =	10.04	mm > 10 JQ/Sy	→ QUALIFIED
Initial ligament b_0 =	4.73	mm > 10 JQ/Sy	→ QUALIFIED

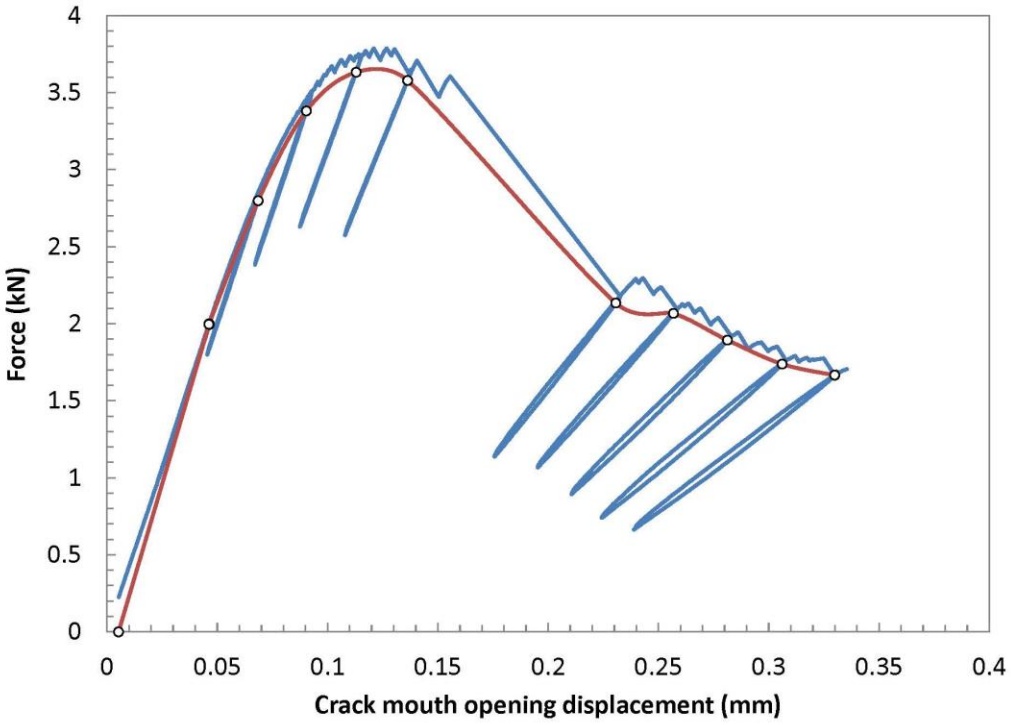
Force (kN)
Crack mouth opening displacement (mm)
0
0.5
1
1.5
2
2.5
3
3.5
4
0.05
0.1
0.15
0.2
0.25
0.3
0.35
0.4

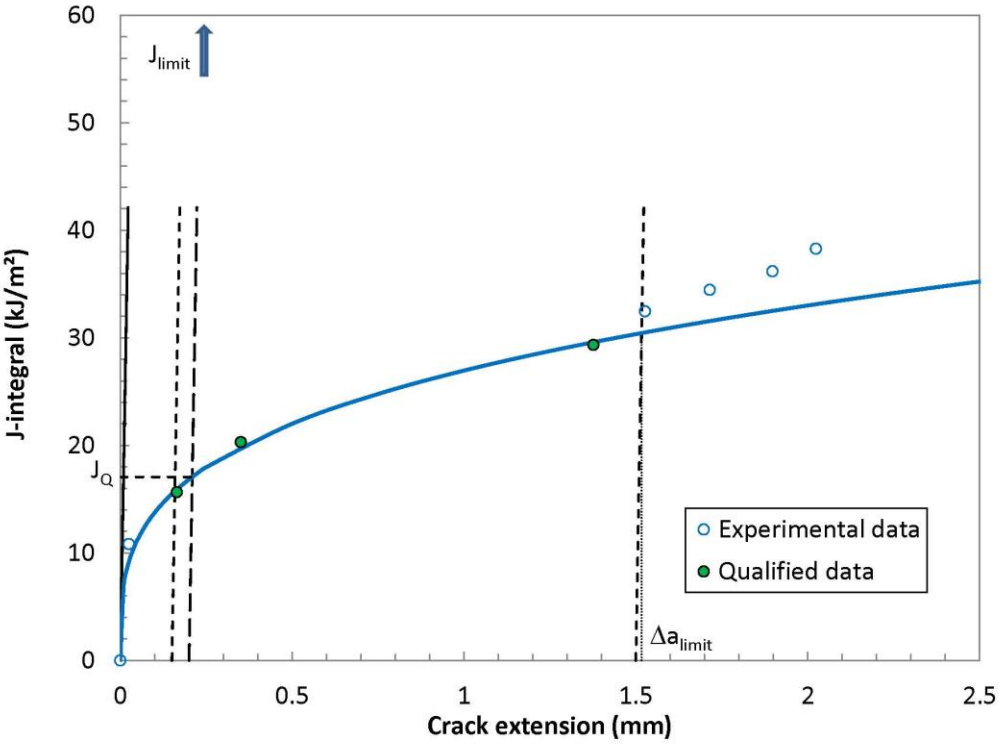
J-integral (kJ/m²)
Crack extension (mm)
J_limit
J_Q
Δa_limit
Experimental data
Qualified data
0
10
20
30
40
50
60
0.5
1
1.5
2
2.5

TEST REPORT

Specimen Information

Type = SE(B)
Identification = W1-F8
Orientation = N/A

Basic dimensions

B =	10.03	mm
B_N =	8.01	mm
W =	10.03	mm

Other dimensions

S =	40.00	mm

Tensile Properties

E =	187	MPa
ν =	0.3	
σ_{YS} =	663.0	MPa
σ_{TS} =	1171.0	MPa

Crack Size Information

a_0 =	5.37	mm
a_{0q} =	5.37	mm
a_f =	8.00	mm
Δa_p =	2.63	mm
$\Delta a_{predicted}$ =	2.36	mm

Test temperature: -269 °C

Analysis of Results

Fracture type = stable tearing

Critical Fracture Toughness

J_Q = 17.56 kJ/m²

TM = 6.1 MPa

QUALIFICATION OF DATA

Estimates of initial crack size:	$a_{0q,1}$ =	5.364	mm	Diff :	0.006	< 0.002W =	0.0201 mm
	$a_{0q,2}$ =	5.374	mm		0.004	< 0.002W =	0.0201 mm
	$a_{0,q3}$ =	5.373	mm		0.003	< 0.002W =	0.0201 mm
	$a_{0,qmean}$ =	5.370	mm				

Qualification of data

Crack extension prediction	Δa_p =	2.63	mm (measured)	
	Δa_{pred} =	2.36	mm (predicted)	
	Difference =	-0.27	mm	PREDICTION NOT ACCEPTABLE

J_Q - Qualification of data

Power coefficient C_2 =	0.328483	< 1.0	→ QUALIFIED
$\lvert a_{0q} - a_0 \rvert$ =	0.00	mm	→ DATA SET ADEQUATE
# of data available to calculate a_{0q} :	5	< 8	→ DATA SET NOT ADEQUATE
# of data between $0.4J_q$ and J_q :	2	< 3	→ NOT QUALIFIED
Correlation coefficient a_{0q} fit :	0.939	< 0.96	→ DATA SET NOT ADEQUATE
Data points distribution :	VALID		
Number of qualified data points :	VALID		

Qualification of J_Q as J_{Ic}

Thickness B =	10.03	mm > 10 JQ/Sy	→ QUALIFIED
Initial ligament b_0 =	4.66	mm > 10 JQ/Sy	→ QUALIFIED

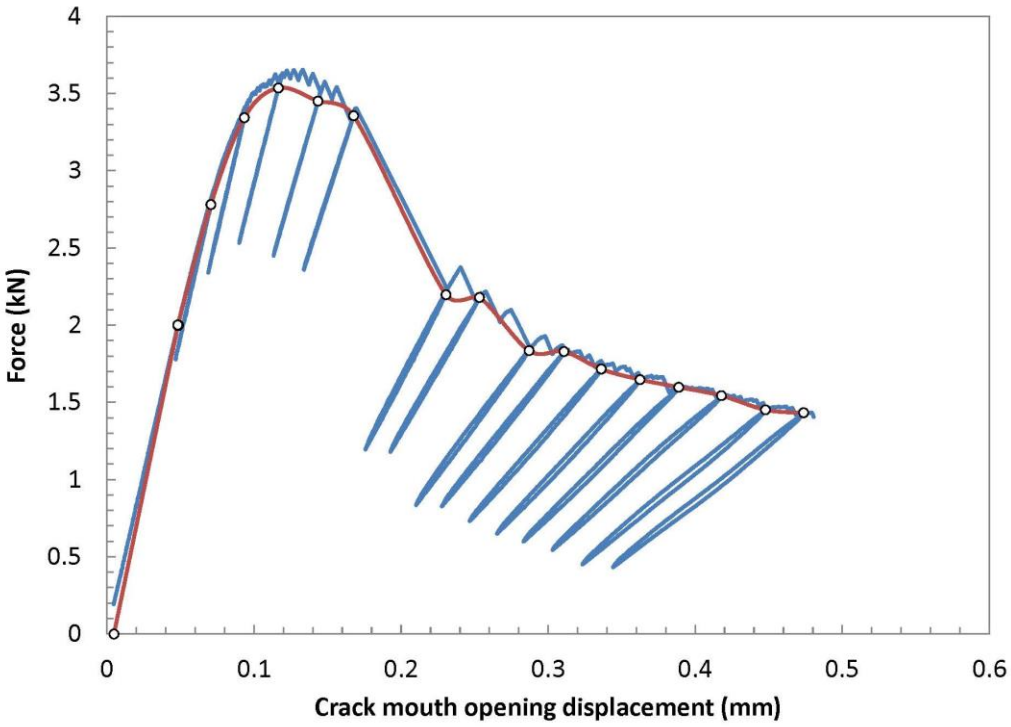
Force (kN)
Crack mouth opening displacement (mm)
0
0.5
1
1.5
2
2.5
3
3.5
4
0
0.1
0.2
0.3
0.4
0.5
0.6

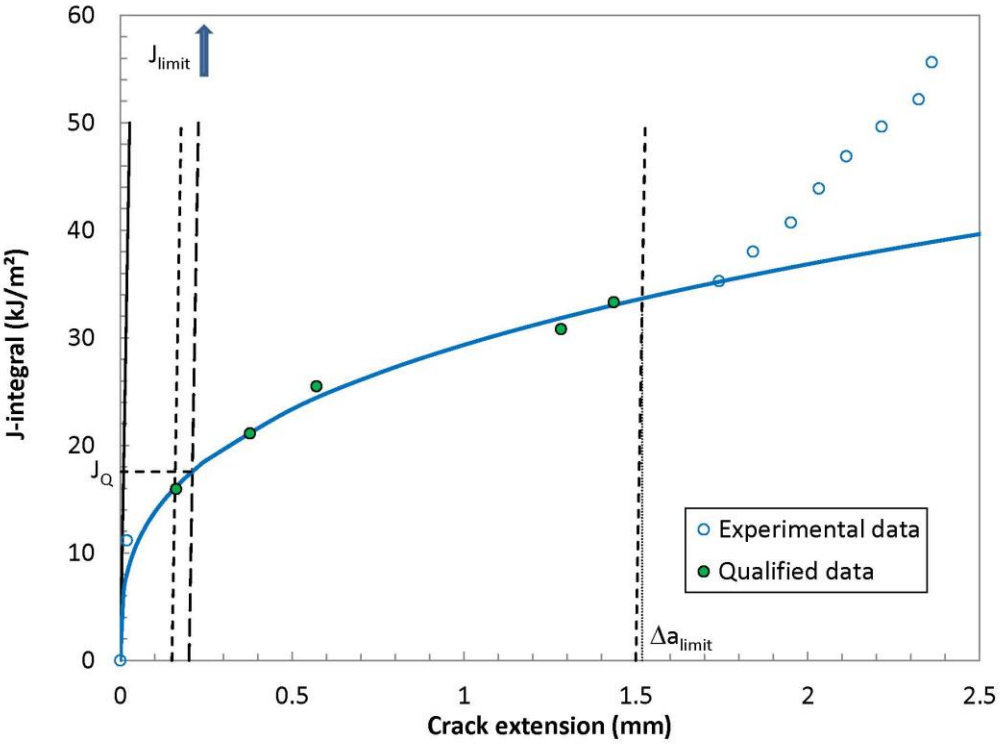
J-integral (kJ/m²)
Crack extension (mm)
J_limit
J_Q
Δa_limit
Experimental data
Qualified data
0
10
20
30
40
50
60
0
0.5
1
1.5
2
2.5

Weld W2, T = 4 K

TEST REPORT

Specimen Information

Type = SE(B)
Identification = W2-F3
Orientation = N/A

Basic dimensions

B =	10.03	mm
B_N =	8.01	mm
W =	10.02	mm

Other dimensions

S =	40.00	mm

Tensile Properties

E =	180	MPa
ν =	0.3	
σ_{YS} =	646.0	MPa
σ_{TS} =	1438.0	MPa

Crack Size Information

a_0 =	5.29	mm
a_{0q} =	5.13	mm
a_f =	8.00	mm
Δa_p =	2.71	mm
$\Delta a_{predicted}$ =	2.44	mm

Test temperature: -269 °C

Analysis of Results

Fracture type = stable tearing

Critical Fracture Toughness

J_Q = 111.72 kJ/m²

TM = 33.4 MPa

QUALIFICATION OF DATA

Estimates of initial crack size:	$a_{0q,1}$ =	5.136	mm	Diff :	0.023	> 0.002W =	0.0200	mm
	$a_{0q,2}$ =	5.127	mm		0.014	< 0.002W =	0.0200	mm
	$a_{0,q3}$ =	5.076	mm		0.037	> 0.002W =	0.0200	mm
	$a_{0,qmean}$ =	5.113	mm					

Qualification of data

Crack extension prediction	Δa_p =	2.71	mm (measured)	
	Δa_{pred} =	2.44	mm (predicted)	
	Difference =	-0.27	mm	PREDICTION NOT ACCEPTABLE

J_Q - Qualification of data

Power coefficient C_2 =	0.457084	< 1.0	→ QUALIFIED
$\lvert a_{0q} - a_0 \rvert$ =	0.16	mm	→ DATA SET ADEQUATE
# of data available to calculate a_{0q} :	14	≥ 8	→ DATA SET ADEQUATE
# of data between $0.4J_q$ and J_q :	6	≥ 3	→ QUALIFIED
Correlation coefficient a_{0q} fit :	0.289	< 0.96	→ DATA SET NOT ADEQUATE
Data points distribution :	VALID		
Number of qualified data points :	VALID		

Qualification of J_Q as J_{Ic}

Thickness B =	10.03	mm > 10 JQ/Sy	→ QUALIFIED
Initial ligament b_0 =	4.73	mm > 10 JQ/Sy	→ QUALIFIED

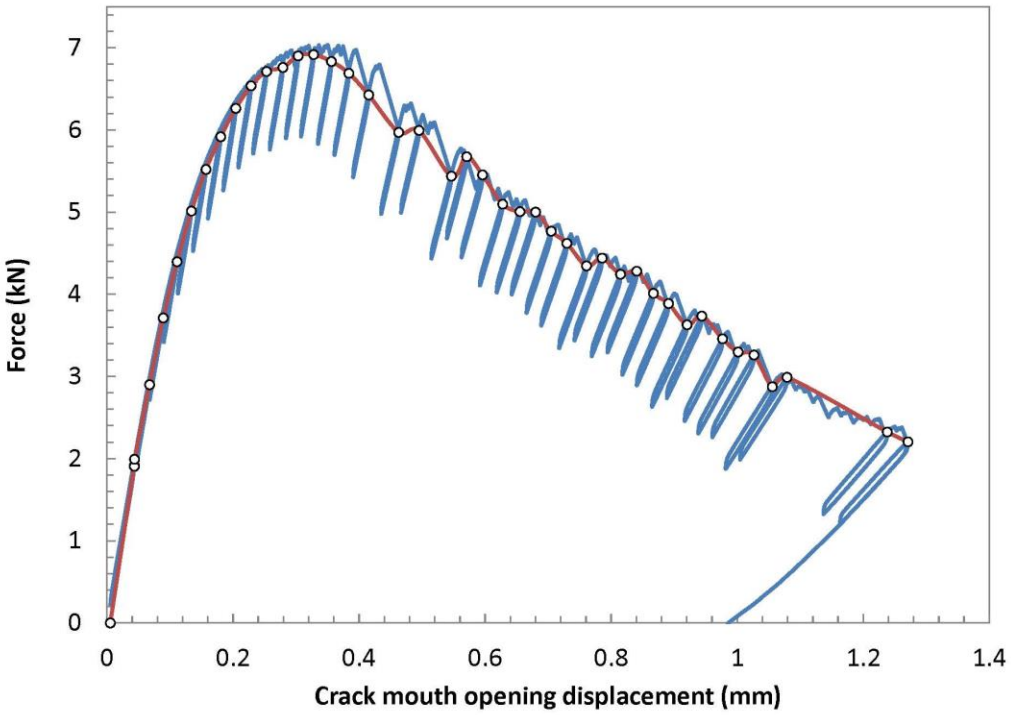
Force (kN)
0
1
2
3
4
5
6
7
0
0.2
0.4
0.6
0.8
1
1.2
1.4
Crack mouth opening displacement (mm)

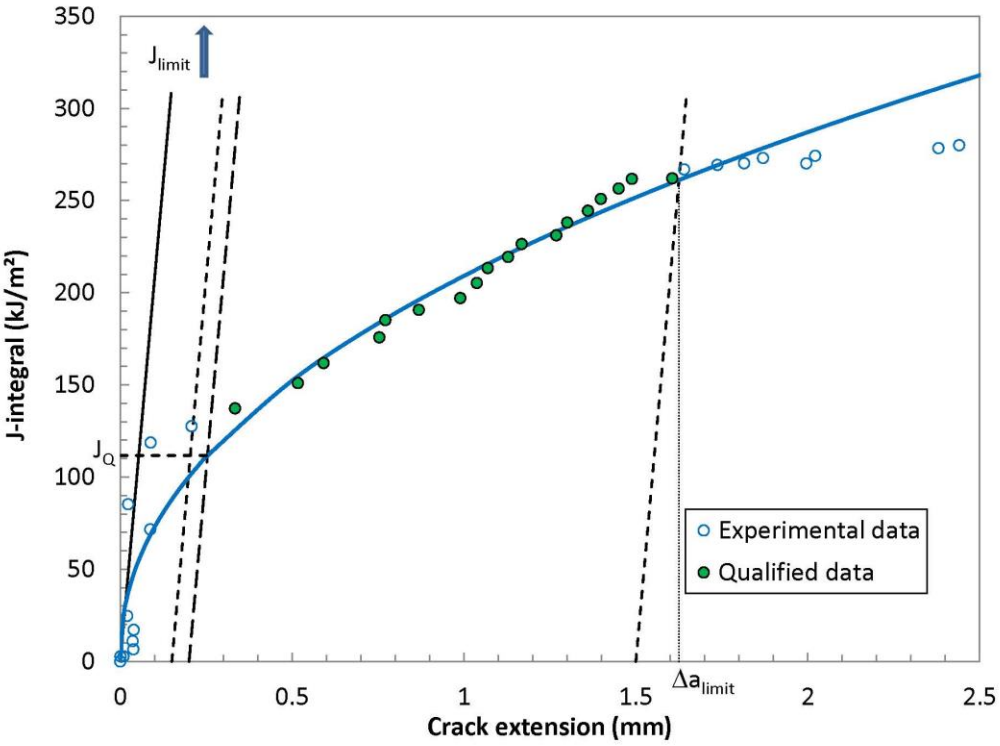
J-integral (kJ/m²)
0
50
100
150
200
250
300
350
J_limit
J_Q
Δa_limit
0
0.5
1
1.5
2
2.5
Crack extension (mm)
Experimental data
Qualified data

TEST REPORT

Specimen Information

Type = SE(B)
Identification = W2-F4
Orientation = N/A

Basic dimensions

B =	10.02	mm
B_N =	8.00	mm
W =	10.02	mm

Other dimensions

S =	40.00	mm

Tensile Properties

E =	180	MPa
ν =	0.3	
σ_{YS} =	646.0	MPa
σ_{TS} =	1438.0	MPa

Crack Size Information

a_0 =	5.18	mm
a_{0q} =	5.16	mm
a_f =	7.78	mm
Δa_p =	2.60	mm
$\Delta a_{predicted}$ =	1.99	mm

Test temperature: -269 °C

Analysis of Results

Fracture type = stable tearing

Critical Fracture Toughness

J_Q = 148.99 kJ/m²

TM = 33.7 MPa

QUALIFICATION OF DATA

Estimates of initial crack size:	$a_{0q,1}$ =	5.189	mm	Diff :	0.007	< 0.002W =	0.0200	mm
	$a_{0q,2}$ =	5.191	mm		0.010	< 0.002W =	0.0200	mm
	$a_{0,q3}$ =	5.164	mm		0.017	< 0.002W =	0.0200	mm
	$a_{0,qmean}$ =	5.181	mm					

Qualification of data

Crack extension prediction	Δa_p =	2.60	mm (measured)	
	Δa_{pred} =	1.99	mm (predicted)	
	Difference =	-0.61	mm	PREDICTION NOT ACCEPTABLE

J_Q - Qualification of data

Power coefficient C_2 =	0.370328	< 1.0	→ QUALIFIED
$\lvert a_{0q} - a_0 \rvert$ =	0.02	mm	→ DATA SET ADEQUATE
# of data available to calculate a_{0q} :	13	≥ 8	→ DATA SET ADEQUATE
# of data between $0.4J_q$ and J_q :	8	≥ 3	→ QUALIFIED
Correlation coefficient a_{0q} fit :	0.582	< 0.96	→ DATA SET NOT ADEQUATE

Data points distribution : VALID
Number of qualified data points : VALID

Qualification of J_Q as J_{Ic}

Thickness B =	10.02	mm > 10 JQ/Sy	→ QUALIFIED
Initial ligament b_0 =	4.84	mm > 10 JQ/Sy	→ QUALIFIED

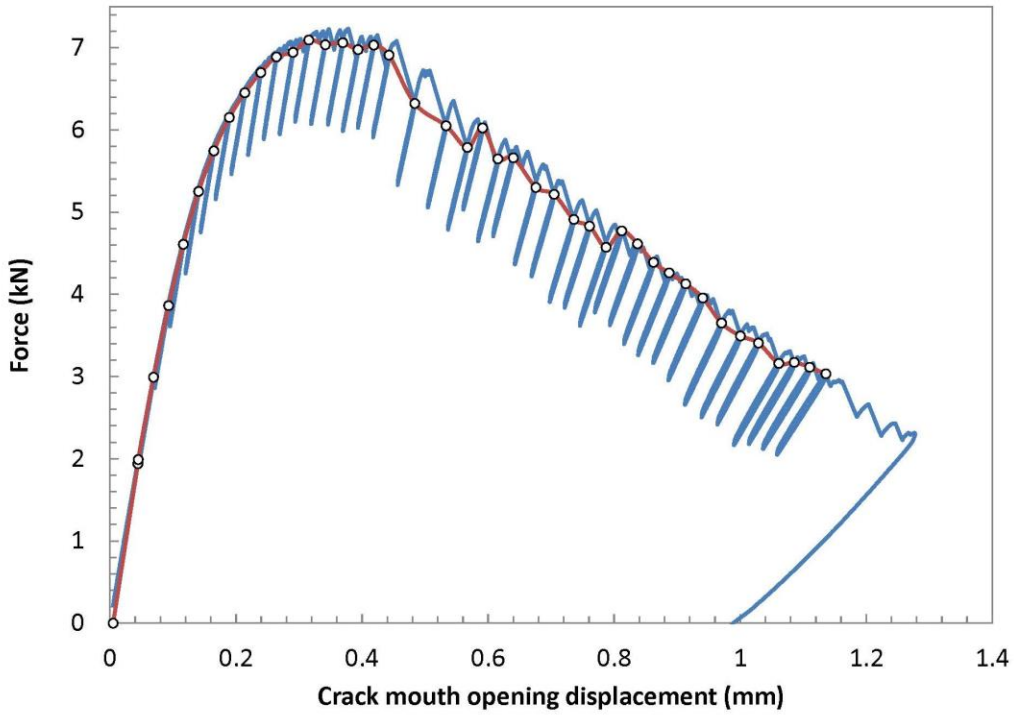
Force (kN)
Crack mouth opening displacement (mm)
0
1
2
3
4
5
6
7
0
0.2
0.4
0.6
0.8
1
1.2
1.4

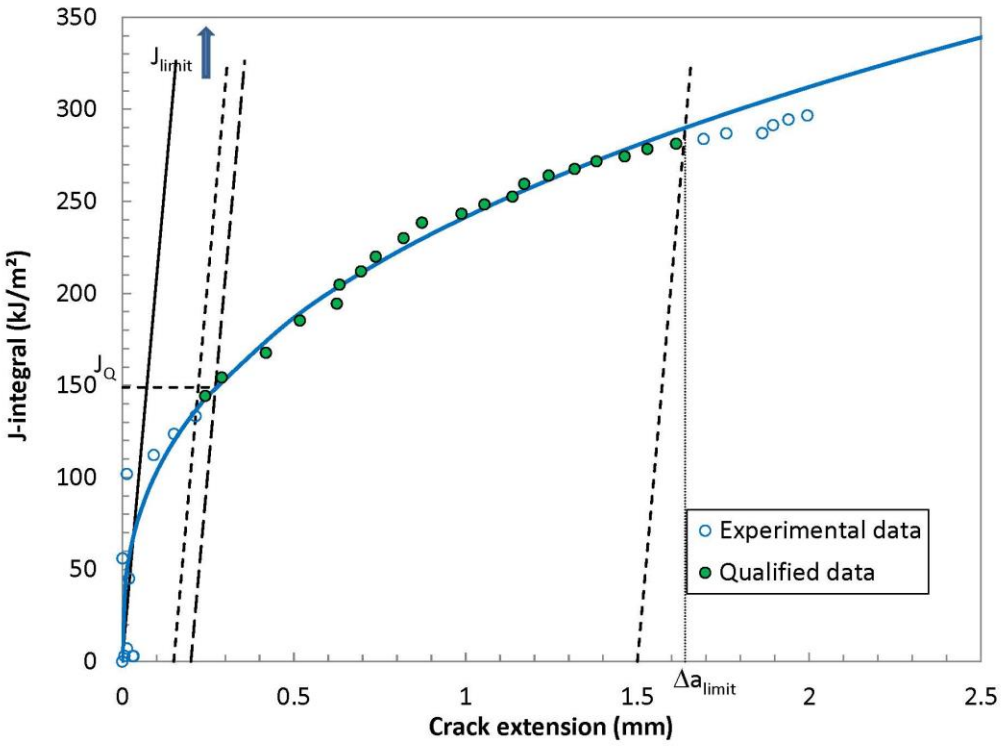
J-integral (kJ/m²)
Crack extension (mm)
J_limit
J_Q
Δa_limit
Experimental data
Qualified data
0
50
100
150
200
250
300
350
0
0.5
1
1.5
2
2.5

TEST REPORT

Specimen Information

Type = SE(B)
Identification = W2-F5
Orientation = N/A

Basic dimensions

B =	10.02	mm
B_N =	8.00	mm
W =	10.02	mm

Other dimensions

S =	40.00	mm

Tensile Properties

E =	180	MPa
ν =	0.3	
σ_{YS} =	646.0	MPa
σ_{TS} =	1438.0	MPa

Crack Size Information

a_0 =	5.12	mm
a_{0q} =	5.15	mm
a_f =	7.80	mm
Δa_p =	2.68	mm
$\Delta a_{predicted}$ =	2.75	mm

Test temperature: -269 °C

Analysis of Results

Fracture type = stable tearing

Critical Fracture Toughness

J_Q = 131.19 kJ/m²

TM = 26.3 MPa

QUALIFICATION OF DATA

Estimates of initial crack size:	$a_{0q,1}$ =	5.157	mm	Diff :	0.005	< 0.002W =	0.0200	mm
	$a_{0q,2}$ =	5.164	mm		0.002	< 0.002W =	0.0200	mm
	$a_{0,q3}$ =	5.164	mm		0.002	< 0.002W =	0.0200	mm
	$a_{0,qmean}$ =	5.162	mm					

Qualification of data

Crack extension prediction	Δa_p =	2.68	mm (measured)	
	Δa_{pred} =	2.75	mm (predicted)	
	Difference =	0.07	mm	(PREDICTION ACCEPTABLE)

J_Q - Qualification of data

Power coefficient C_2 =	0.318003	< 1.0	→ QUALIFIED
$\lvert a_{0q} - a_0 \rvert$ =	0.03	mm	→ DATA SET ADEQUATE
# of data available to calculate a_{0q} :	13	≥ 8	→ DATA SET ADEQUATE
# of data between $0.4J_q$ and J_q :	7	≥ 3	→ QUALIFIED
Correlation coefficient a_{0q} fit :	0.244	< 0.96	→ DATA SET NOT ADEQUATE

Data points distribution : VALID
Number of qualified data points : VALID

Qualification of J_Q as J_{Ic}

Thickness B =	10.02	mm > 10 JQ/Sy	→ QUALIFIED
Initial ligament b_0 =	4.90	mm > 10 JQ/Sy	→ QUALIFIED

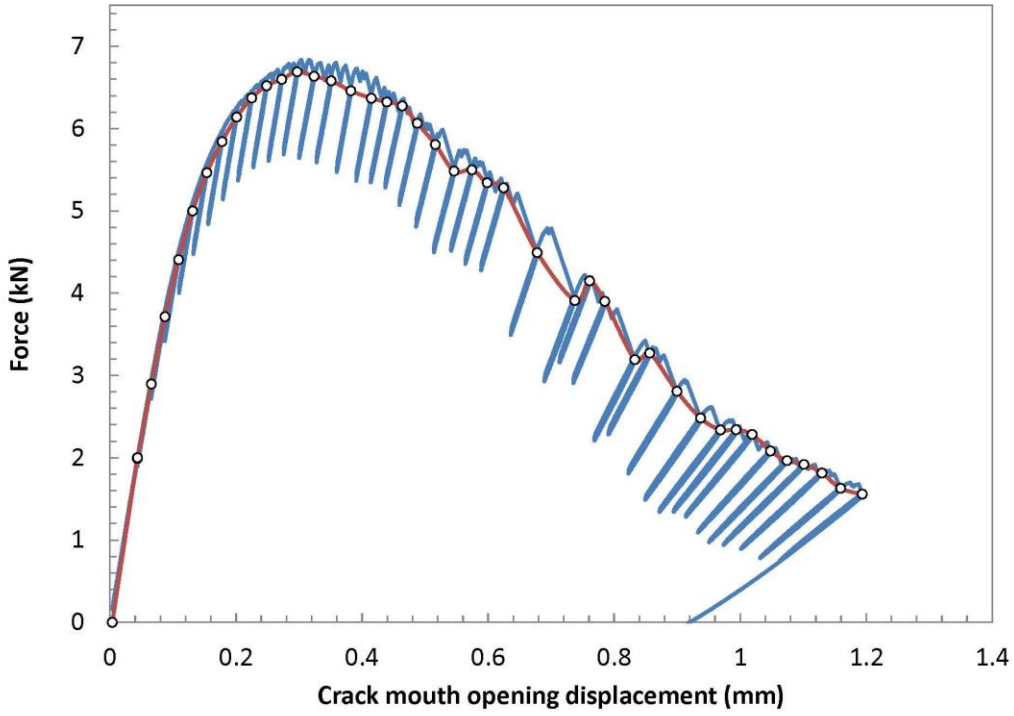
Force (kN)
Crack mouth opening displacement (mm)
0
1
2
3
4
5
6
7
0
0.2
0.4
0.6
0.8
1
1.2
1.4

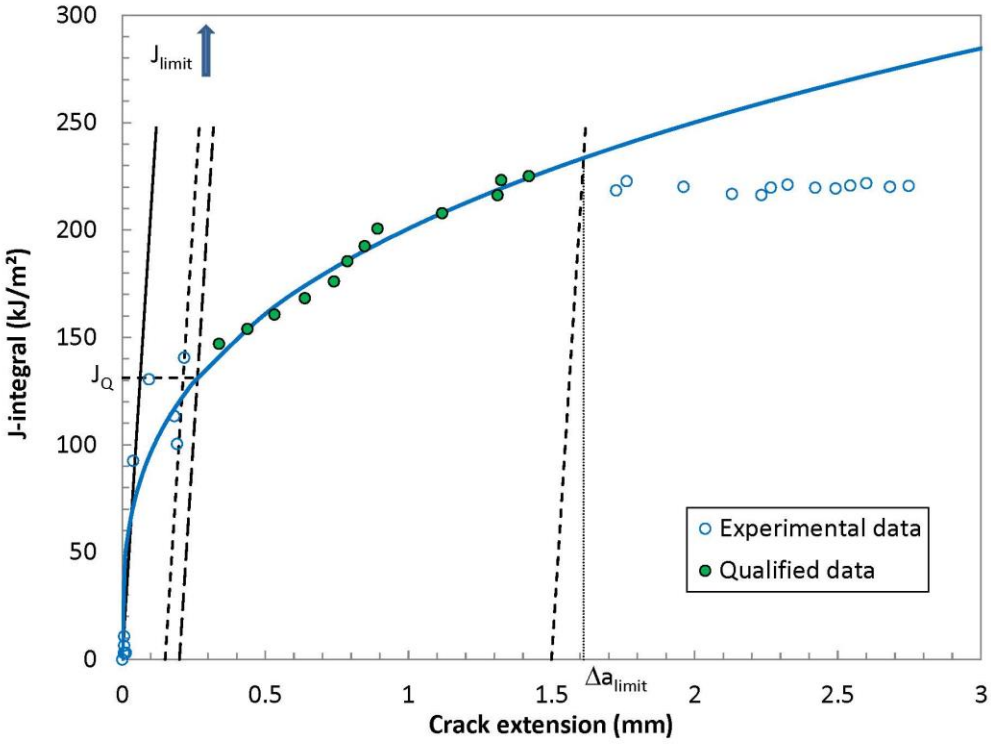
J-integral (kJ/m²)
Crack extension (mm)
J_limit
J_Q
Δa_limit
Experimental data
Qualified data
0
50
100
150
200
250
300
0
0.5
1
1.5
2
2.5
3

TEST REPORT

Specimen Information

Type = SE(B)
Identification = W2-F6
Orientation = N/A

Basic dimensions

B =	10.01	mm
B_N =	8.01	mm
W =	10.02	mm

Other dimensions

S =	40.00	mm

Tensile Properties

E =	180	MPa
ν =	0.3	
σ_{YS} =	646.0	MPa
σ_{TS} =	1438.0	MPa

Crack Size Information

a_0 =	5.13	mm
a_{0q} =	5.15	mm
a_f =	8.20	mm
Δa_p =	3.07	mm
$\Delta a_{predicted}$ =	2.85	mm

Test temperature: -269 °C

Analysis of Results

Fracture type = stable tearing

Critical Fracture Toughness

J_Q = 164.59 kJ/m²

TM = 29.1 MPa

QUALIFICATION OF DATA

Estimates of initial crack size:	$a_{0q,1}$ =	5.157	mm	Diff :	0.003	< 0.002W =	0.0200	mm
	$a_{0q,2}$ =	5.153	mm		0.001	< 0.002W =	0.0200	mm
	$a_{0,q3}$ =	5.152	mm		0.002	< 0.002W =	0.0200	mm
	$a_{0,qmean}$ =	5.154	mm					

Qualification of data

Crack extension prediction	Δa_p =	3.07	mm (measured)	
	Δa_{pred} =	2.85	mm (predicted)	
	Difference =	-0.22	mm	PREDICTION NOT ACCEPTABLE

J_Q - Qualification of data

Power coefficient C_2 =	0.297953	< 1.0	→ QUALIFIED
$\lvert a_{0q} - a_0 \rvert$ =	0.02	mm	→ DATA SET ADEQUATE
# of data available to calculate a_{0q} :	15	≥ 8	→ DATA SET ADEQUATE
# of data between $0.4J_q$ and J_q :	8	≥ 3	→ QUALIFIED
Correlation coefficient a_{0q} fit :	0.740	< 0.96	→ DATA SET NOT ADEQUATE
Data points distribution :	VALID		
Number of qualified data points :	VALID		

Qualification of J_Q as J_{Ic}

Thickness B =	10.01	mm > 10 JQ/Sy	→ QUALIFIED
Initial ligament b_0 =	4.89	mm > 10 JQ/Sy	→ QUALIFIED

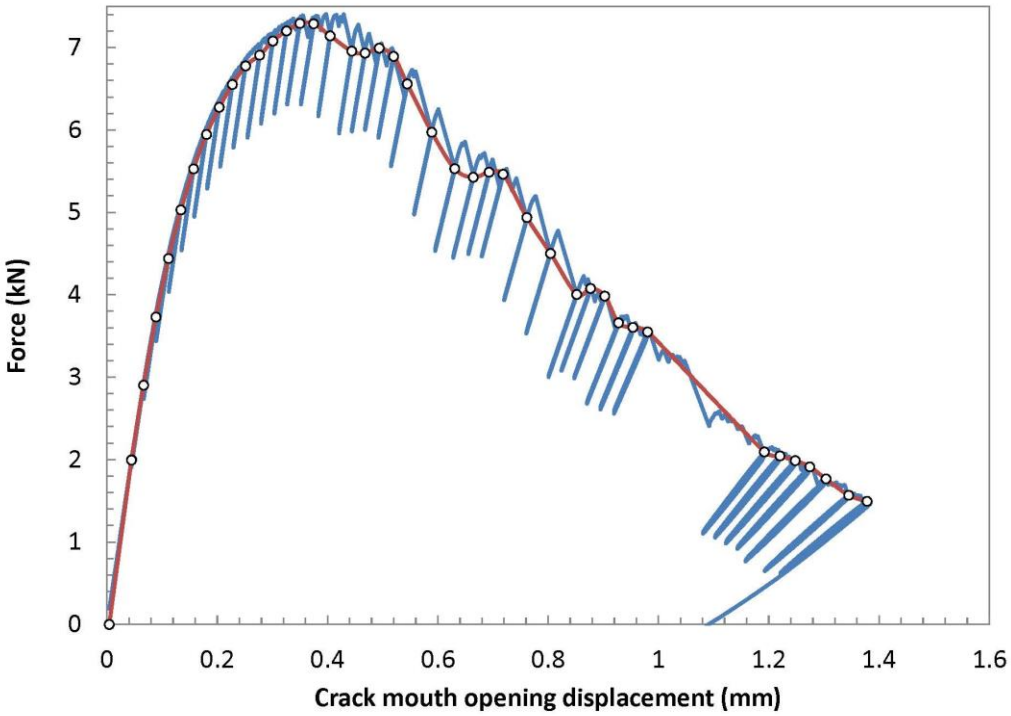
Force (kN)
Crack mouth opening displacement (mm)
0
1
2
3
4
5
6
7
0
0.2
0.4
0.6
0.8
1
1.2
1.4
1.6

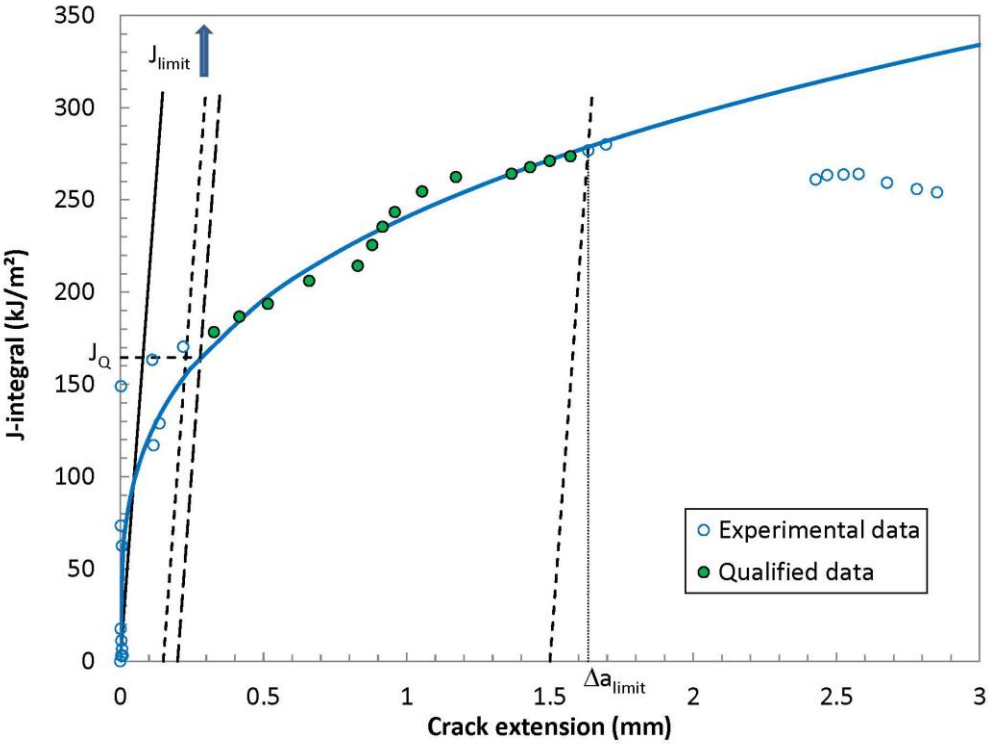
J-integral (kJ/m²)
Crack extension (mm)
J_limit
J_Q
Δa_limit
Experimental data
Qualified data
0
50
100
150
200
250
300
350
0
0.5
1
1.5
2
2.5
3

TEST REPORT

Specimen Information

Type = SE(B)
Identification = W2-F7
Orientation = N/A

Basic dimensions

B =	10.01	mm
B_N =	8.00	mm
W =	10.03	mm

Other dimensions

S =	40.00	mm

Tensile Properties

E =	180	MPa
ν =	0.3	
σ_{YS} =	646.0	MPa
σ_{TS} =	1438.0	MPa

Crack Size Information

a_0 =	5.28	mm
a_{0q} =	5.18	mm
a_f =	8.30	mm
Δa_p =	3.02	mm
$\Delta a_{predicted}$ =	2.68	mm

Test temperature: -269 °C

Analysis of Results

Fracture type = stable tearing

Critical Fracture Toughness

J_Q = 173.37 kJ/m²

TM = 39.0 MPa

QUALIFICATION OF DATA

Estimates of initial crack size:	$a_{0q,1}$ =	5.151	mm	Diff :	0.003	< 0.002W =	0.0201	mm
	$a_{0q,2}$ =	5.148	mm		0.000	< 0.002W =	0.0201	mm
	$a_{0,q3}$ =	5.146	mm		0.002	< 0.002W =	0.0201	mm
	$a_{0,qmean}$ =	5.148	mm					

Qualification of data

Crack extension prediction	Δa_p =	3.02	mm (measured)	
	Δa_{pred} =	2.68	mm (predicted)	
	Difference =	-0.34	mm	PREDICTION NOT ACCEPTABLE

J_Q - Qualification of data

Power coefficient C_2 =	0.384224	< 1.0	→ QUALIFIED
$\lvert a_{0q} - a_0 \rvert$ =	0.10	mm	→ DATA SET ADEQUATE
# of data available to calculate a_{0q} :	17	≥ 8	→ DATA SET ADEQUATE
# of data between $0.4J_q$ and J_q :	10	≥ 3	→ QUALIFIED
Correlation coefficient a_{0q} fit :	0.647	< 0.96	→ DATA SET NOT ADEQUATE

Data points distribution : VALID
Number of qualified data points : VALID

Qualification of J_Q as J_{Ic}

Thickness B =	10.01	mm > 10 JQ/Sy	→ QUALIFIED
Initial ligament b_0 =	4.75	mm > 10 JQ/Sy	→ QUALIFIED

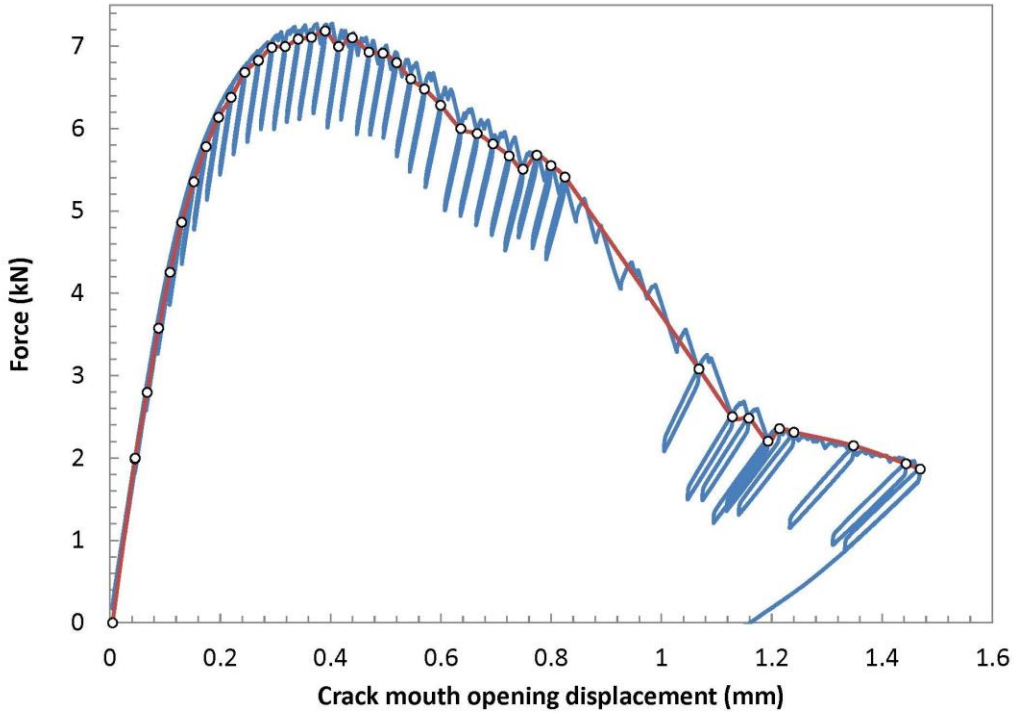
Force (kN)
0
1
2
3
4
5
6
7
0
0.2
0.4
0.6
0.8
1
1.2
1.4
1.6
Crack mouth opening displacement (mm)

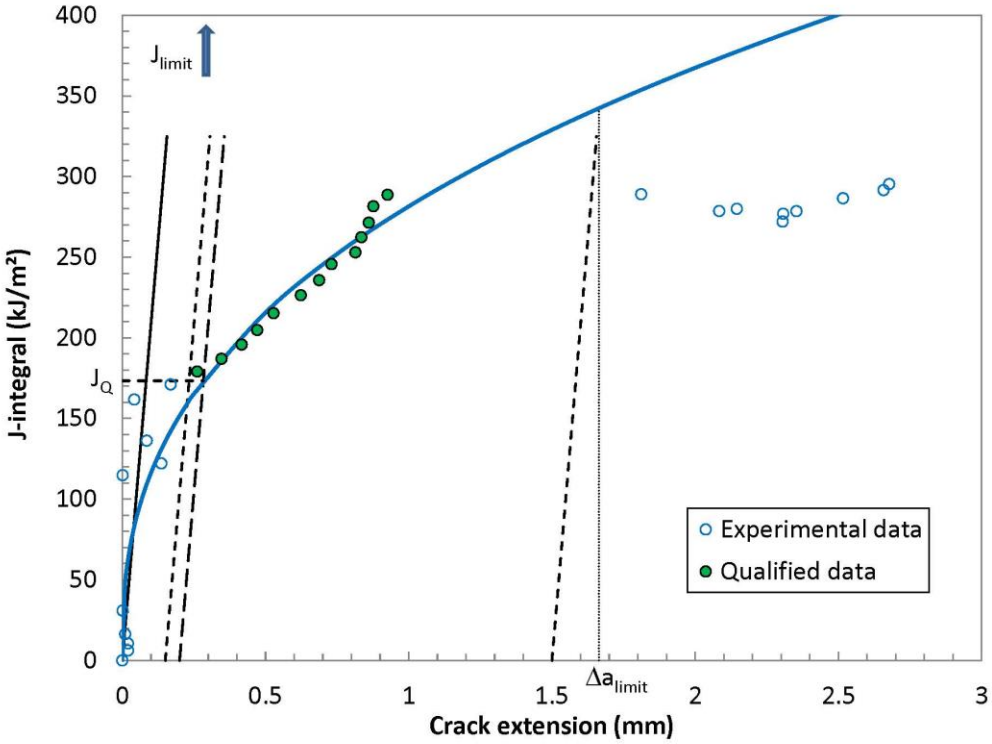
J-integral (kJ/m²)
400
350
300
250
200
150
100
50
0
J_limit
J_Q
Δa_limit
0
0.5
1
1.5
2
2.5
3
Crack extension (mm)
Experimental data
Qualified data

Weld W3, T = 4 K

TEST REPORT

Specimen Information

Type =	SE(B)
Identification =	**W3-F3**
Orientation =	N/A

Basic dimensions

B =	10.01	mm
B_N =	8.06	mm
W =	10.02	mm

Other dimensions

S =	40.00	mm

Tensile Properties

E =	177	MPa
ν =	0.3	
σ_{YS} =	626.0	MPa
σ_{TS} =	1197.0	MPa

Crack Size Information

a_0 =	5.29	mm
a_{0q} =	5.21	mm
a_f =	6.88	mm
Δa_p =	1.59	mm
$\Delta a_{predicted}$ =	1.29	mm

Test temperature: -269 °C

Analysis of Results

Fracture type = stable tearing

Critical Fracture Toughness

J_Q = 85.51 kJ/m²

TM = 36.3 MPa

QUALIFICATION OF DATA

Estimates of initial crack size:

$a_{0q,1}$ =	5.212	mm	Diff :	0.000	< 0.002W =	0.0200 mm
$a_{0q,2}$ =	5.214	mm		0.001	< 0.002W =	0.0200 mm
$a_{0,q3}$ =	5.212	mm		0.001	< 0.002W =	0.0200 mm
$a_{0,qmean}$ =	5.213	mm				

Qualification of data

Crack extension prediction	Δa_p =	1.59	mm (measured)	
	Δa_{pred} =	1.29	mm (predicted)	
	Difference =	-0.30	mm	PREDICTION NOT ACCEPTABLE

J_Q - Qualification of data

Power coefficient C_2 =	0.49181	< 1.0	→ QUALIFIED
$\lvert a_{0q} - a_0 \rvert$ =	0.08	mm	→ DATA SET ADEQUATE
# of data available to calculate a_{0q} :	11	≥ 8	→ DATA SET ADEQUATE
# of data between $0.4J_q$ and J_q :	6	≥ 3	→ QUALIFIED
Correlation coefficient a_{0q} fit :	0.984	≥ 0.96	→ DATA SET ADEQUATE
Data points distribution :	VALID		
Number of qualified data points :	VALID		

Qualification of J_Q as J_{Ic}

Thickness B =	10.01	mm > 10 JQ/Sy	→ QUALIFIED
Initial ligament b_0 =	4.73	mm > 10 JQ/Sy	→ QUALIFIED

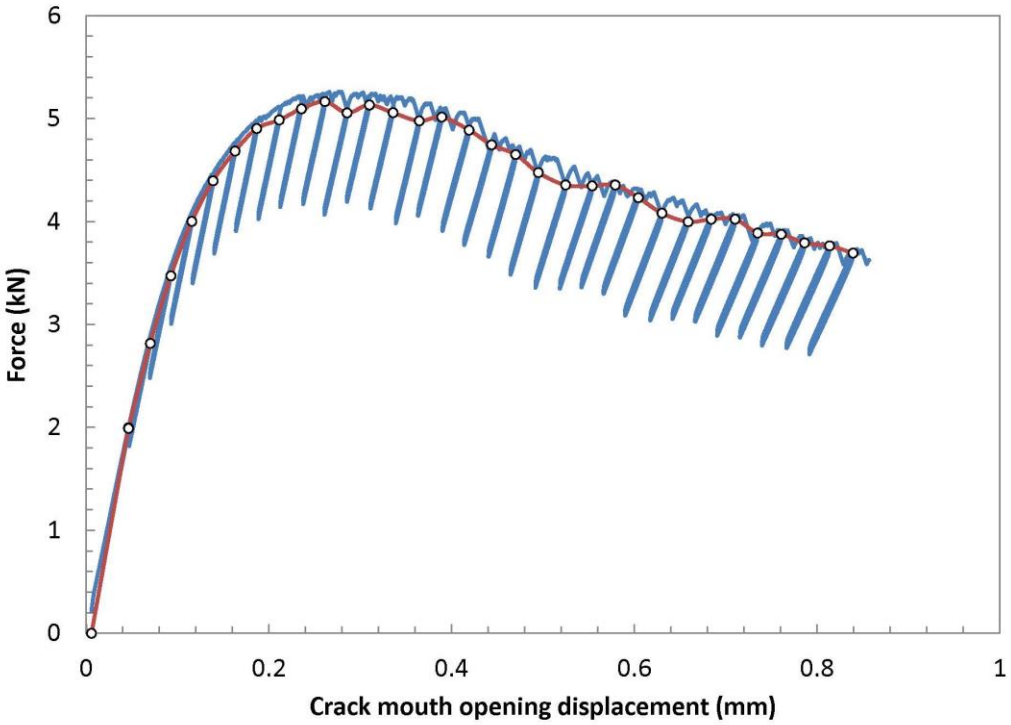
Force (kN)
Crack mouth opening displacement (mm)
0
1
2
3
4
5
6
0
0.2
0.4
0.6
0.8
1

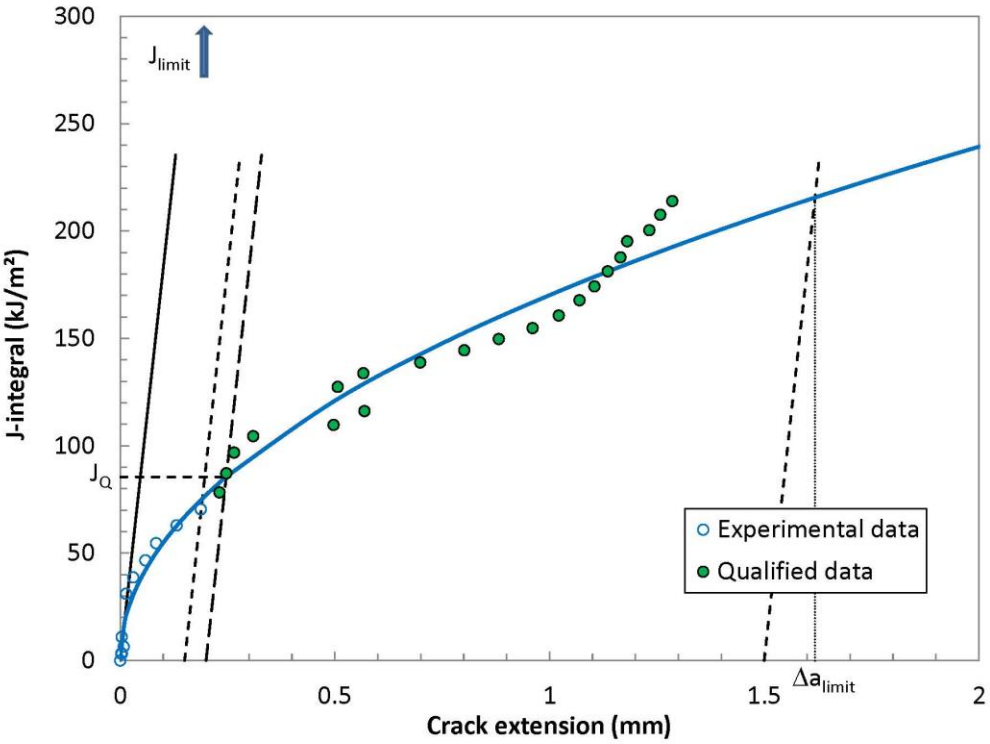
J-integral (kJ/m²)
Crack extension (mm)
J_limit
J_Q
Δa_limit
Experimental data
Qualified data
0
50
100
150
200
250
300
0
0.5
1
1.5
2

TEST REPORT

Specimen Information

Type = SE(B)
Identification = W3-F4
Orientation = N/A

Basic dimensions

B =	10.02	mm
B_N =	8.00	mm
W =	10.02	mm

Other dimensions

S =	40.00	mm

Tensile Properties

E =	177	MPa
ν =	0.3	
σ_{YS} =	626.0	MPa
σ_{TS} =	1197.0	MPa

Crack Size Information

a_0 =	5.24	mm
a_{0q} =	5.19	mm
a_f =	6.96	mm
Δa_p =	1.72	mm
$\Delta a_{predicted}$ =	1.51	mm

Test temperature: -269 °C

Analysis of Results

Fracture type = stable tearing

Critical Fracture Toughness

J_Q = 98.14 kJ/m²

TM = 37.7 MPa

QUALIFICATION OF DATA

Estimates of initial crack size:	$a_{0q,1}$ =	5.196	mm	Diff :	0.004	< 0.002W =	0.0200	mm
	$a_{0q,2}$ =	5.193	mm		0.000	< 0.002W =	0.0200	mm
	$a_{0,q3}$ =	5.189	mm		0.004	< 0.002W =	0.0200	mm
	$a_{0,qmean}$ =	5.193	mm					

Qualification of data

Crack extension prediction	Δa_p =	1.72	mm (measured)	
	Δa_{pred} =	1.51	mm (predicted)	
	Difference =	-0.21	mm	PREDICTION NOT ACCEPTABLE

J_Q - Qualification of data

Power coefficient C_2 =	0.457835	< 1.0	→ QUALIFIED
$\lvert a_{0q} - a_0 \rvert$ =	0.05	mm	→ DATA SET ADEQUATE
# of data available to calculate a_{0q} :	13	≥ 8	→ DATA SET ADEQUATE
# of data between $0.4J_q$ and J_q :	7	≥ 3	→ QUALIFIED
Correlation coefficient a_{0q} fit :	0.983	≥ 0.96	→ DATA SET ADEQUATE
Data points distribution :	VALID		
Number of qualified data points :	VALID		

Qualification of J_Q as J_{Ic}

Thickness B =	10.02	mm > 10 JQ/Sy	→ QUALIFIED
Initial ligament b_0 =	4.78	mm > 10 JQ/Sy	→ QUALIFIED

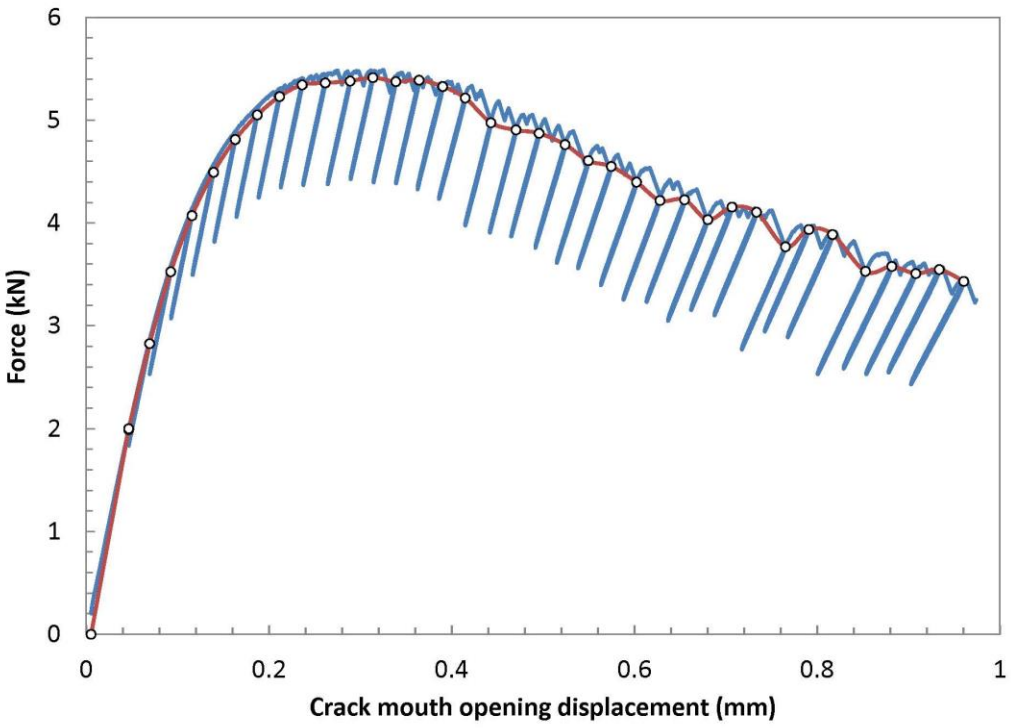
Force (kN)
Crack mouth opening displacement (mm)
0
1
2
3
4
5
6
0
0.2
0.4
0.6
0.8
1

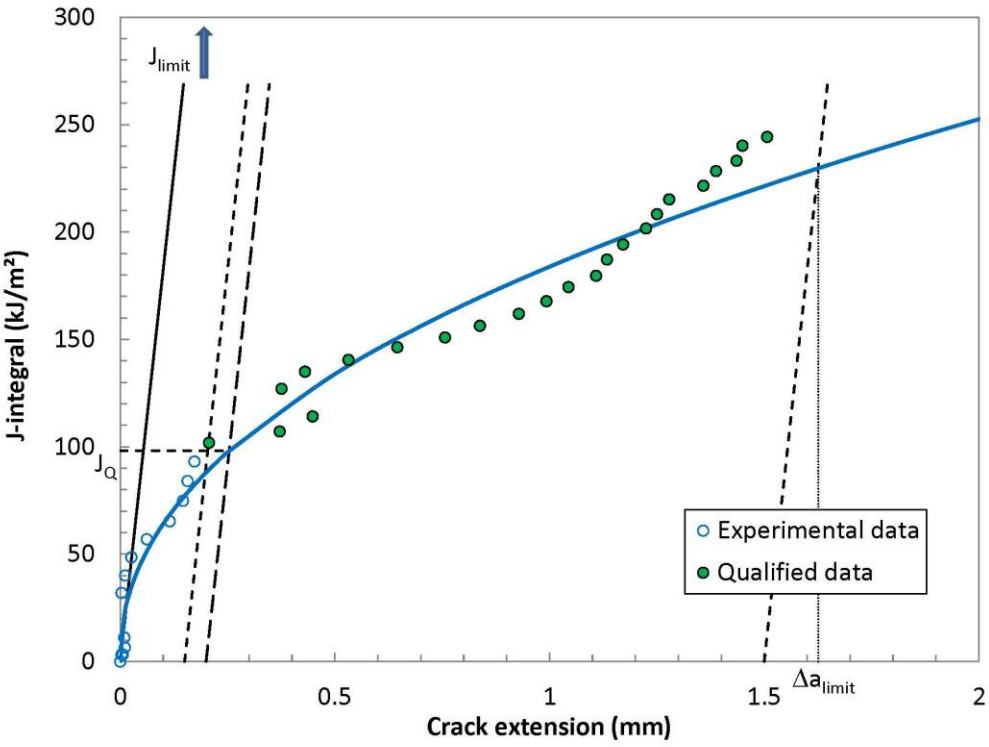
J-integral (kJ/m²)
Crack extension (mm)
J_limit
J_Q
Δa_limit
Experimental data
Qualified data
0
50
100
150
200
250
300
0
0.5
1
1.5
2

TEST REPORT

Specimen Information

Type = SE(B)
Identification = W3-F5
Orientation = N/A

Basic dimensions

B =	9.96	mm
B_N =	8.06	mm
W =	10.02	mm

Other dimensions

S =	40.00	mm

Tensile Properties

E =	177	MPa
ν =	0.3	
σ_{YS} =	626.0	MPa
σ_{TS} =	1197.0	MPa

Crack Size Information

a_0 =	5.24	mm
a_{0q} =	5.04	mm
a_f =	7.66	mm
Δa_p =	2.42	mm
$\Delta a_{predicted}$ =	2.25	mm

Test temperature: -269 °C

Analysis of Results

Fracture type = stable tearing

Critical Fracture Toughness

J_Q = 101.38 kJ/m²

TM = 30.1 MPa

QUALIFICATION OF DATA

Estimates of initial crack size:	$a_{0q,1}$ =	5.045	mm	Diff :	0.004	< 0.002W =	0.0200	mm
	$a_{0q,2}$ =	5.043	mm		0.002	< 0.002W =	0.0200	mm
	$a_{0,q3}$ =	5.035	mm		0.006	< 0.002W =	0.0200	mm
	$a_{0,qmean}$ =	5.041	mm					

Qualification of data

Crack extension prediction	Δa_p =	2.42	mm (measured)	
	Δa_{pred} =	2.25	mm (predicted)	
	Difference =	-0.17	mm	PREDICTION NOT ACCEPTABLE

J_Q - Qualification of data

Power coefficient C_2 =	0.356689	< 1.0	→ QUALIFIED
$\lvert a_{0q} - a_0 \rvert$ =	0.20	mm	→ DATA SET ADEQUATE
# of data available to calculate a_{0q} :	12	≥ 8	→ DATA SET ADEQUATE
# of data between $0.4J_q$ and J_q :	7	≥ 3	→ QUALIFIED
Correlation coefficient a_{0q} fit :	0.978	≥ 0.96	→ DATA SET ADEQUATE

Data points distribution : VALID
Number of qualified data points : VALID

Qualification of J_Q as J_{Ic}

Thickness B =	9.96	mm > 10 JQ/Sy	→ QUALIFIED
Initial ligament b_0 =	4.78	mm > 10 JQ/Sy	→ QUALIFIED

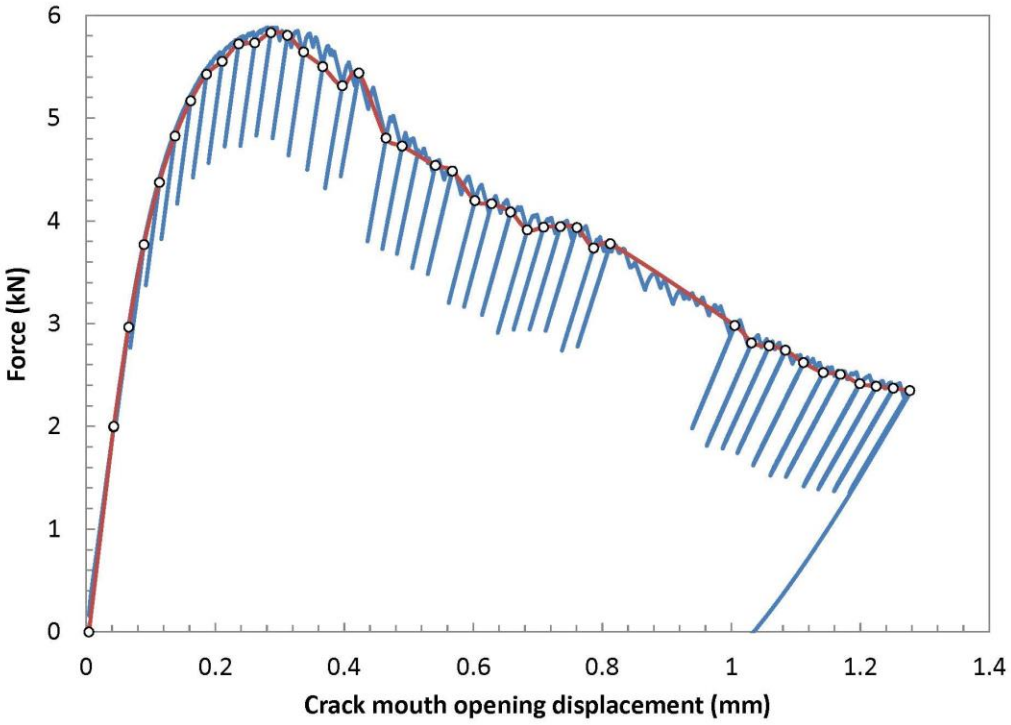
Force (kN)
Crack mouth opening displacement (mm)
0
1
2
3
4
5
6
0
0.2
0.4
0.6
0.8
1
1.2
1.4

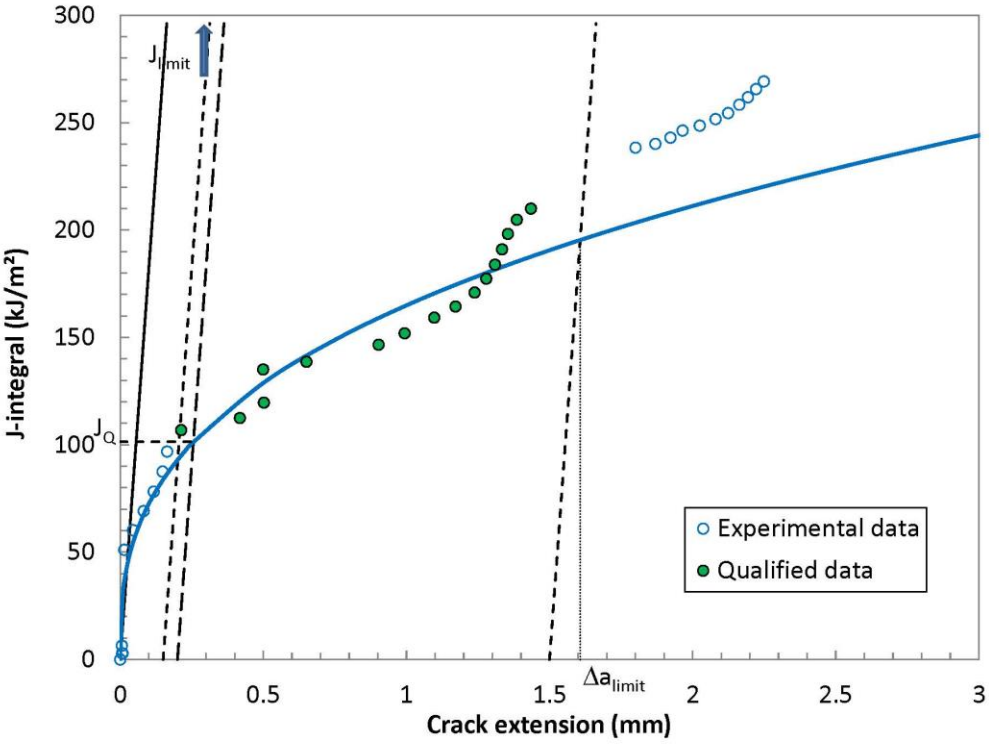
J-integral (kJ/m²)
Crack extension (mm)
J_limit
J_Q
Δa_limit
Experimental data
Qualified data
0
50
100
150
200
250
300
0
0.5
1
1.5
2
2.5
3

TEST REPORT

Specimen Information

Type = SE(B)
Identification = W3-F6
Orientation = N/A

Basic dimensions

B =	10.01	mm
B_N =	8.00	mm
W =	9.96	mm

Other dimensions

S =	40.00	mm

Tensile Properties

E =	177	MPa
ν =	0.3	
σ_{YS} =	626.0	MPa
σ_{TS} =	1197.0	MPa

Crack Size Information

a_0 =	5.32	mm
a_{0q} =	5.17	mm
a_f =	7.14	mm
Δa_p =	1.82	mm
$\Delta a_{predicted}$ =	2.11	mm

Test temperature: -269 °C

Analysis of Results

Fracture type = stable tearing

Critical Fracture Toughness

J_Q = 96.08 kJ/m²

TM = 29.1 MPa

QUALIFICATION OF DATA

Estimates of initial crack size:	$a_{0q,1}$ =	5.186	mm	Diff :	0.005	< 0.002W =	0.0199	mm
	$a_{0q,2}$ =	5.174	mm		0.008	< 0.002W =	0.0199	mm
	$a_{0,q3}$ =	5.184	mm		0.003	< 0.002W =	0.0199	mm
	$a_{0,qmean}$ =	5.181	mm					

Qualification of data

Crack extension prediction	Δa_p =	1.82	mm (measured)	
	Δa_{pred} =	2.11	mm (predicted)	
	Difference =	0.29	mm	PREDICTION NOT ACCEPTABLE

J_Q - Qualification of data

Power coefficient C_2 =	0.359323	< 1.0	→ QUALIFIED
$\lvert a_{0q} - a_0 \rvert$ =	0.15	mm	→ DATA SET ADEQUATE
# of data available to calculate a_{0q} :	13	≥ 8	→ DATA SET ADEQUATE
# of data between $0.4J_q$ and J_q :	7	≥ 3	→ QUALIFIED
Correlation coefficient a_{0q} fit :	0.976	≥ 0.96	→ DATA SET ADEQUATE

Data points distribution : VALID
Number of qualified data points : VALID

Qualification of J_Q as J_{Ic}

Thickness B =	10.01	mm > 10 JQ/Sy	→ QUALIFIED
Initial ligament b_0 =	4.64	mm > 10 JQ/Sy	→ QUALIFIED

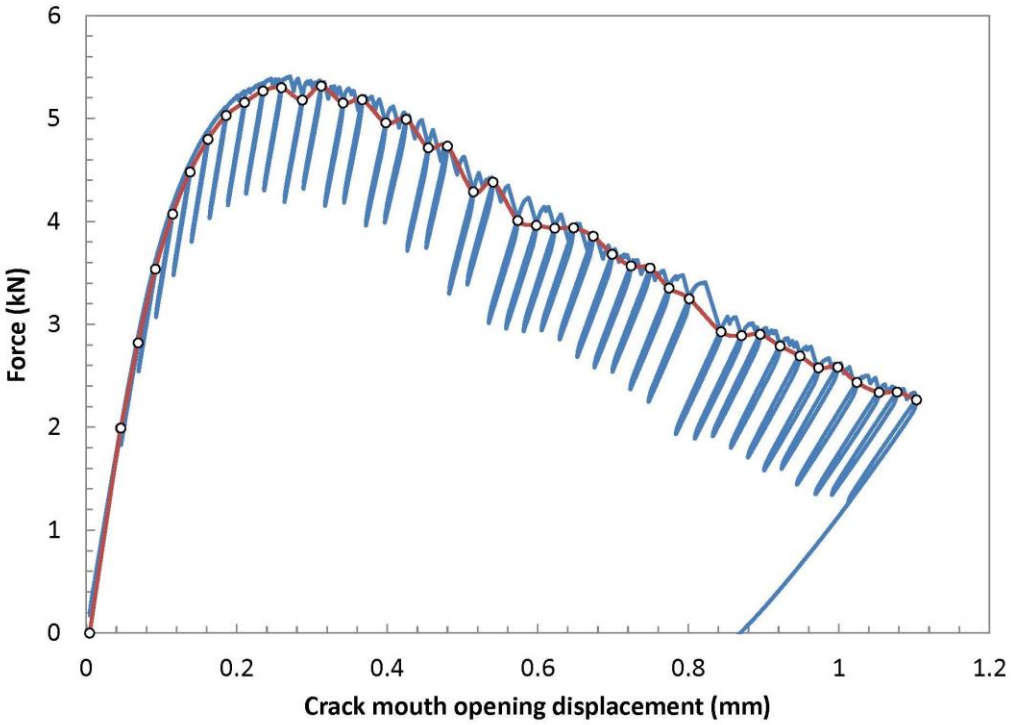
Force (kN)
Crack mouth opening displacement (mm)
0
1
2
3
4
5
6
0
0.2
0.4
0.6
0.8
1
1.2

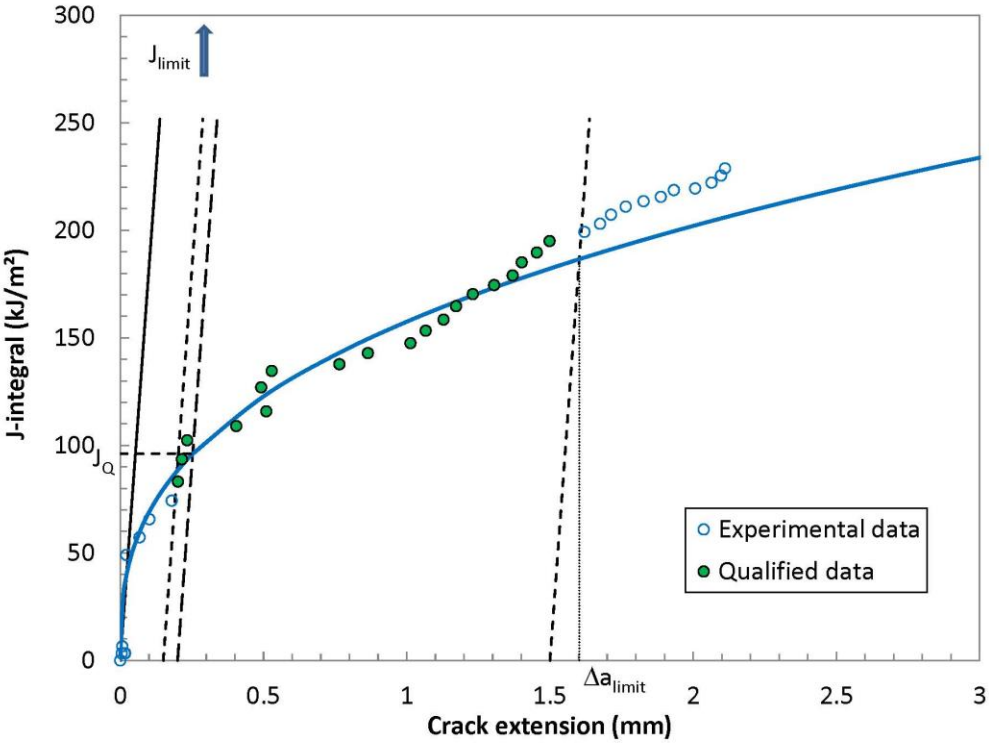
J-integral (kJ/m²)
Crack extension (mm)
J_limit
J_Q
Δa_limit
Experimental data
Qualified data
0
50
100
150
200
250
300
0
0.5
1
1.5
2
2.5
3

TEST REPORT

Specimen Information

Type = SE(B)
Identification = W3-F7
Orientation = N/A

Basic dimensions

B =	10.01	mm
B_N =	8.07	mm
W =	9.92	mm

Other dimensions

S =	40.00	mm

Tensile Properties

E =	177	MPa
ν =	0.3	
σ_{YS} =	626.0	MPa
σ_{TS} =	1197.0	MPa

Crack Size Information

a_0 =	5.30	mm
a_{0q} =	5.15	mm
a_f =	7.16	mm
Δa_p =	1.86	mm
$\Delta a_{predicted}$ =	1.73	mm

Test temperature: -269 °C

Analysis of Results

Fracture type = stable tearing

Critical Fracture Toughness

J_Q = 104.36 kJ/m²

TM = 32.2 MPa

QUALIFICATION OF DATA

Estimates of initial crack size:

$a_{0q,1}$ =	5.160	mm	Diff :	0.012	< 0.002W =	0.0198	mm
$a_{0q,2}$ =	5.137	mm		0.010	< 0.002W =	0.0198	mm
$a_{0,q3}$ =	5.146	mm		0.002	< 0.002W =	0.0198	mm
$a_{0,qmean}$ =	5.148	mm					

Qualification of data

Crack extension prediction	Δa_p =	1.86	mm (measured)	
	Δa_{pred} =	1.73	mm (predicted)	
	Difference =	-0.13	mm	(PREDICTION ACCEPTABLE)

J_Q - Qualification of data

Power coefficient C_2 =	0.372105	< 1.0	→ QUALIFIED
$\lvert a_{0q} - a_0 \rvert$ =	0.15	mm	→ DATA SET ADEQUATE
# of data available to calculate a_{0q} :	14	≥ 8	→ DATA SET ADEQUATE
# of data between $0.4J_q$ and J_q :	7	≥ 3	→ QUALIFIED
Correlation coefficient a_{0q} fit :	0.661	< 0.96	→ DATA SET NOT ADEQUATE

Data points distribution : VALID
Number of qualified data points : VALID

Qualification of J_Q as J_{Ic}

Thickness B =	10.01	mm > 10 JQ/Sy	→ QUALIFIED
Initial ligament b_0 =	4.62	mm > 10 JQ/Sy	→ QUALIFIED

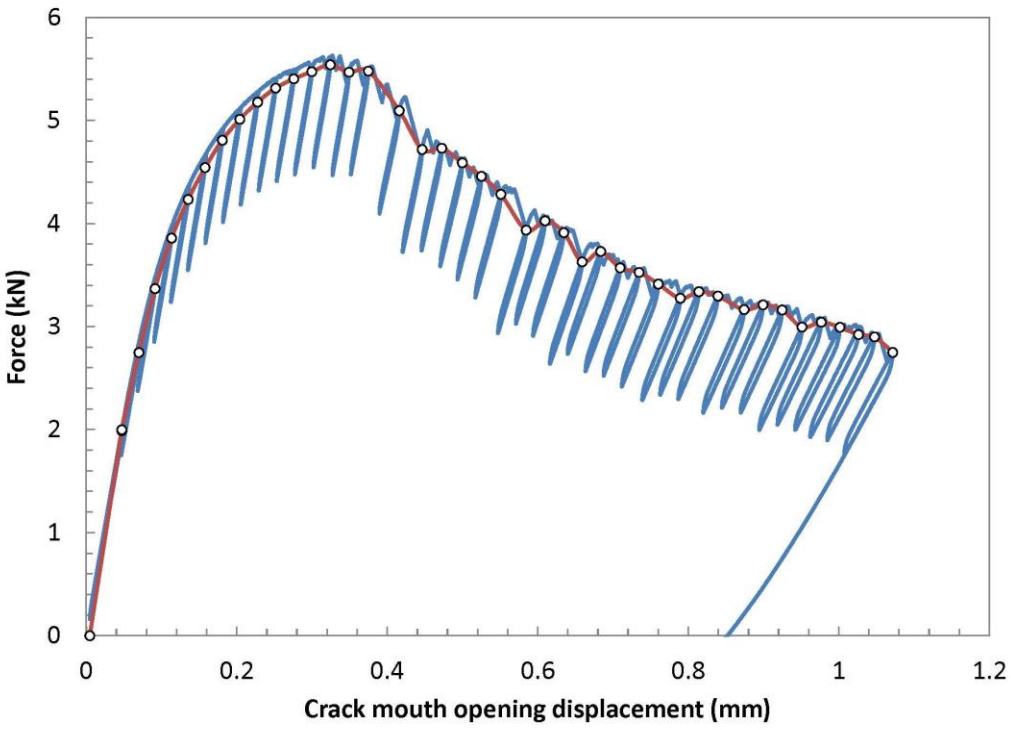
Force (kN)
Crack mouth opening displacement (mm)
0
1
2
3
4
5
6
0
0.2
0.4
0.6
0.8
1
1.2

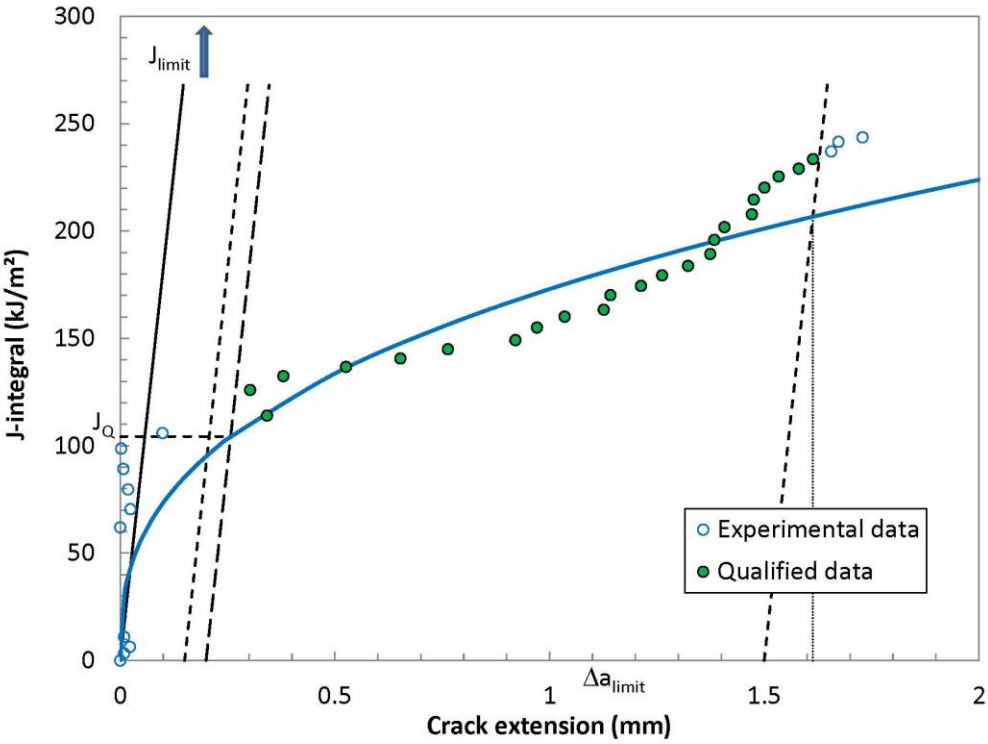
J-integral (kJ/m²)
Crack extension (mm)
J_limit
J_Q
Δa_limit
Experimental data
Qualified data
0
50
100
150
200
250
300
0
0.5
1
1.5
2

Weld W4, T = 4 K

TEST REPORT

Specimen Information

Type = SE(B)
Identification = W4-F3
Orientation = N/A

Basic dimensions

B =	9.98	mm
B_N =	8.01	mm
W =	10.01	mm

Other dimensions

S =	40.00	mm

Tensile Properties

E =	166	MPa
ν =	0.3	
σ_{YS} =	648.0	MPa
σ_{TS} =	1534.0	MPa

Crack Size Information

a_0 =	5.24	mm
a_{0q} =	5.12	mm
a_f =	8.15	mm
Δa_p =	2.91	mm
$\Delta a_{predicted}$ =	2.57	mm

Test temperature: -269 °C

Analysis of Results

Fracture type = stable tearing

Critical Fracture Toughness

J_Q = #N/A kJ/m²

TM = #N/A MPa

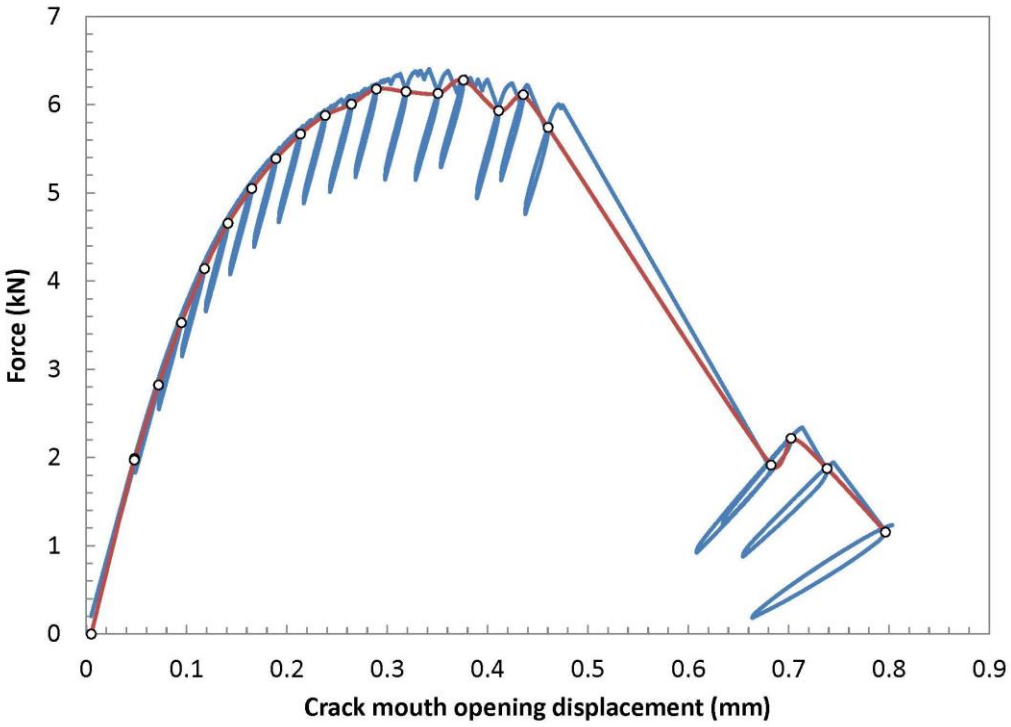

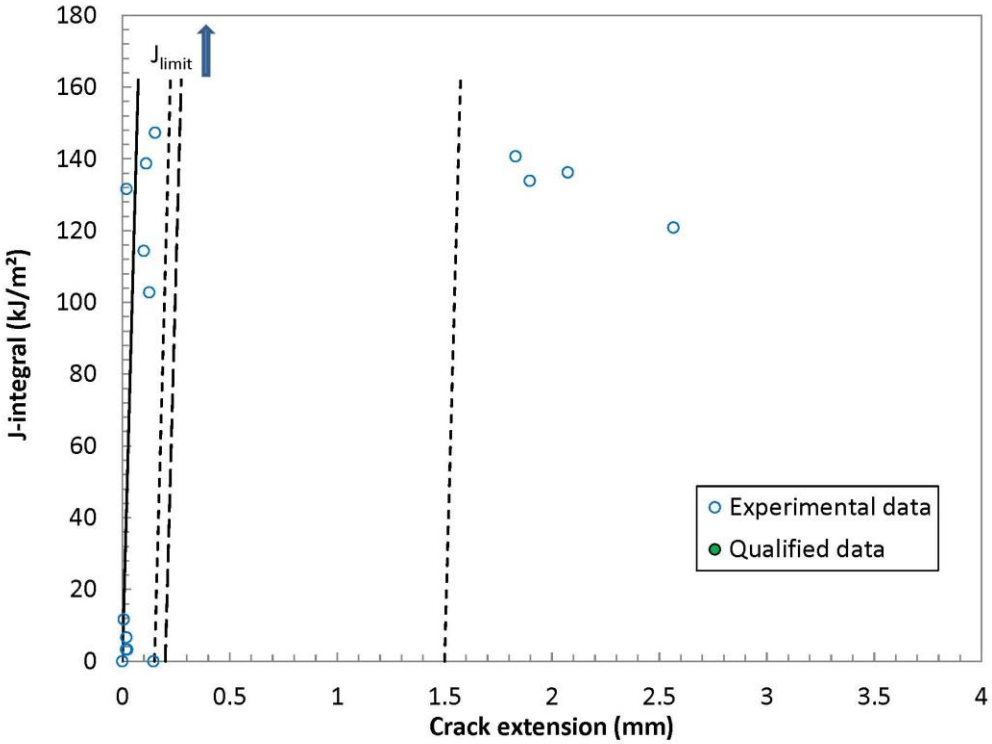

Specimen :	W4-F3			Δa =	0.16	mm	
F_c =	5.99	kN		K_e =	77.04	MPa√m	
B =	9.9822	mm		J_e =	32.54	kJ/m²	
B_N =	8.0055	mm					
W =	10.01	mm		η =	2.635224		
a_0 =	5.240	mm					
a_0/W =	0.524			J_{pl} =	133.25	kJ/m²	
S =	40	mm					
				J_c =	**164.31**	**kJ/m²**	NOT VALID
f(a/W) =	2.874868			**K_{Jc} =**	**173.13**	**MPa√m**	
T =	-269	°C		σ_Y =	1091	MPa	
E =	166.00	GPa =	163000 MPa	.00 J_{Qc}/σ_Y =	15.1	mm	
ν =	0.3						
A_{tot} =	2.36	kN.mm					
				Limits for compliance calculation:		F_{low} =	0.5 kN
C_o =	0.024035	mm/kN				F_{high} =	2 kN
A_{el} =	0.43	kN.mm					
A_{pl} =	1.93	kN.mm				Intercept:	-0.00508 mm

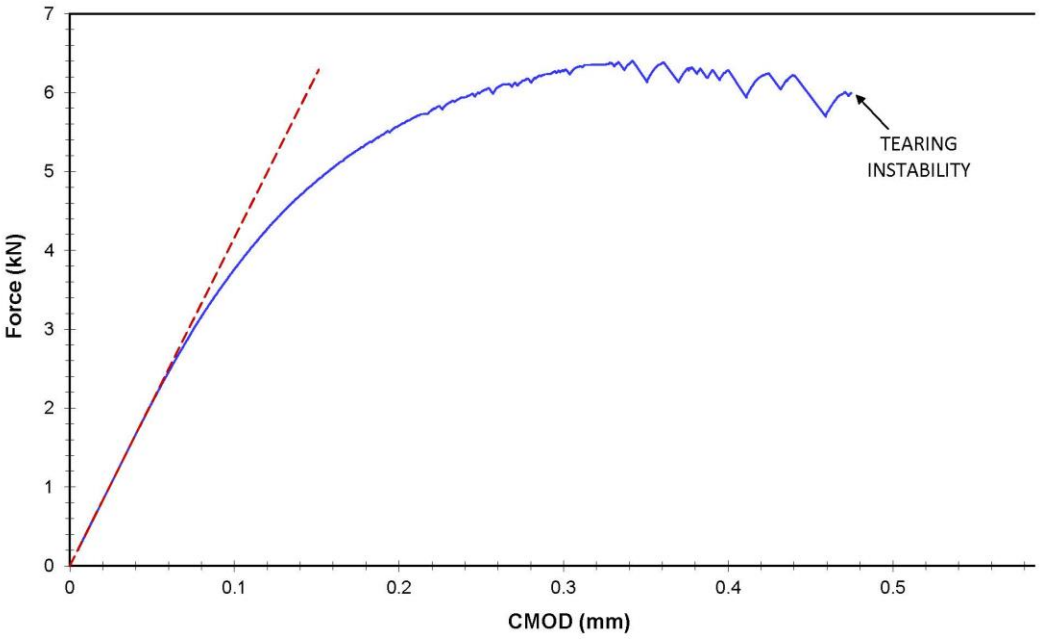
Force (kN)
CMOD (mm)
TEARING
INSTABILITY
0
1
2
3
4
5
6
7
0
0.1
0.2
0.3
0.4
0.5

TEST REPORT

Specimen Information

Type = SE(B)
Identification = W4-F4
Orientation = N/A

Basic dimensions

B =	10.02	mm
B_N =	8.01	mm
W =	9.99	mm

Other dimensions

S =	40.00	mm

Tensile Properties

E =	166	MPa
ν =	0.3	
σ_{YS} =	648.0	MPa
σ_{TS} =	1534.0	MPa

Crack Size Information

a_0 =	5.22	mm
a_{0q} =	5.06	mm
a_f =	8.56	mm
Δa_p =	3.34	mm
$\Delta a_{predicted}$ =	3.39	mm

Test temperature: -269 °C

Analysis of Results

Fracture type = stable tearing

Critical Fracture Toughness

J_Q = 42.01 kJ/m²

TM = 6.0 MPa

QUALIFICATION OF DATA

Estimates of initial crack size:	$a_{0q,1}$ =	5.056	mm	Diff :	0.000	< 0.002W =	0.0200 mm
	$a_{0q,2}$ =	5.058	mm		0.003	< 0.002W =	0.0200 mm
	a_{0q3} =	5.053	mm		0.003	< 0.002W =	0.0200 mm
	$a_{0,qmean}$ =	5.056	mm				

Qualification of data

Crack extension prediction	Δa_p =	3.34	mm (measured)	
	Δa_{pred} =	3.39	mm (predicted)	
	Difference =	0.05	mm	(PREDICTION ACCEPTABLE)

J_Q - Qualification of data

Power coefficient C_2 =	0.223864	< 1.0	→ QUALIFIED
$\lvert a_{0q} - a_0 \rvert$ =	0.16	mm	→ DATA SET ADEQUATE
# of data available to calculate a_{0q} :	8	≥ 8	→ DATA SET ADEQUATE
# of data between $0.4J_q$ and J_q :	4	≥ 3	→ QUALIFIED
Correlation coefficient a_{0q} fit :	0.981	≥ 0.96	→ DATA SET ADEQUATE
Data points distribution :	VALID		
Number of qualified data points :	NOT VALID		

Qualification of J_Q as J_{Ic}

Thickness B =	10.02	mm > 10 JQ/Sy	→ QUALIFIED
Initial ligament b_0 =	4.77	mm > 10 JQ/Sy	→ QUALIFIED

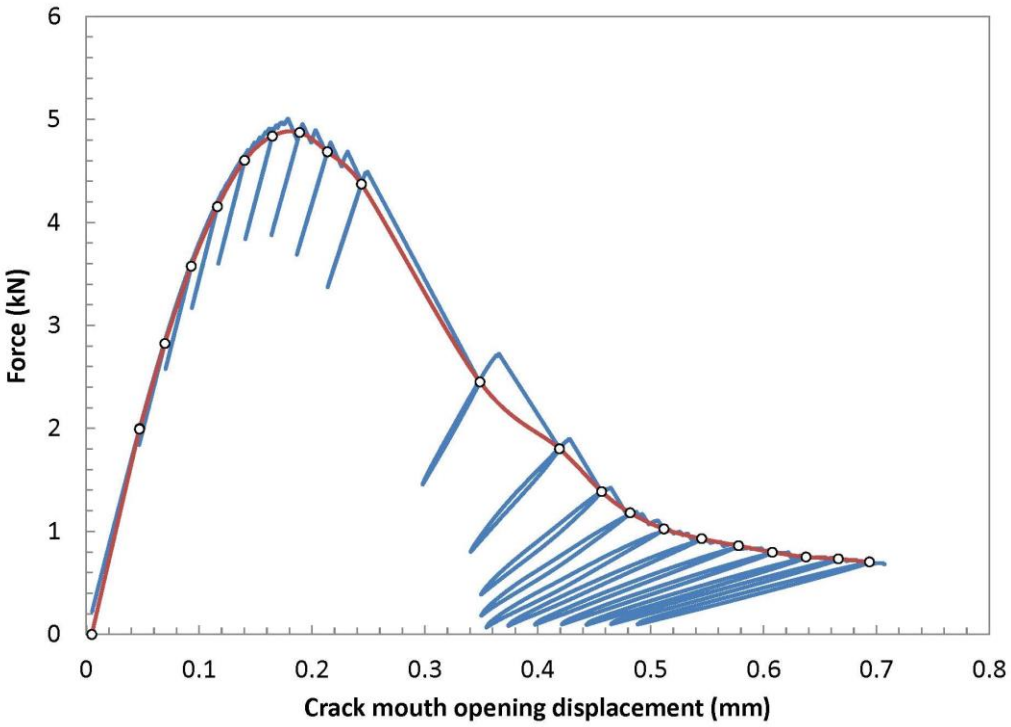
Force (kN)
Crack mouth opening displacement (mm)
0
1
2
3
4
5
6
0
0.1
0.2
0.3
0.4
0.5
0.6
0.7
0.8

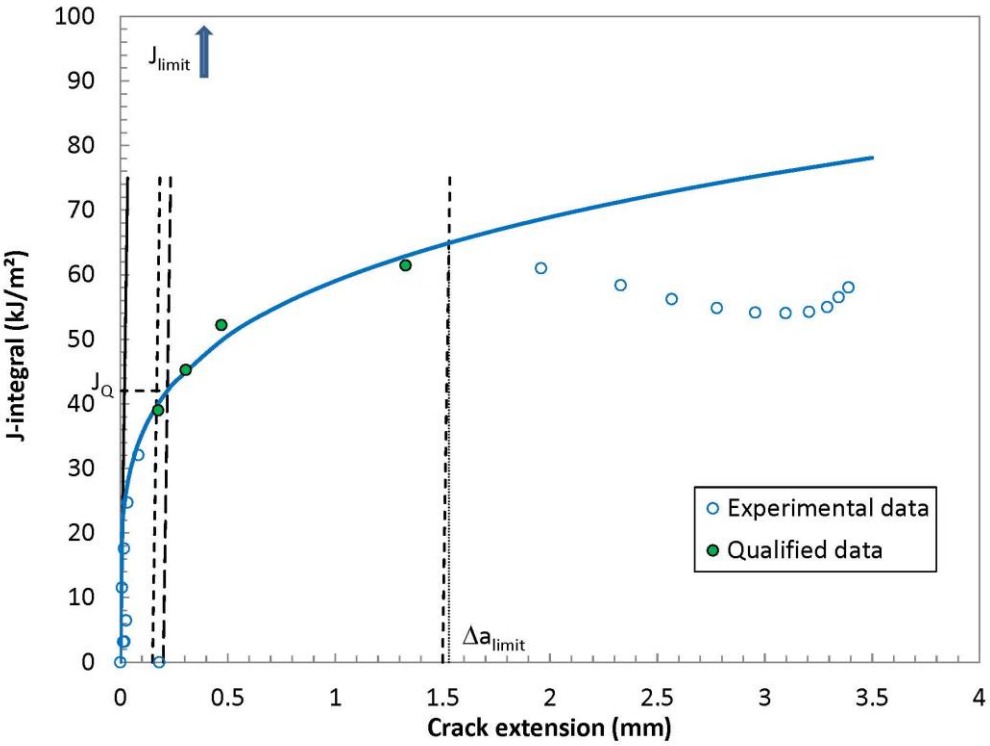
J-integral (kJ/m²)
Crack extension (mm)
J_limit
J_Q
Δa_limit
Experimental data
Qualified data
0
10
20
30
40
50
60
70
80
90
100
0
0.5
1
1.5
2
2.5
3
3.5
4

TEST REPORT

Specimen Information

Type = SE(B)
Identification = W4-F5
Orientation = N/A

Basic dimensions

B =	10.04	mm
B_N =	8.02	mm
W =	10.01	mm

Other dimensions

S =	40.00	mm

Tensile Properties

E =	166	MPa
ν =	0.3	
σ_{YS} =	648.0	MPa
σ_{TS} =	1534.0	MPa

Crack Size Information

a_0 =	5.23	mm
a_{0q} =	5.01	mm
a_f =	8.75	mm
Δa_p =	3.52	mm
$\Delta a_{predicted}$ =	3.62	mm

Test temperature: -269 °C

Analysis of Results

Fracture type = stable tearing

Critical Fracture Toughness

J_Q = 70.32 kJ/m²

TM = 7.9 MPa

QUALIFICATION OF DATA

Estimates of initial crack size:	$a_{0q,1}$ =	5.018	mm	Diff :	0.000	< 0.002W =	0.0200	mm
	$a_{0q,2}$ =	5.018	mm		0.000	< 0.002W =	0.0200	mm
	$a_{0,q3}$ =	5.019	mm		0.000	< 0.002W =	0.0200	mm
	$a_{0,qmean}$ =	5.018	mm					

Qualification of data

Crack extension prediction	Δa_p =	3.52	mm (measured)	
	Δa_{pred} =	3.62	mm (predicted)	
	Difference =	0.10	mm	(PREDICTION ACCEPTABLE)

J_Q - Qualification of data

Power coefficient C_2 =	0.187764	< 1.0	→ QUALIFIED
$\lvert a_{0q} - a_0 \rvert$ =	0.22	mm	→ DATA SET ADEQUATE
# of data available to calculate a_{0q} :	11	≥ 8	→ DATA SET ADEQUATE
# of data between $0.4J_q$ and J_q :	14	≥ 3	→ QUALIFIED
Correlation coefficient a_{0q} fit :	0.995	≥ 0.96	→ DATA SET ADEQUATE
Data points distribution :	VALID		
Number of qualified data points :	NOT VALID		

Qualification of J_Q as J_{Ic}

Thickness B =	10.04	mm > 10 JQ/Sy	→ QUALIFIED
Initial ligament b_0 =	4.78	mm > 10 JQ/Sy	→ QUALIFIED

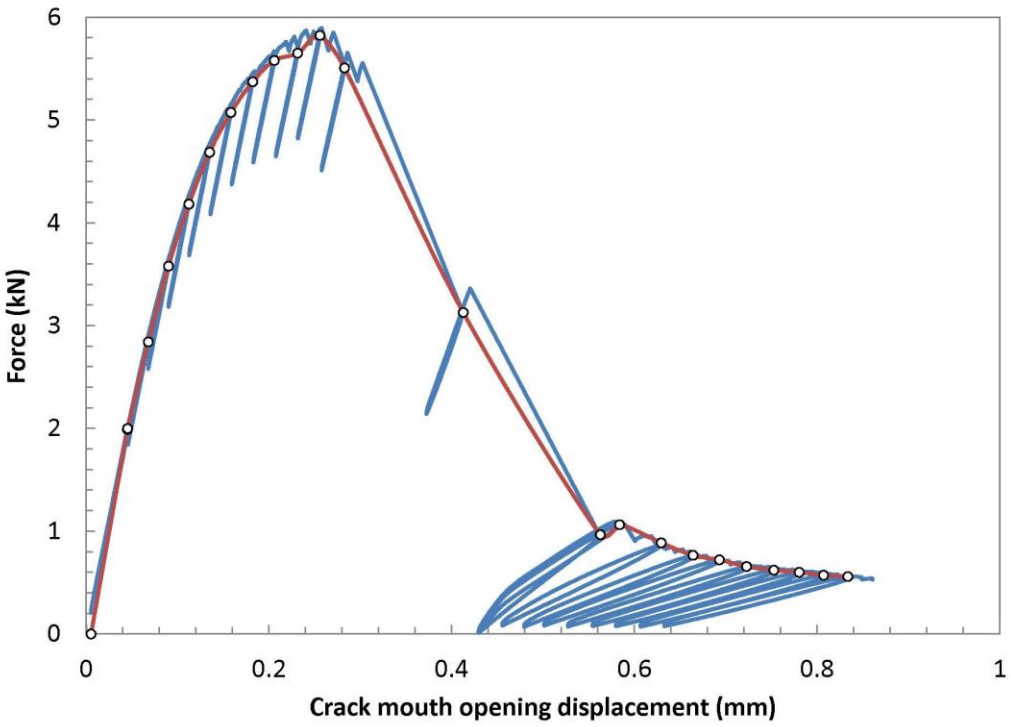
Force (kN)
Crack mouth opening displacement (mm)
0
1
2
3
4
5
6
0
0.2
0.4
0.6
0.8
1

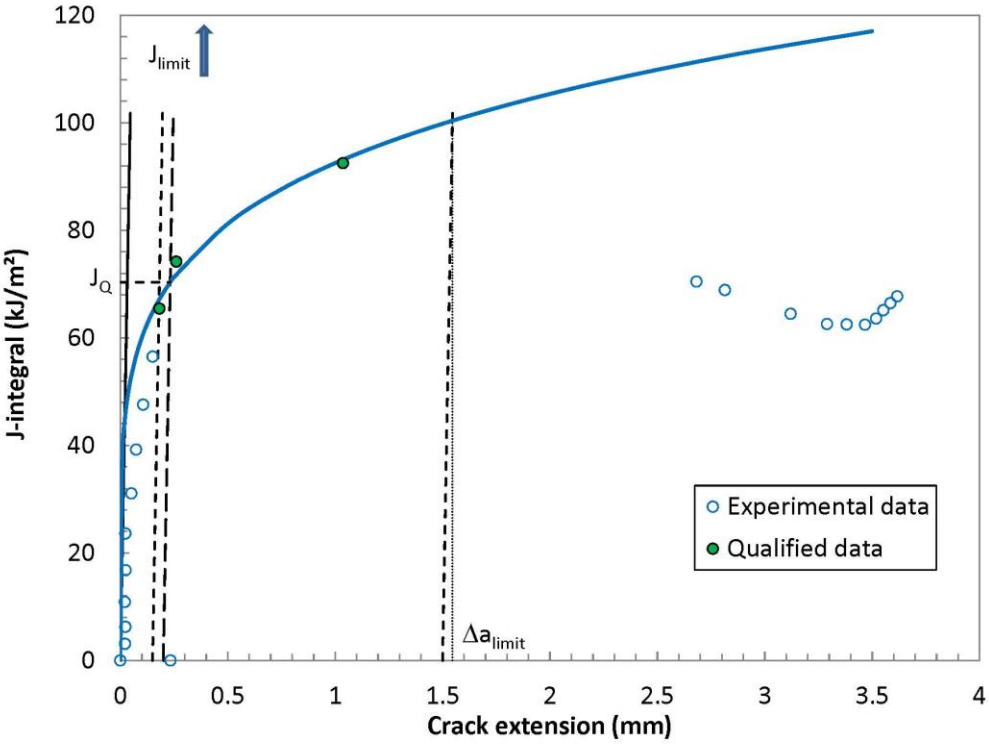
J-integral (kJ/m²)
Crack extension (mm)
J_limit
J_Q
Δa_limit
Experimental data
Qualified data
0
20
40
60
80
100
120
0
0.5
1
1.5
2
2.5
3
3.5
4

TEST REPORT

Specimen Information

Type = SE(B)
Identification = W4-F6
Orientation = N/A

Basic dimensions

B =	10.02	mm
B_N =	8.00	mm
W =	10.00	mm

Other dimensions

S =	40.00	mm

Tensile Properties

E =	166	MPa
ν =	0.3	
σ_{YS} =	648.0	MPa
σ_{TS} =	1534.0	MPa

Crack Size Information

a_0 =	5.18	mm
a_{0q} =	4.99	mm
a_f =	8.82	mm
Δa_p =	3.64	mm
$\Delta a_{predicted}$ =	3.66	mm

Test temperature: -269 °C

Analysis of Results

Fracture type = stable tearing

Critical Fracture Toughness

J_Q = #N/A kJ/m²

TM = #N/A MPa

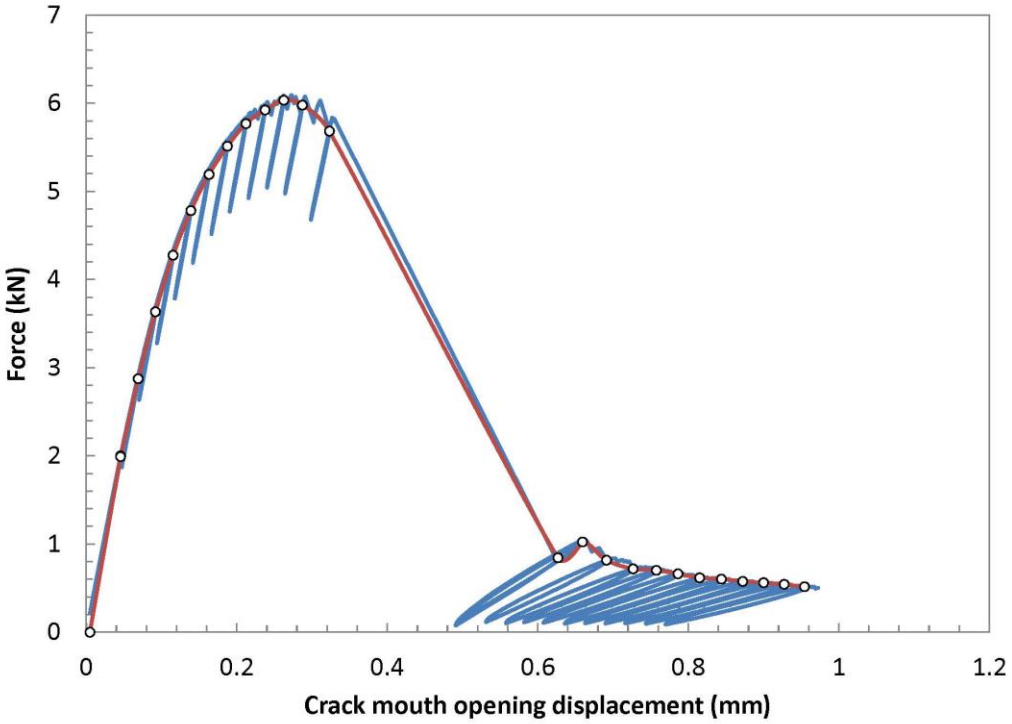

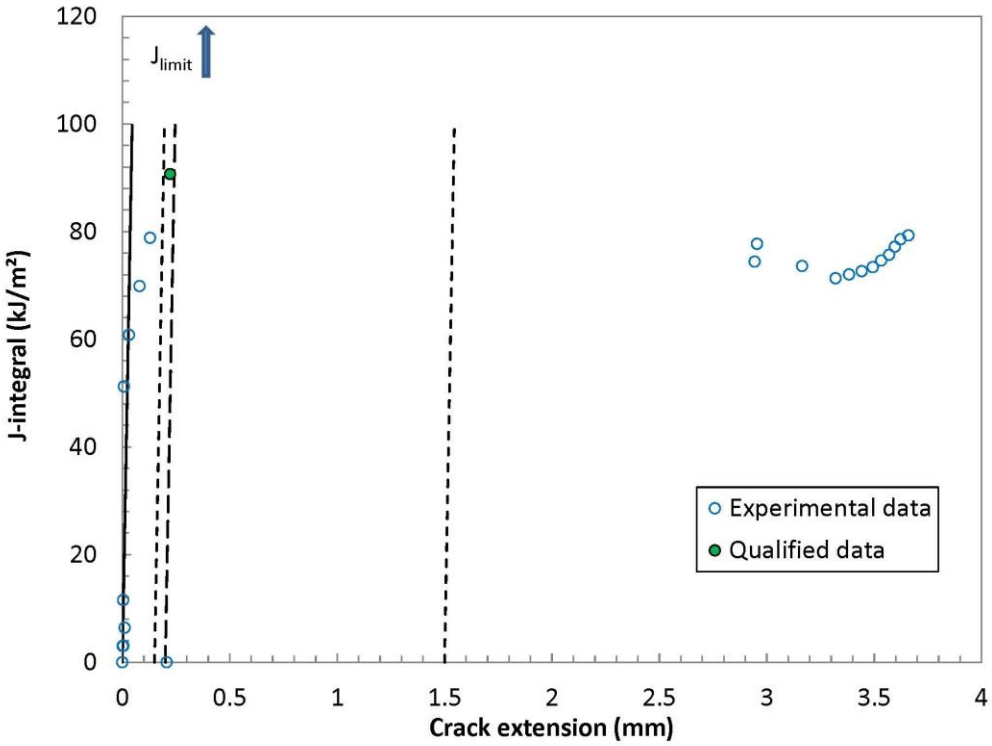

Specimen :	W4-F6			Δa =	0.15	mm	
F_c =	5.82	kN		K_e =	73.45	MPa√m	
B =	10.0239	mm		J_e =	30.12	kJ/m²	
B_N =	7.9994	mm					
W =	10.00	mm		η =	2.644868		
a_0 =	5.180	mm					
a_0/W =	0.518			J_{pl} =	74.61	kJ/m²	
S =	40	mm					
				J_c =	**103.96**	**kJ/m²**	NOT VALID
f(a/W) =	2.823069			**K_{Jc} =**	**136.46**	**MPa√m**	
T =	-269	°C			σ_Y =	923	MPa
E =	163.00	GPa =	163000 MPa	.00	J_{Qc}/σ_Y =	11.3	mm
ν =	0.3						
A_{tot} =	1.48	kN.mm					
			Limits for compliance calculation:		F_{low} =	0.5	kN
C_o =	0.022974	mm/kN			F_{high} =	2	kN
A_{el} =	0.39	kN.mm					
A_{pl} =	1.09	kN.mm			Intercept:	-0.00531	mm

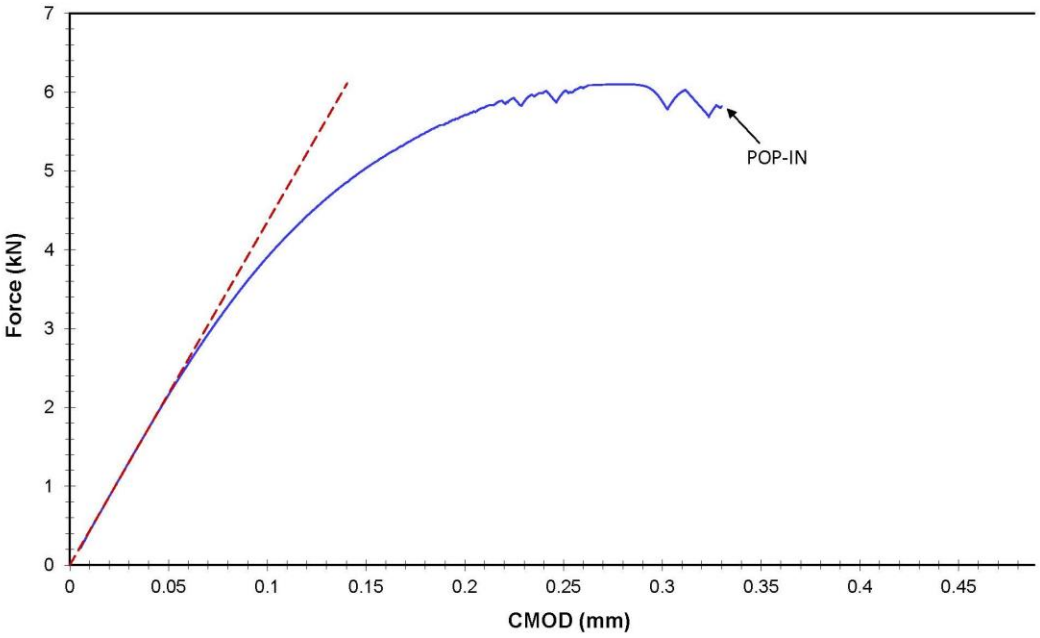
Force (kN)
CMOD (mm)
POP-IN
0
1
2
3
4
5
6
7
0
0.05
0.1
0.15
0.2
0.25
0.3
0.35
0.4
0.45

TEST REPORT

Specimen Information

Type = SE(B)
Identification = W4-F7
Orientation = N/A

Basic dimensions

B =	10.01	mm
B_N =	8.01	mm
W =	10.01	mm

Other dimensions

S =	40.00	mm

Tensile Properties

E =	166	MPa
ν =	0.3	
σ_{YS} =	648.0	MPa
σ_{TS} =	1534.0	MPa

Crack Size Information

a_0 =	5.13	mm
a_{0q} =	5.12	mm
a_f =	8.31	mm
Δa_p =	3.18	mm
$\Delta a_{predicted}$ =	3.18	mm

Test temperature: -269 °C

Analysis of Results

Fracture type = stable tearing

Critical Fracture Toughness

J_Q = 26.99 kJ/m²

TM = 6.4 MPa

QUALIFICATION OF DATA

Estimates of initial crack size:	$a_{0q,1}$ =	5.100	mm	Diff :	0.007	< 0.002W =	0.0200	mm
	$a_{0q,2}$ =	5.108	mm		0.000	< 0.002W =	0.0200	mm
	$a_{0,q3}$ =	5.114	mm		0.006	< 0.002W =	0.0200	mm
	$a_{0,qmean}$ =	5.107	mm					

Qualification of data

Crack extension prediction	Δa_p =	3.18	mm (measured)	
	Δa_{pred} =	3.18	mm (predicted)	
	Difference =	0.00	mm	(PREDICTION ACCEPTABLE)

J_Q - Qualification of data

Power coefficient C_2 =	0.360808	< 1.0	→ QUALIFIED
$\lvert a_{0q} - a_0 \rvert$ =	0.01	mm	→ DATA SET ADEQUATE
# of data available to calculate a_{0q} :	7	< 8	→ DATA SET NOT ADEQUATE
# of data between 0.4J_q and J_q :	3	≥ 3	→ QUALIFIED
Correlation coefficient a_{0q} fit :	0.994	≥ 0.96	→ DATA SET ADEQUATE
Data points distribution :	VALID		
Number of qualified data points :	VALID		

Qualification of J_Q as J_{Ic}

Thickness B =	10.01	mm > 10 JQ/Sy	→ QUALIFIED
Initial ligament b_0 =	4.88	mm > 10 JQ/Sy	→ QUALIFIED

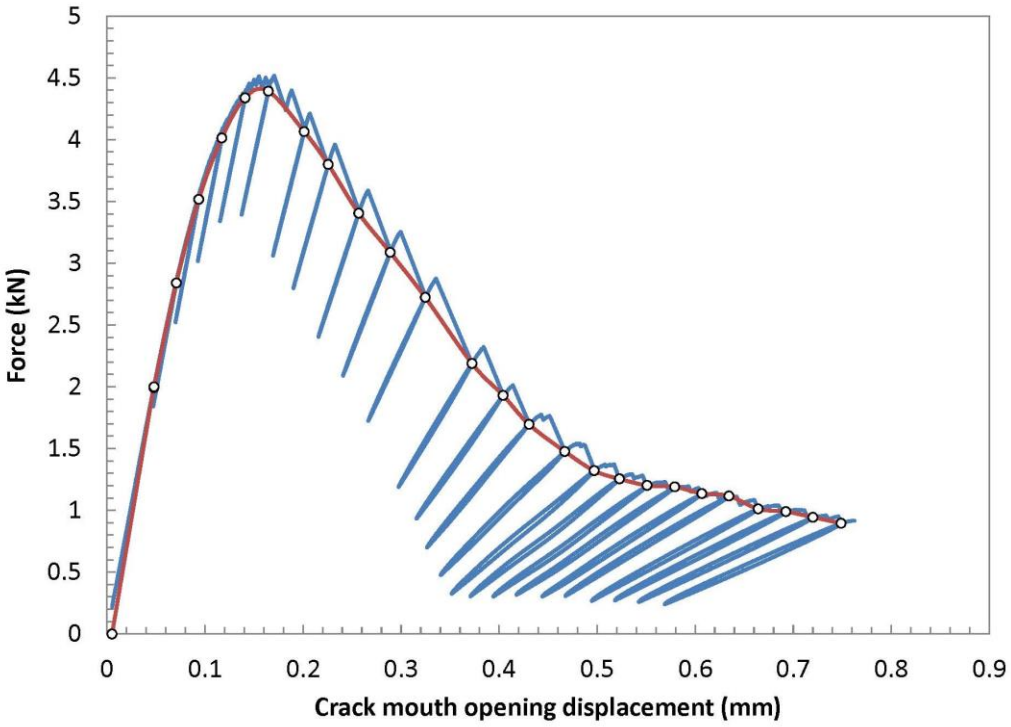
Force (kN)
Crack mouth opening displacement (mm)
0
0.5
1
1.5
2
2.5
3
3.5
4
4.5
5
0.1
0.2
0.3
0.4
0.5
0.6
0.7
0.8
0.9

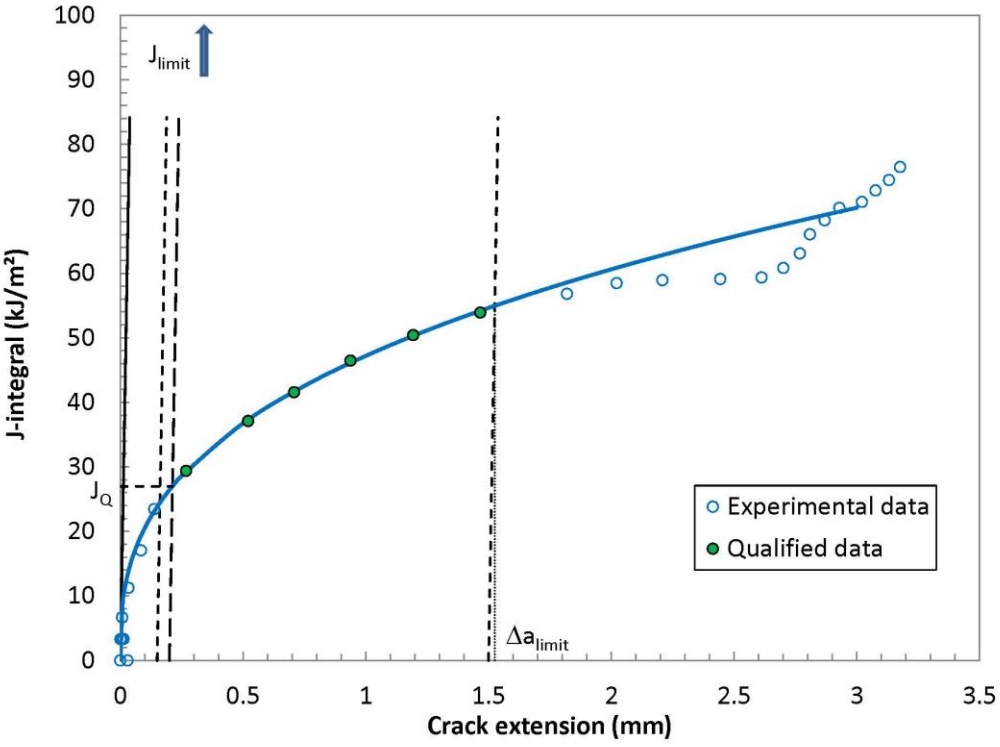
J-integral (kJ/m²)
Crack extension (mm)
J_limit
J_Q
Δa_limit
Experimental data
Qualified data
0
10
20
30
40
50
60
70
80
90
100
0.5
1
1.5
2
2.5
3
3.5

TEST REPORT

Specimen Information

Type = SE(B)
Identification = W4-F8
Orientation = N/A

Basic dimensions

B =	10.02	mm
B_N =	8.00	mm
W =	10.02	mm

Other dimensions

S =	40.00	mm

Tensile Properties

E =	166	MPa
ν =	0.3	
σ_{YS} =	648.0	MPa
σ_{TS} =	1534.0	MPa

Crack Size Information

a_0 =	5.26	mm
a_{0q} =	5.07	mm
a_f =	7.25	mm
Δa_p =	1.99	mm
$\Delta a_{predicted}$ =	3.59	mm

Test temperature: -269 °C

Analysis of Results

Fracture type = stable tearing

Critical Fracture Toughness

J_Q = #N/A kJ/m²

TM = #N/A MPa

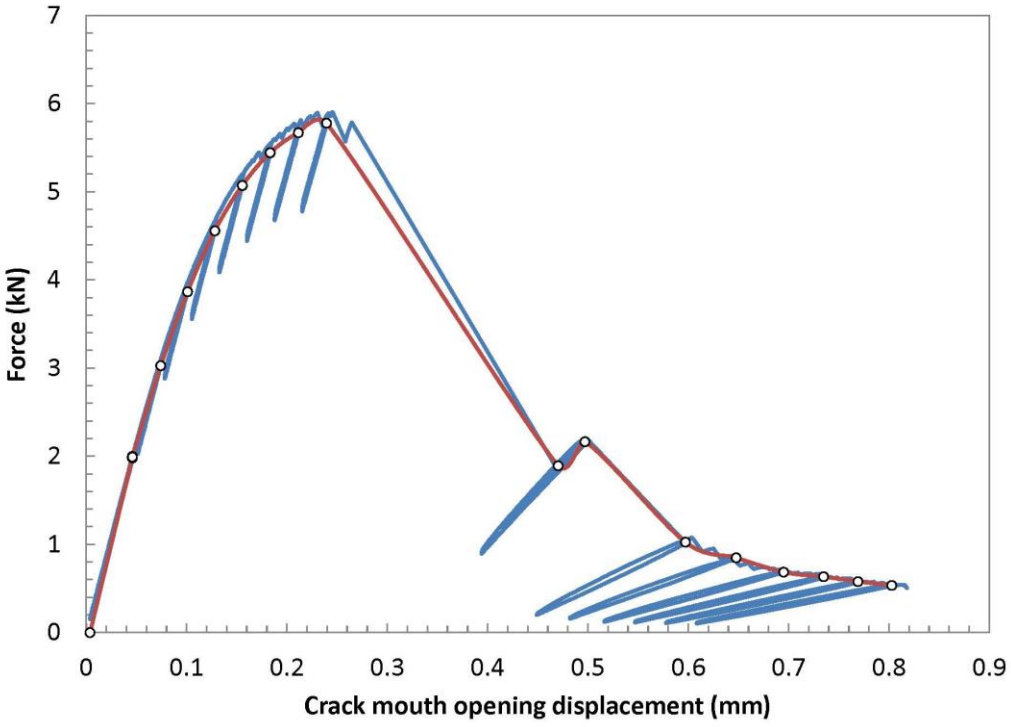

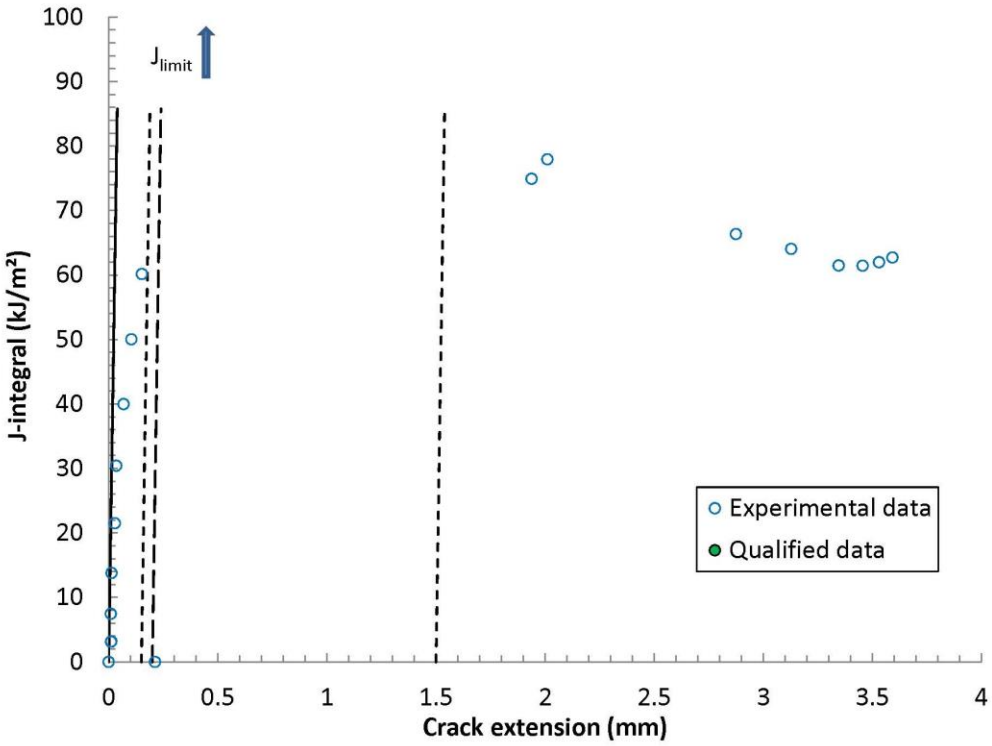

Specimen :	W4-F8			Δa =	0.15	mm
F_c =	5.77	kN		K_e =	68.65	MPa√m
B =	10.021	mm		J_e =	26.31	kJ/m²
B_N =	8.0034	mm				
W =	10.02	mm		η =	2.67486	
a_0 =	5.020	mm				
a_0/W =	0.501			J_{pl} =	26.29	kJ/m²
S =	40	mm				
				J_c =	**52.34**	**kJ/m²** NOT VALID
f(a/W) =	2.671589			**K_{Jc} =**	**96.83**	**MPa√m**
T =	-268.93	°C		σ_Y =	923	MPa
E =	163.00	GPa =	163000 MPa	.00 J_{Qc}/σ_Y =	5.7	mm
ν =	0.3					
A_{tot} =	0.78	kN.mm				
			Limits for compliance calculation:	F_{low} =	0.5	kN
C_o =	0.02312	mm/kN		F_{high} =	2	kN
A_{el} =	0.38	kN.mm				
A_{pl} =	0.39	kN.mm		Intercept:	-0.00409	mm

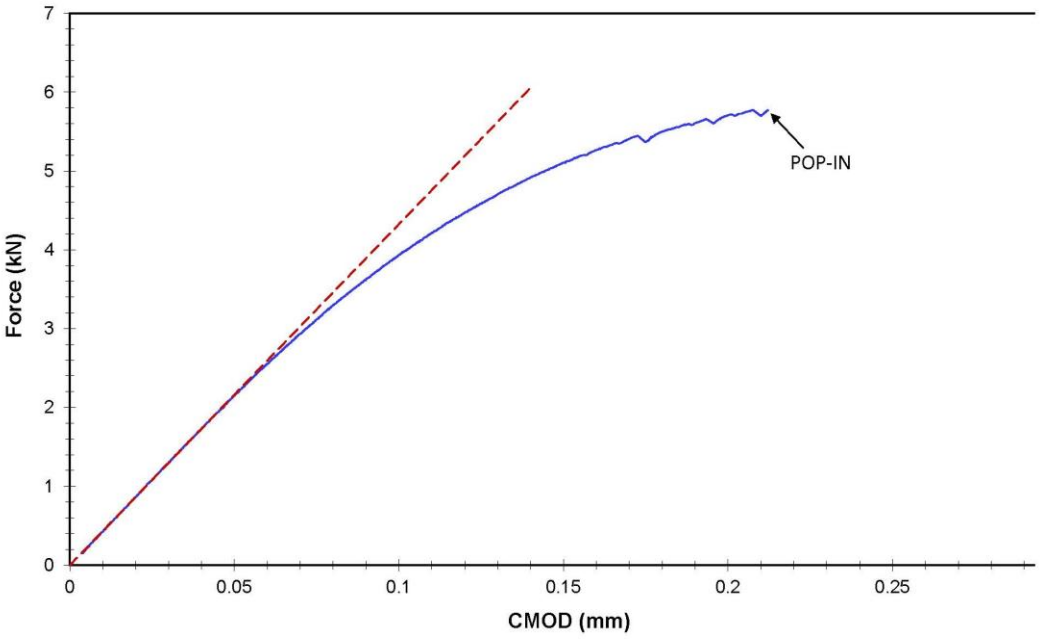
Force (kN)
CMOD (mm)
POP-IN
0
1
2
3
4
5
6
7
0
0.05
0.1
0.15
0.2
0.25

Appendix E: Fractography – Optical Images

Weld W1, T = 4 K

W1 F4

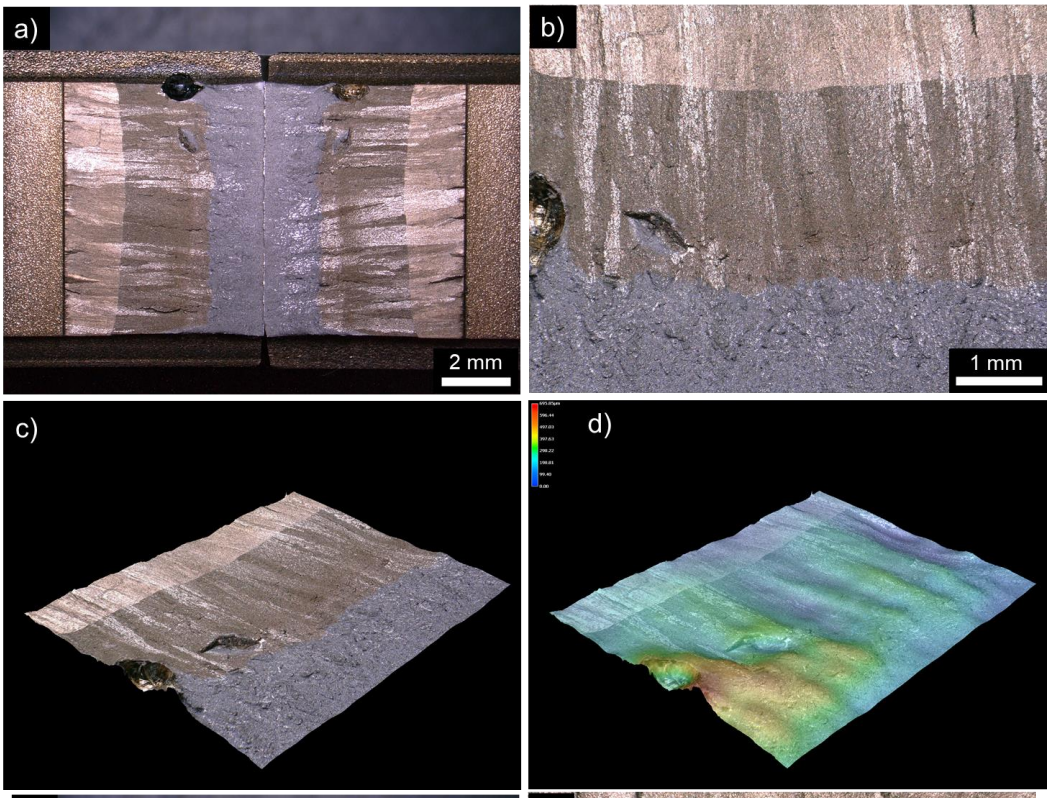

W1 F5

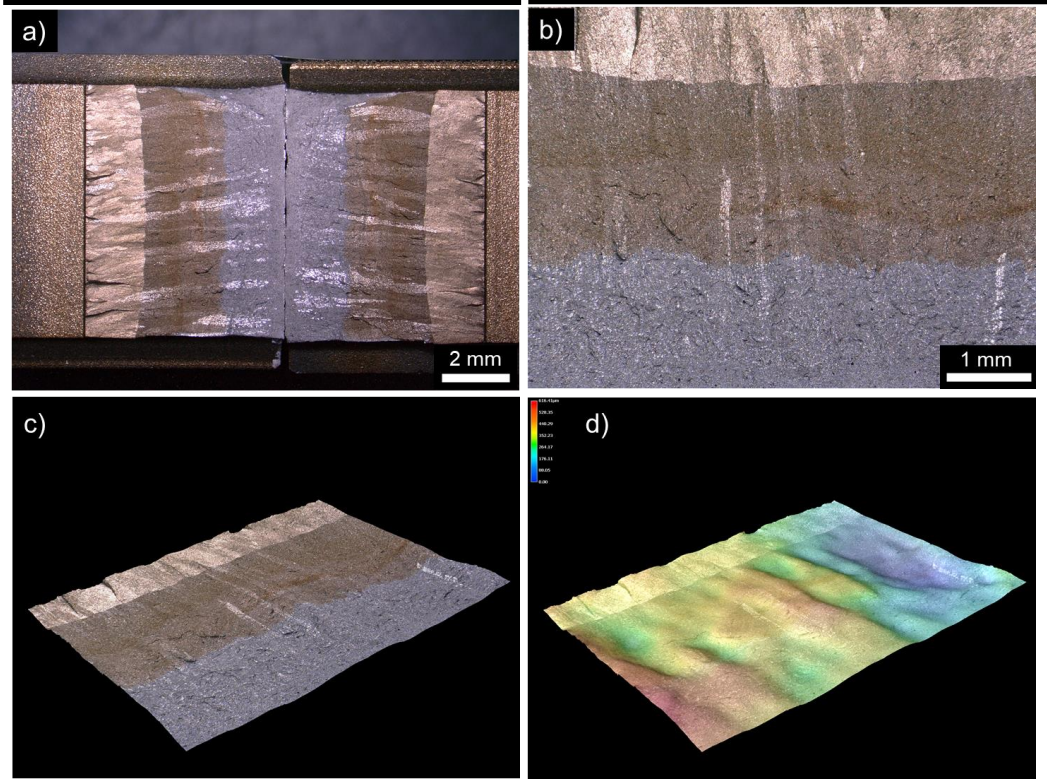

W1 F6

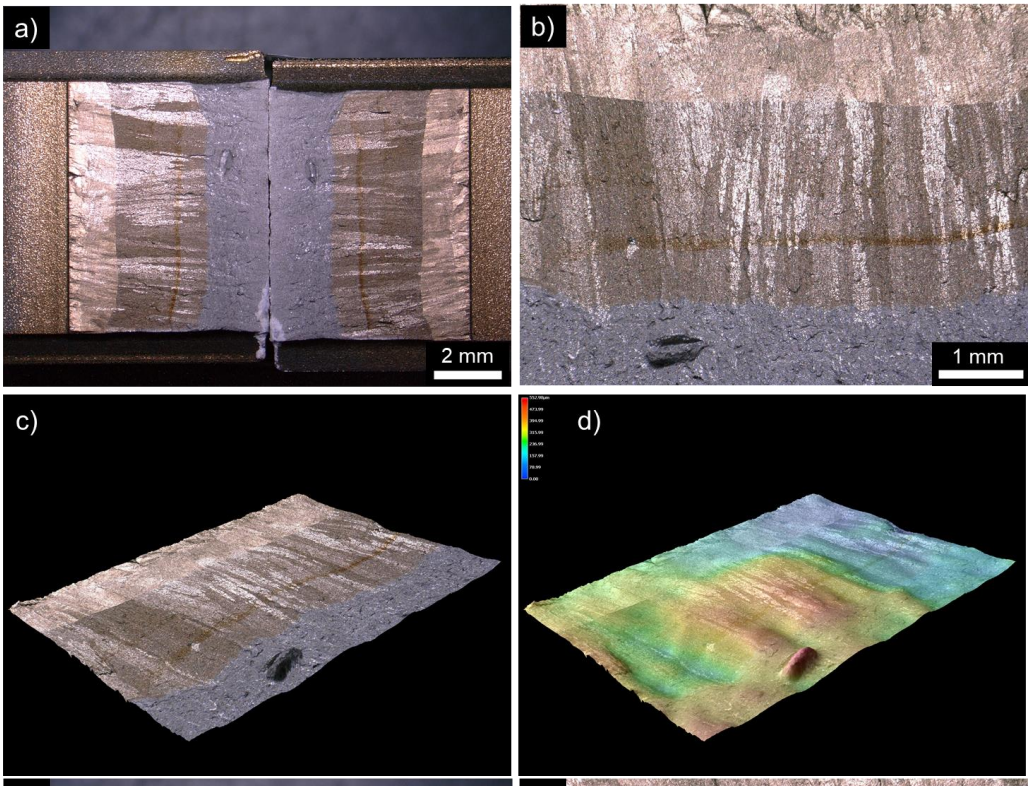

W1 F7

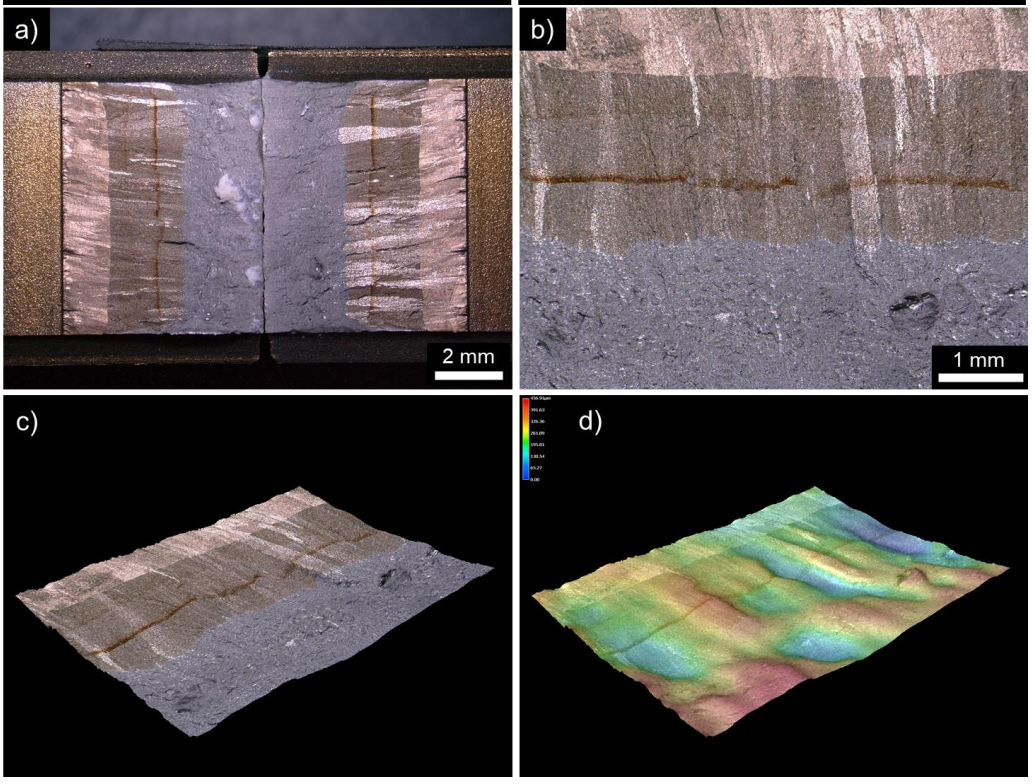

W1 F8

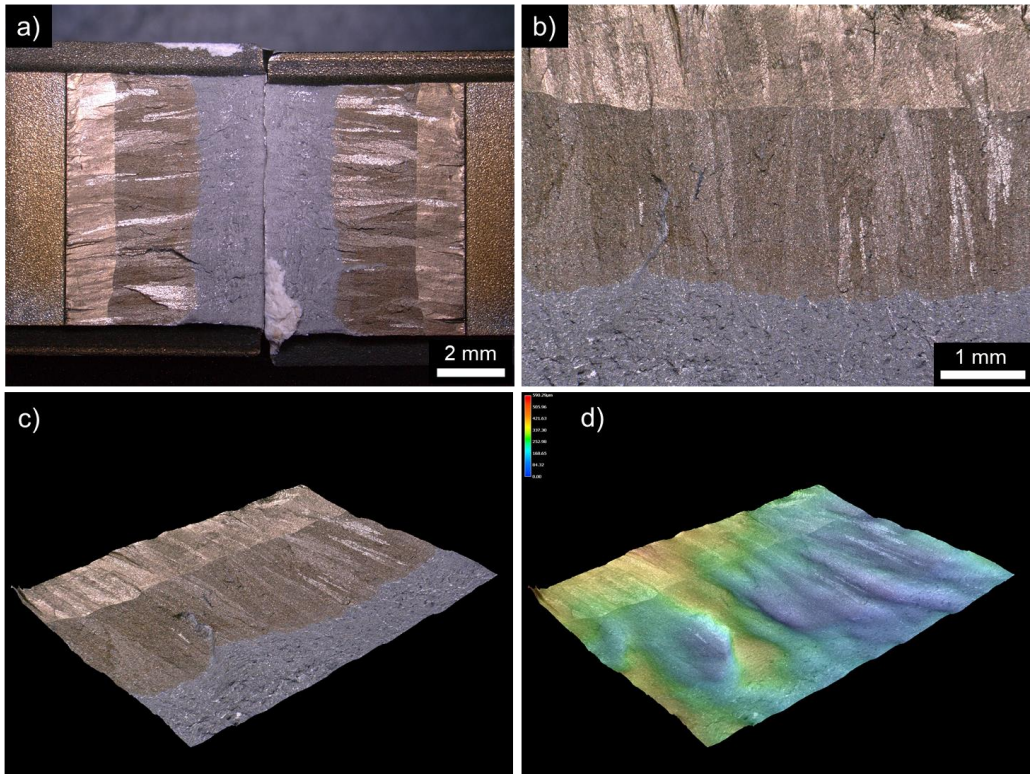

Weld W1, T = 77 K

W1 F9

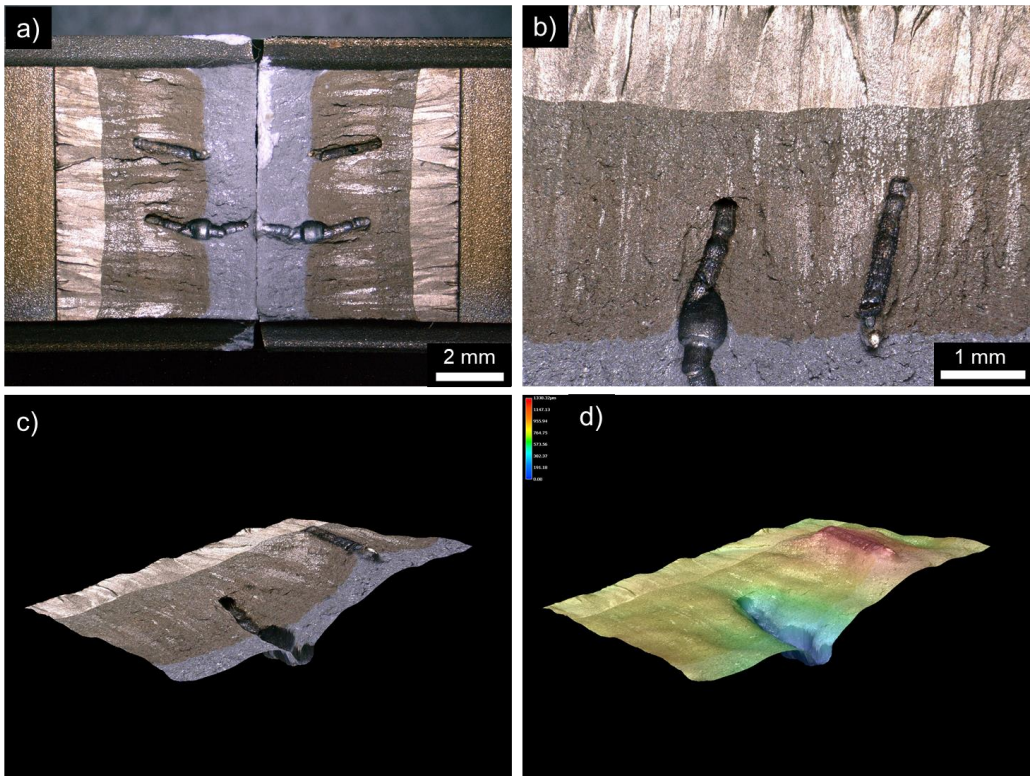

W1 F10

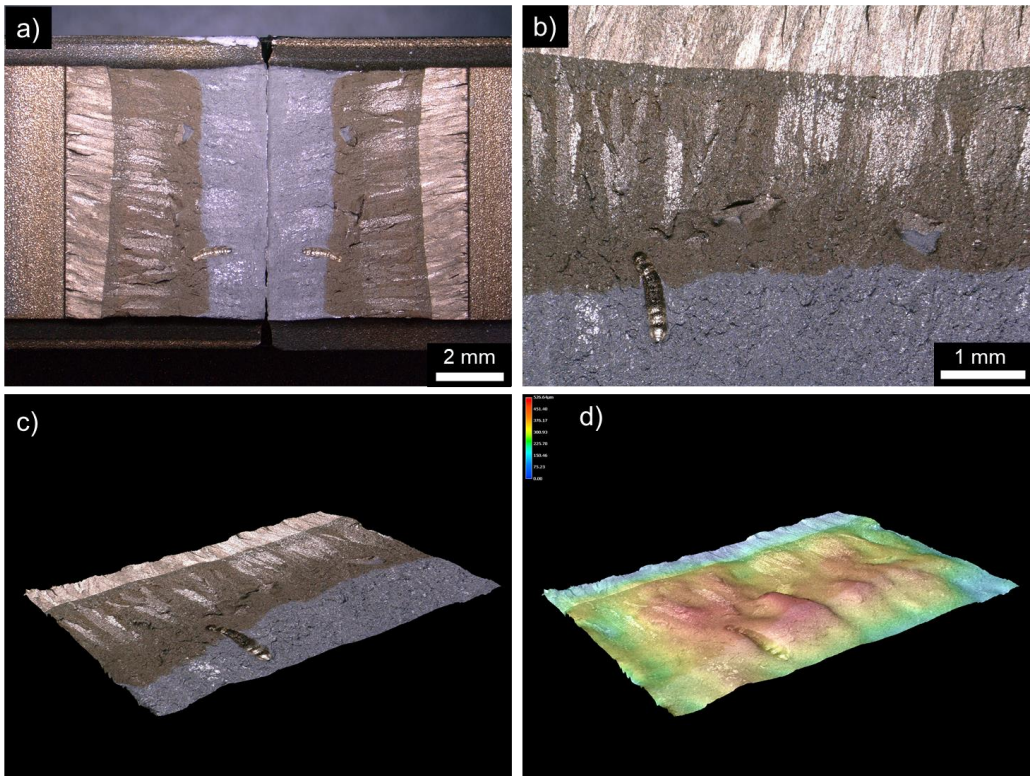

W1 F11

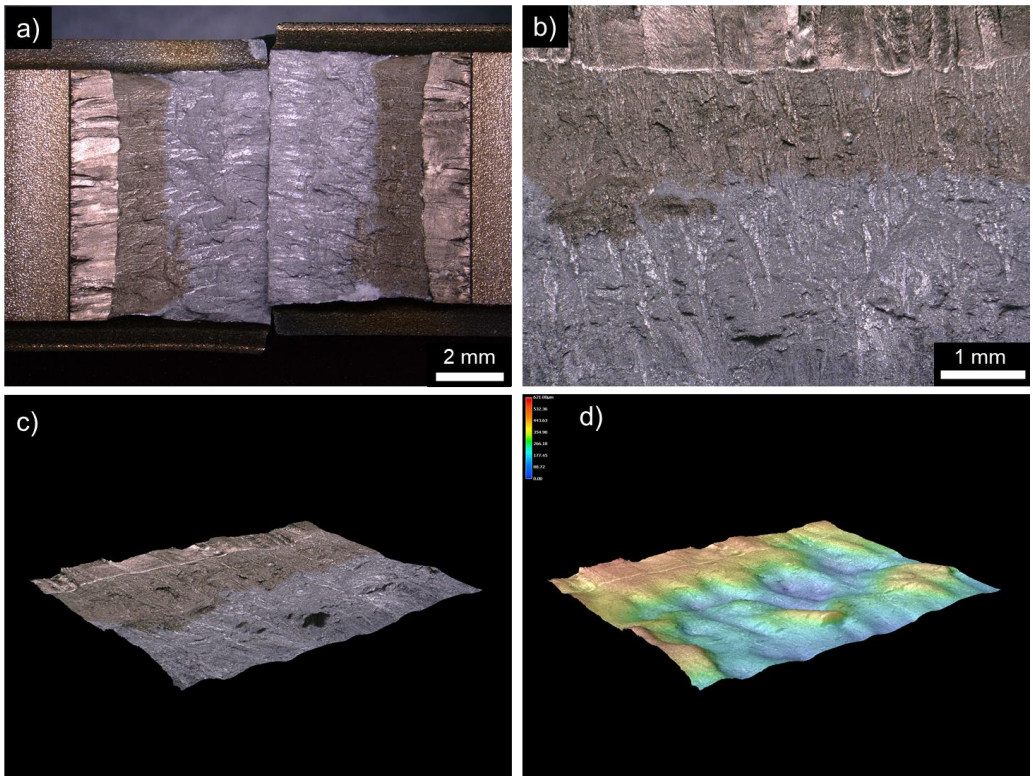

W1 F12

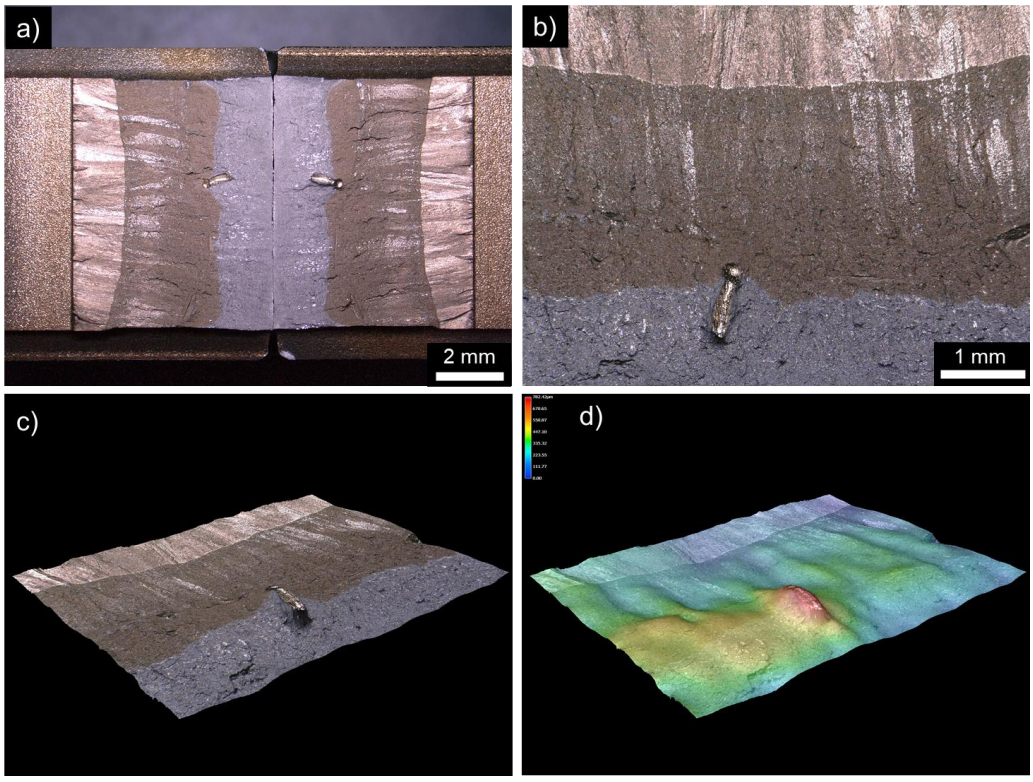

W1 F13

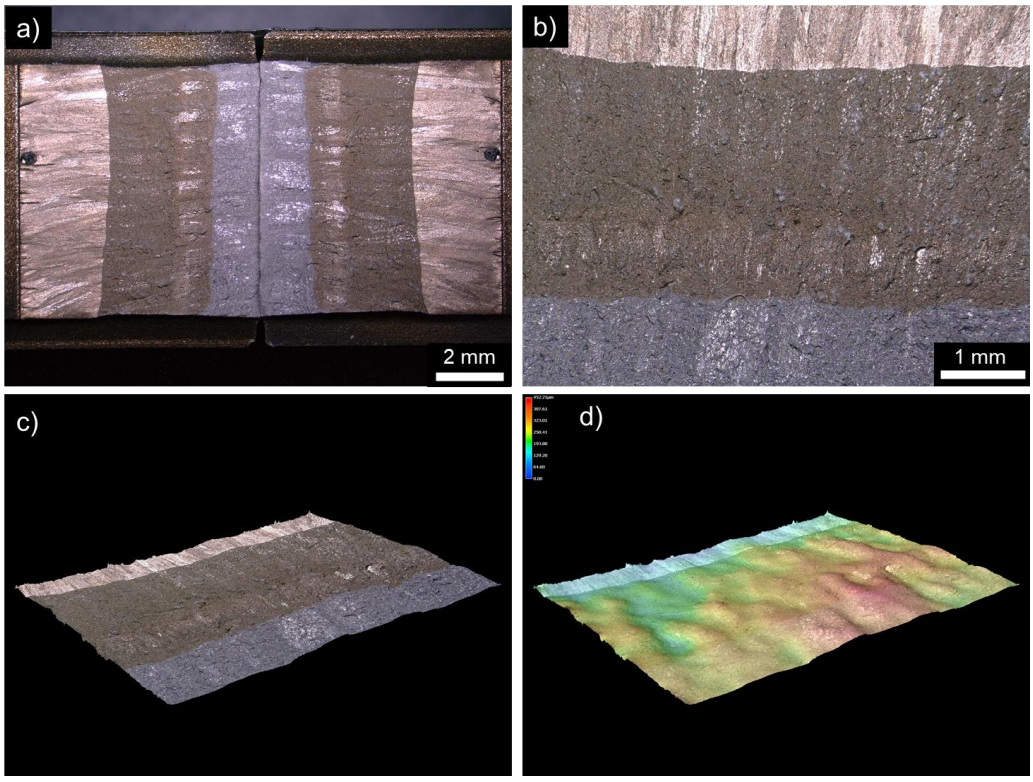

W1 F14

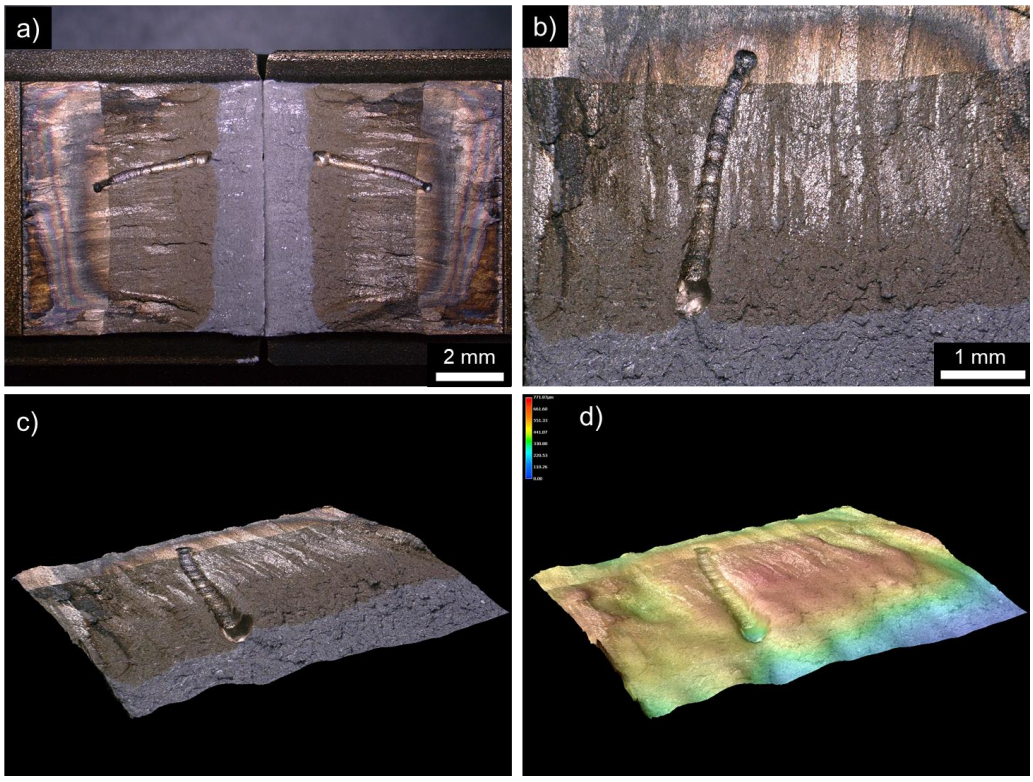

Weld W2, T = 4 K

W2 F3

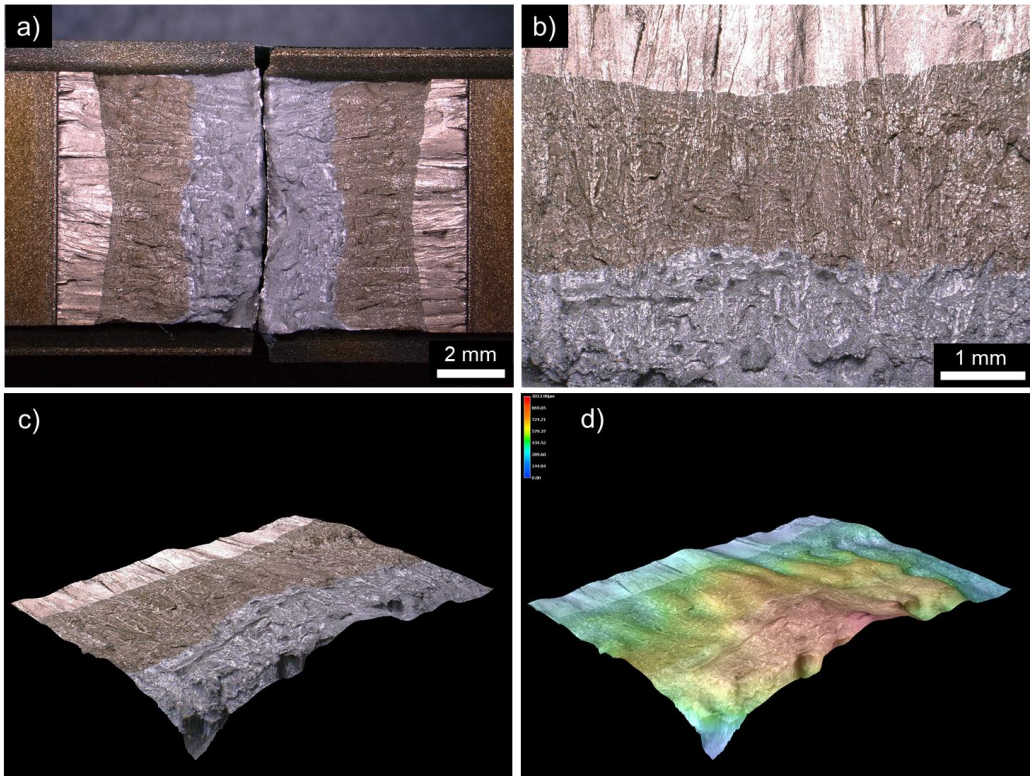

W2 F4

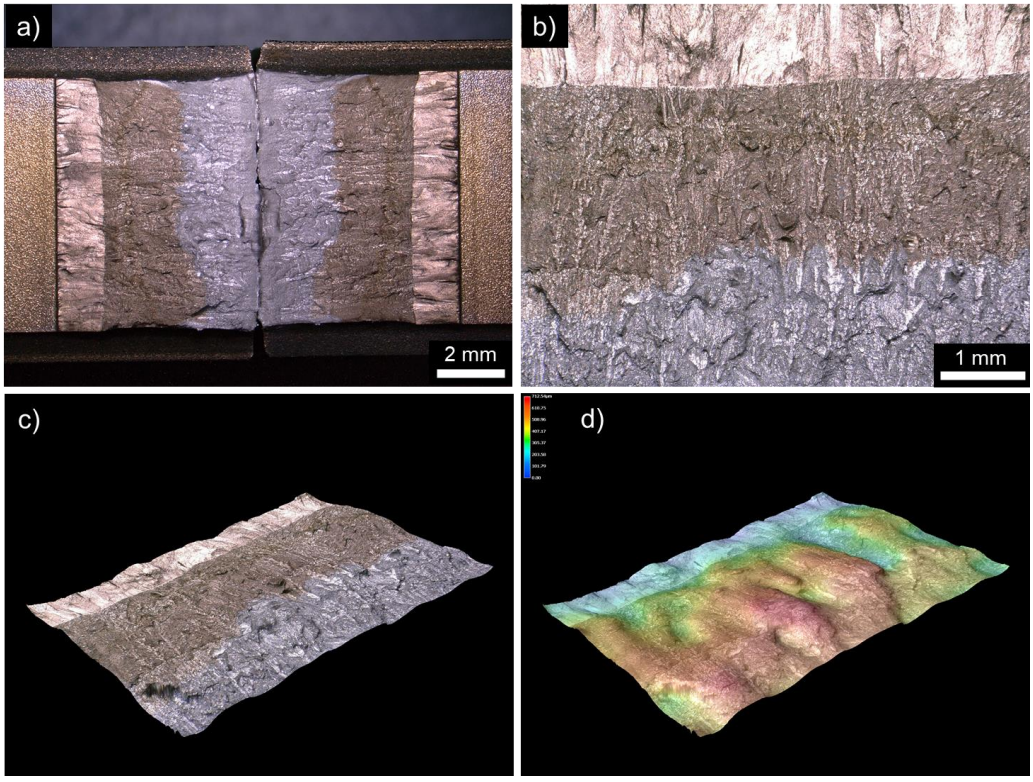

W2 F5

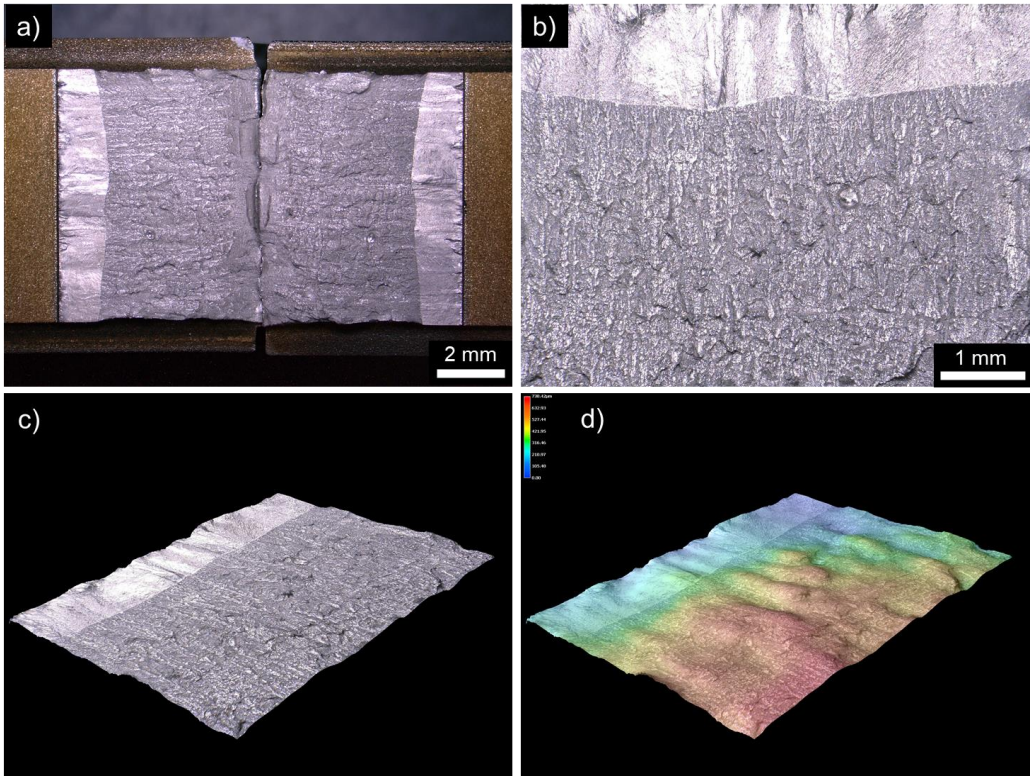

W2 F6

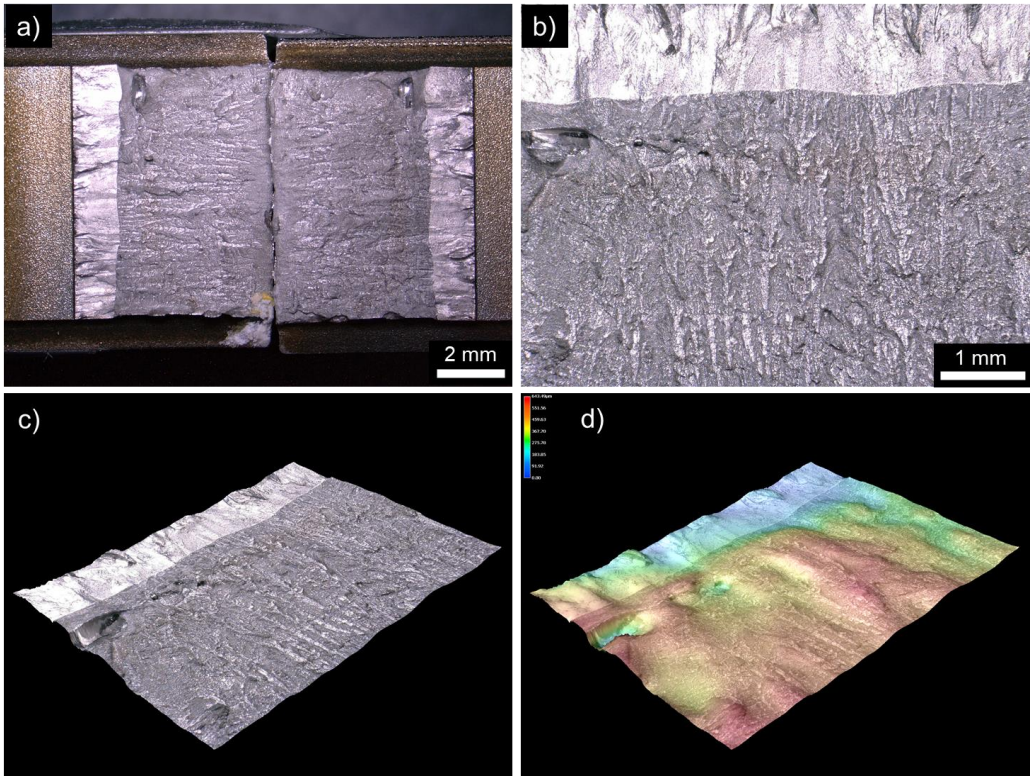

W2 F7

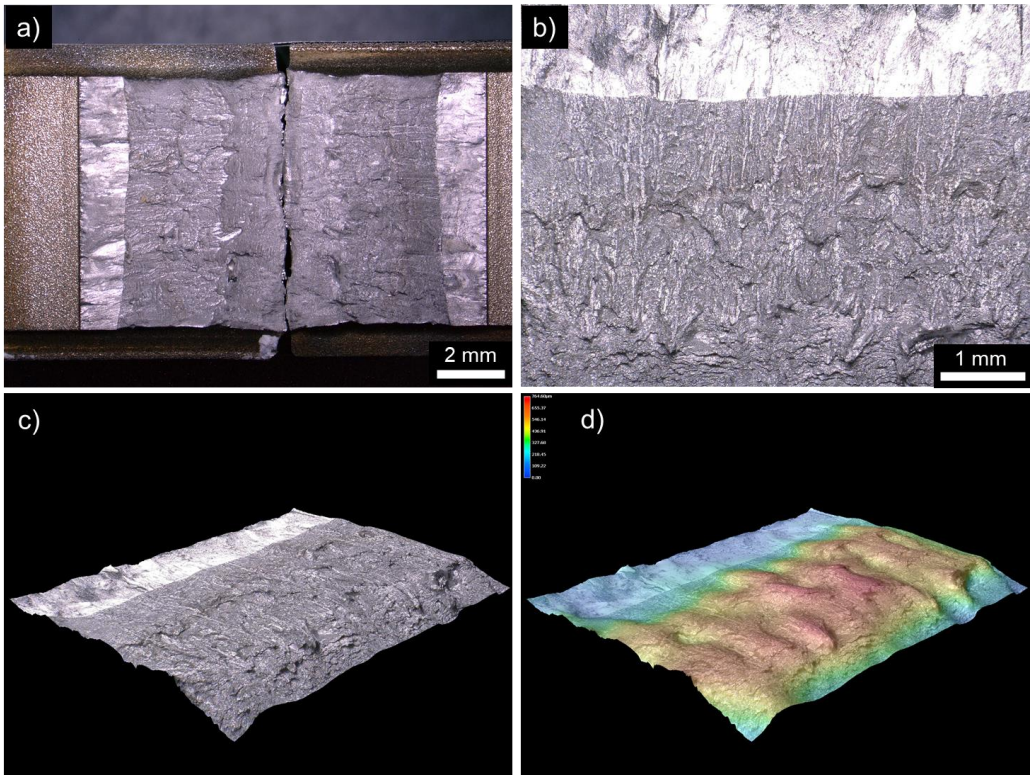

Weld W2, T = 77 K

W2 F8

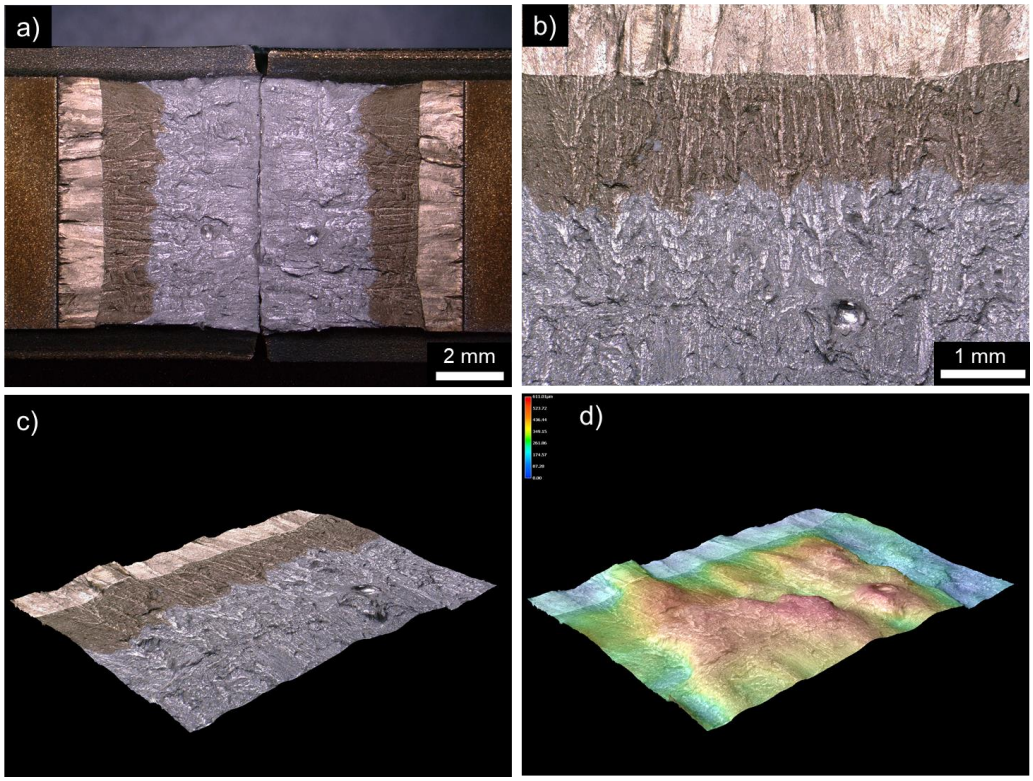

W2 F9

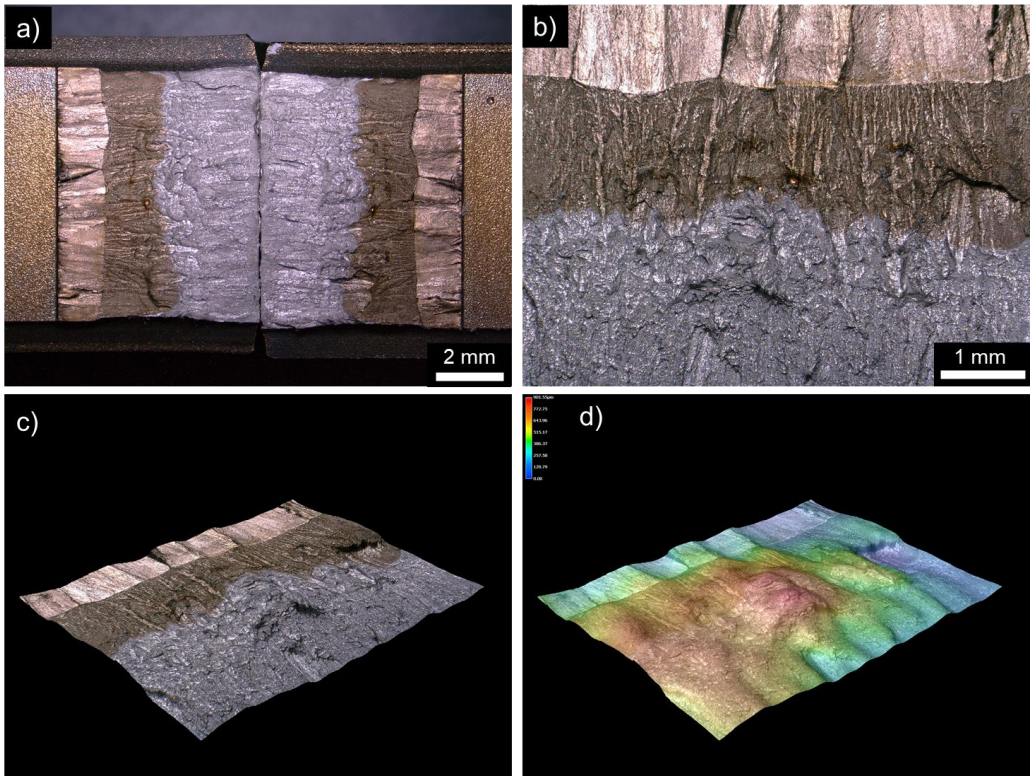

W2 F10

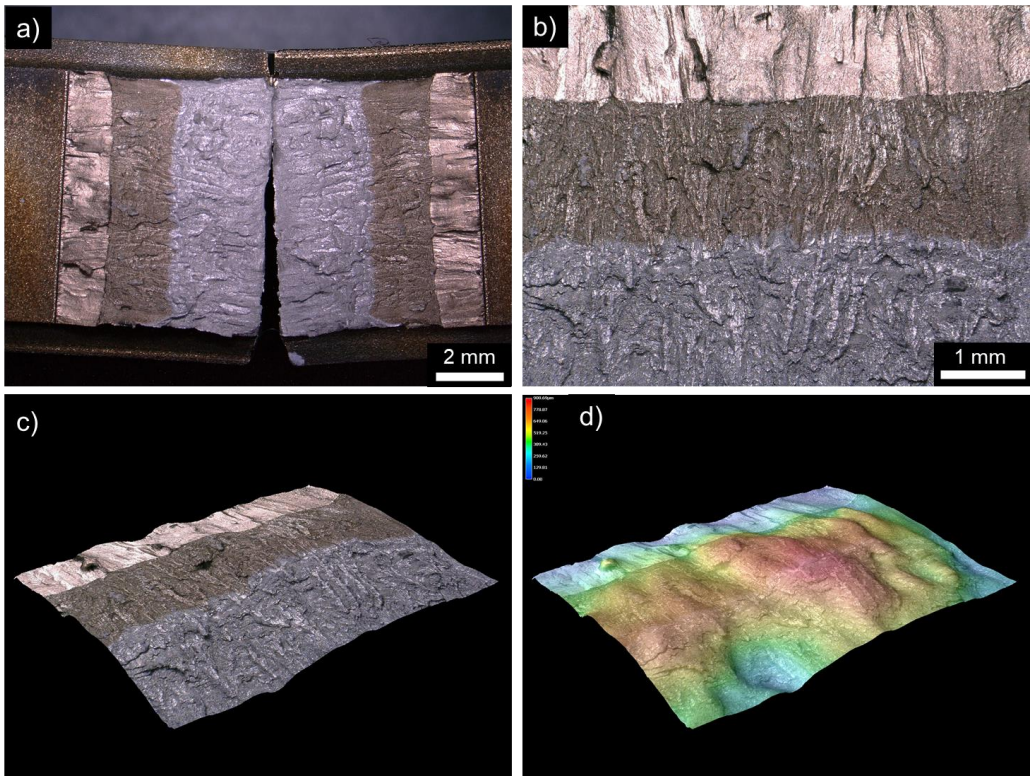

W2 F11

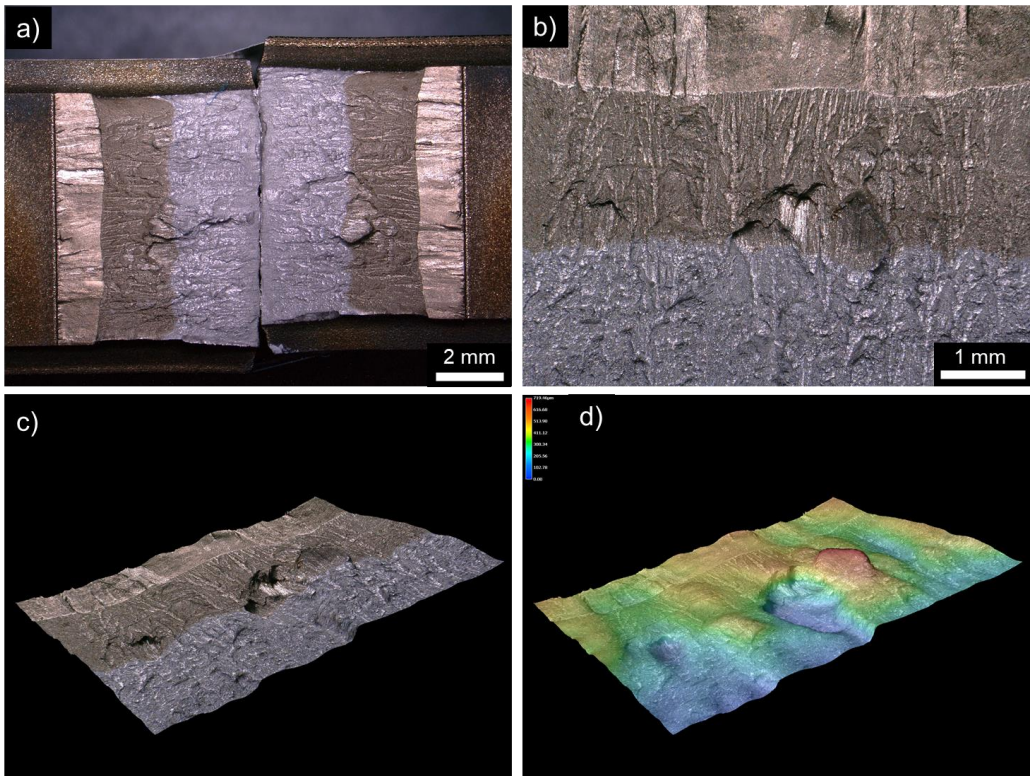

W2 F12

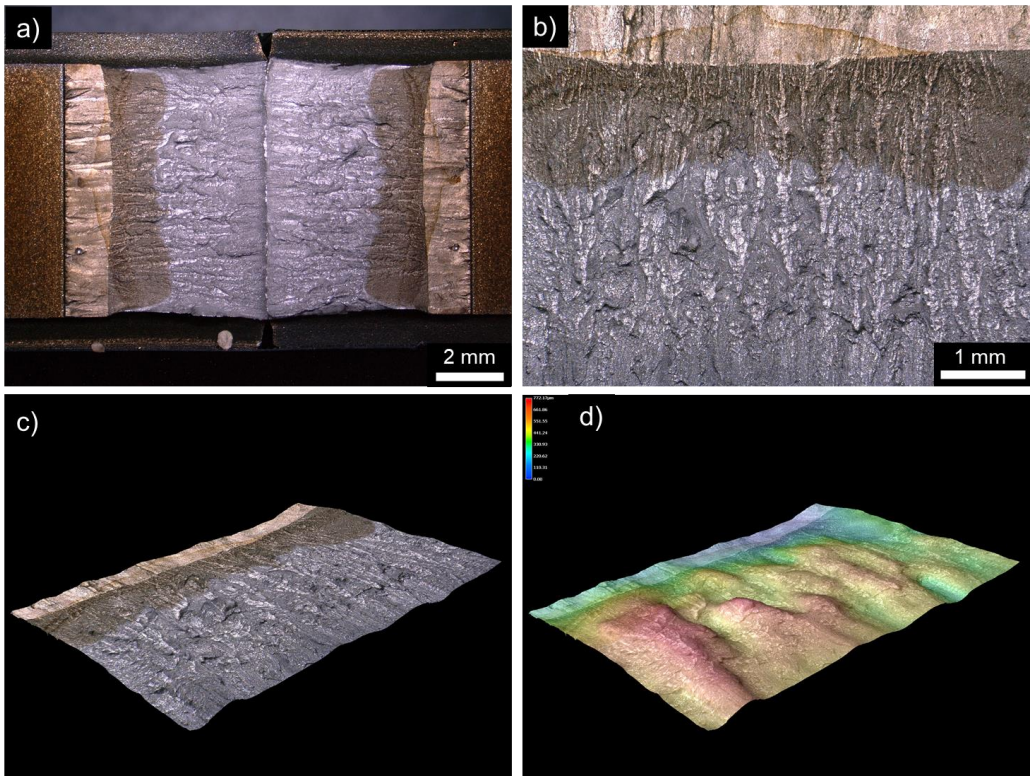

Weld W3, T = 4 K

W3 F3

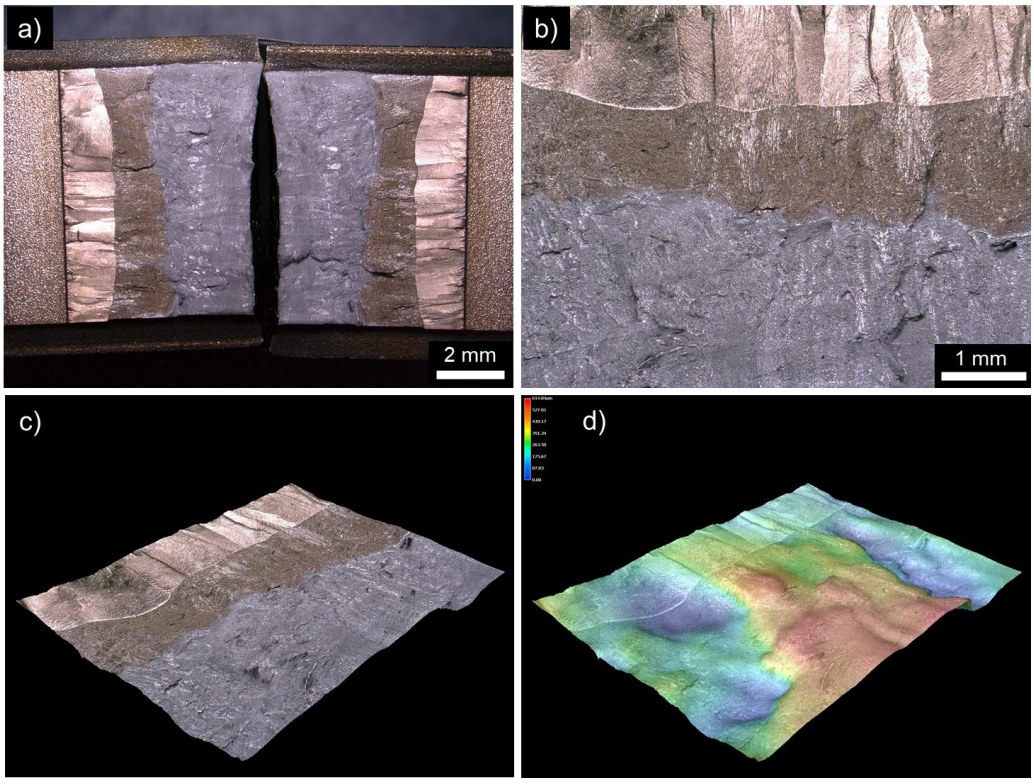

W3 F4

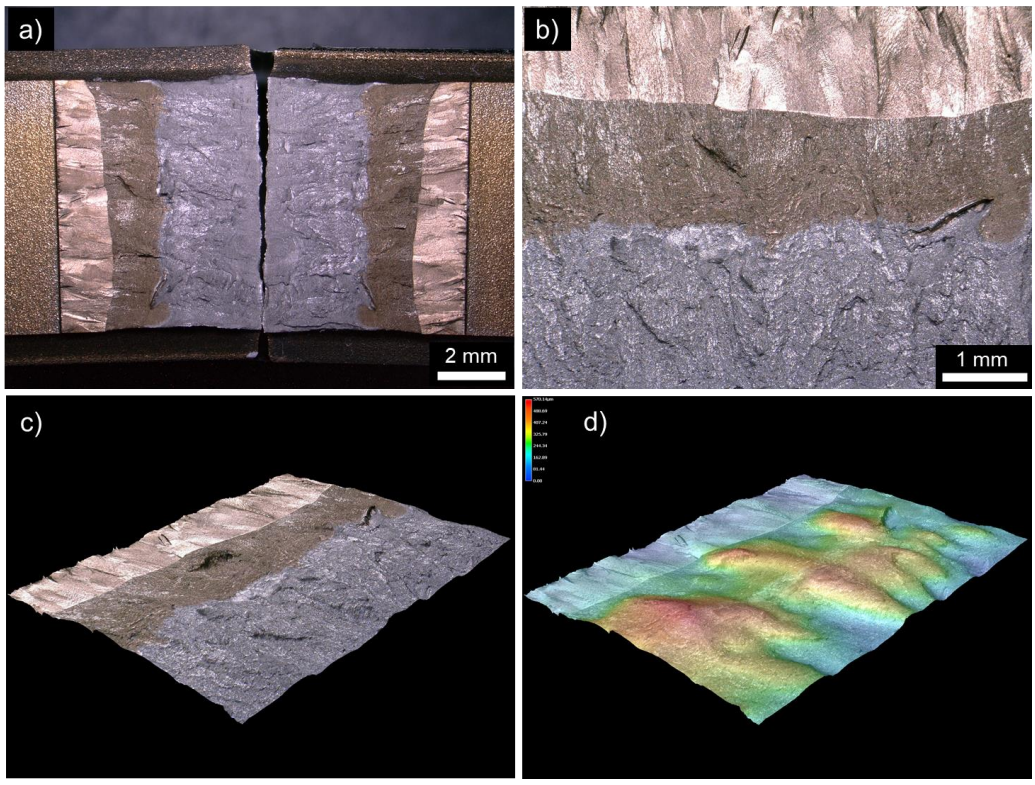

W3 F5

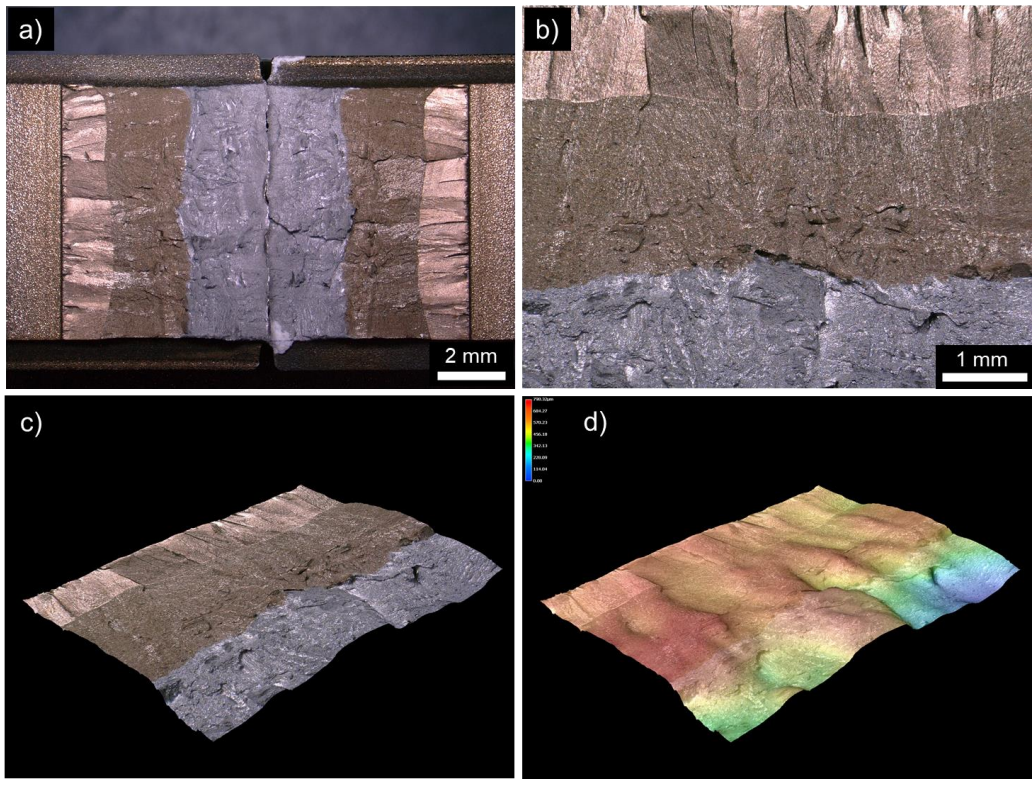

W3 F6

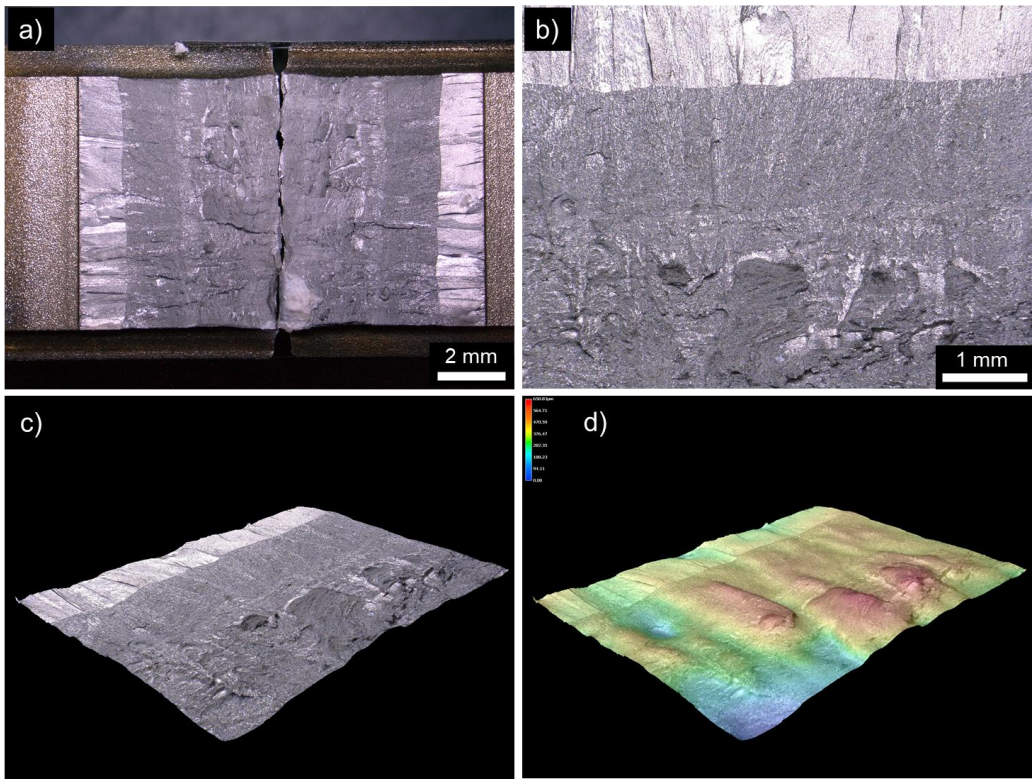

W3 F7

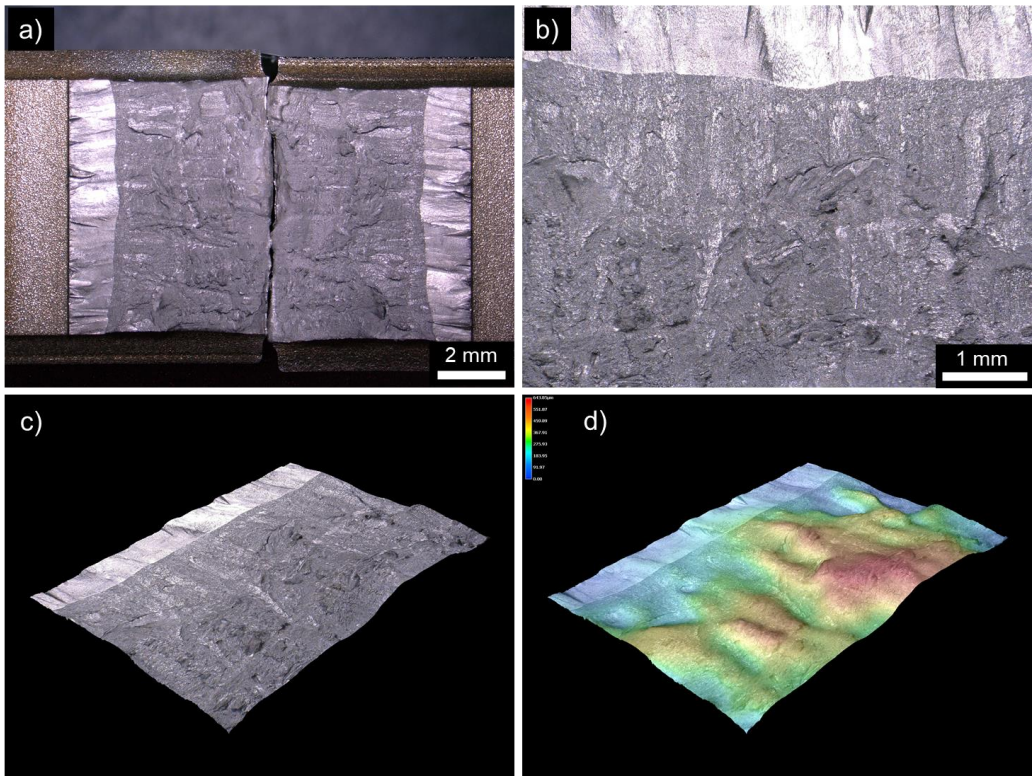

Weld W3, T = 77 K

W3 F8

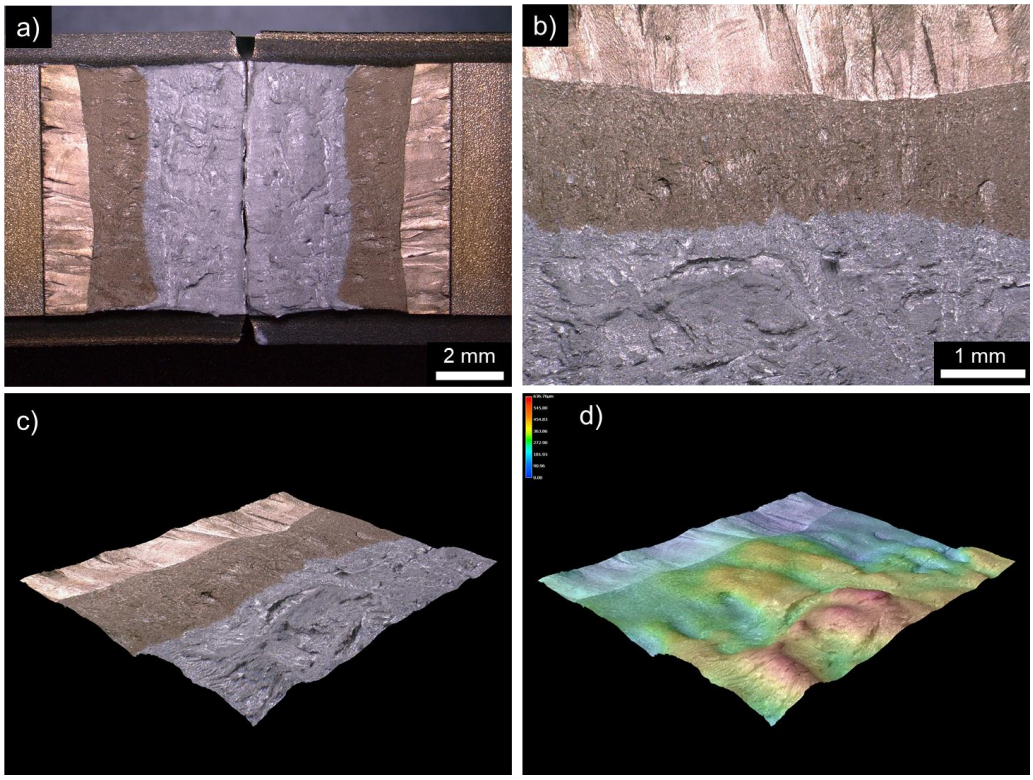

W3 F9

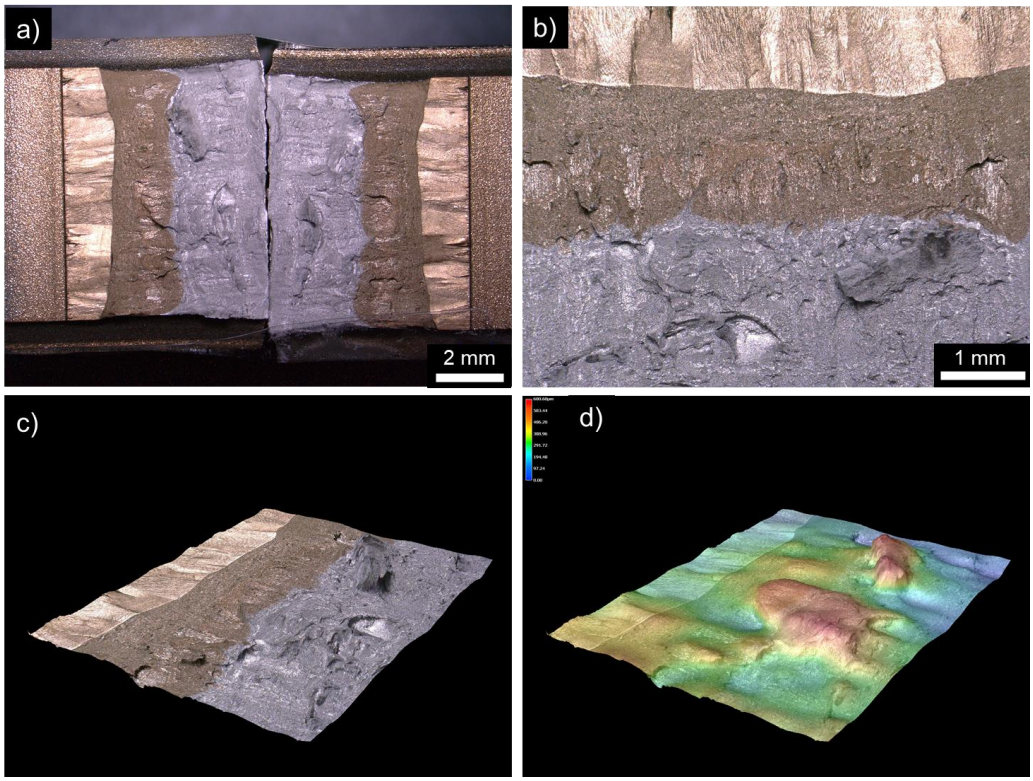

W3 F10

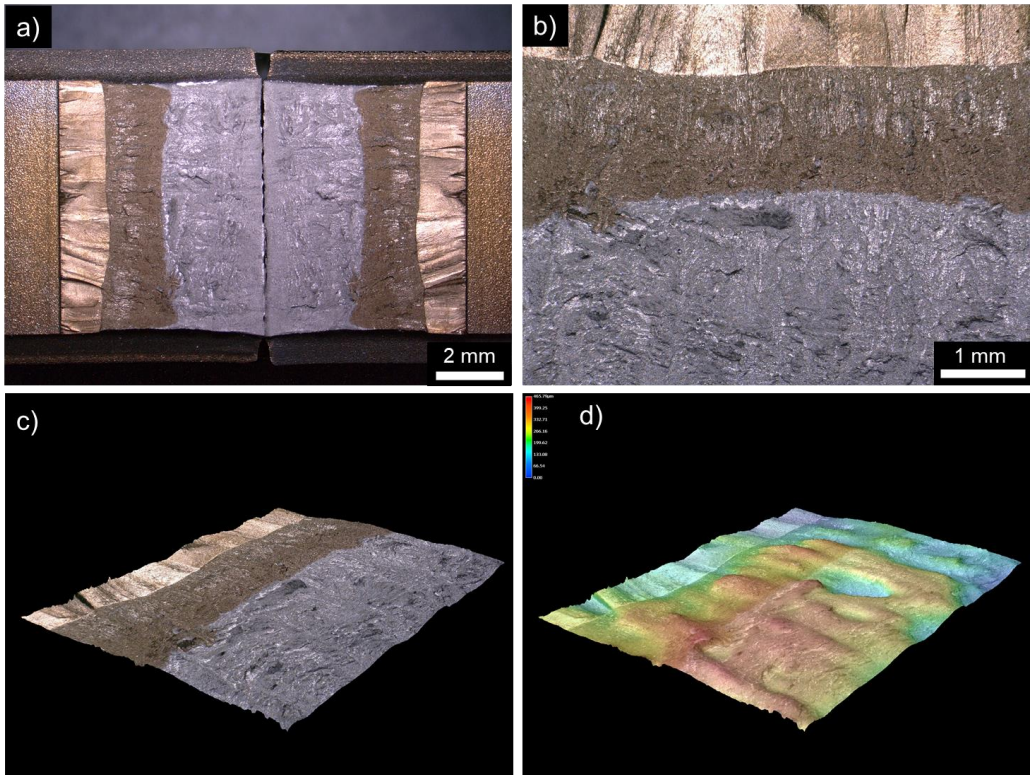

W3 F11

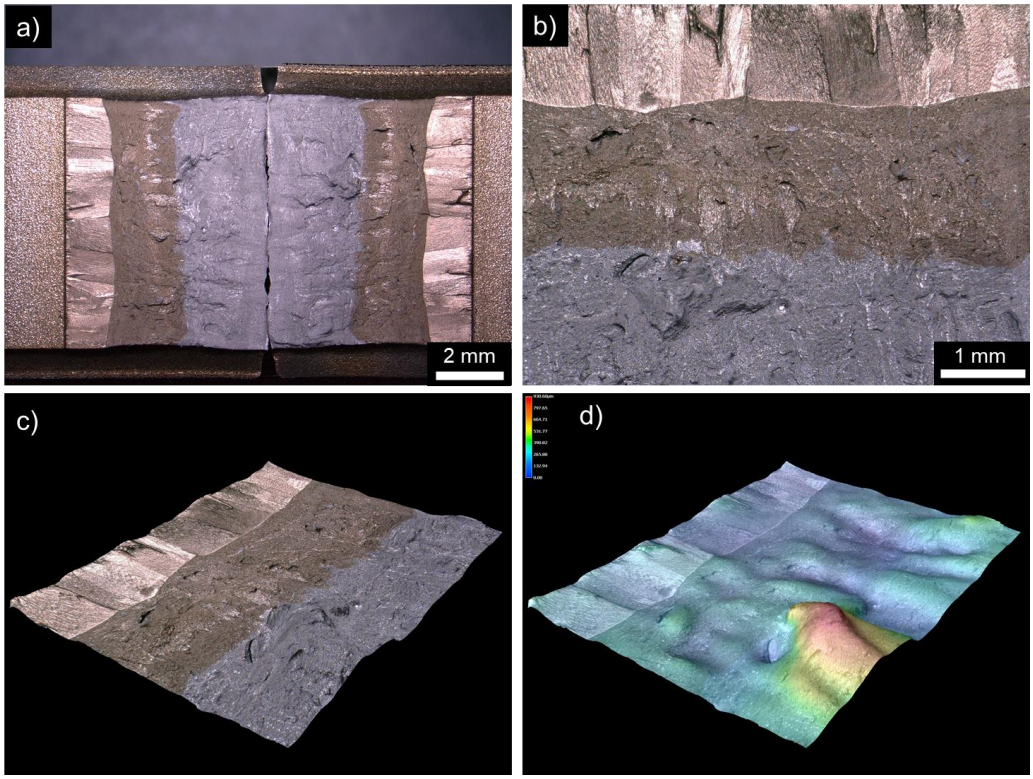

W3 F12

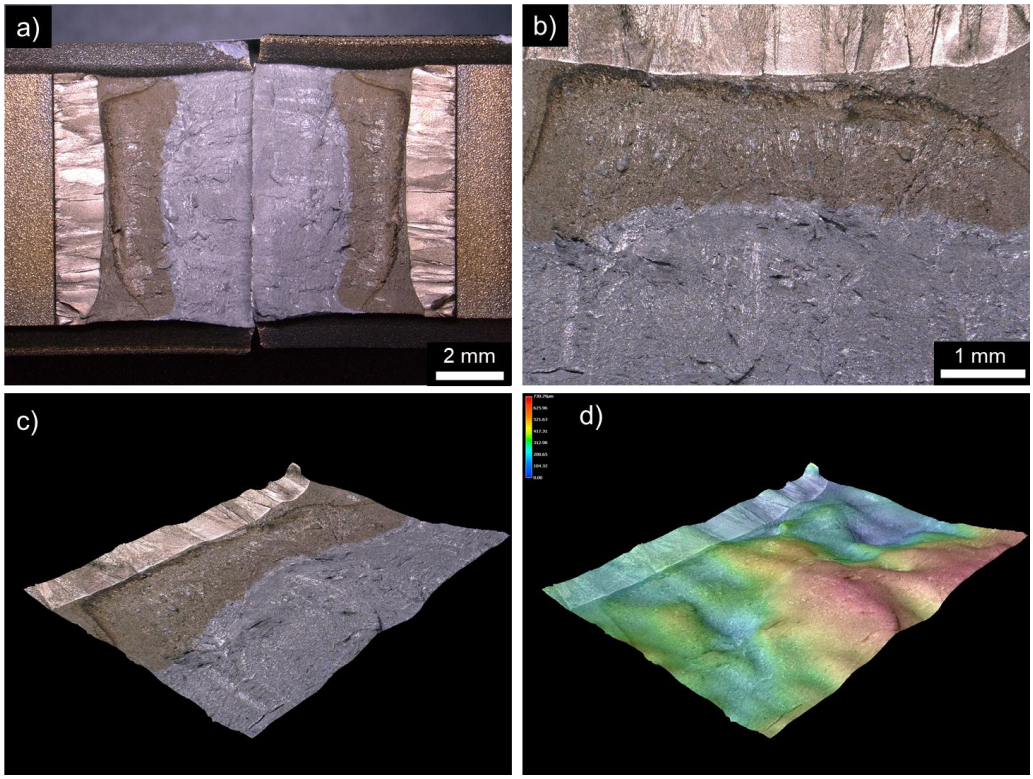

W3 F13

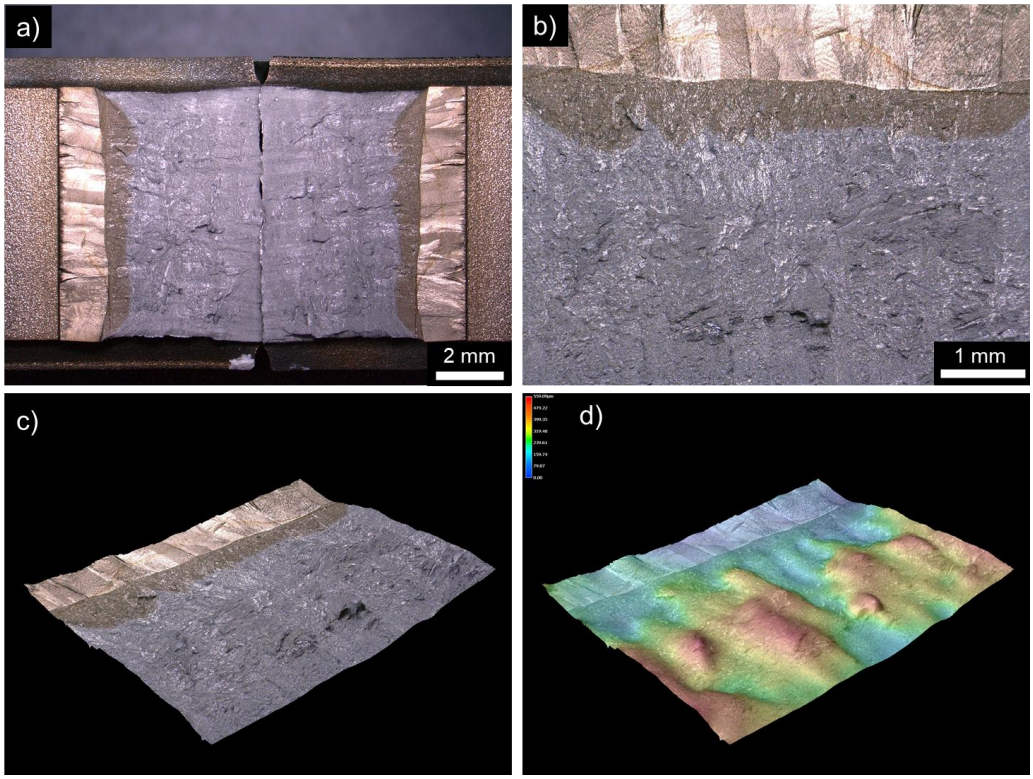

Weld W4, T = 4 K

W4 F3

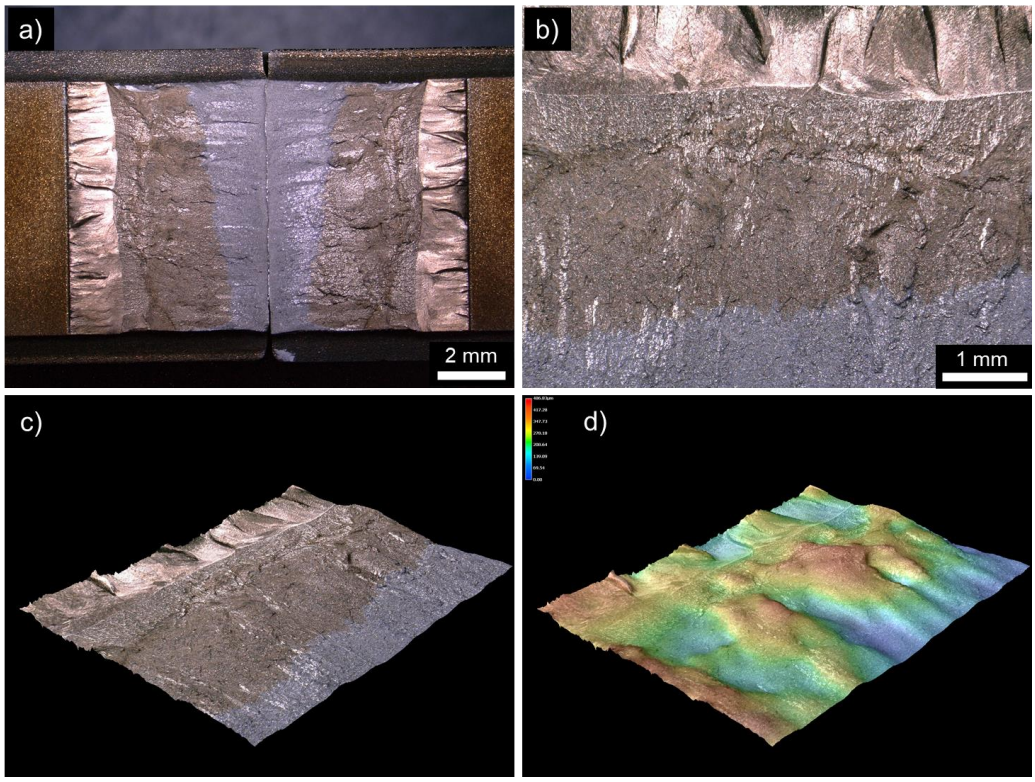

W4 F4

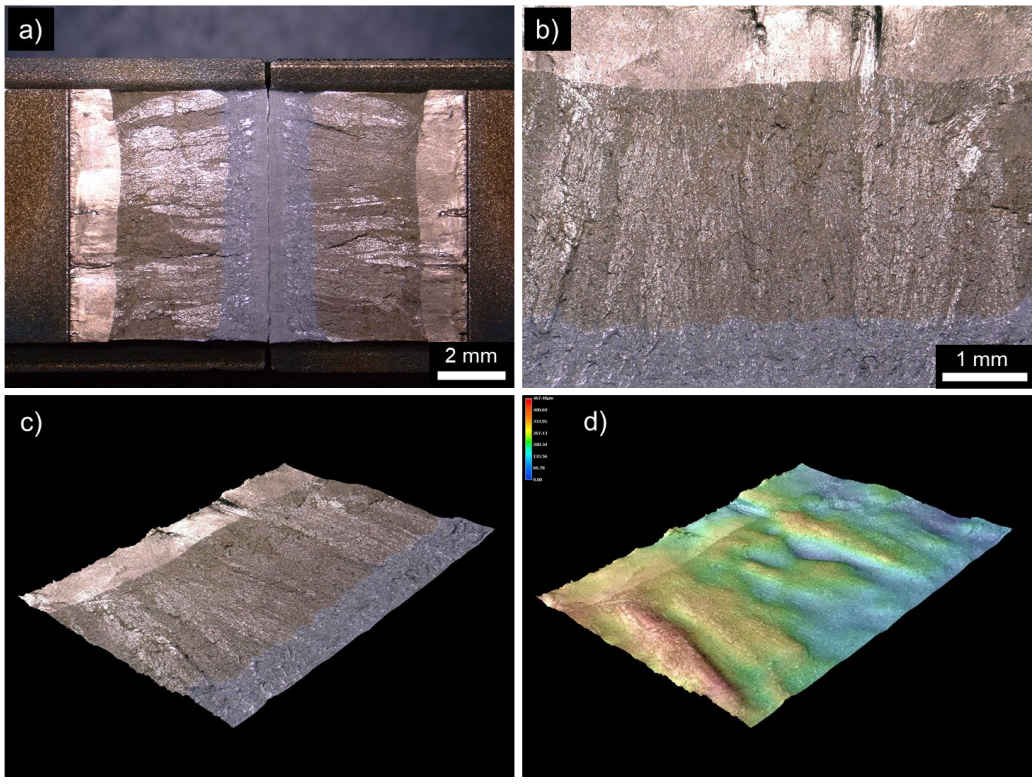

W4 F5

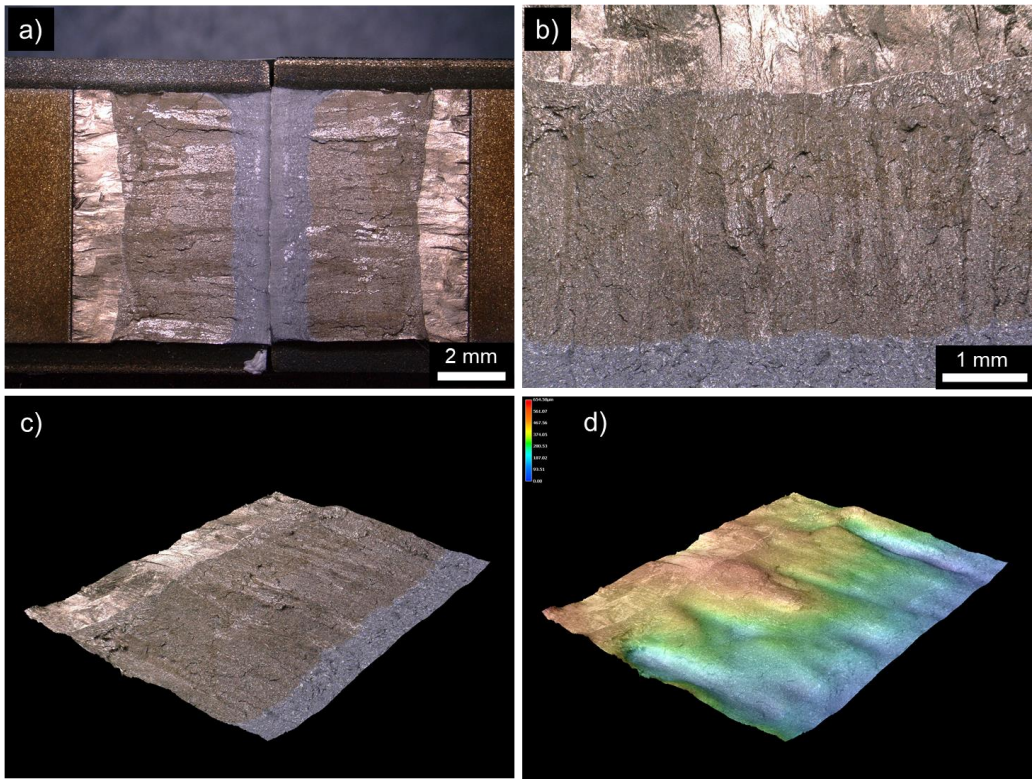

W4 F6

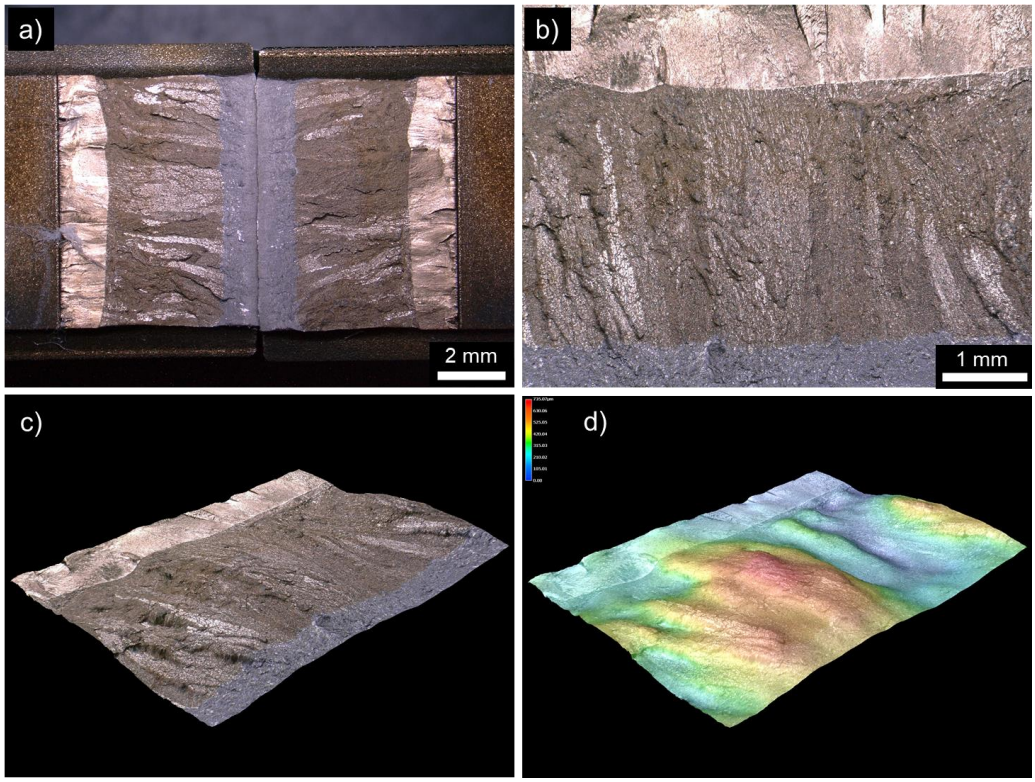

W4 F7

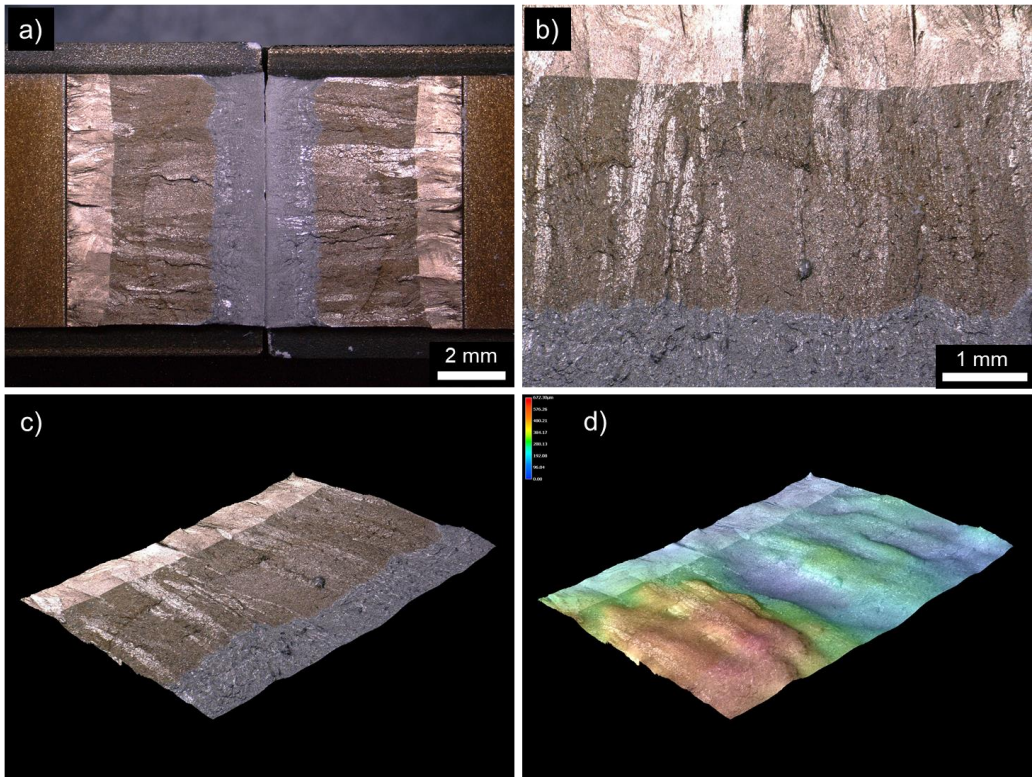

W4 F8

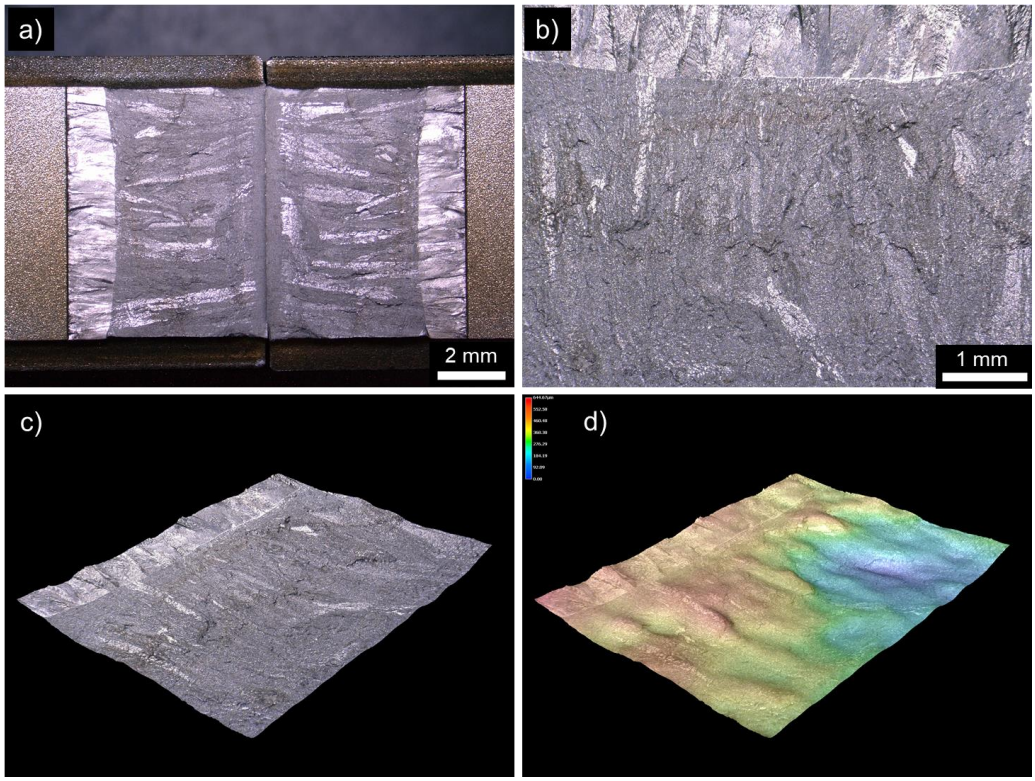

Weld W4, T = 4 K

W4 F9

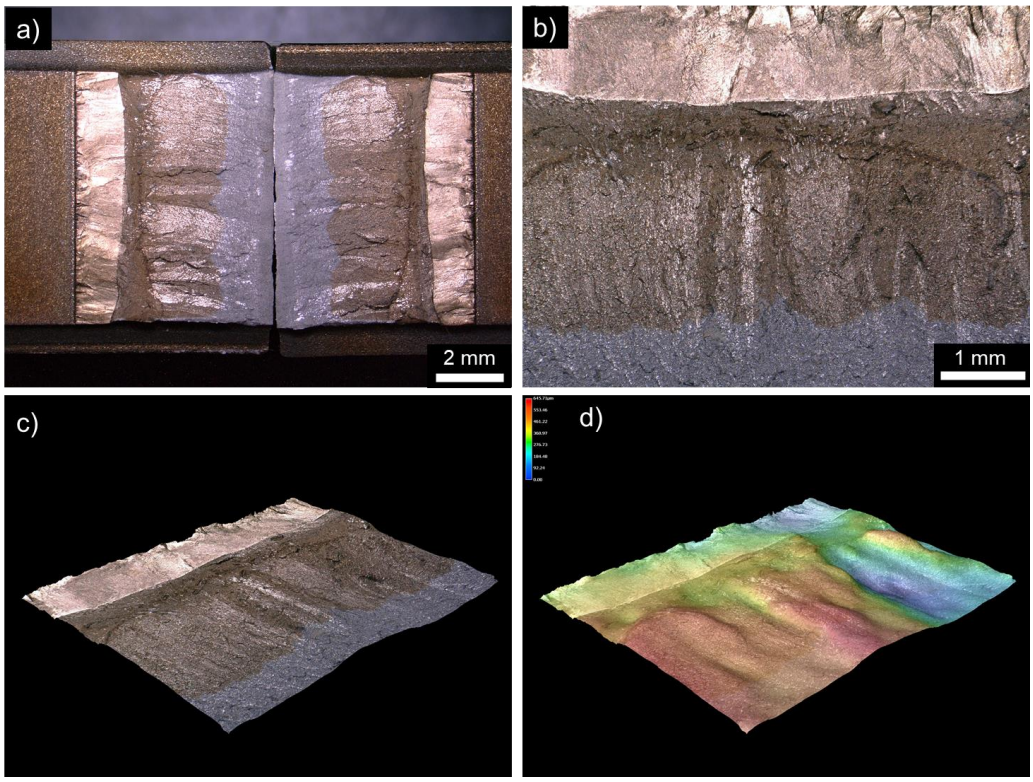

W4 F10

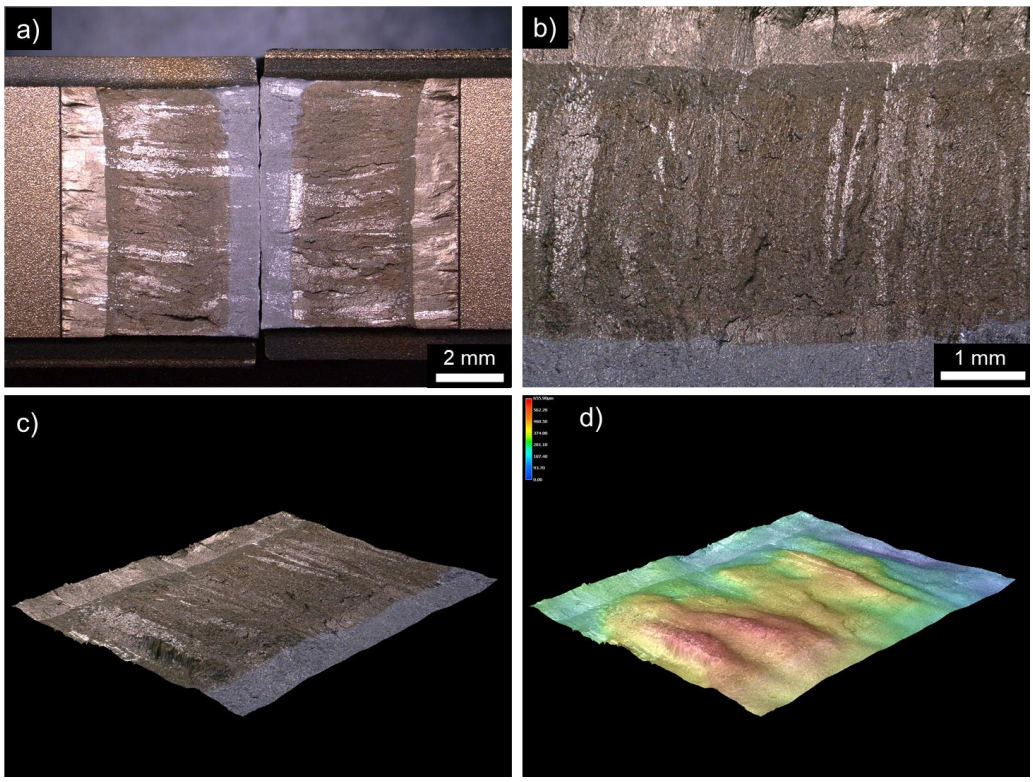

W4 F11

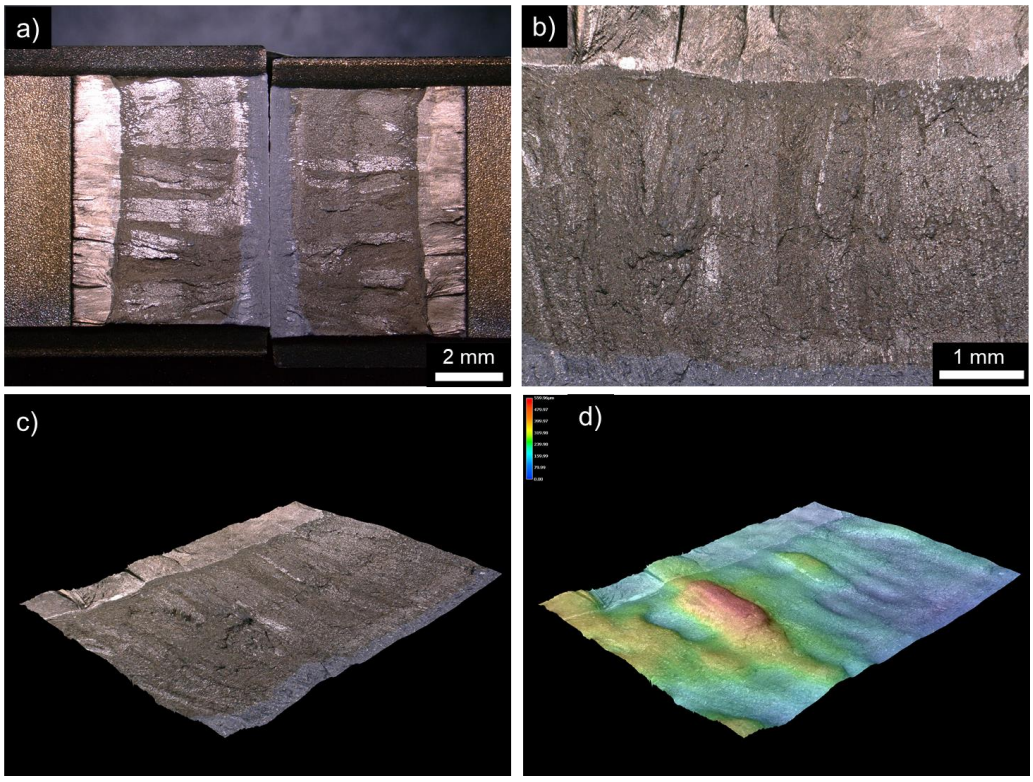

W4 F12

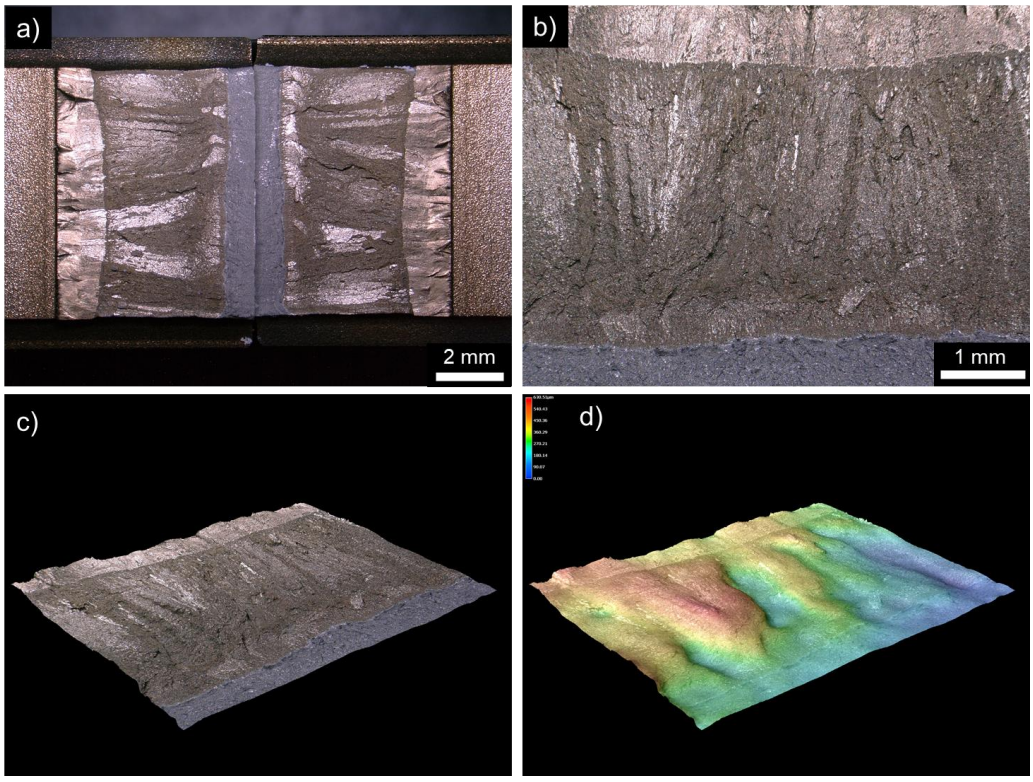

W4 F13

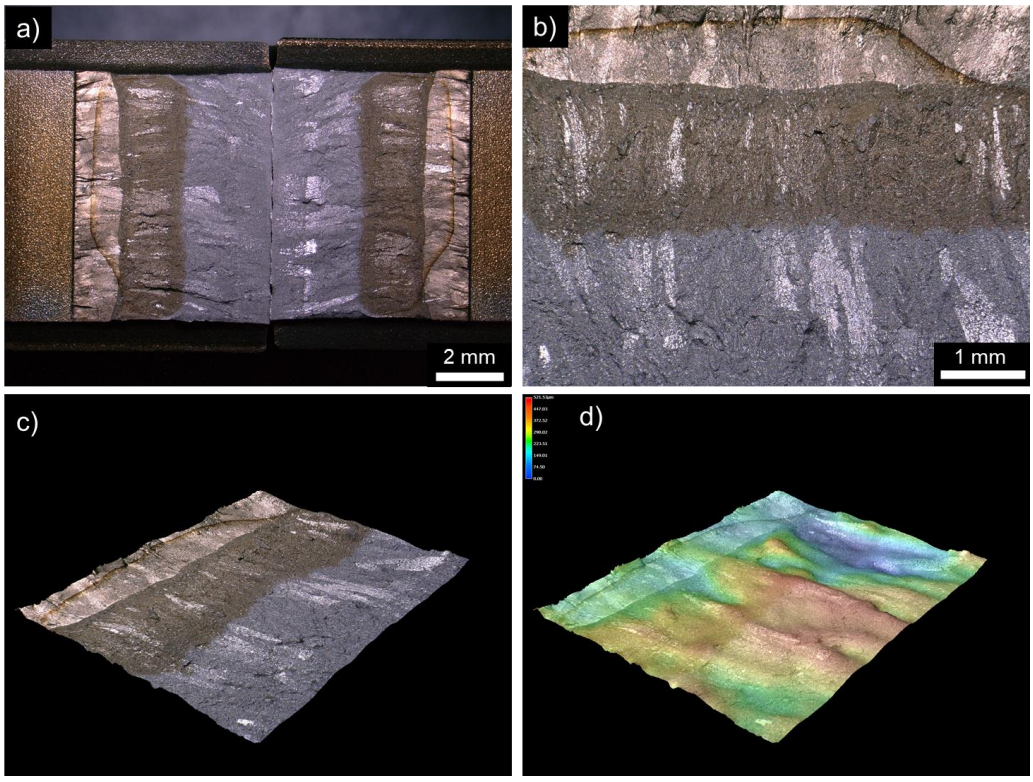

Appendix F: Fractography – SEM Images and EDS Spectra

Weld W1

W1-F4 (4 K)

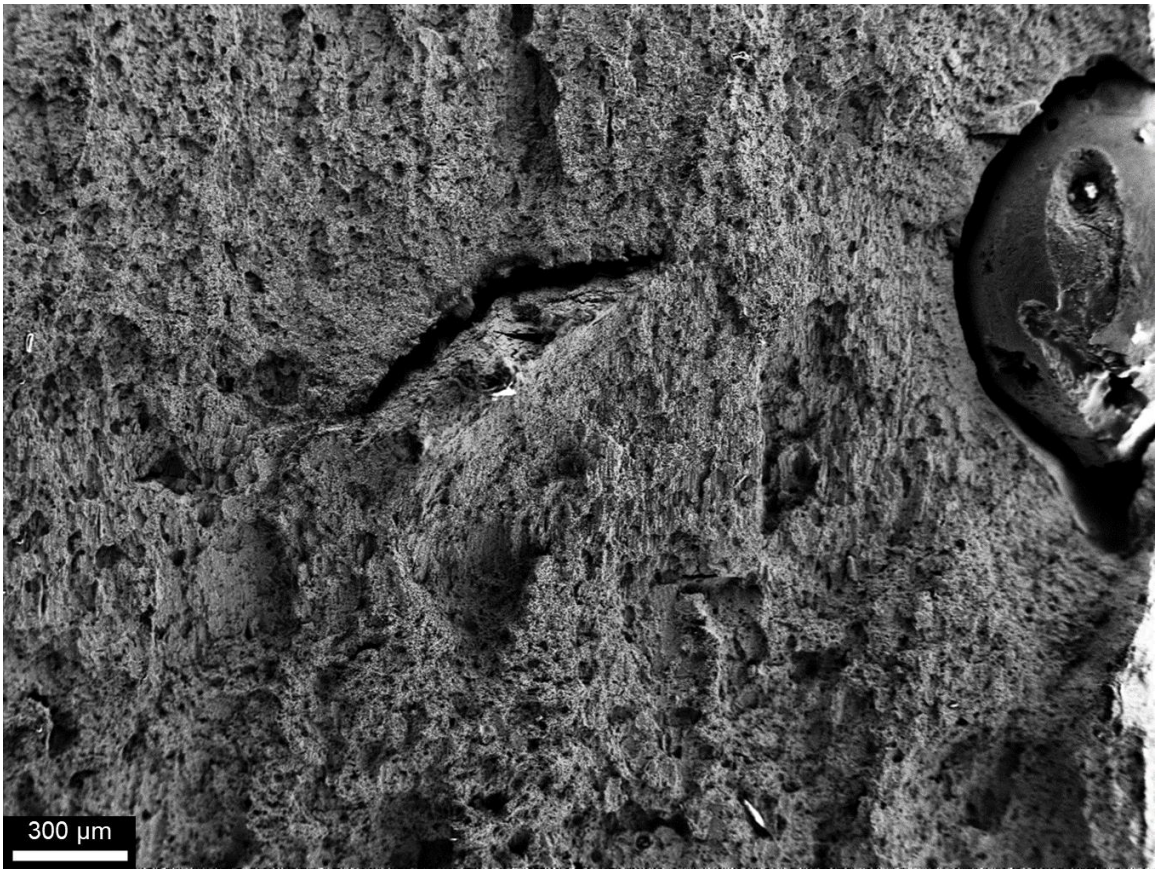

Large FOV displaying a crack jump and lack of fusion pore.

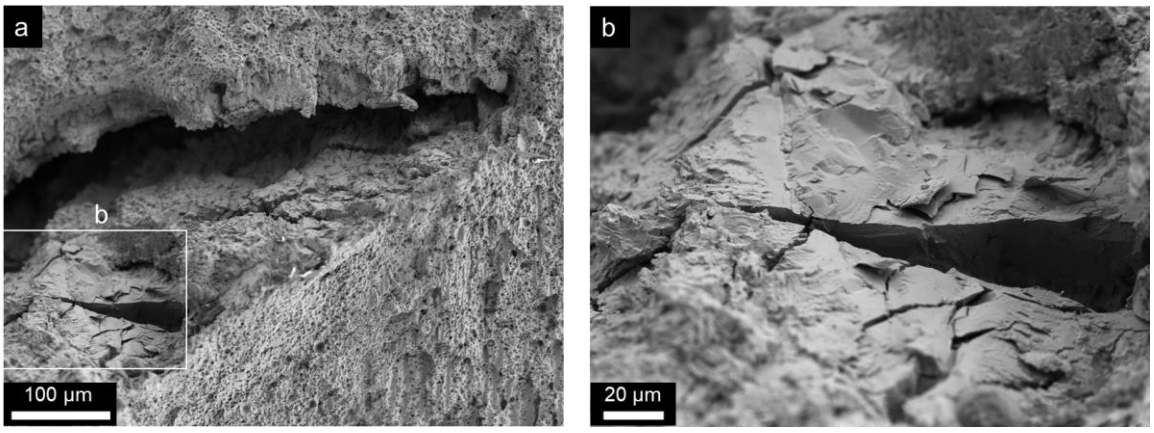

a) Crack jump, b) cleavage fracture

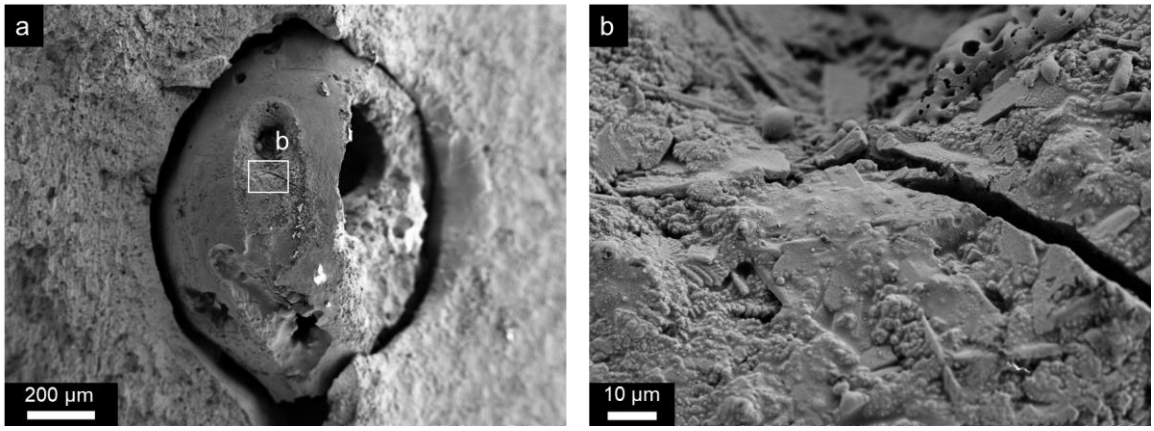

a) Lack of fusion pore, b) feature on the surface of the feature.

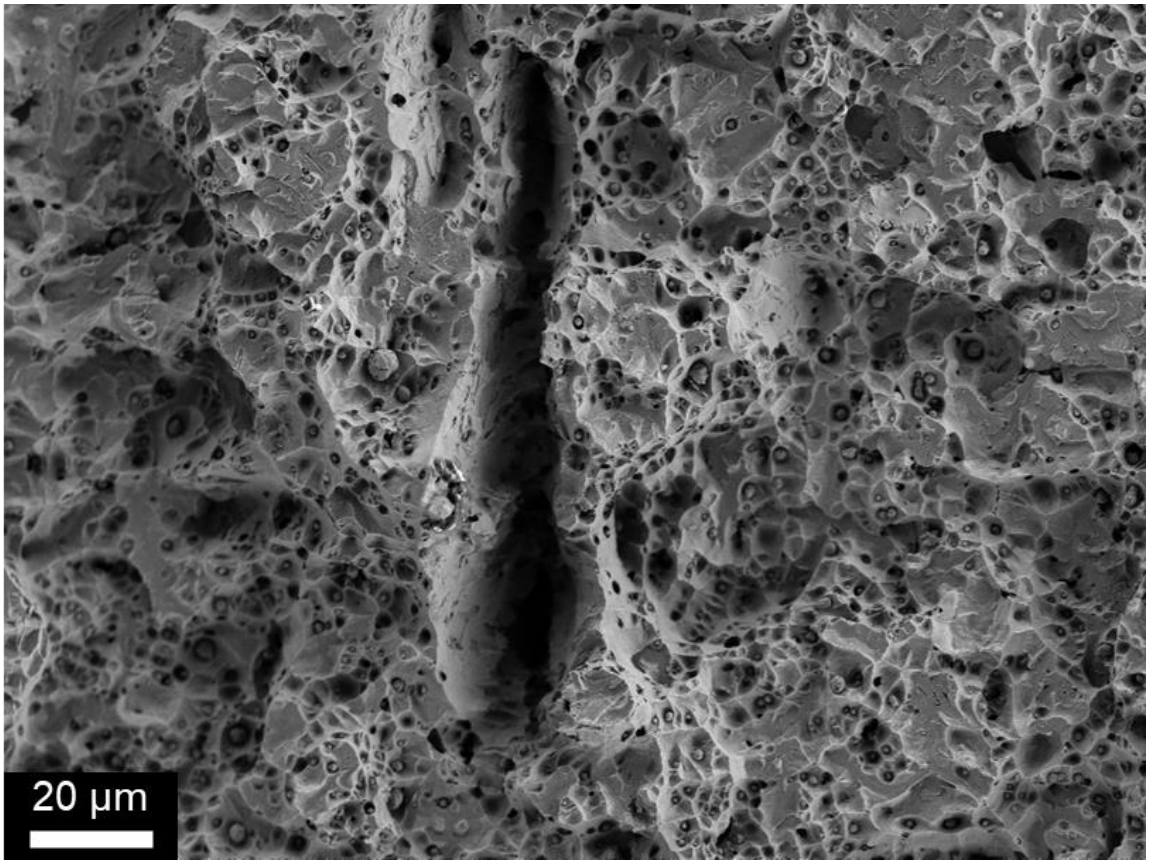

Elongated lack of fusion pore.

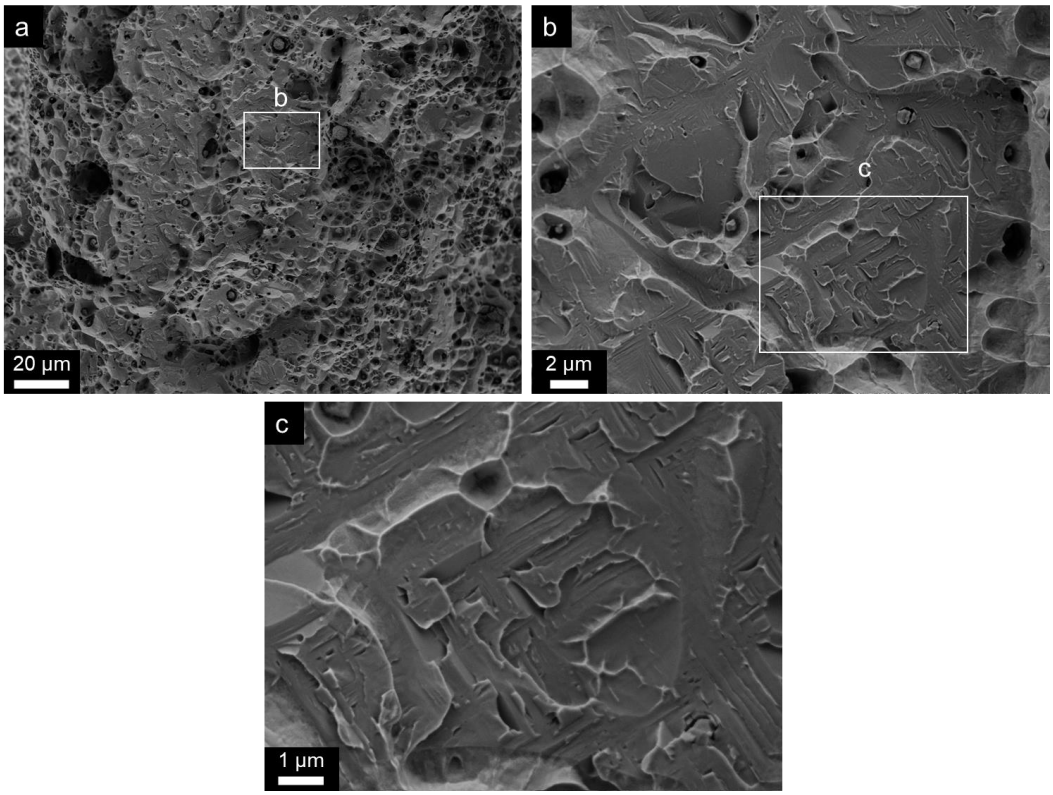

a) Crack paths showing brittle fracture, b—c) higher magnification of the cleavage facets.

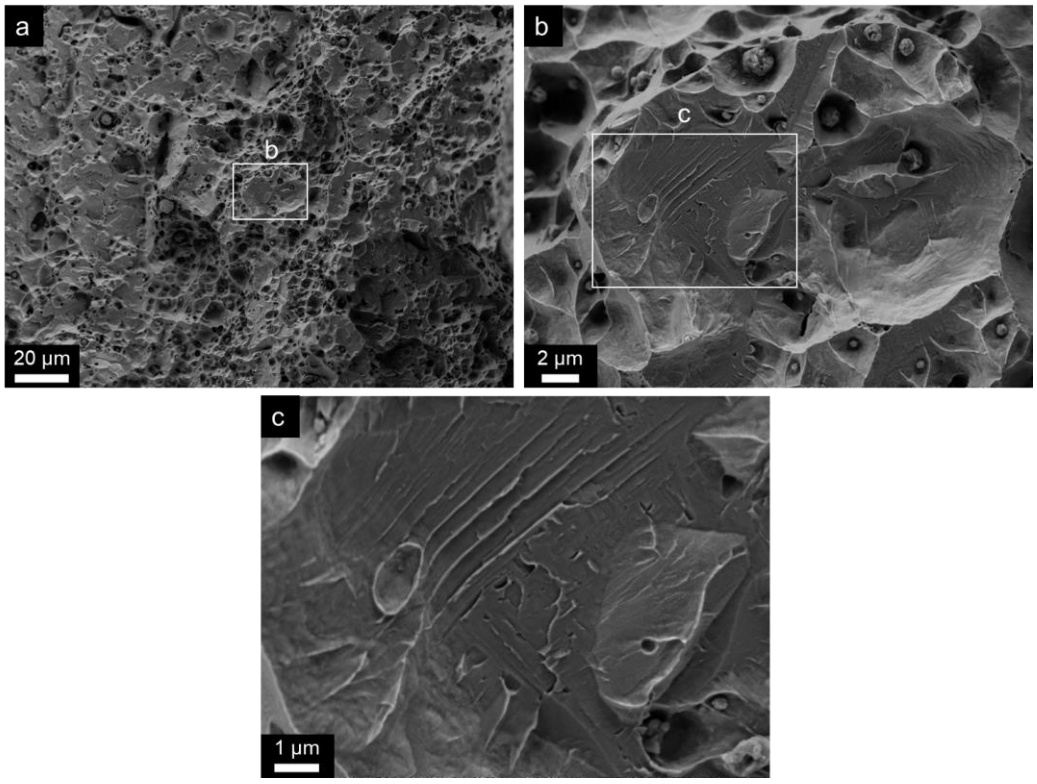

a) Crack paths showing brittle fracture and MVC, b-c) higher magnification of the cleavage facets.

W1-F8 (4K)

Large FOV of the fracture surface displaying a crack jump.

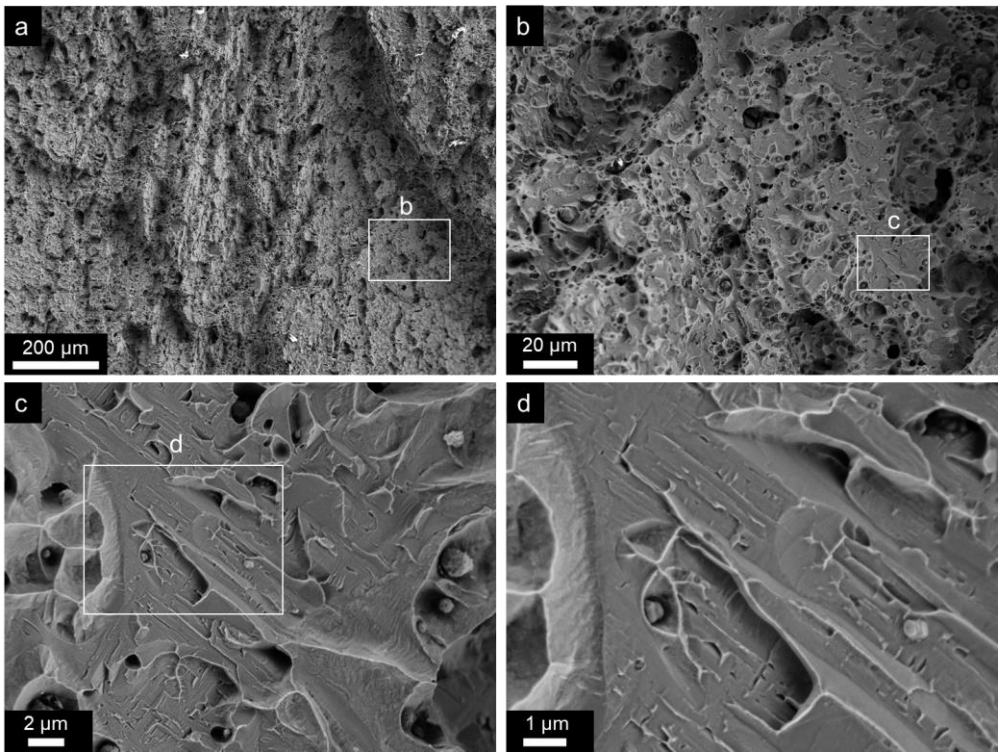

a) Crack jump, b) surface of the brittle fracture, c-d) higher magnification of the cleavage fracture.

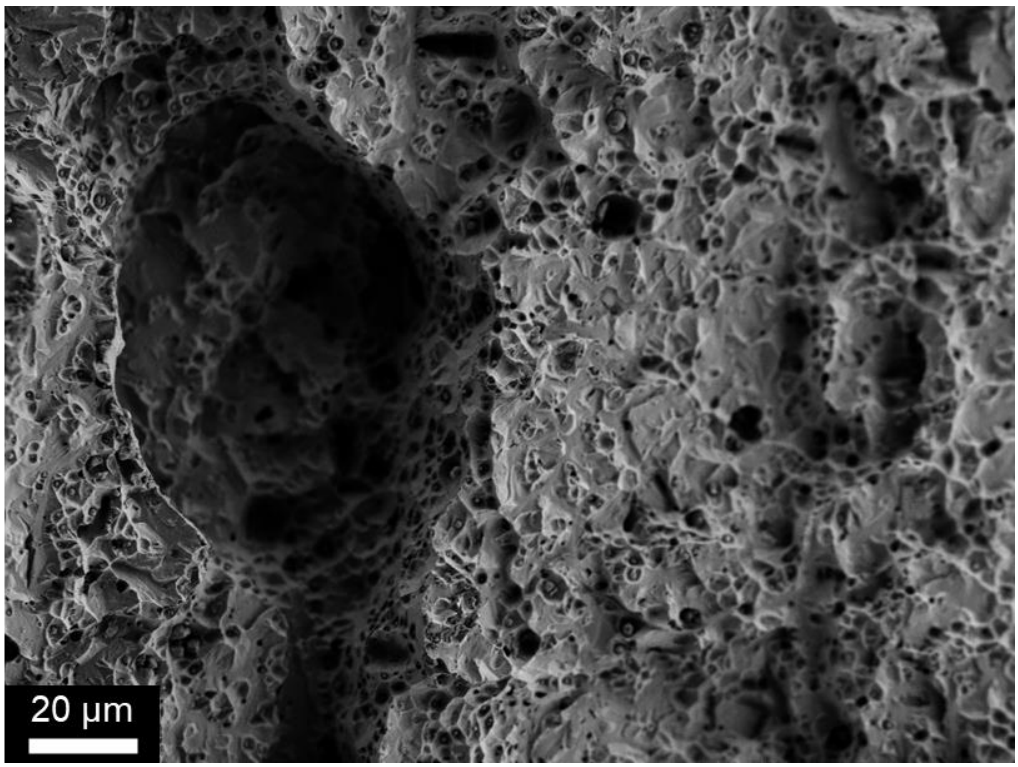

Lack of fusion pore surrounded by both cleavage fracture and MVC.

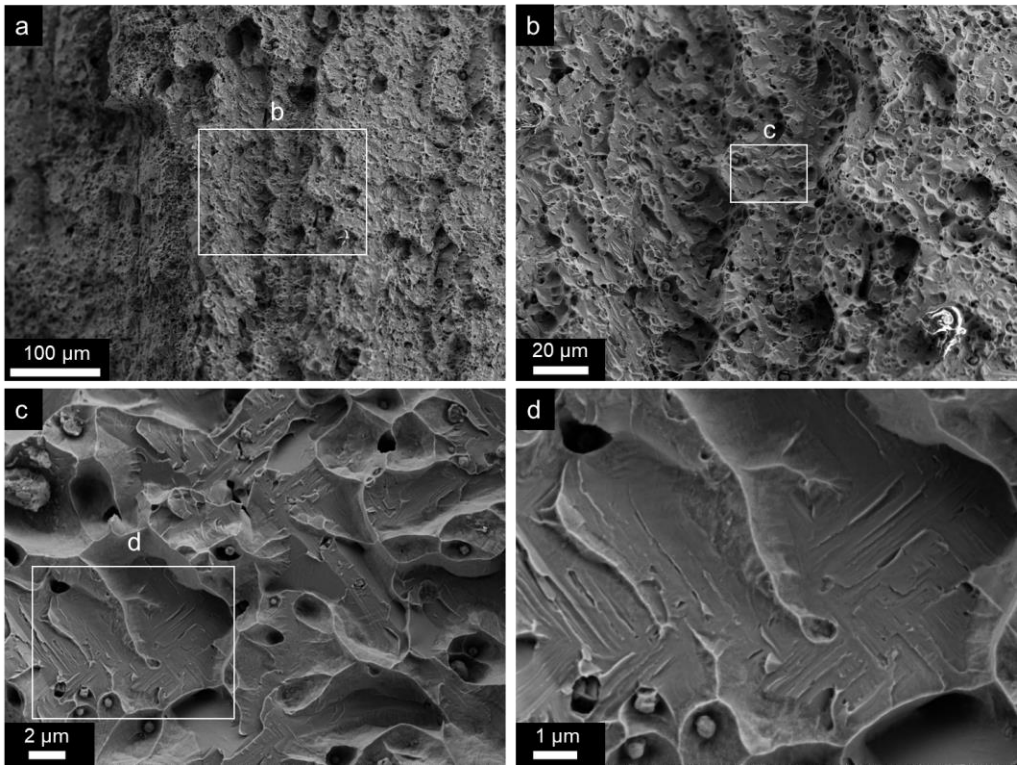

a-b) View of the crack paths, c-d) higher magnification of the MVC and cleavage fractures.

W1-F13 (77 K)

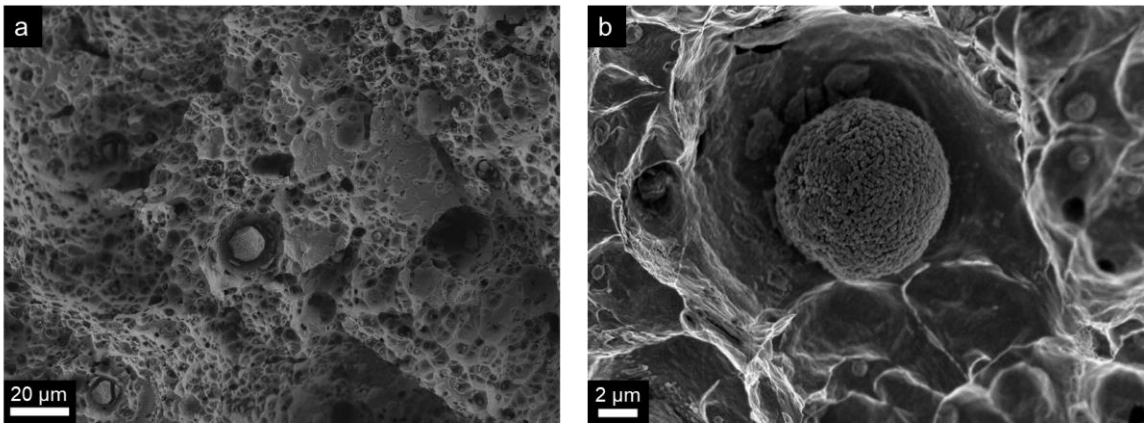

a) MVC surface morphology, b) typical inclusion within a microvoid.

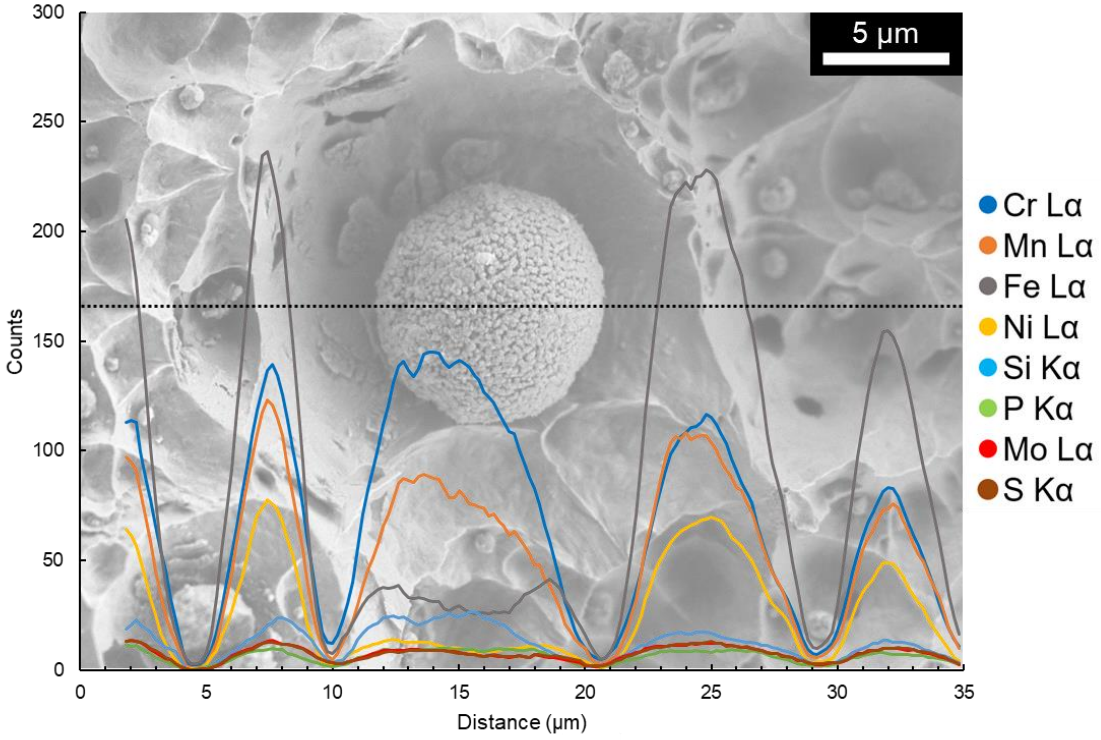

EDS line scan of an inclusion found within a microvoid.

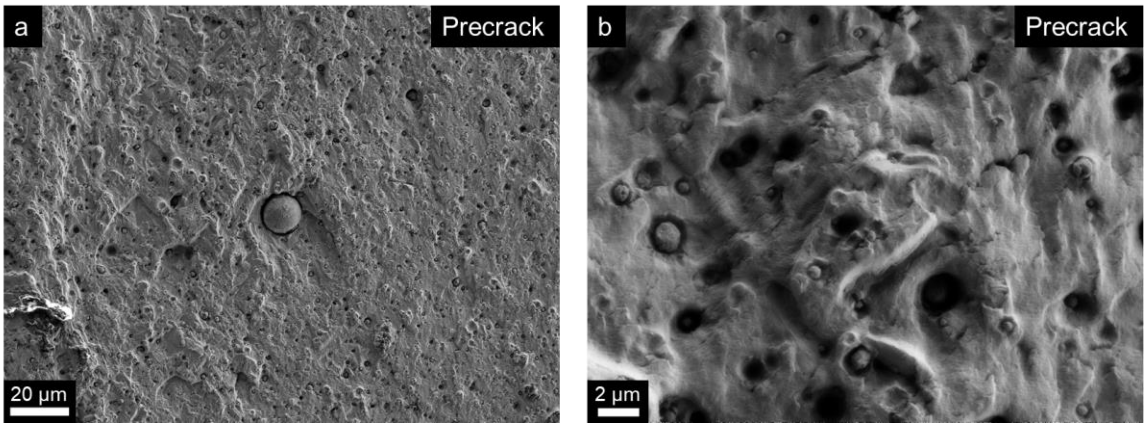

Precracked regions displaying inclusions exposed to the surface.

W1-F14 (77 K)

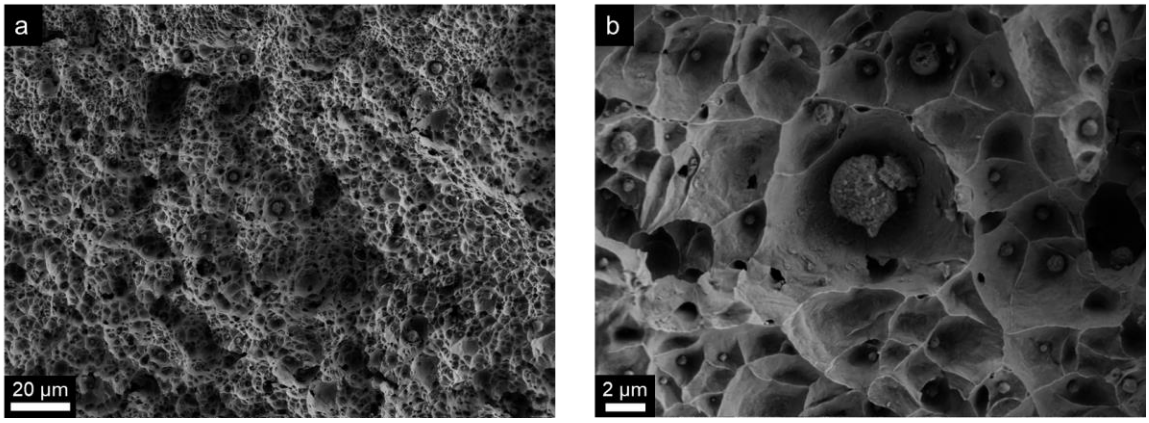

a) Typical MVC morphology, b) inclusion within a microvoid.

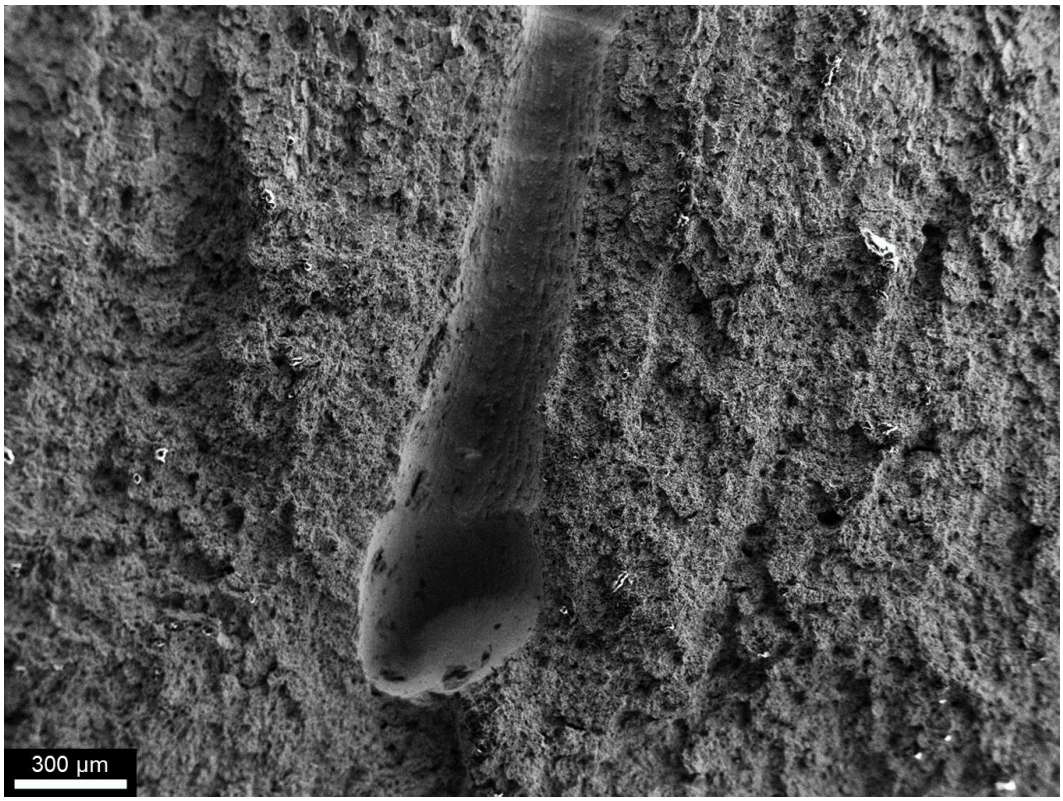

Wormhole pore

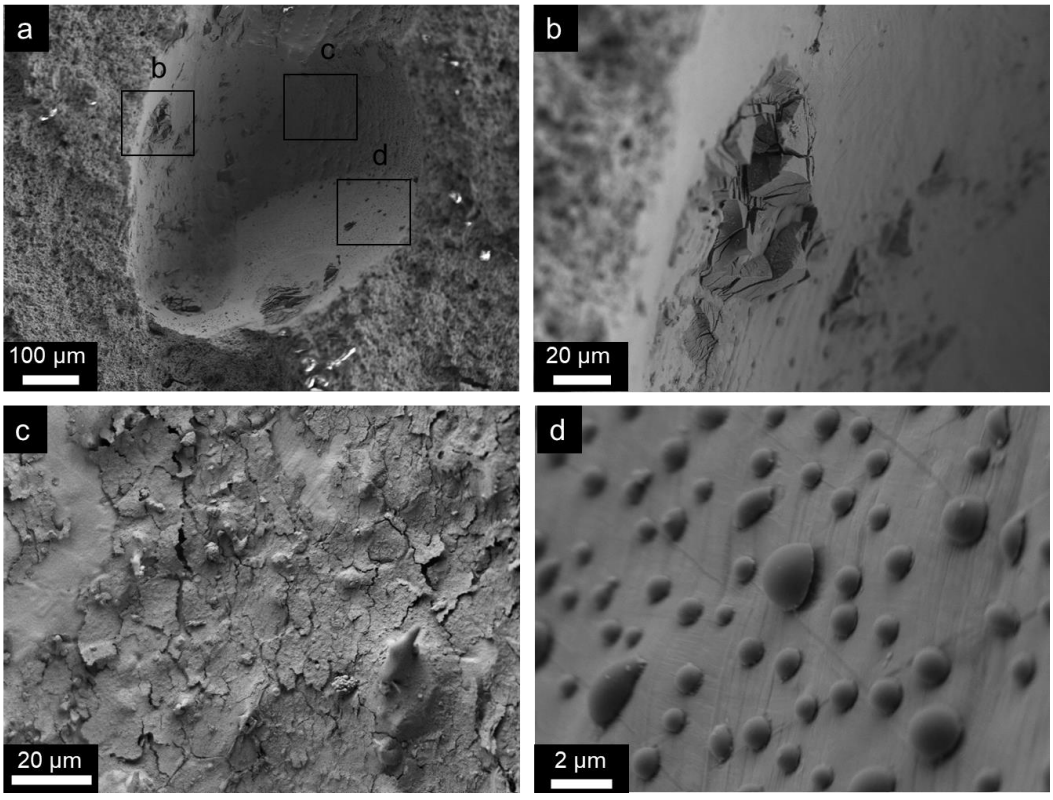

a) Wormhole pore head, b) remnants in the cavity, c) cavity bottom, d) oxides.

Weld W2

W2-F4 (4 K)

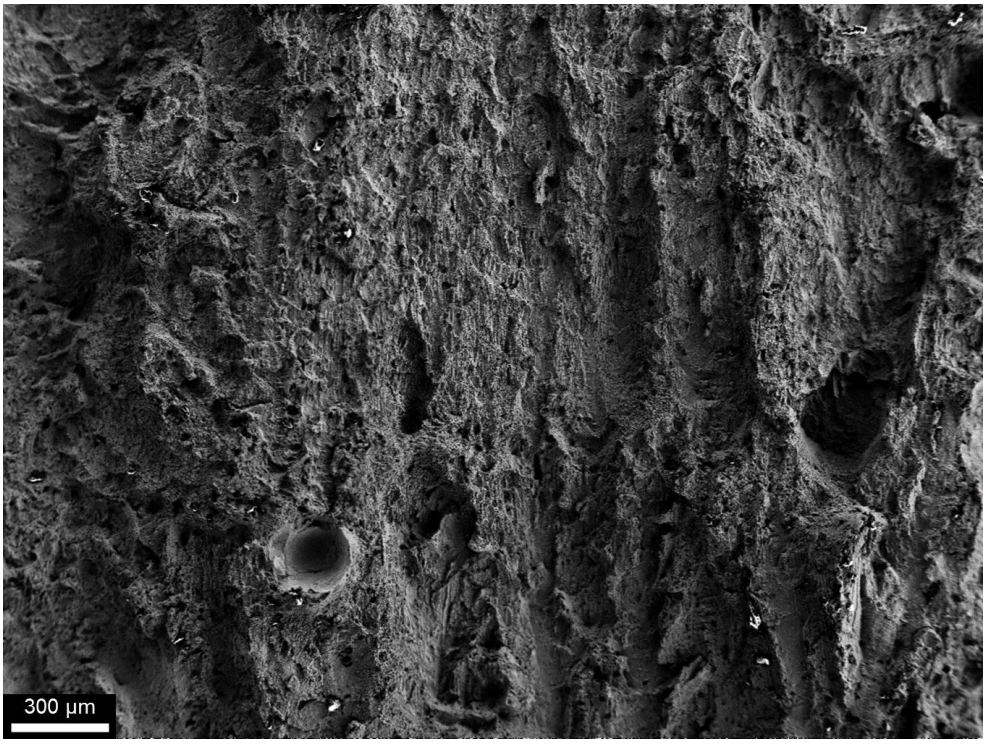

Large FOV of the fracture surface displaying lack of fusion porosity.

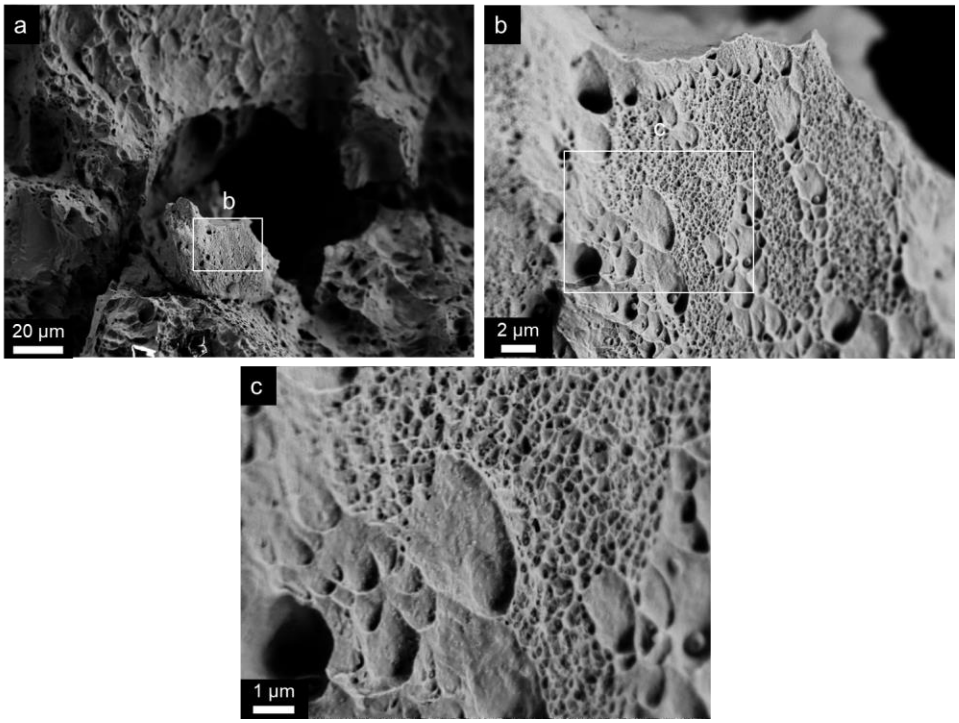

a) lack of fusion porosity, b) sheared microvoids, c) nanovoids.

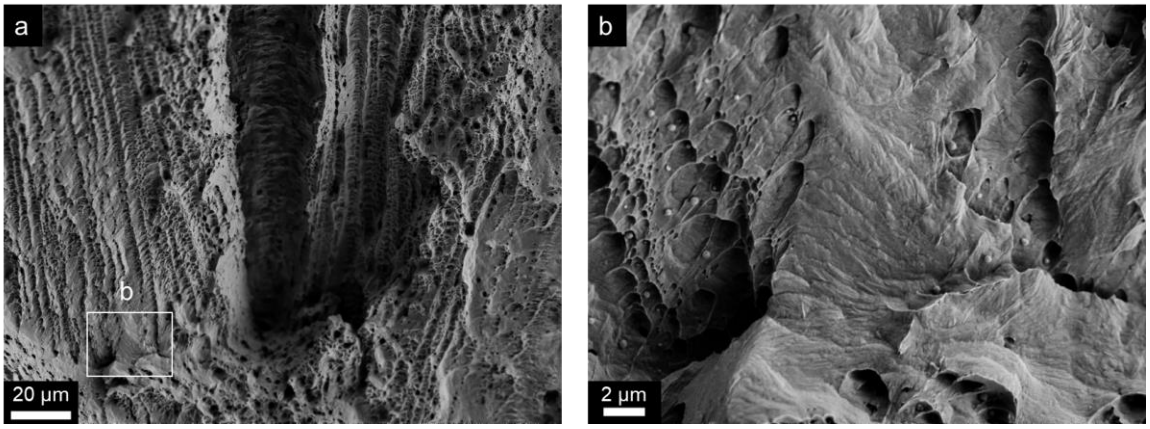

a) sheared microvoids, b) higher magnification.

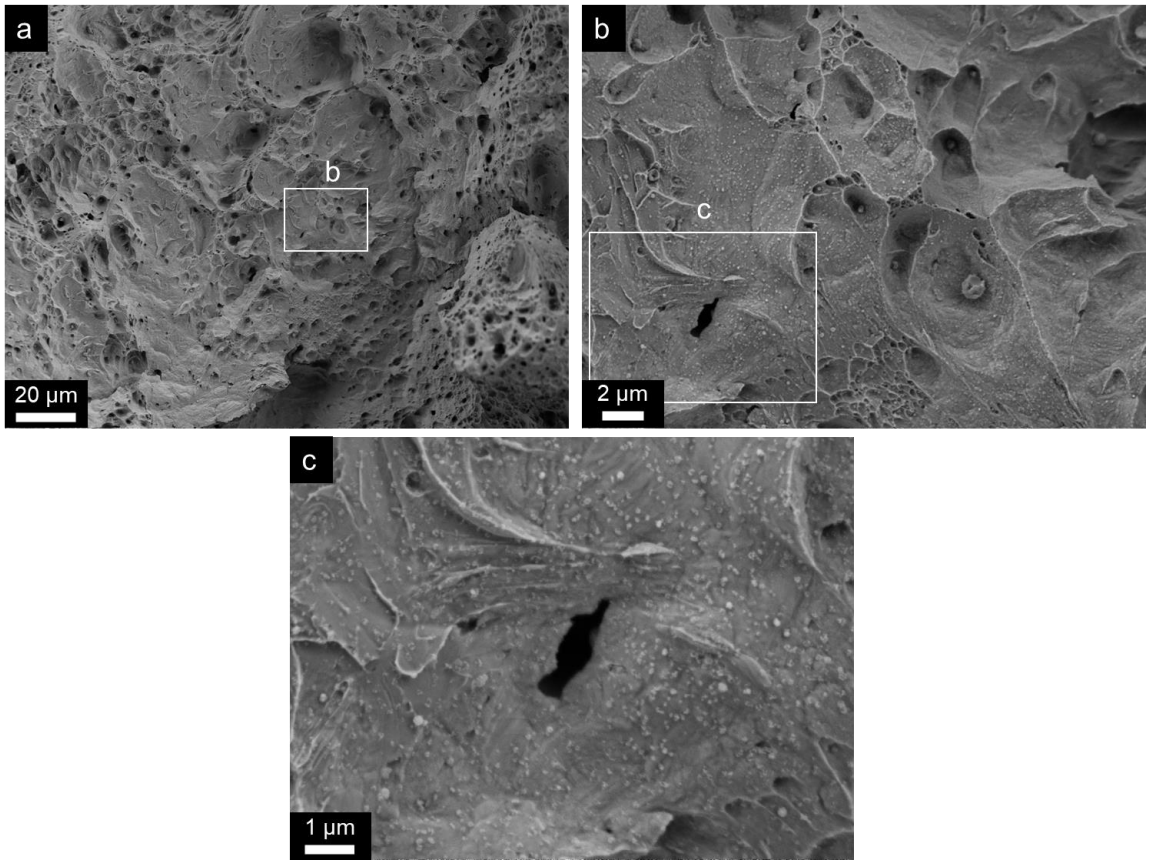

a) MVC, b-c) small pore.

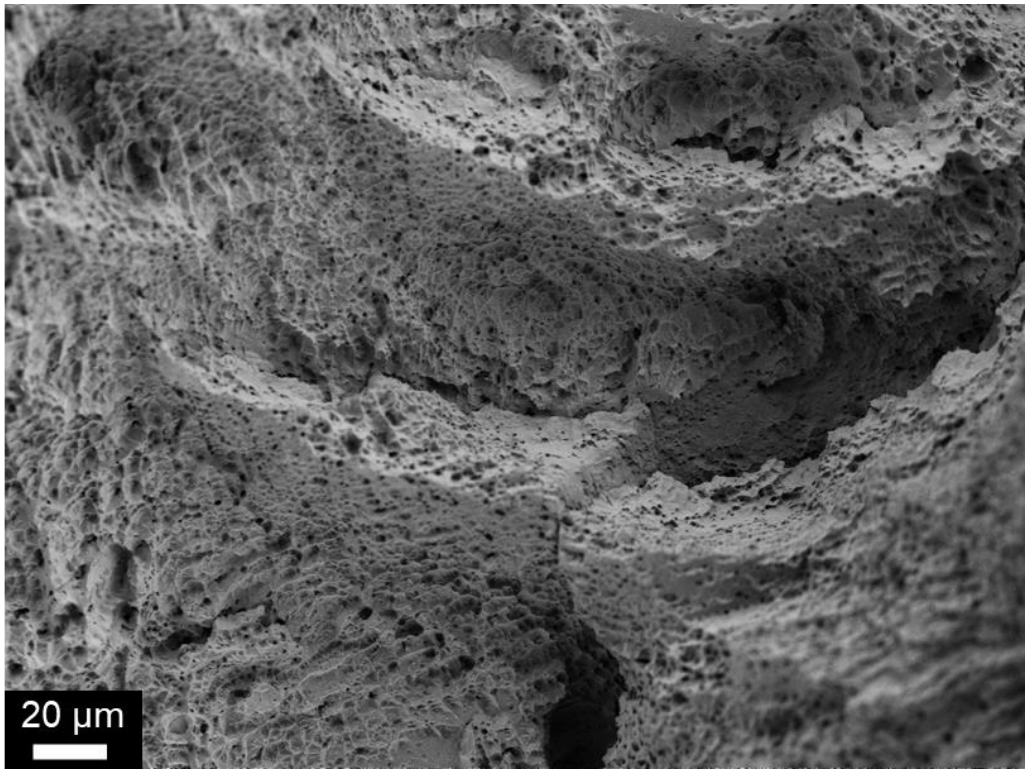

MVC and crack jumps

W2-F9 (77 K)

Large FOV of the fracture surface displaying lack of fusion porosity

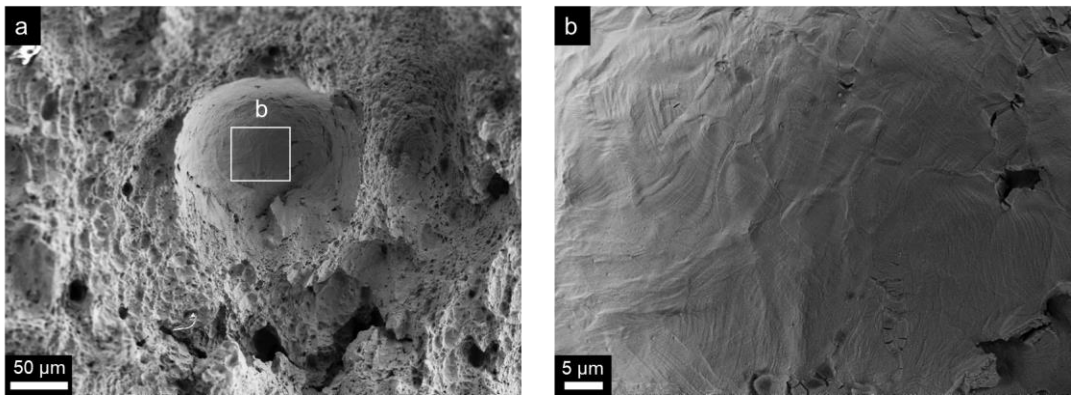

a) Lack of fusion pore, b) surface at the bottom of the pore cavity.

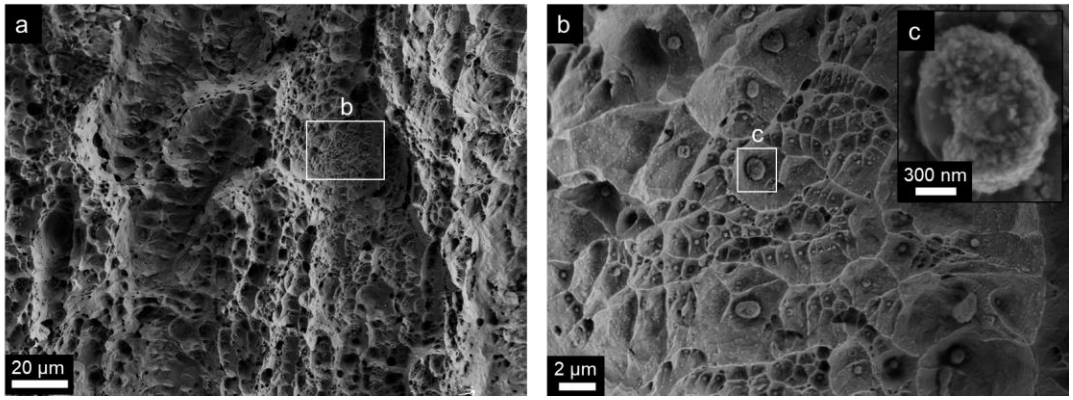

a) MVC, b) Inclusions

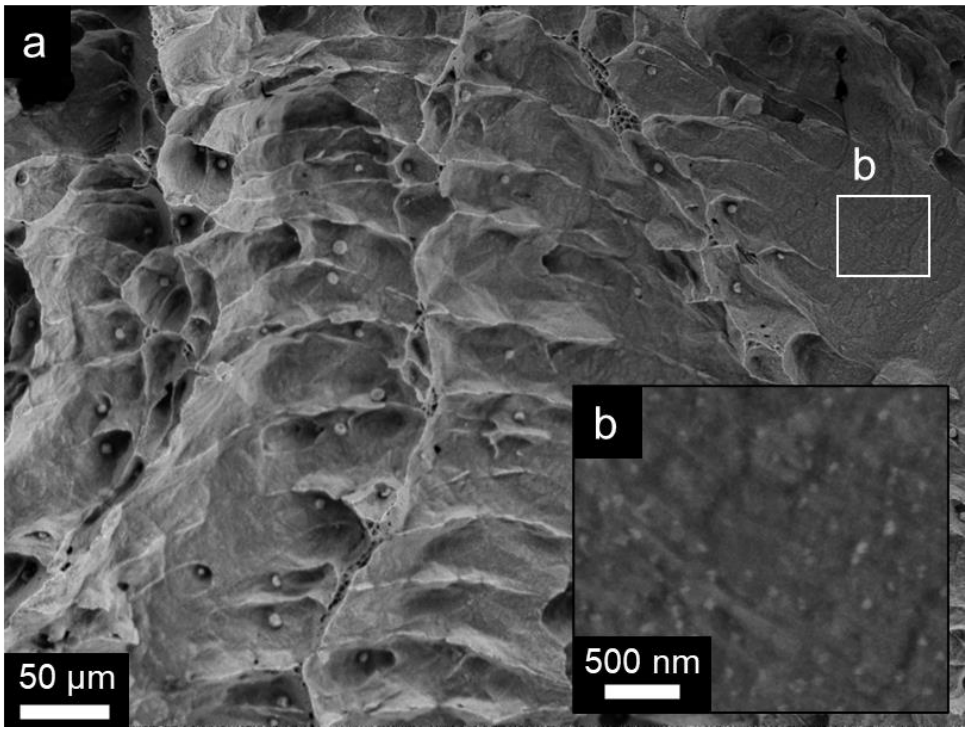

a) Sheared MVC, b) small inclusions on the surface.

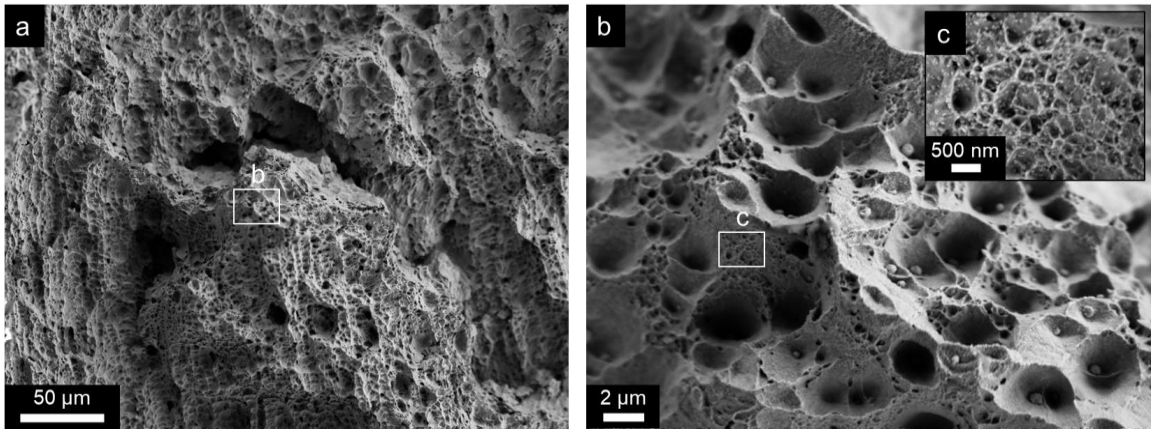

a) Crack jump, b) MVC, c) nanovoids.

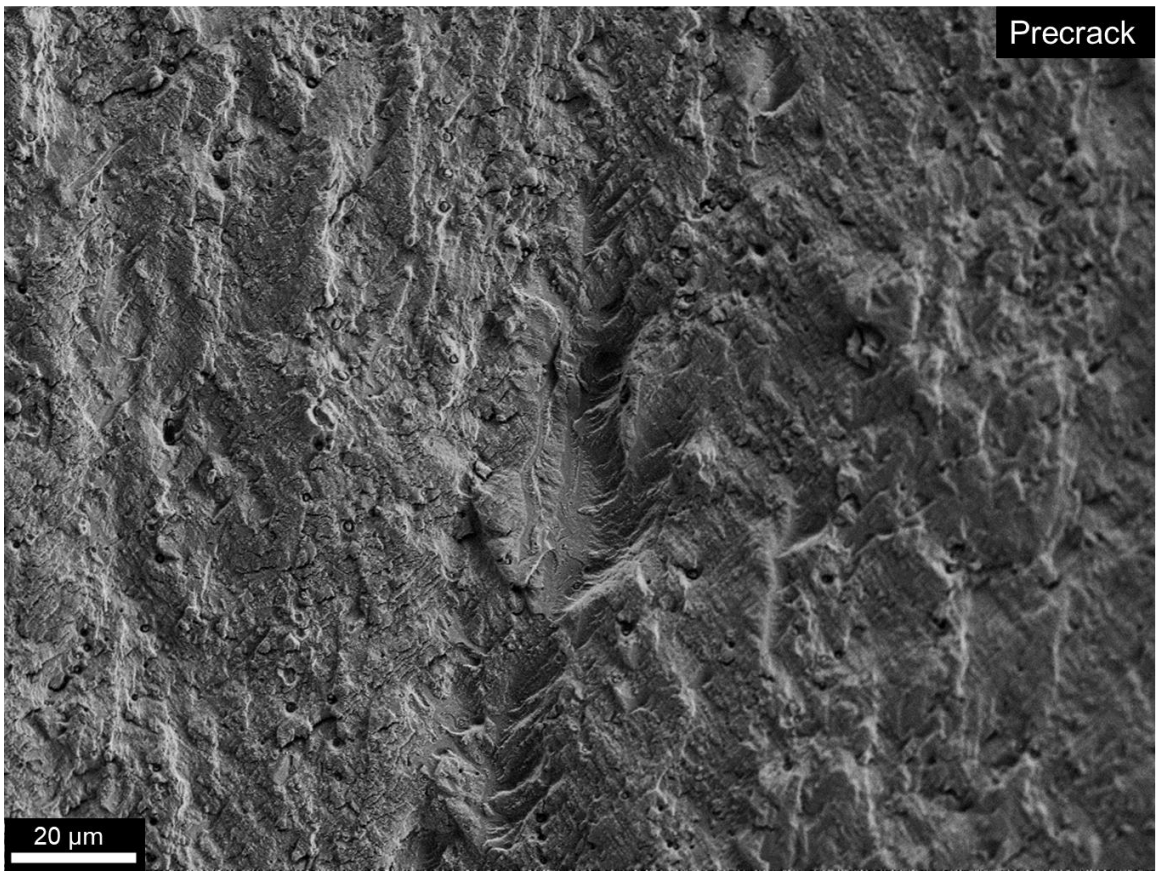

Large FOV of the precracked region.

Weld W3

W3-F4 (4 K)

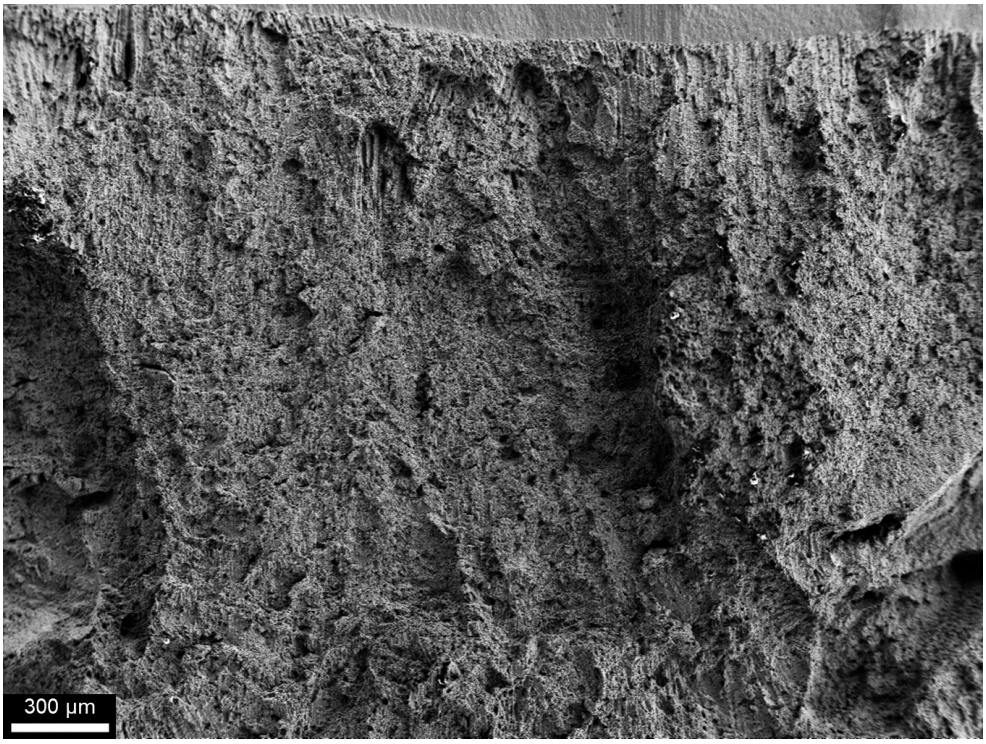

Large FOV of the fracture surface.

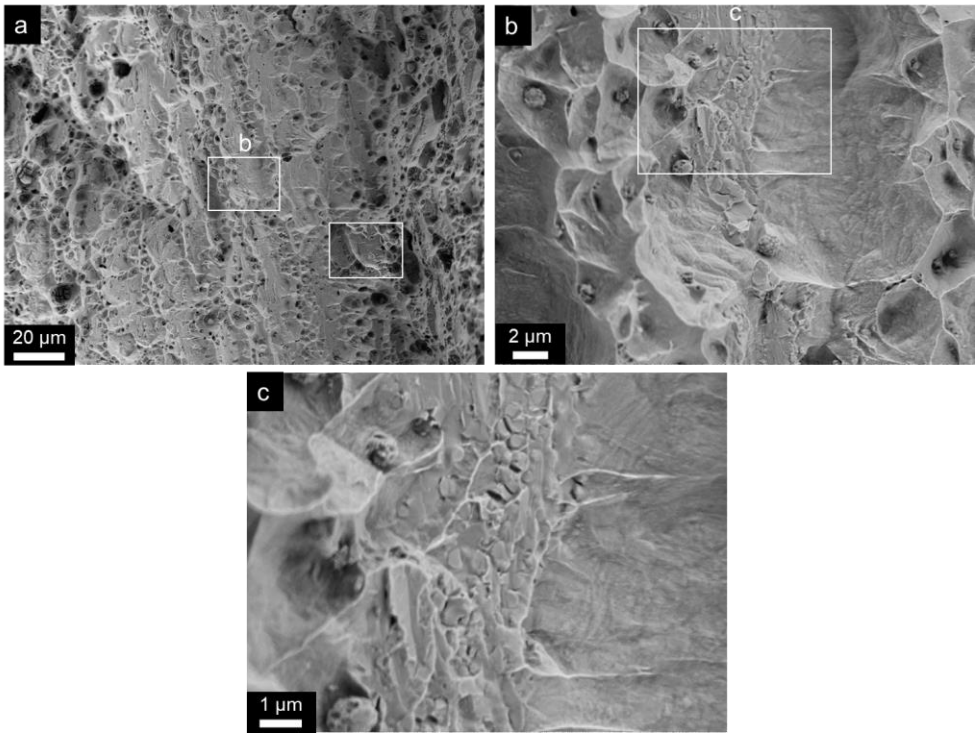

a) Crack paths, b-c) Intergranular fracture.

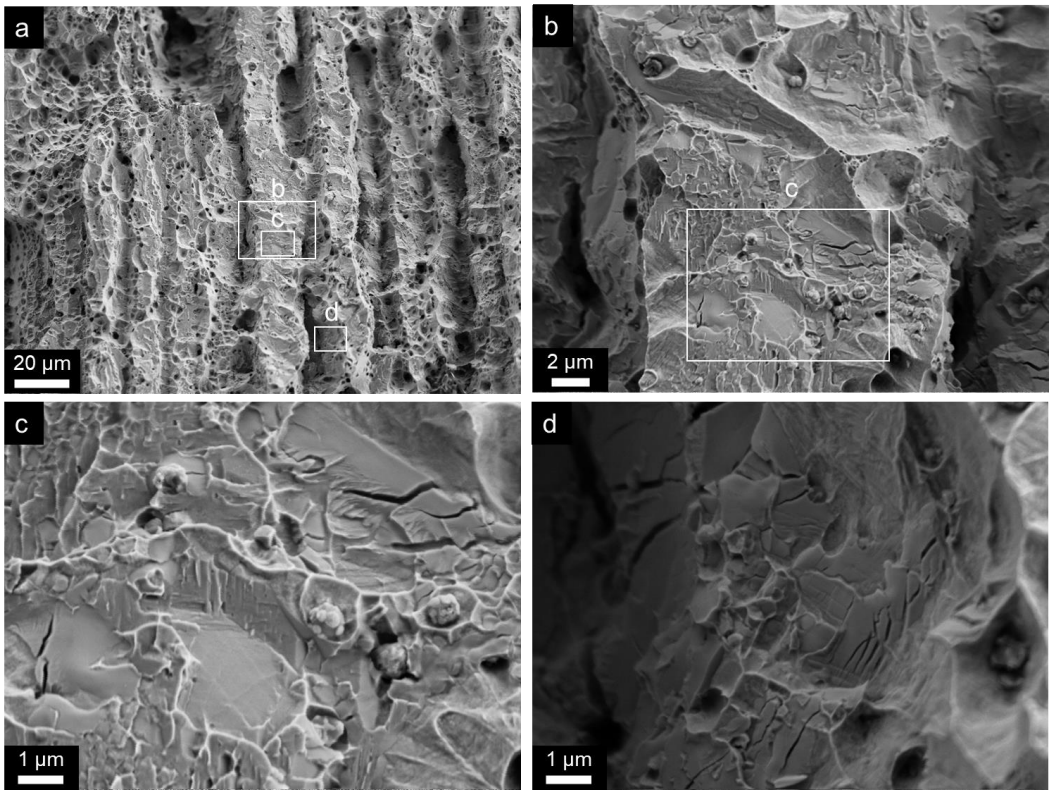

a) Crack paths, b) brittle fracture) c-d) intergranular and intragranular fracture.

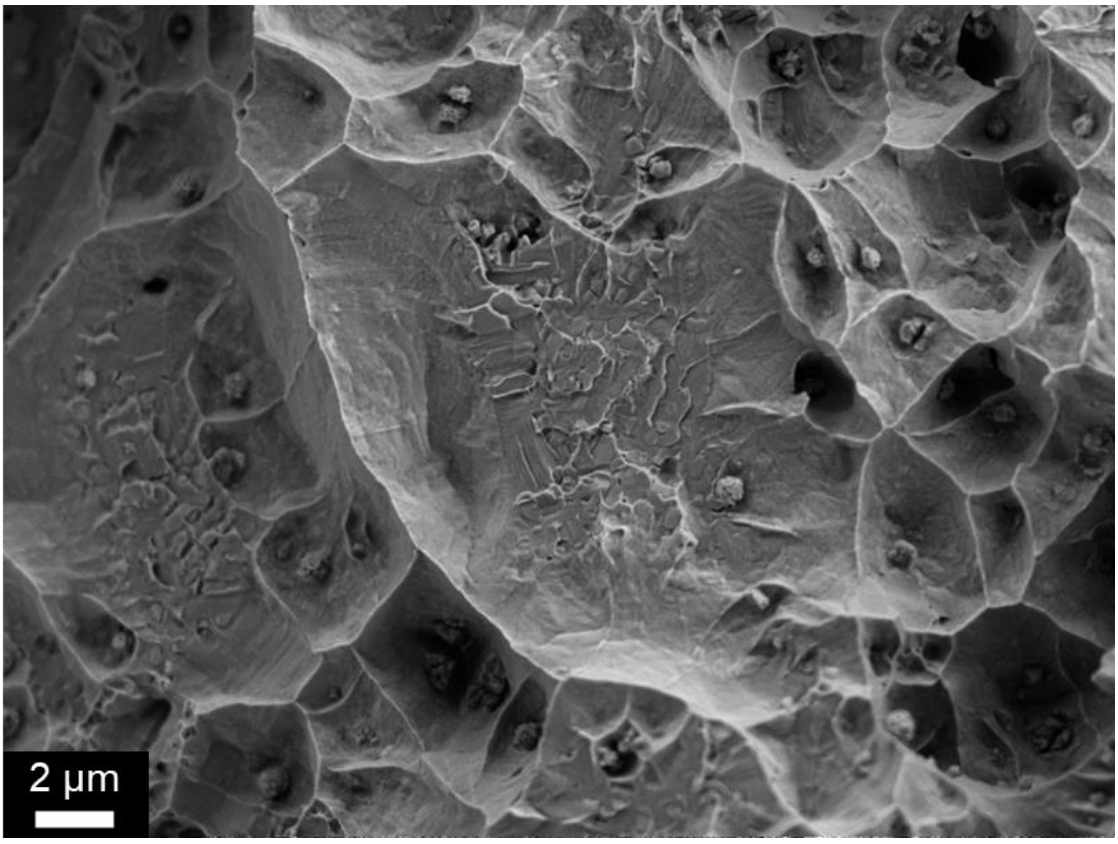

Partially formed microvoid interrupted by cleavage fracture.

W3-F5 (4 K)

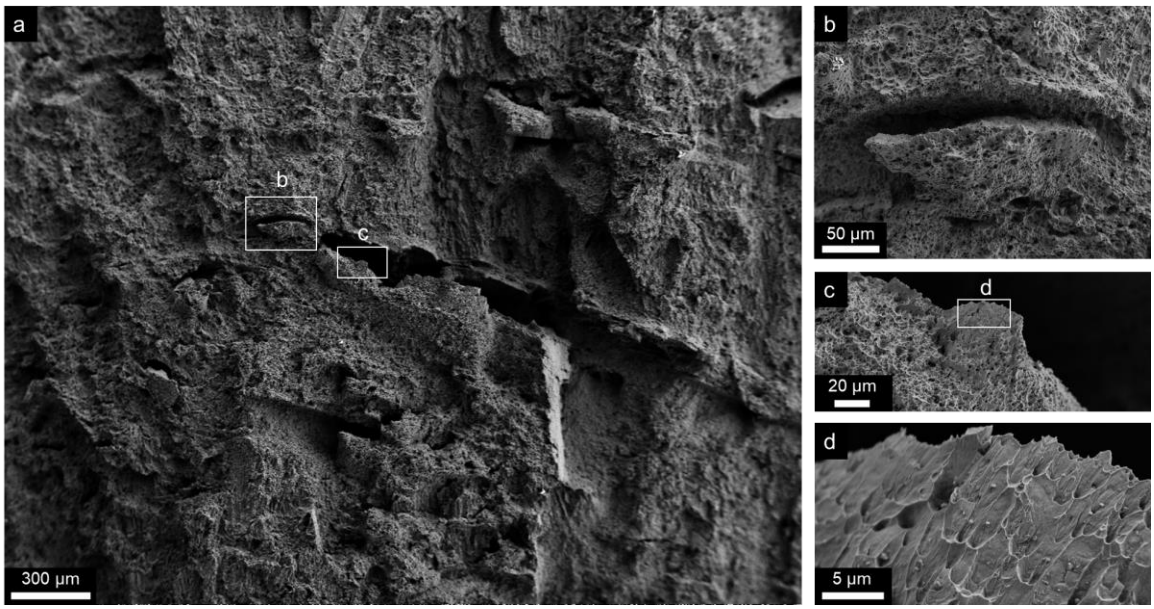

a) Crack jumps, b) higher magnification of a crack jump, c-d) MVC at the crack jump surface.

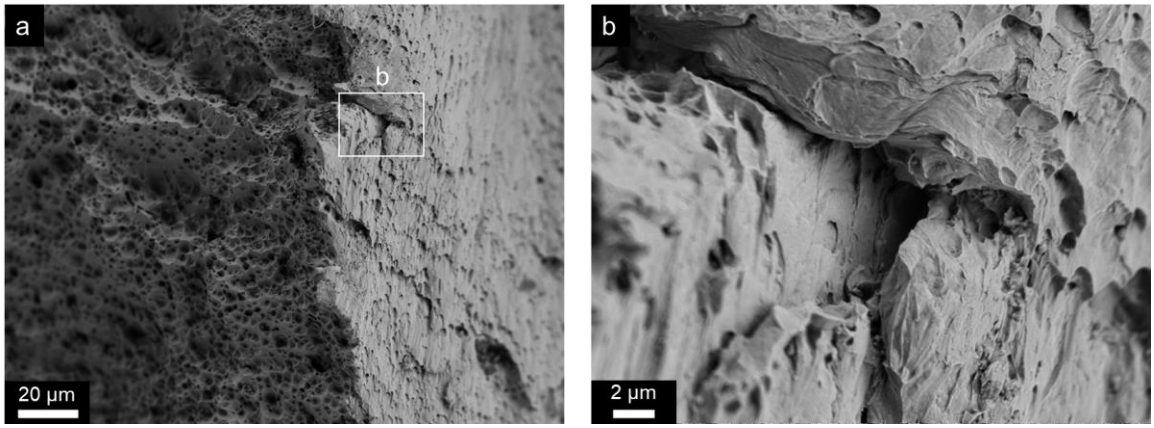

a-b) Plastic deformation features

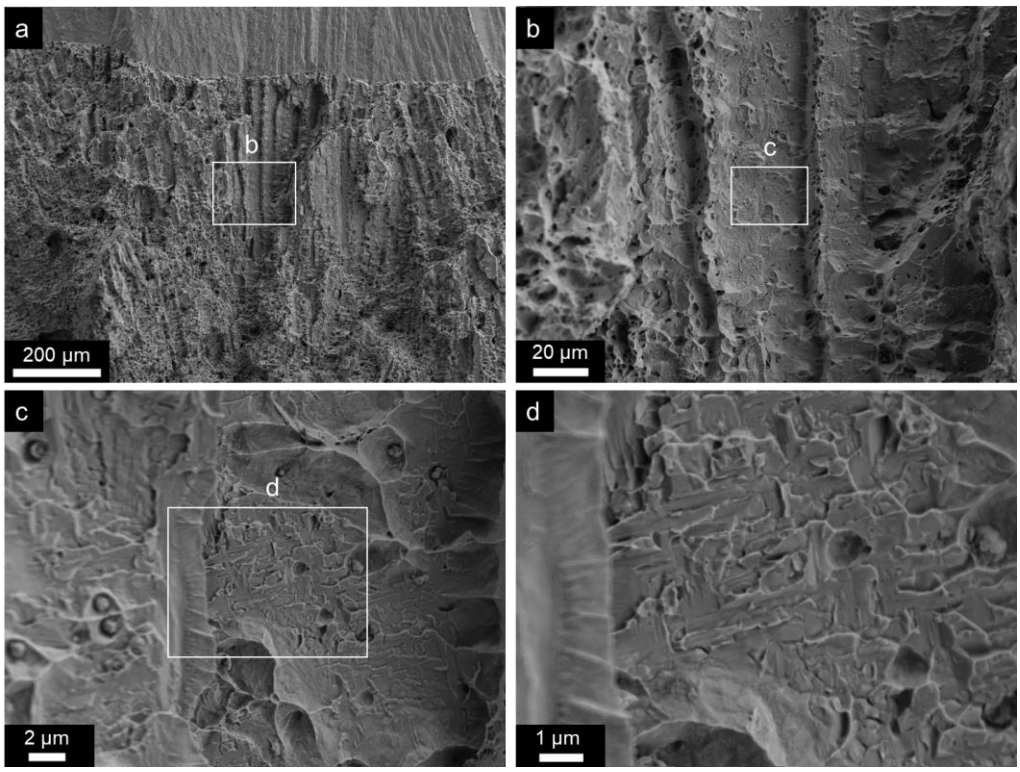

a) Crack paths near the precracked region, b) enlarged view, c—d) cleavage facets.

W3-F9 (77 K)

Large FOV displaying crack jumps.

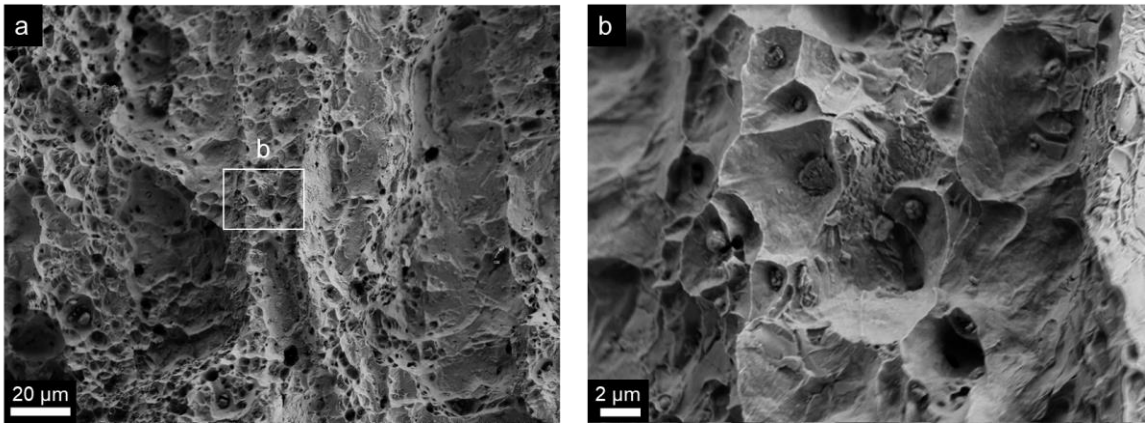

MVC.

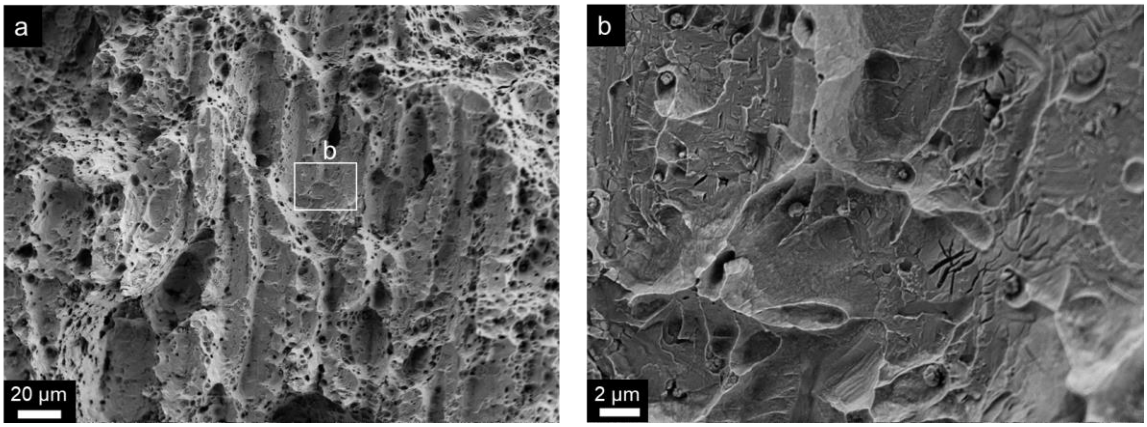

a) Crack paths, b) MVC

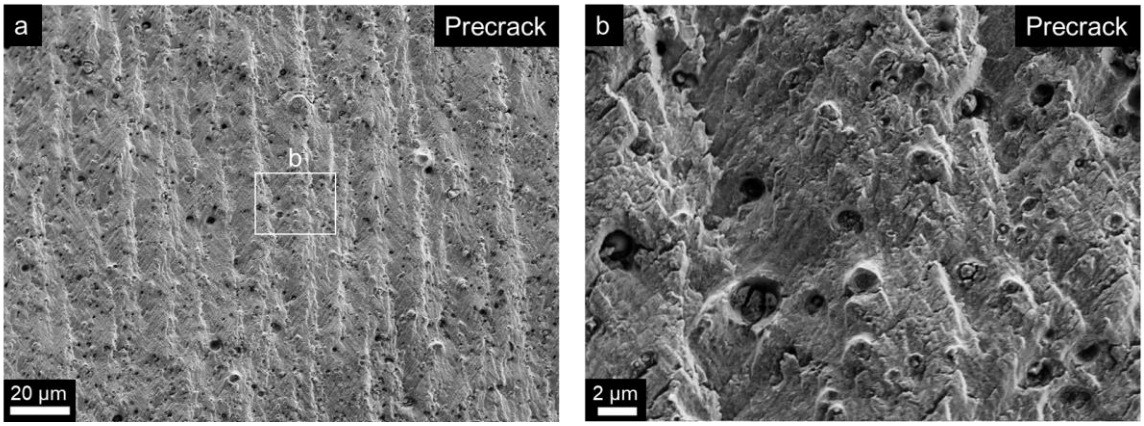

a) Precracked region, b) Inclusions exposed to the surface.

Weld W4

W4-F4 (4 K)

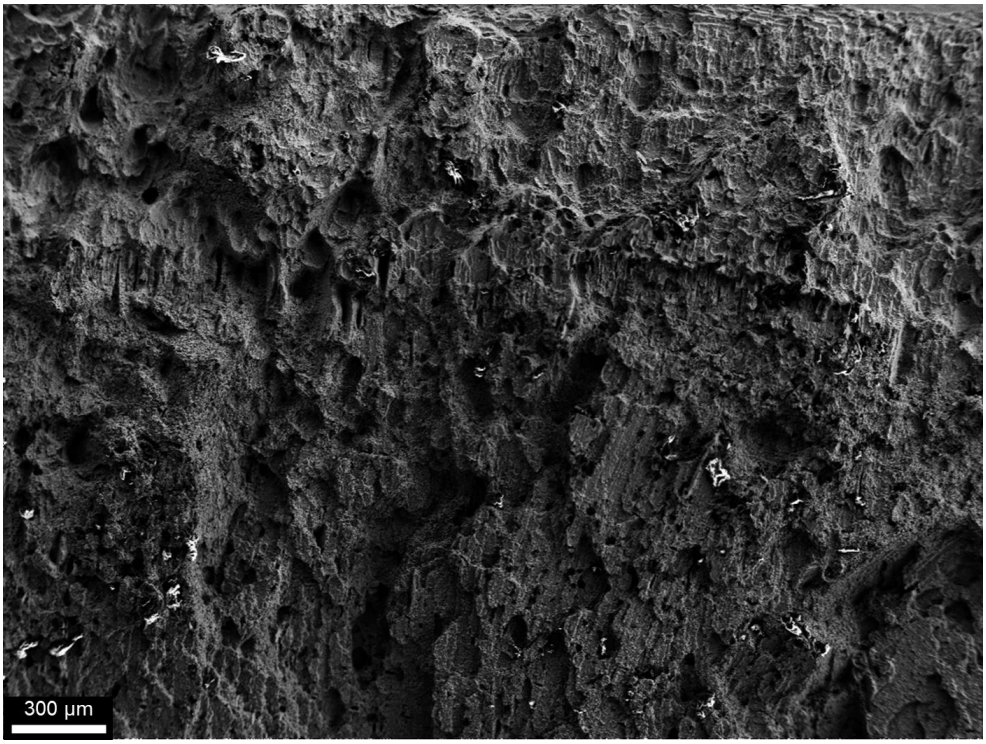

Large FOV displaying lack of fusion porosity.

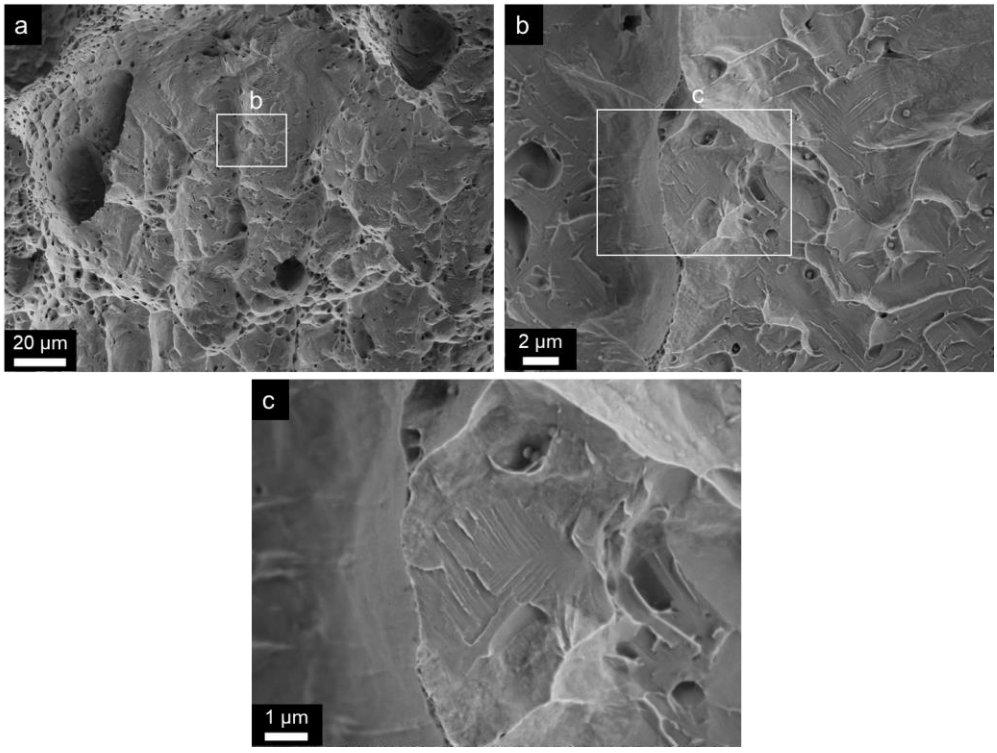

a) Mixed mode fracture and inclusion lift-outs, b-c) cleavage fracture surface.

W4-F6 (4 K)

Large FOV of the fracture surface.

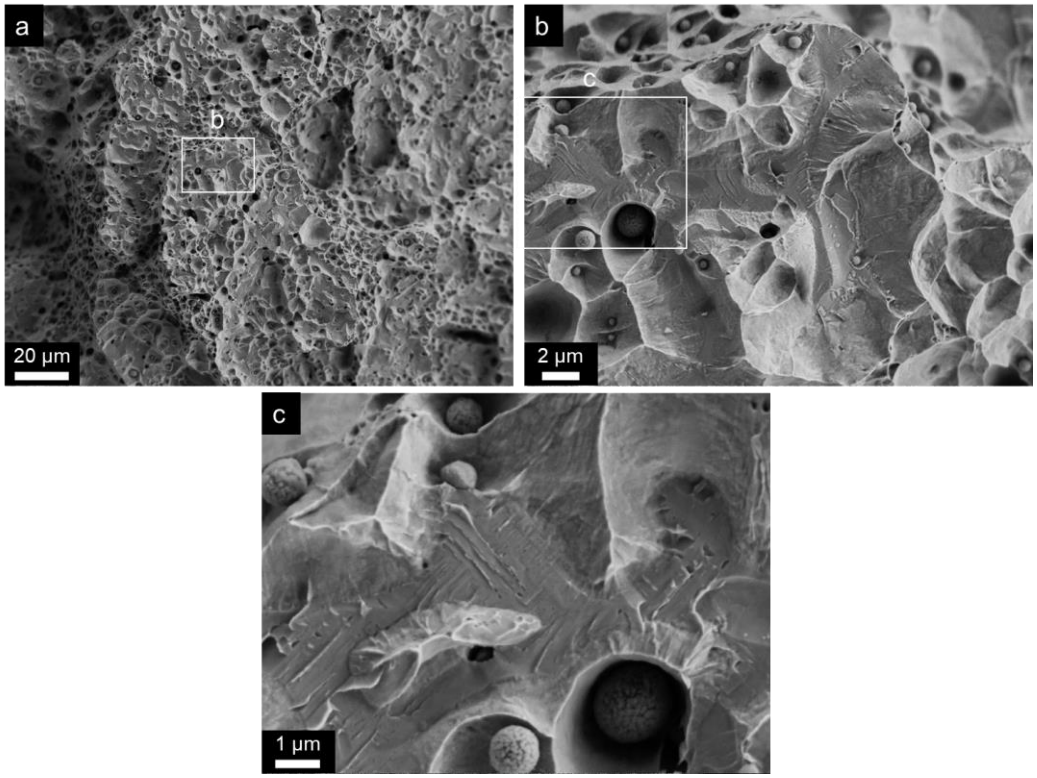

a) Mixed mode fracture (MVC and cleavage), b-c) inclusions exposed to the surface.

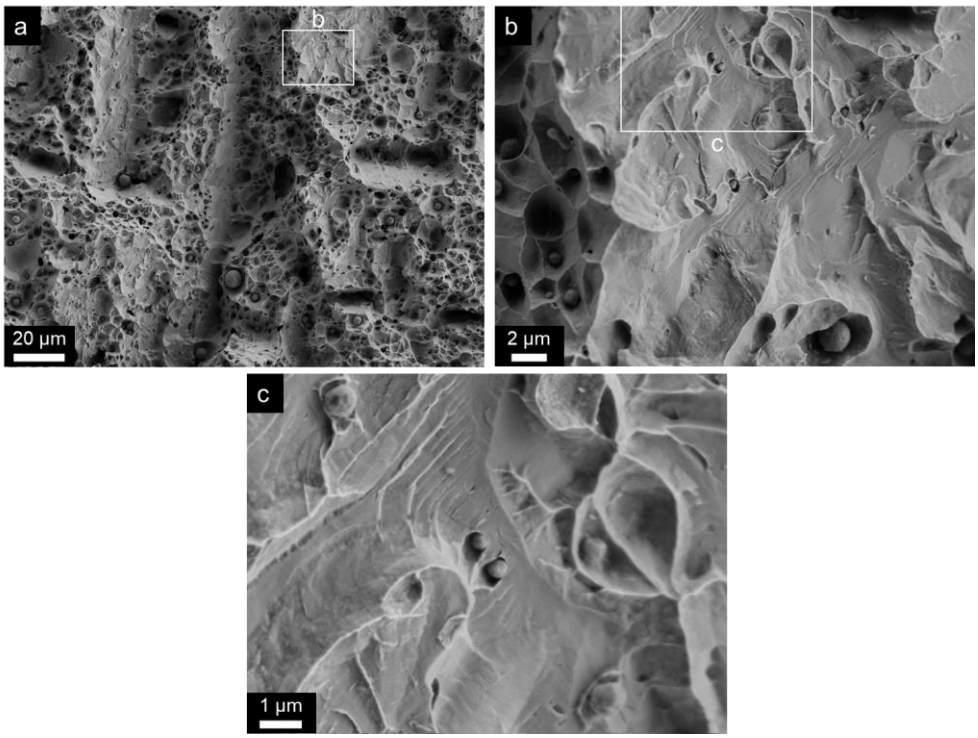

a) Crack paths among MVC and cleavage fracture, b-c) inclusions exposed to the surface.

W4-F7 (4 K)

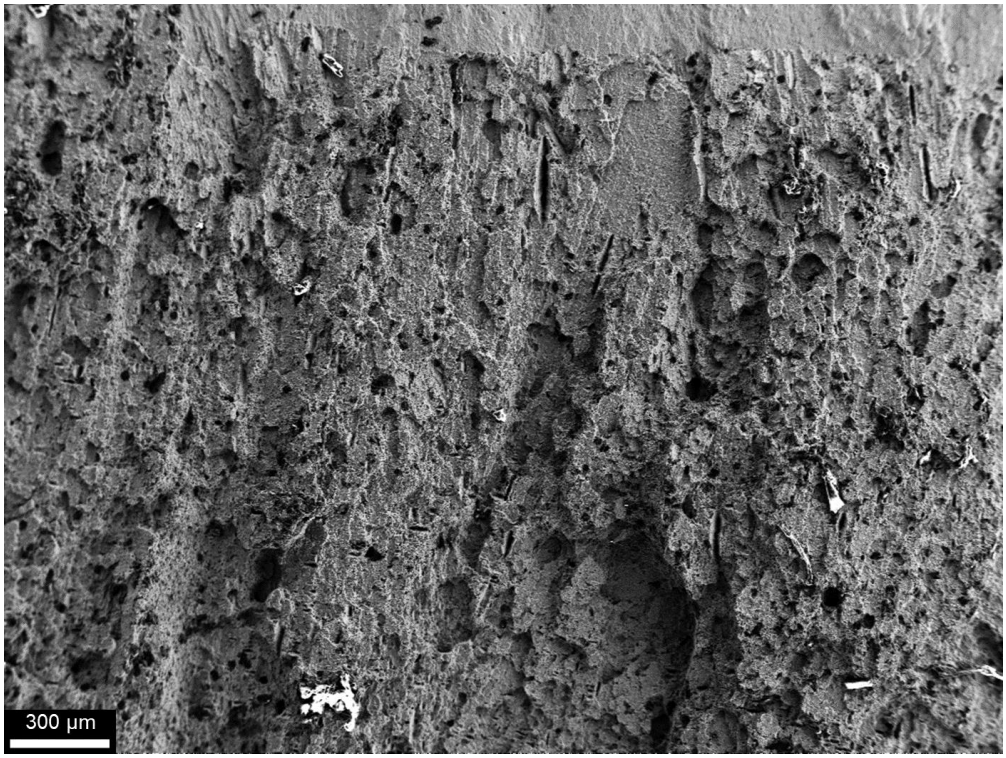

Large FOV of the fracture surface displaying regions of brittle fracture and elongated lack of fusion pores.

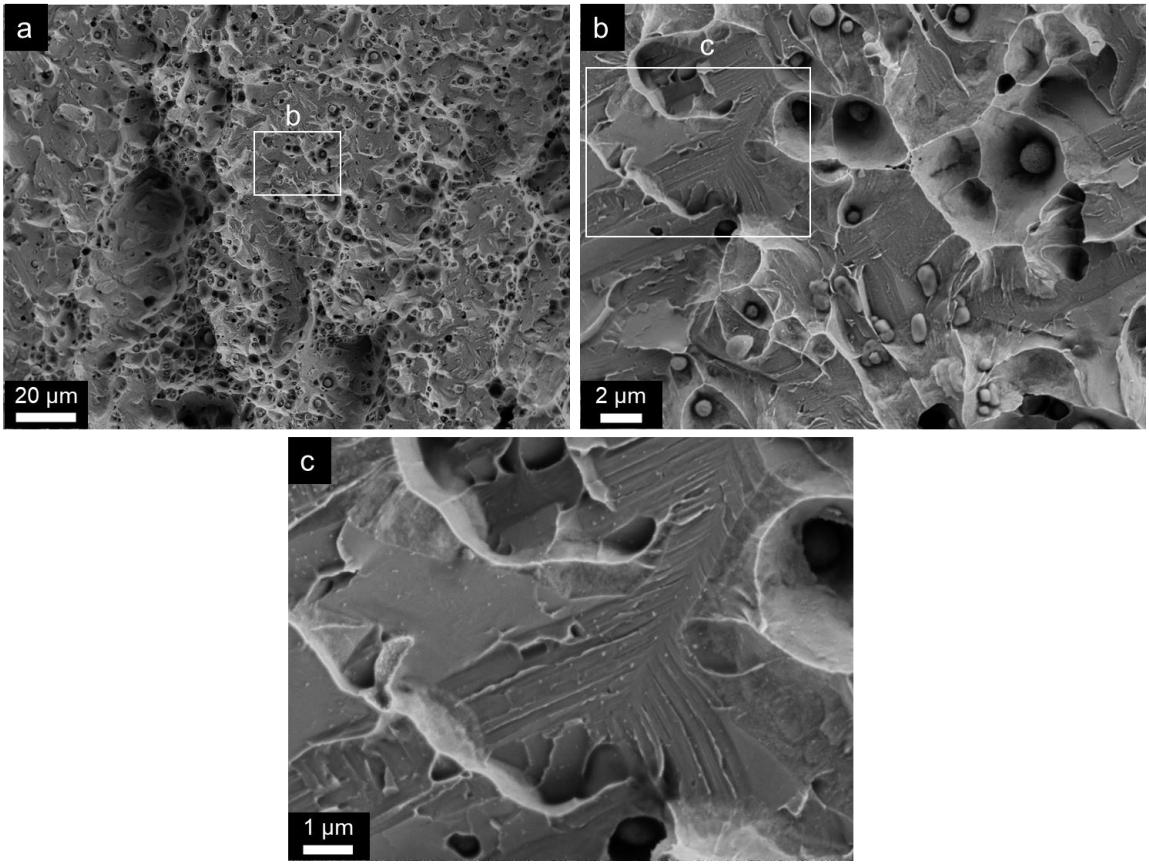

a) Mixed MVC and brittle fracture, b-c) enlarged view of the mixed fractures.

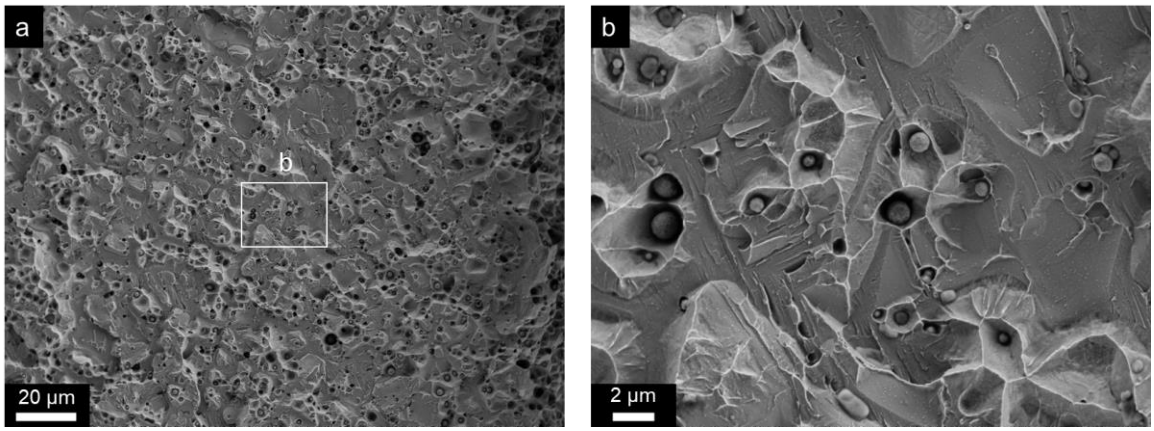

a) Mixed MVC and brittle fracture, b-c) enlarged view of the mixed fractures.

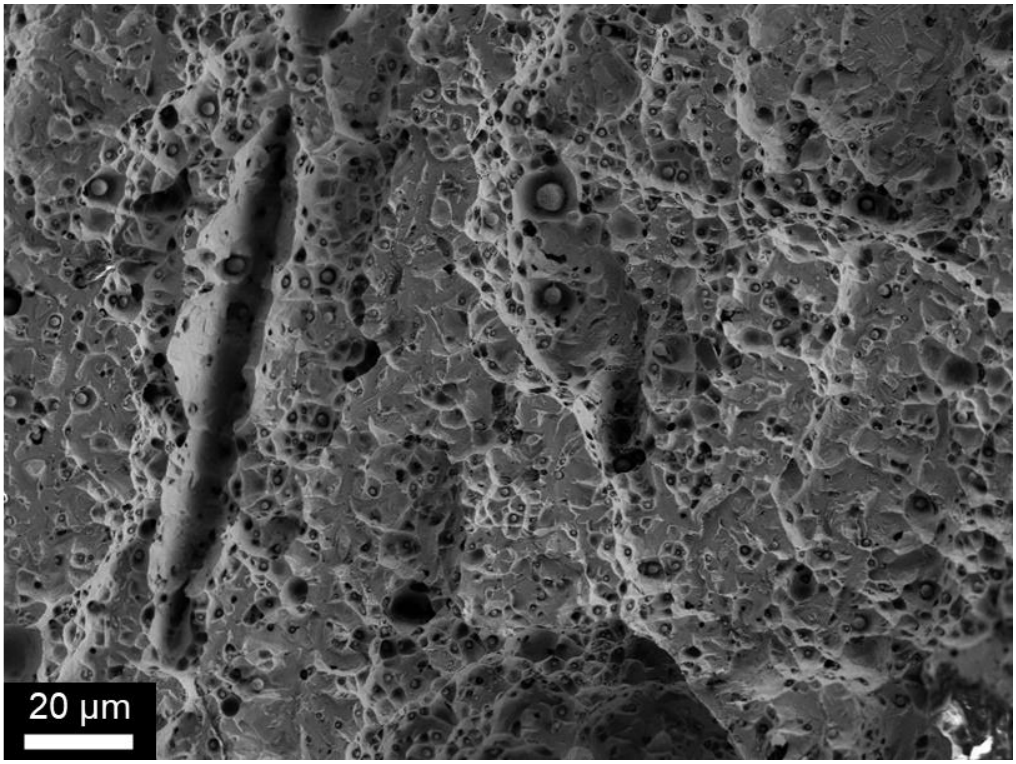

Mixed MVC and brittle fracture near an elongated lack of fusion pore.

W4-F12 (77 K)

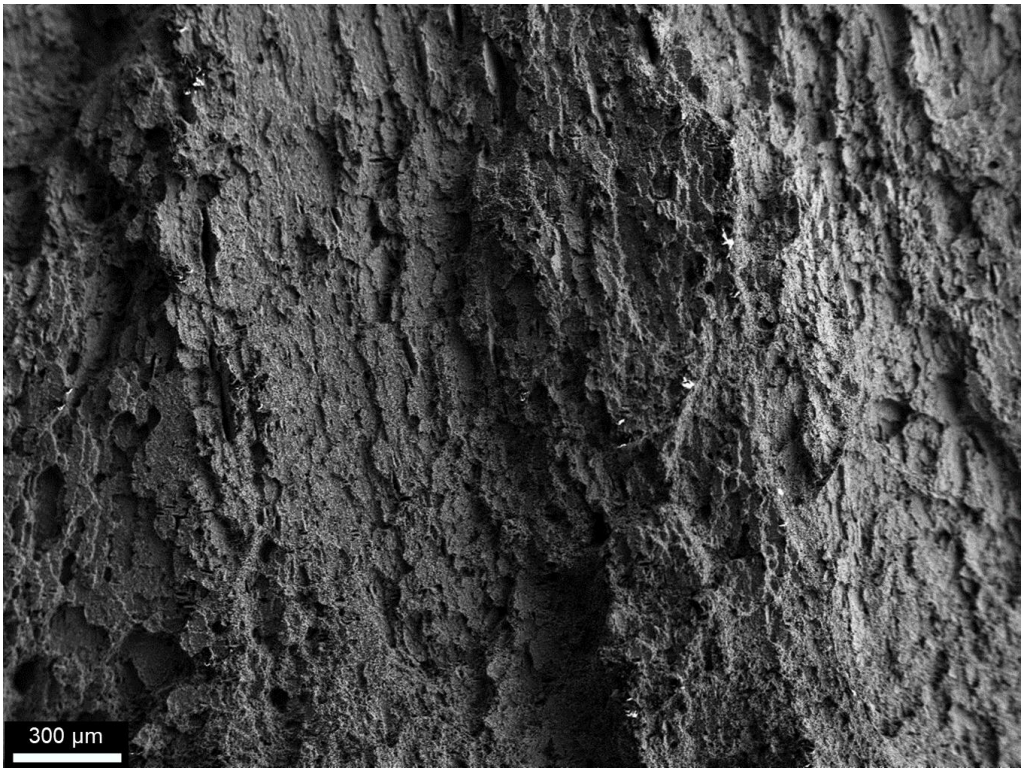

Large FOV of the fracture surface and crack paths.

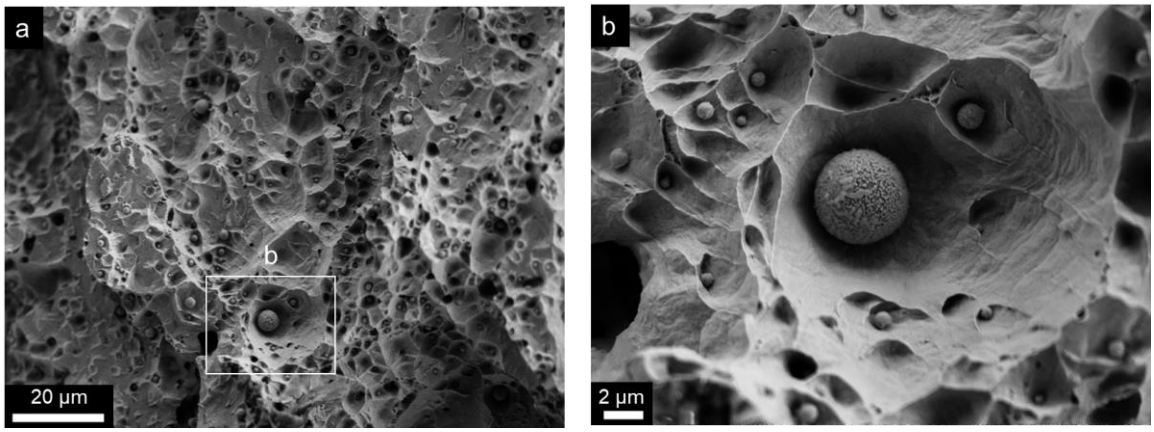

MVC.

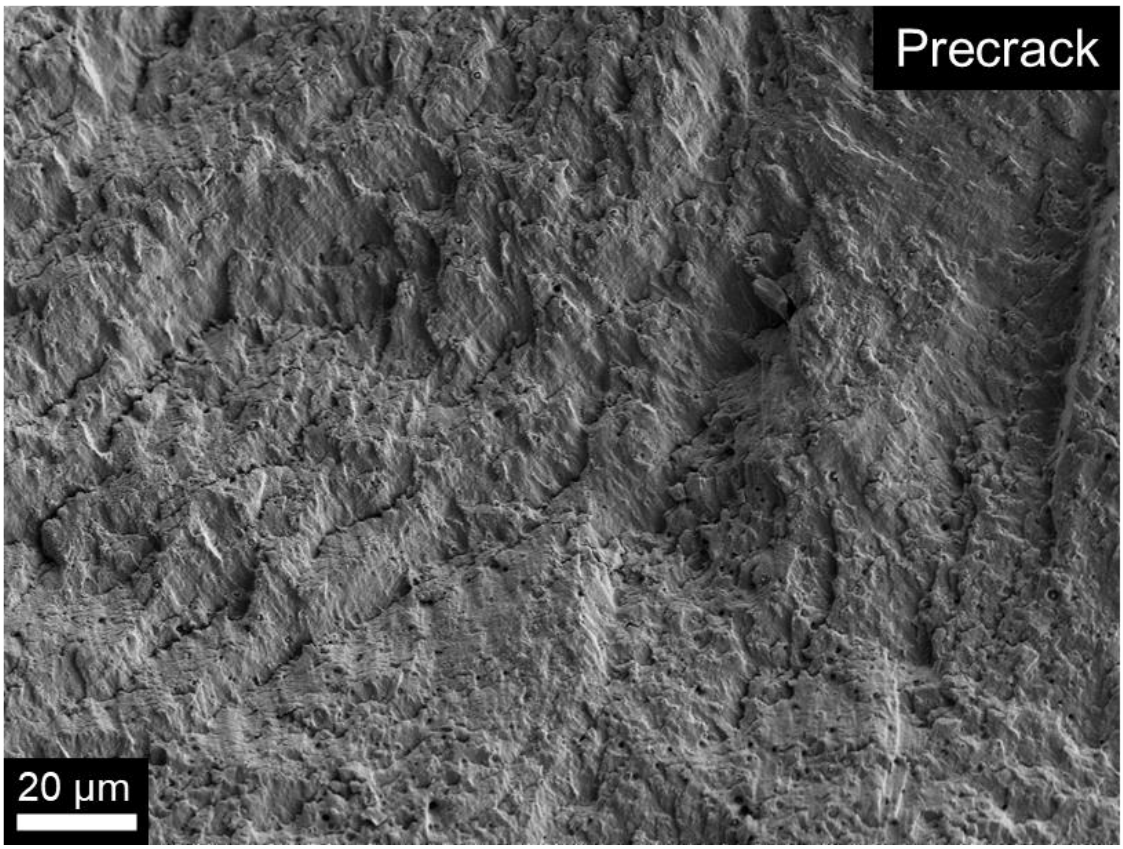

Precracked region.